

## APPENDIX F

### SUMMARY OF FIGURES

This appendix provides a full list of figures produced in an effort to validate the ability to characterize the anomalous rate increase observed in field data. Organization of this appendix follows a similar pattern as the main body. The dimensionless rate plot will be followed by the dimensionless rate derivative, dimensionless cumulative production and time-normalized dimensionless cumulative rate for each parameter, for each time-dependent model, per flow regime. The author notes, all values of the  $\tau$ -parameter will equal  $\tau = 0.01$  unless otherwise stated.

#### F.1 Power-Law Flow Relation

*Power-Law Flow Relation with Cumulative Exponential Time-Dependent Skin*

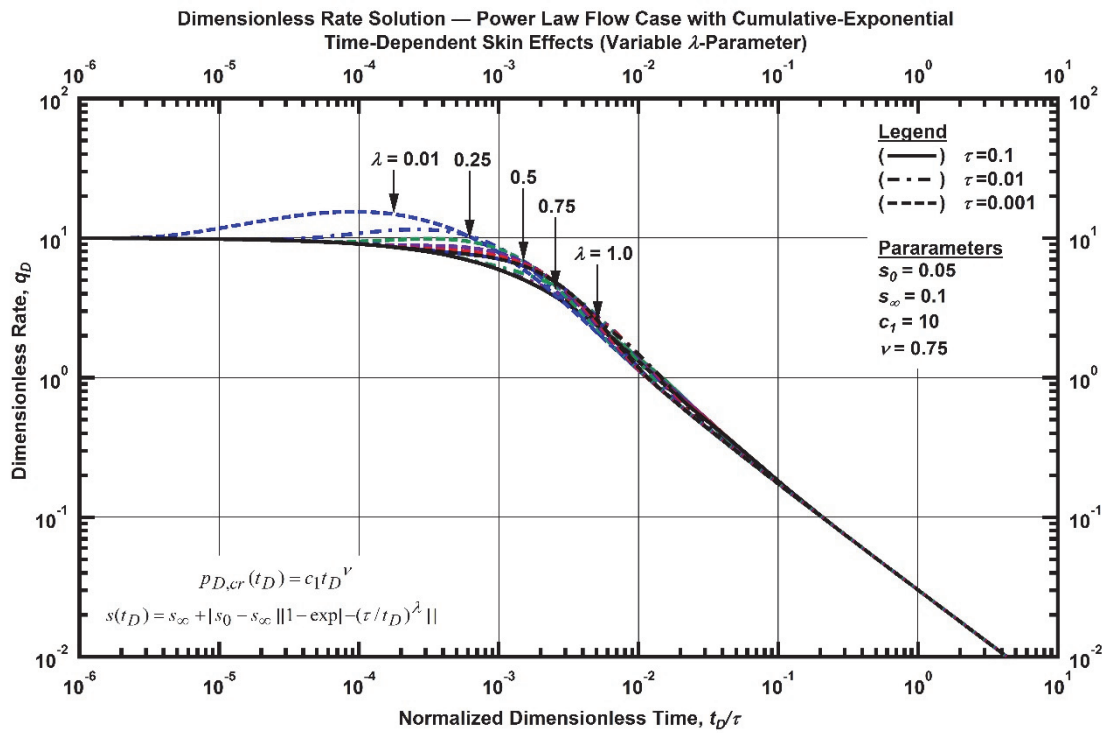


Figure F. 1 — Log-log plot (constant pressure dimensionless rate solution) for the power-law flow model combined with the cumulative-exponential time-dependent skin effects for select values of  $\lambda$ -parameter.

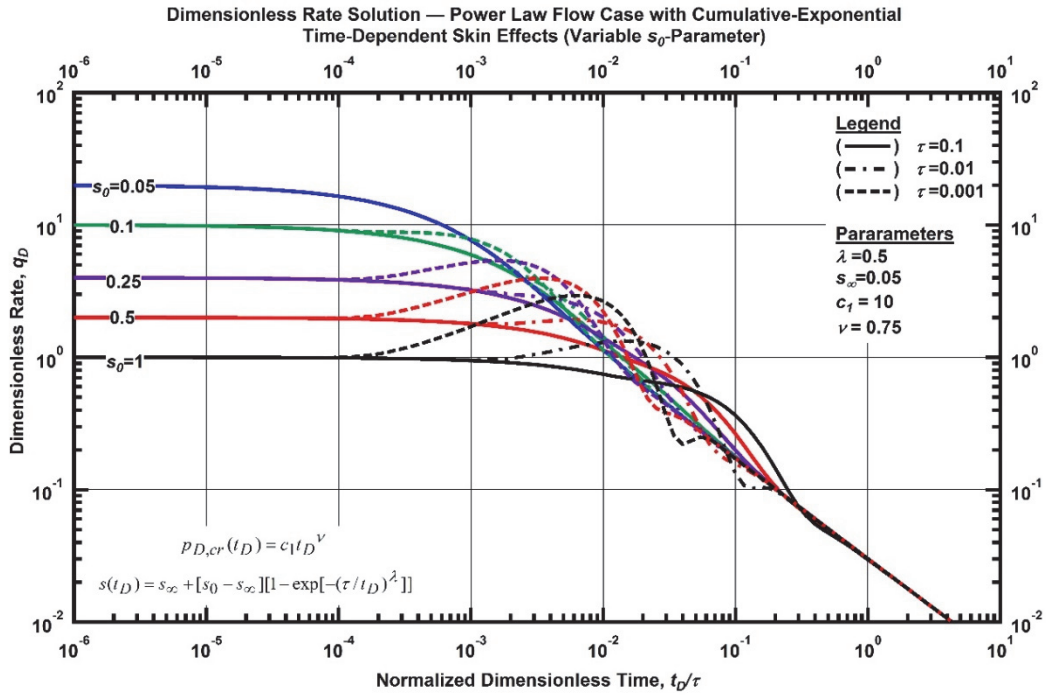


Figure F. 2 — Log-log plot (constant pressure dimensionless rate solution) for the power law flow model combined with the cumulative-exponential time-dependent skin effects for select values of  $s_0$ -parameter.

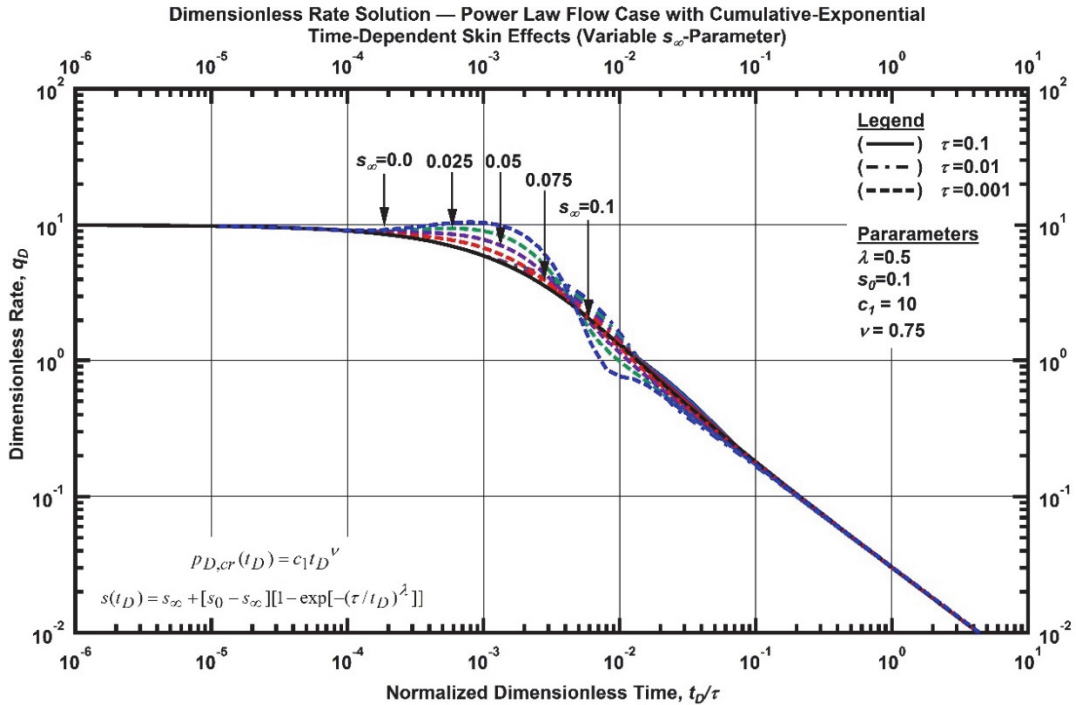


Figure F. 3 — Log-log plot (constant pressure dimensionless rate solution) for the power law flow model combined with the cumulative-exponential time-dependent skin effects for select values of  $s_\infty$ -parameter.

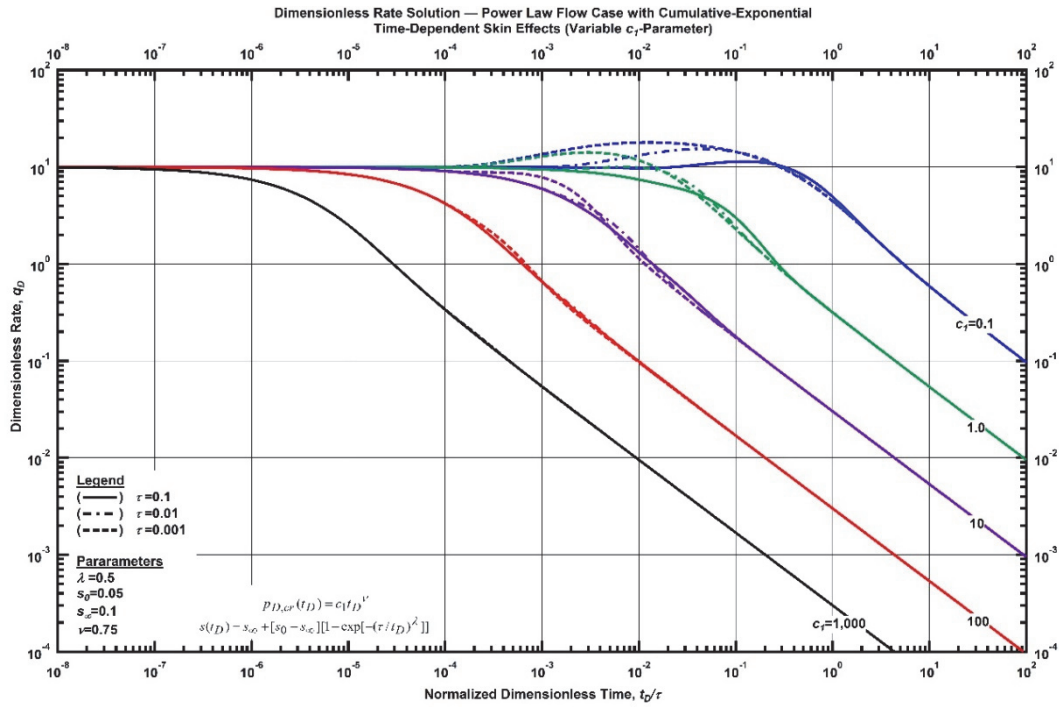


Figure F. 4 — Log-log plot (constant pressure dimensionless rate solution) for the power law flow model combined with the cumulative-exponential time-dependent skin effects for select values of  $c_1$ -parameter.

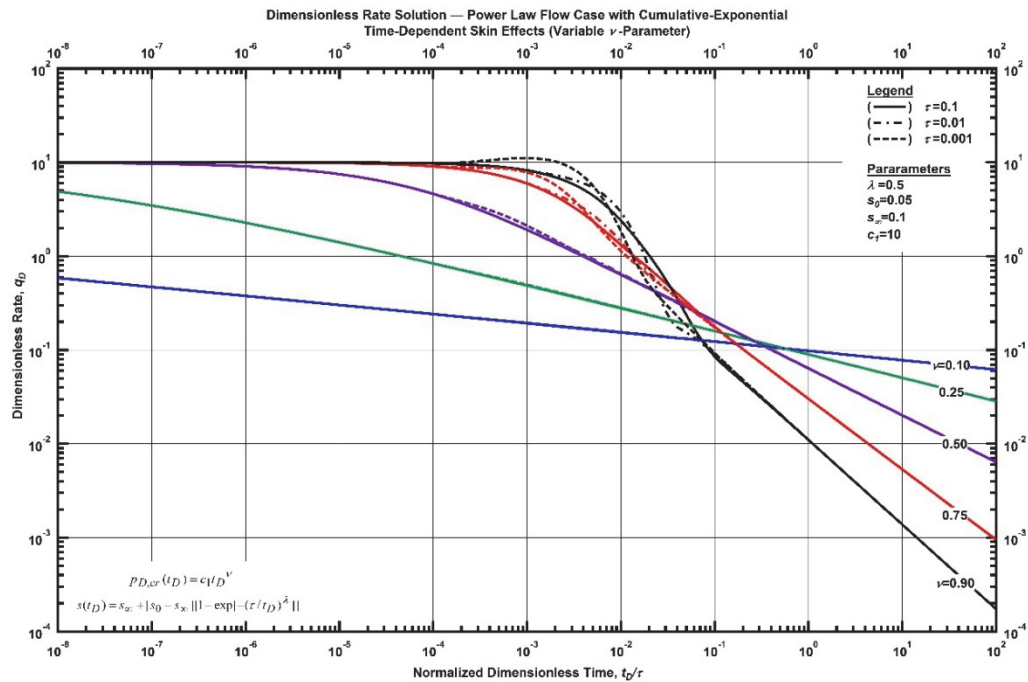


Figure F. 5 — Log-log plot (constant pressure dimensionless rate solution) for the power law flow model combined with the cumulative-exponential time-dependent skin effects for select values of  $\nu$ -parameter.

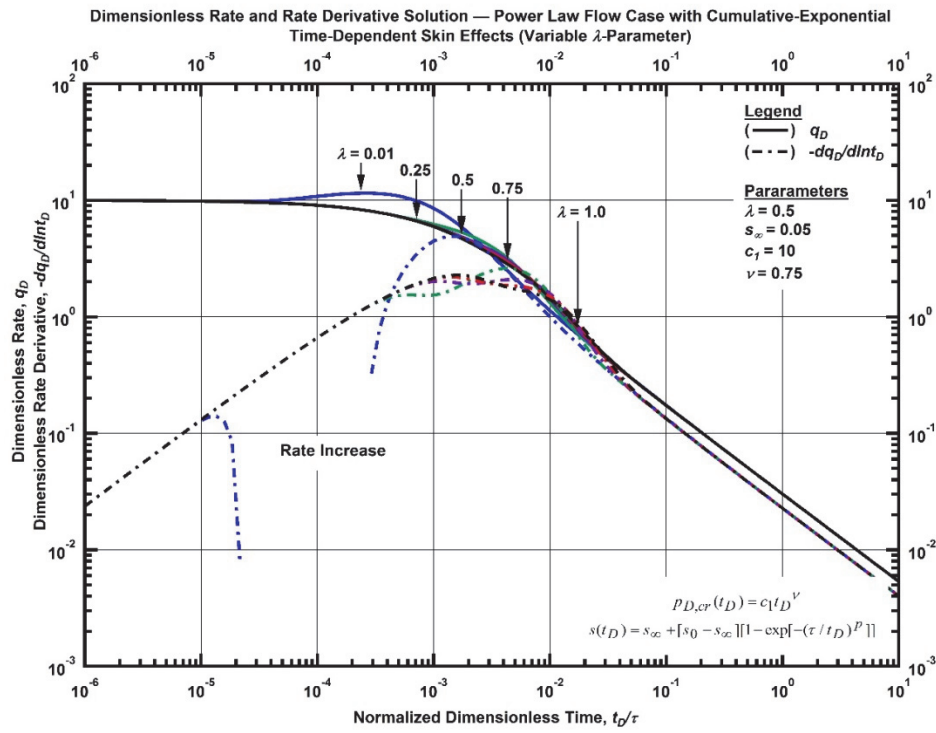


Figure F. 6 — Log-log plot (constant pressure dimensionless rate derivative solution) for the power-law flow model combined with the cumulative-exponential time-dependent skin effects for select values of  $\lambda$ -parameter.

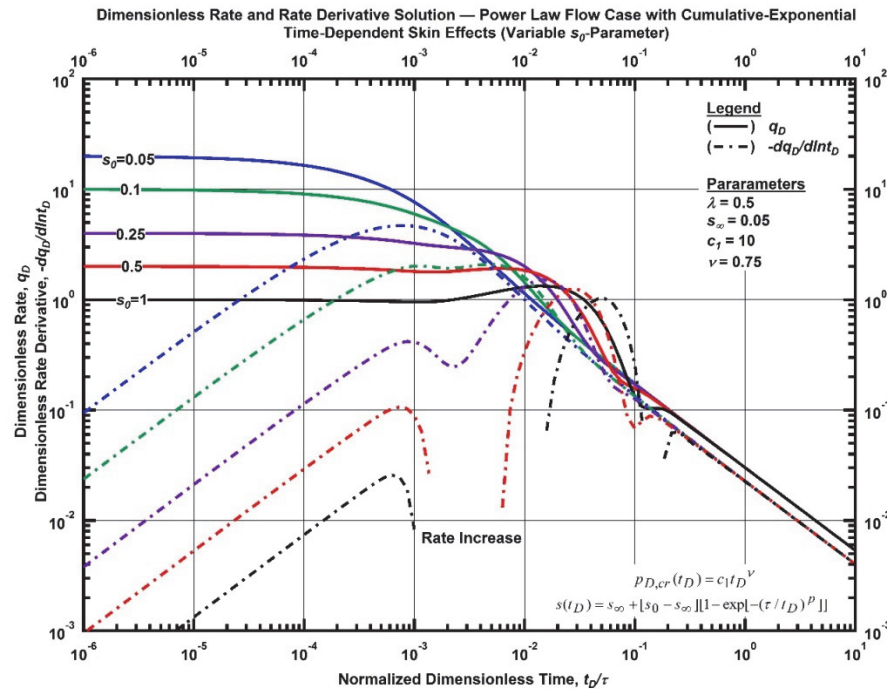


Figure F. 7 — Log-log plot (constant pressure dimensionless rate derivative solution) for the power law flow model combined with the cumulative-exponential time-dependent skin effects for select values of  $s_0$ -parameter.

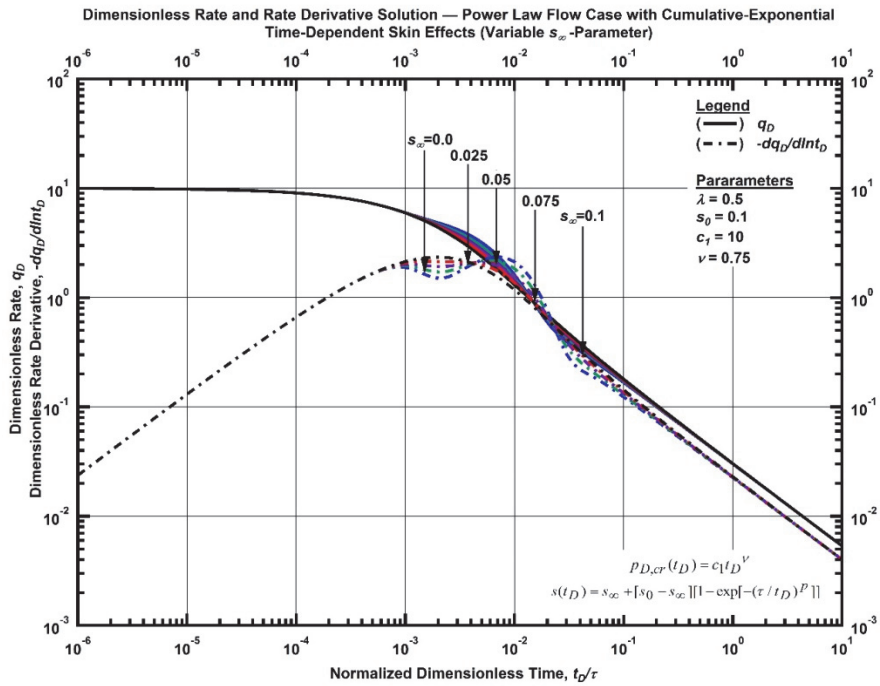


Figure F. 8 — Log-log plot (constant pressure dimensionless rate derivative solution) for the power law flow model combined with the cumulative-exponential time-dependent skin effects for select values of  $s_\infty$ -parameter.

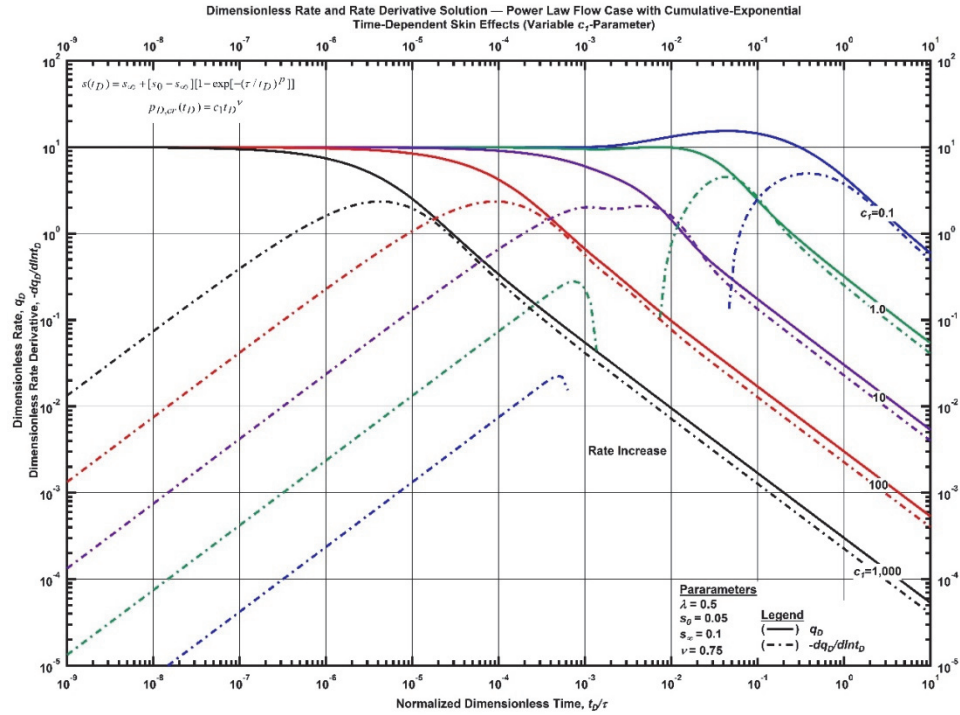


Figure F. 9 — Log-log plot (constant pressure dimensionless rate derivative solution) for the power law flow model combined with the cumulative-exponential time-dependent skin effects for select values of  $c_1$ -parameter.

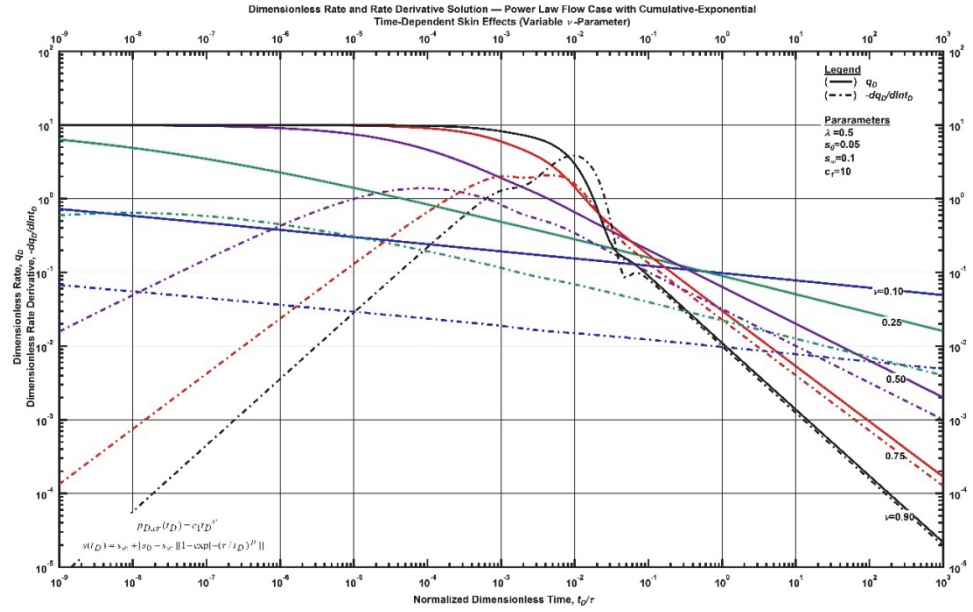


Figure F. 10—Log-log plot (constant pressure dimensionless rate derivative solution) for the power law flow model combined with the cumulative-exponential time-dependent skin effects for select values of  $\nu$ -parameter.

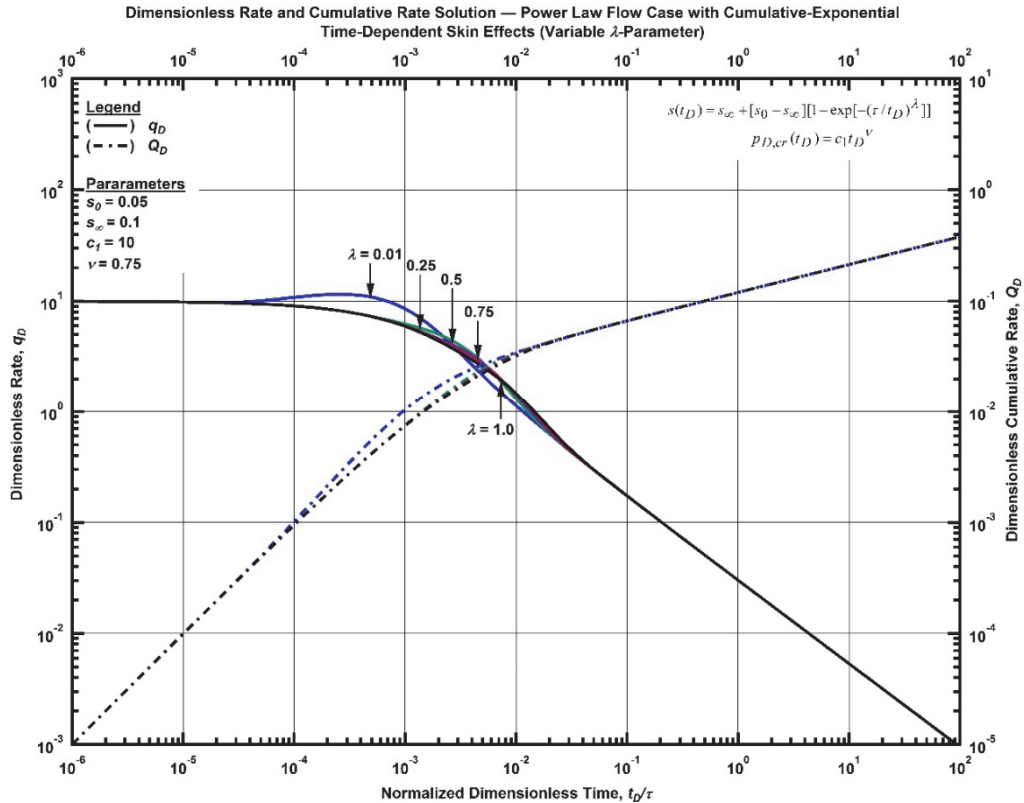


Figure F. 11—Log-log plot (constant pressure dimensionless cumulative production solution) for the power-law flow model combined with the cumulative-exponential time-dependent skin effects for select values of  $\lambda$ -parameter.

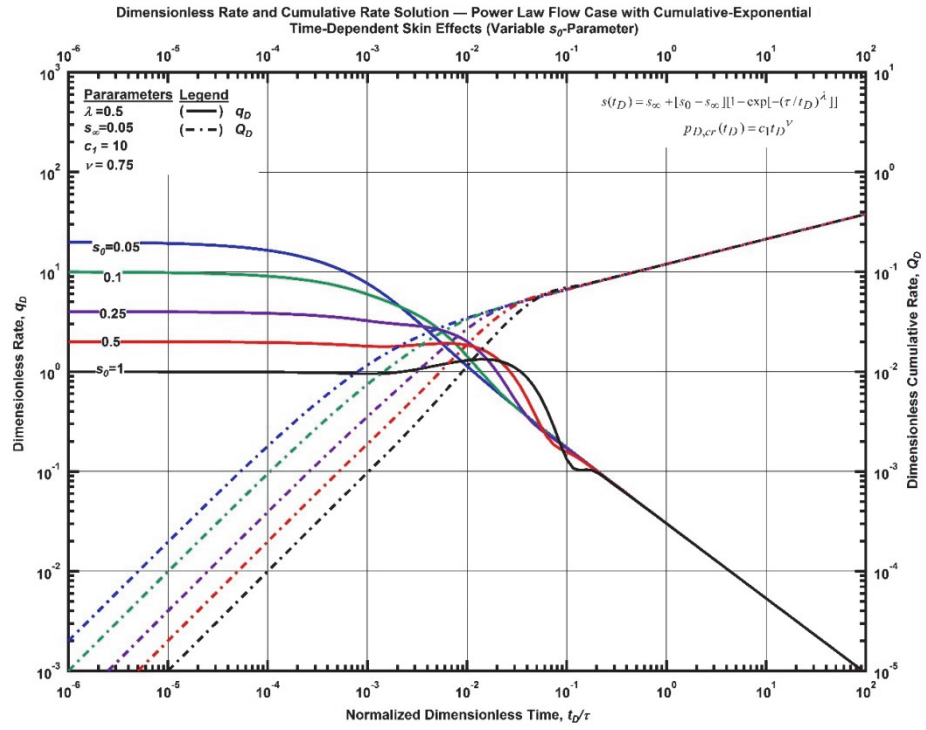


Figure F. 12—Log-log plot (constant pressure dimensionless cumulative production solution) for the power law flow model combined with the cumulative-exponential time-dependent skin effects for select values of  $s_0$ -parameter.

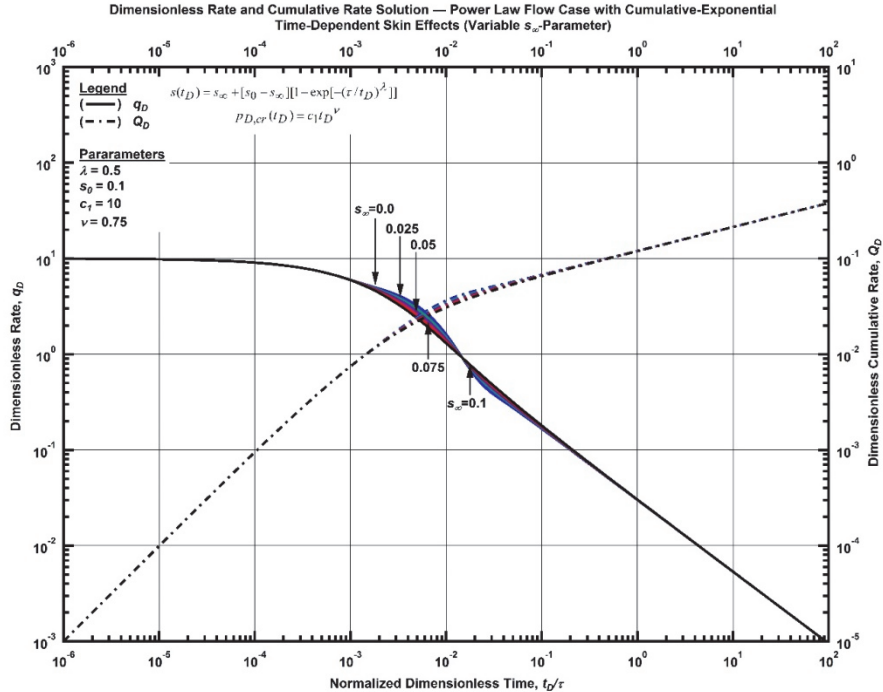


Figure F. 13—Log-log plot (constant pressure dimensionless cumulative production solution) for the power law flow model combined with the cumulative-exponential time-dependent skin effects for select values of  $s_\infty$ -parameter.

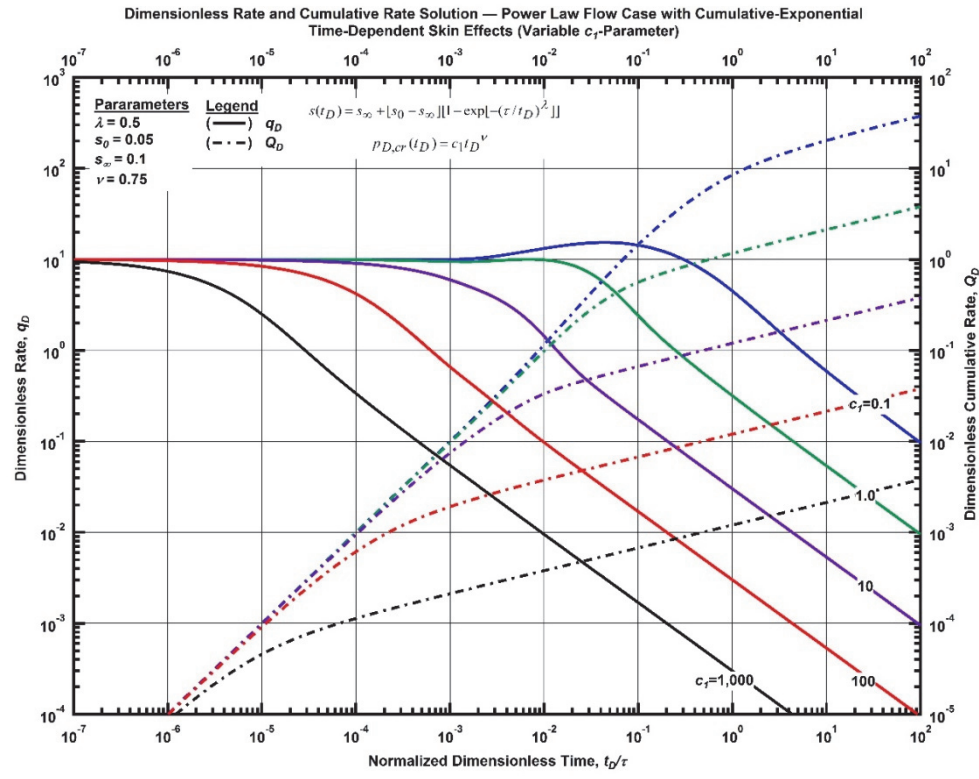


Figure F. 14—Log-log plot (constant pressure dimensionless cumulative production solution) for the power law flow model combined with the cumulative-exponential time-dependent skin effects for select values of  $c_1$ -parameter.

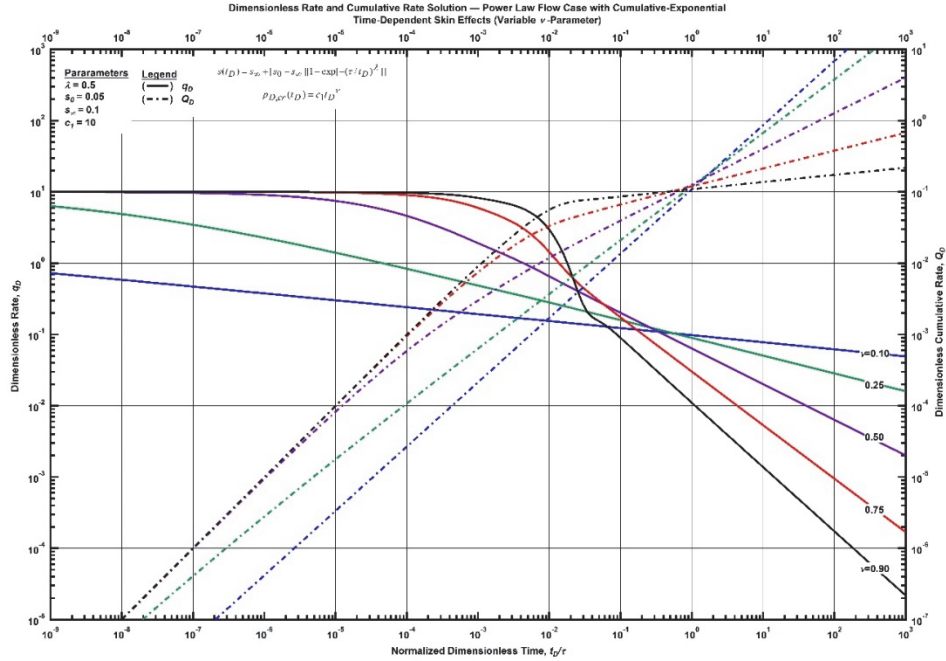


Figure F. 15—Log-log plot (constant pressure dimensionless cumulative production solution) for the power law flow model combined with the cumulative-exponential time-dependent skin effects for select values of  $v$ -parameter.

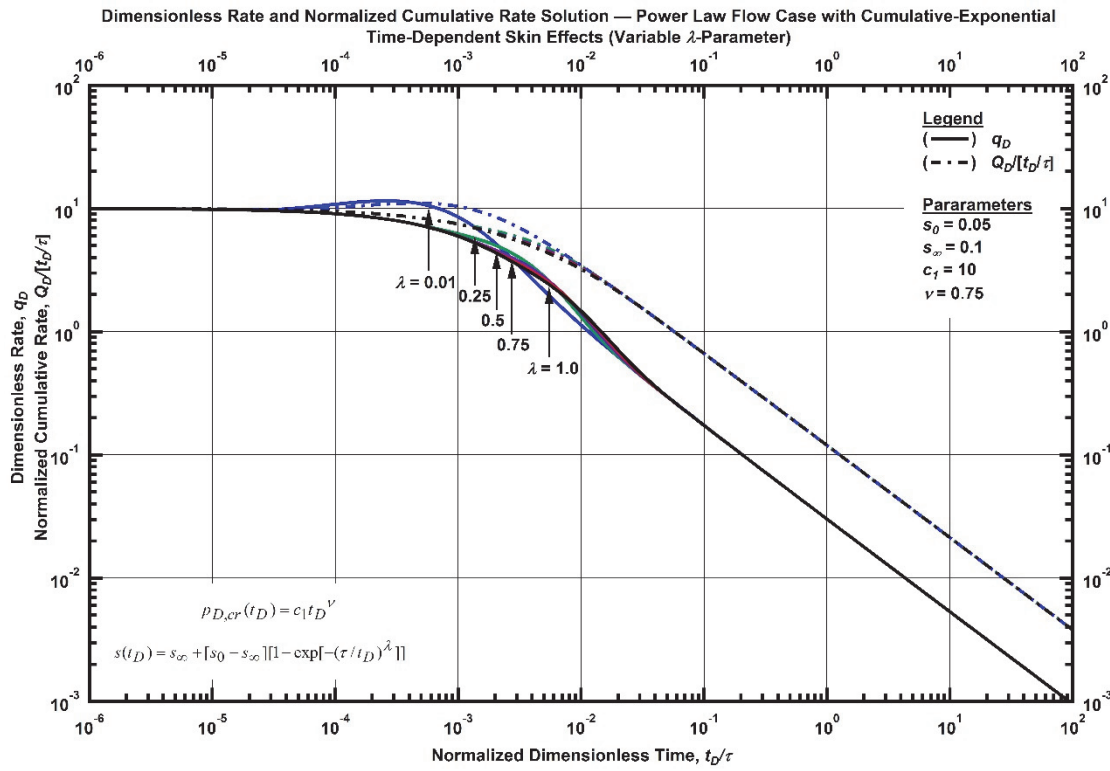


Figure F. 16—Log-log plot (constant pressure time-normalized dimensionless cumulative rate solution) for the power-law flow model combined with the cumulative-exponential time-dependent skin effects for select values of  $\lambda$ -parameter.

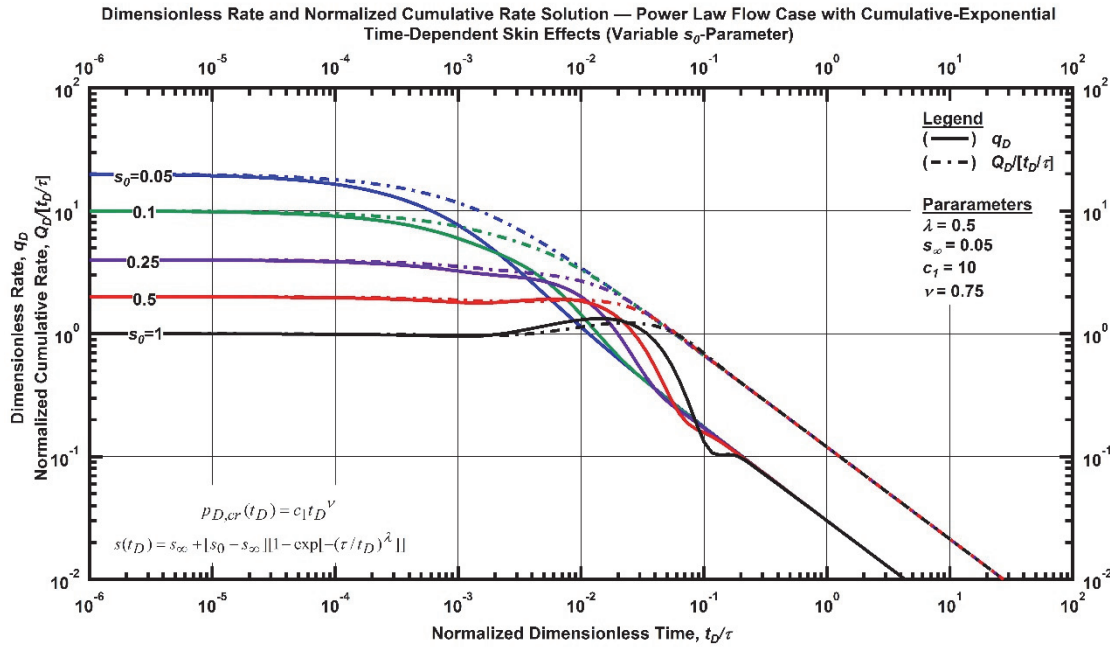


Figure F. 17—Log-log plot (constant pressure time-normalized dimensionless cumulative rate solution) for the power law flow model combined with the cumulative-exponential time-dependent skin effects for select values of  $s_0$ -parameter.

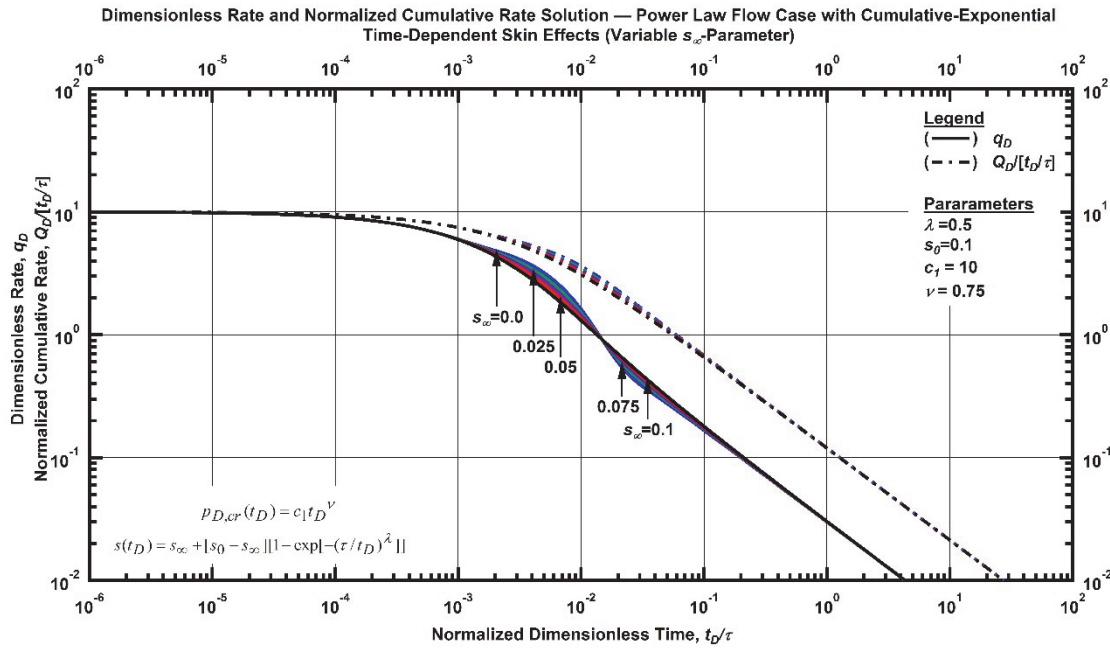


Figure F. 18—Log-log plot (constant pressure time-normalized dimensionless cumulative rate solution) for the power law flow model combined with the cumulative-exponential time-dependent skin effects for select values of  $s_\infty$ -parameter.

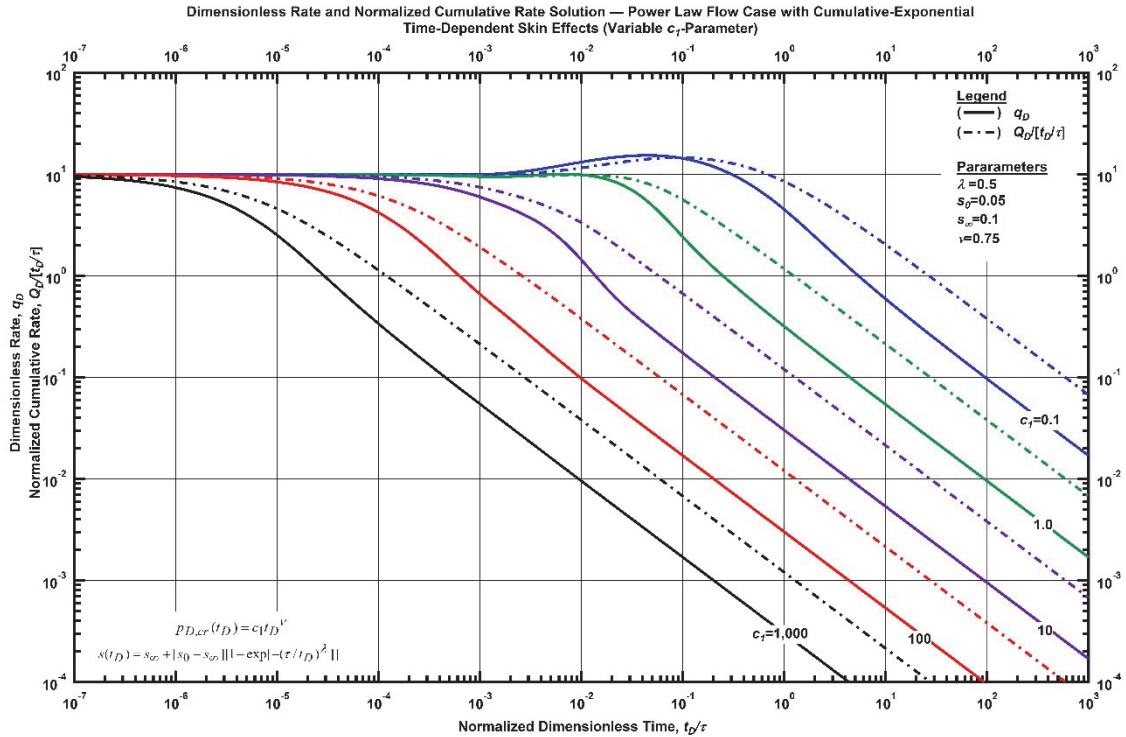


Figure F. 19—Log-log plot (constant pressure time-normalized dimensionless cumulative rate solution) for the power law flow model combined with the cumulative-exponential time-dependent skin effects for select values of  $c_1$ -parameter.

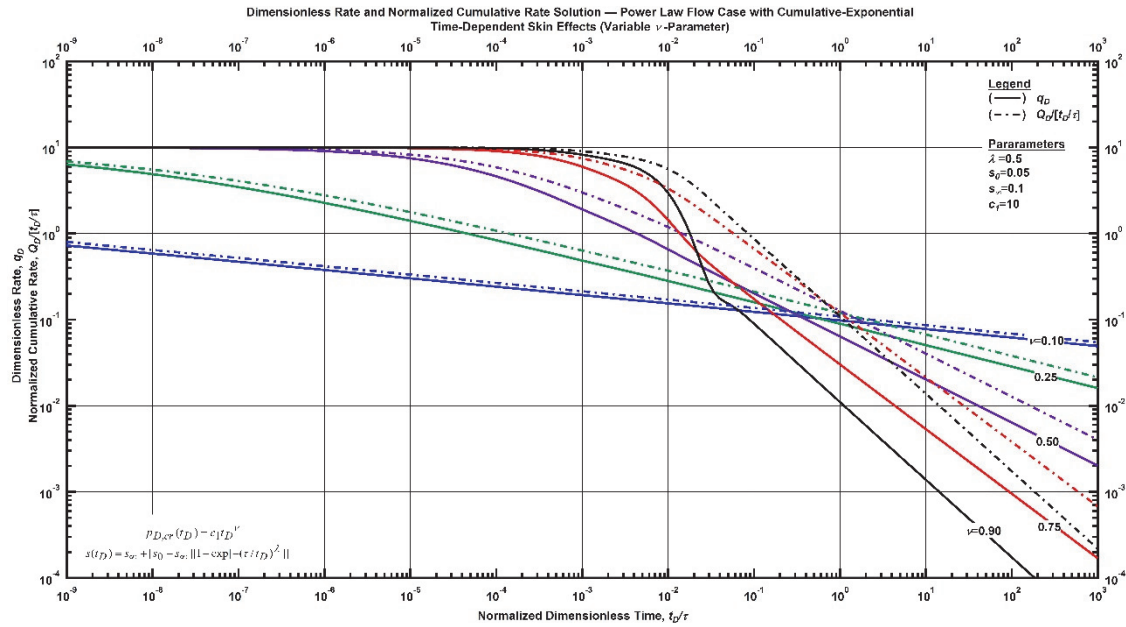


Figure F. 20—Log-log plot (constant pressure dimensionless rate solution) for the power law flow model combined with the cumulative-exponential time-dependent skin effects for select values of  $\nu$ -parameter.

*Power-Law Flow Relation with Exponential Time-Dependent Skin*

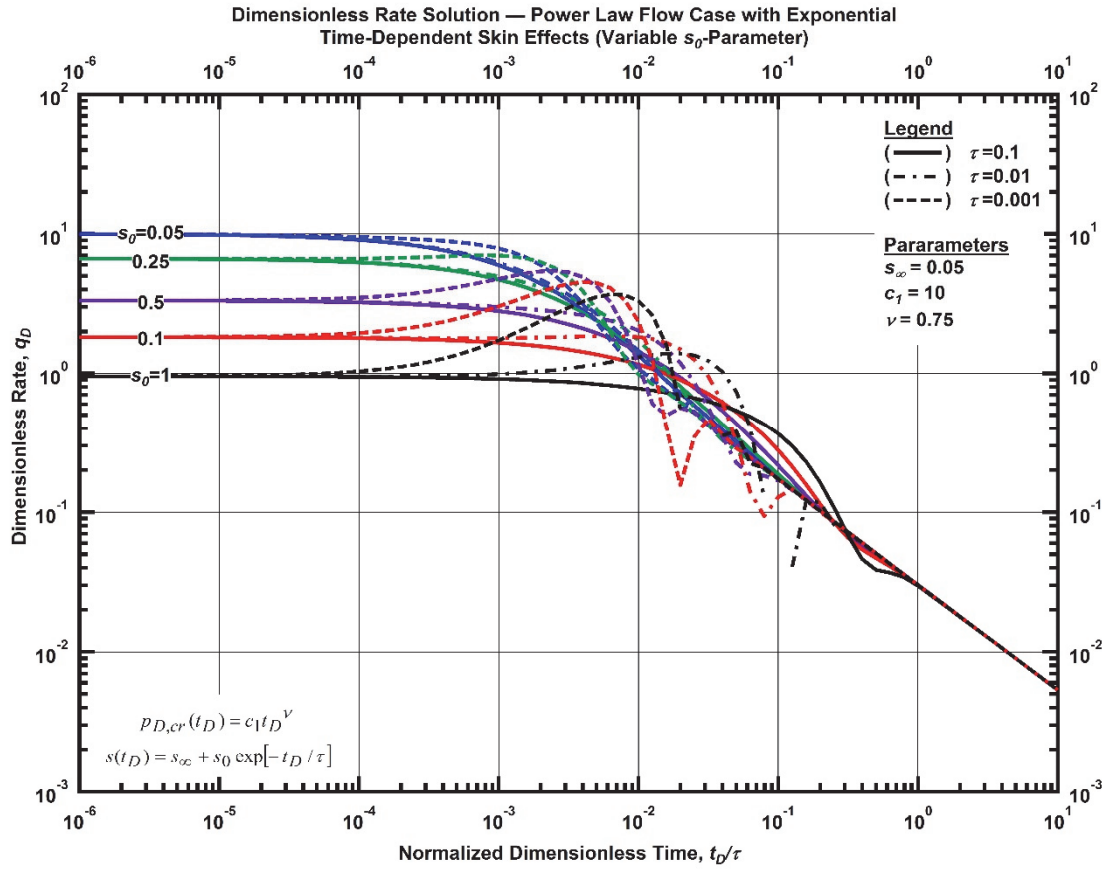


Figure F. 21—Log-log plot (constant pressure dimensionless rate solution) for the power law flow model combined with the exponential time-dependent skin effects for select values of  $s_0$ -parameter.

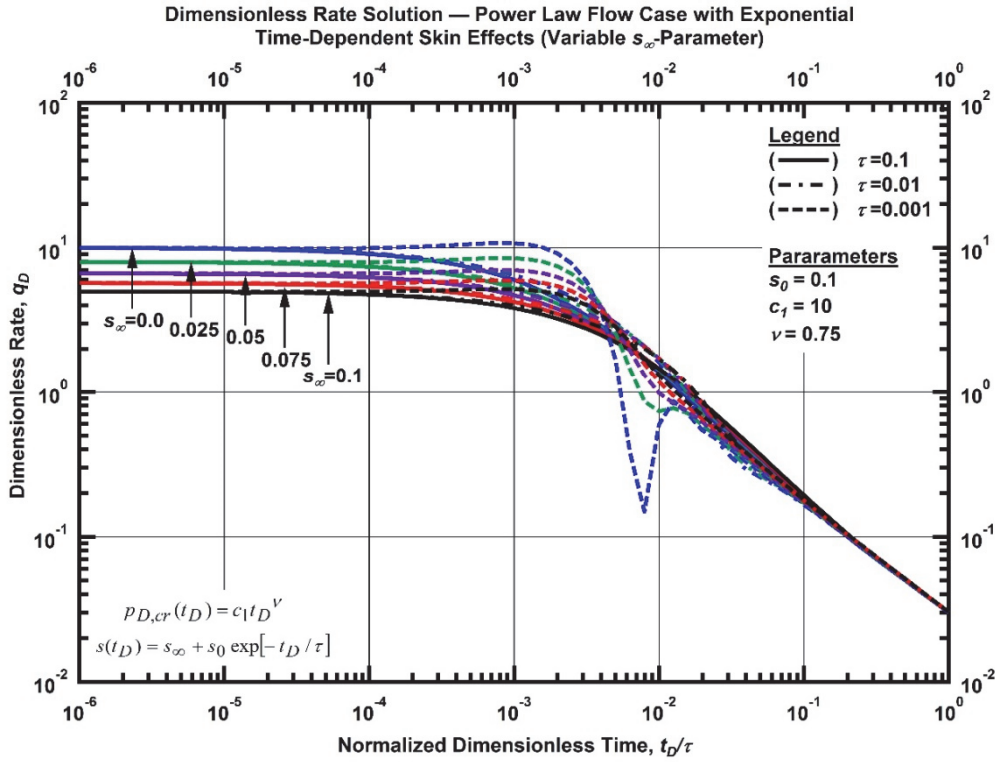


Figure F. 22—Log-log plot (constant pressure dimensionless rate solution) for the power law flow model combined with the exponential time-dependent skin effects for select values of  $s_\infty$ -parameter.

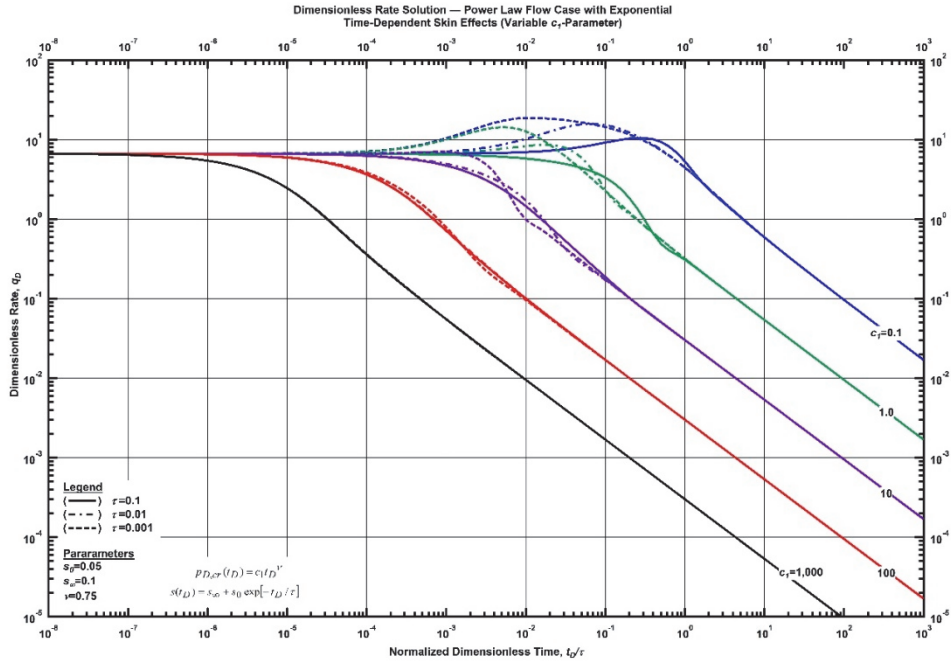


Figure F. 23—Log-log plot (constant pressure dimensionless rate solution) for the power law flow model combined with the exponential time-dependent skin effects for select values of  $c_1$ -parameter.

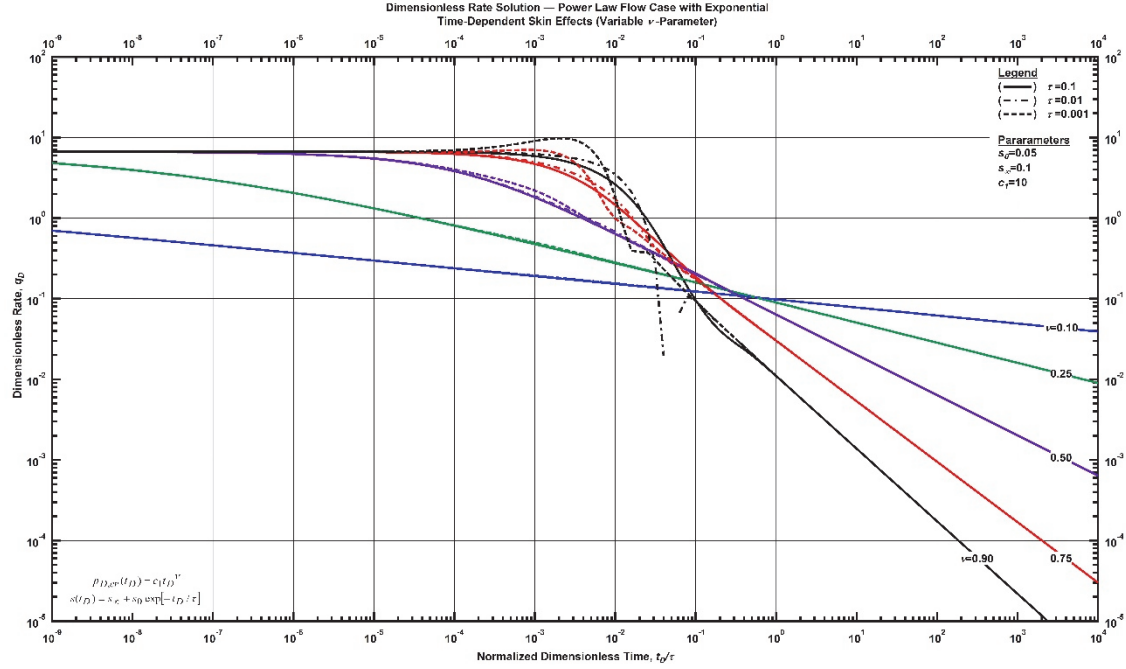


Figure F. 24—Log-log plot (constant pressure dimensionless rate solution) for the power law flow model combined with the exponential time-dependent skin effects for select values of  $\nu$ -parameter.

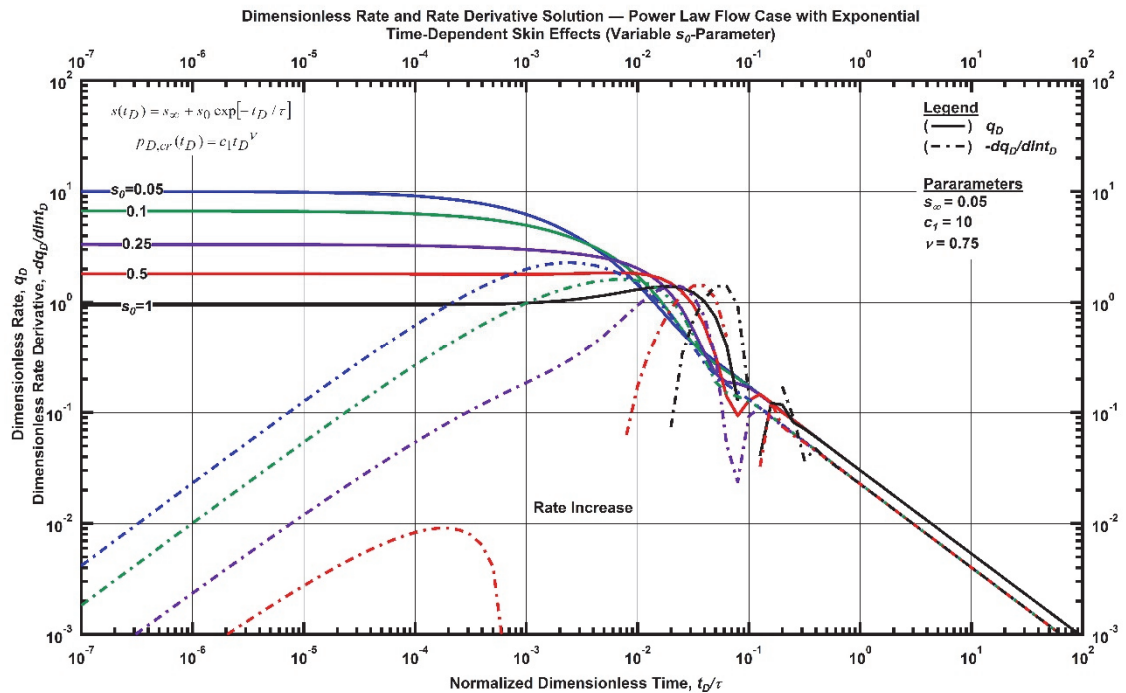


Figure F. 25—Log-log plot (constant pressure dimensionless rate derivative solution) for the power law flow model combined with the exponential time-dependent skin effects for select values of  $s_0$ -parameter.

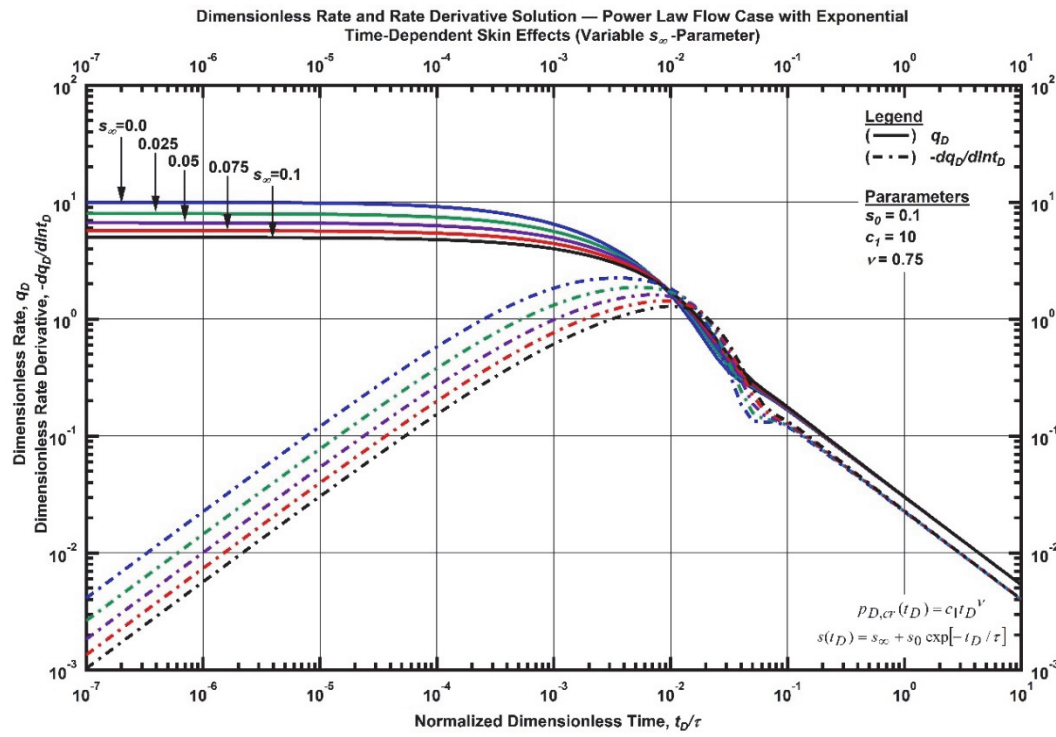


Figure F. 26—Log-log plot (constant pressure dimensionless rate derivative solution) for the power law flow model combined with the exponential time-dependent skin effects for select values of  $s_\infty$ -parameter.

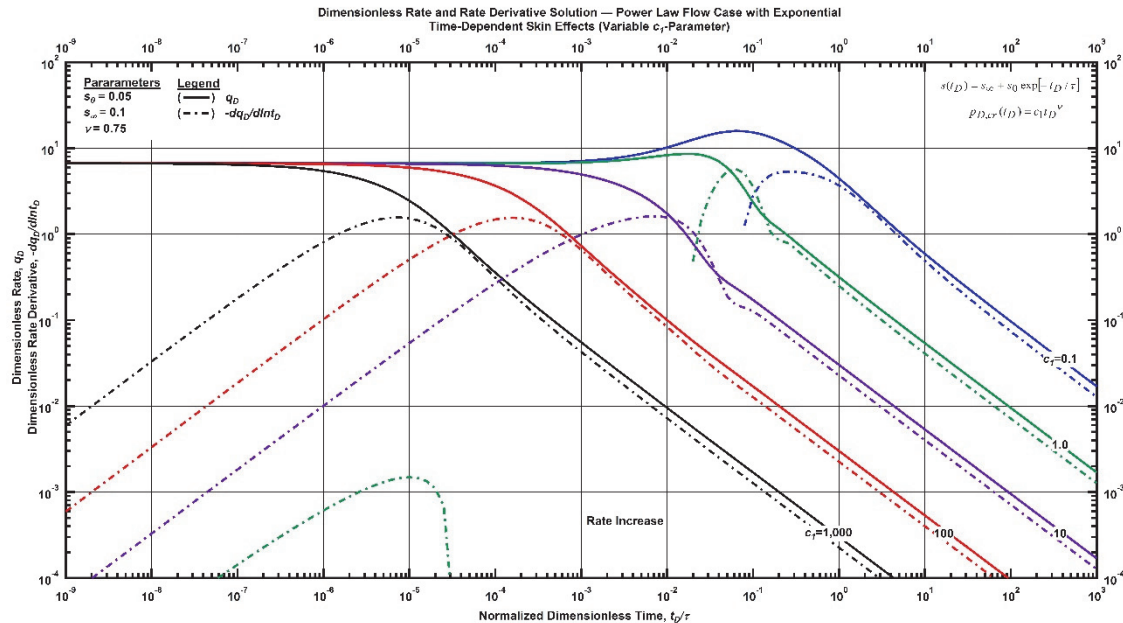


Figure F. 27—Log-log plot (constant pressure dimensionless rate derivative solution) for the power law flow model combined with the exponential time-dependent skin effects for select values of  $c_1$ -parameter.

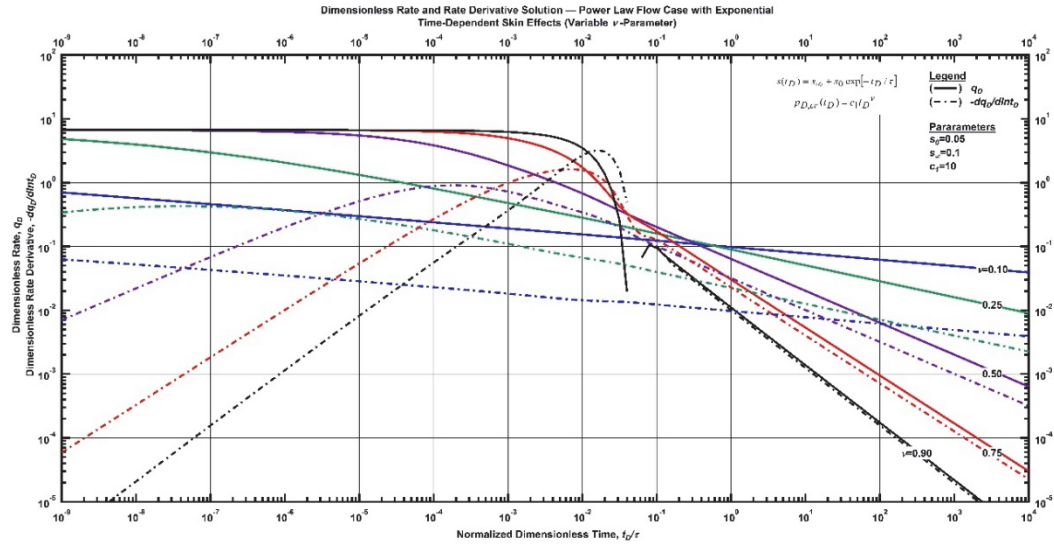


Figure F. 28—Log-log plot (constant pressure dimensionless rate derivative solution) for the power law flow model combined with the exponential time-dependent skin effects for select values of  $\nu$ -parameter.

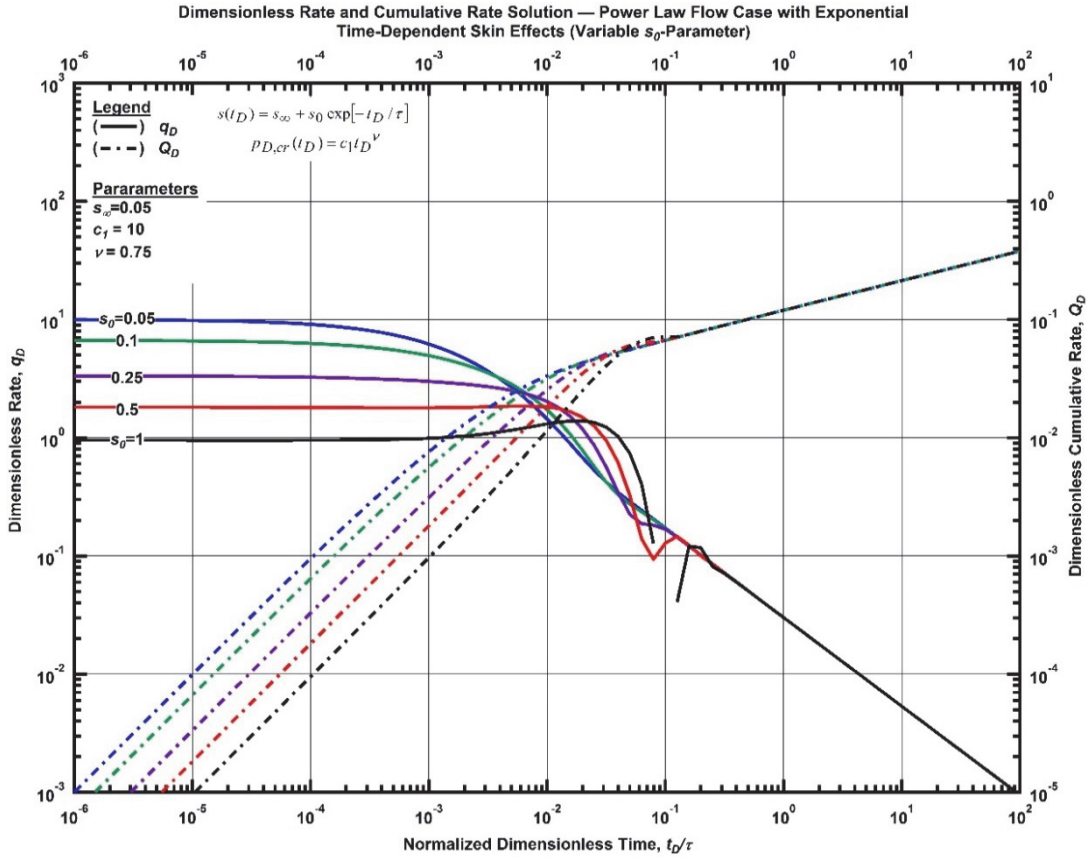


Figure F. 29—Log-log plot (constant pressure dimensionless cumulative production solution) for the power law flow model combined with the exponential time-dependent skin effects for select values of  $s_0$ -parameter.

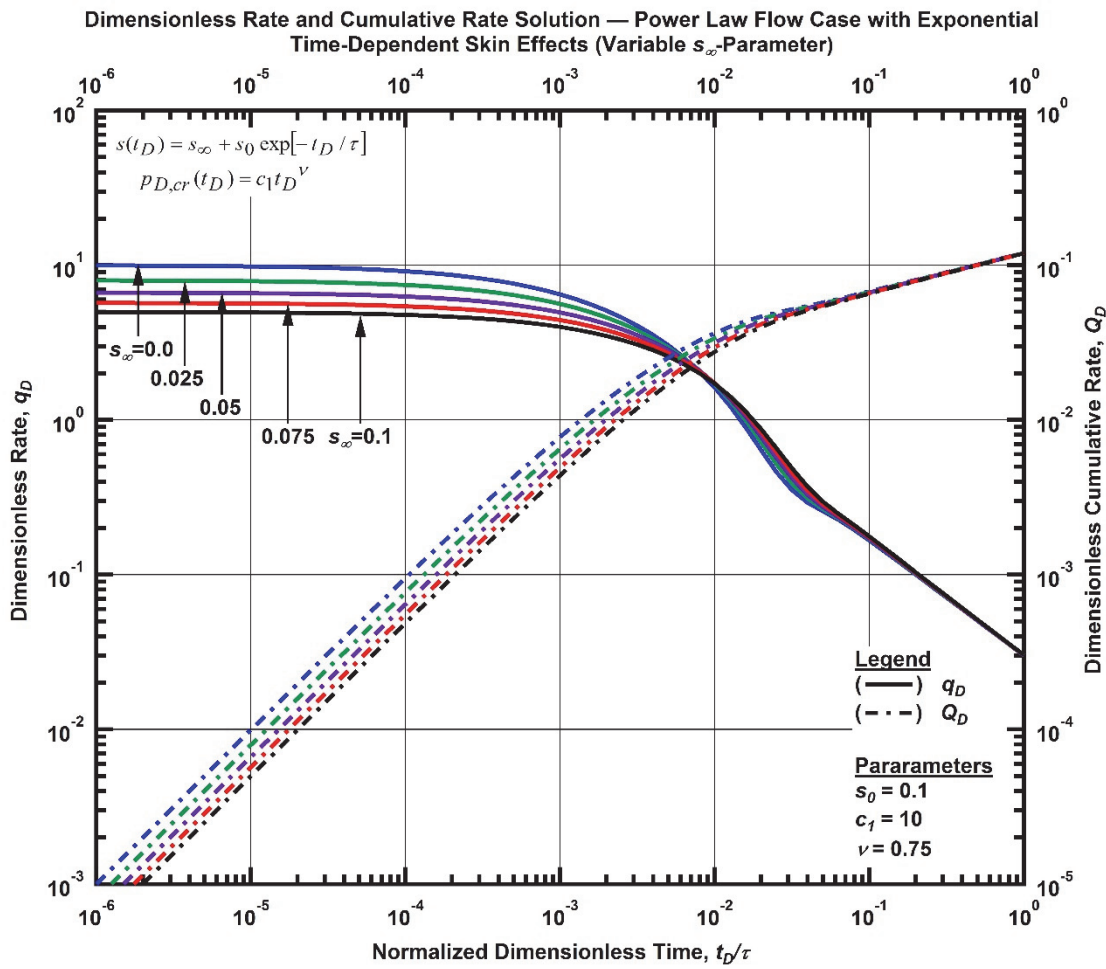


Figure F. 30—Log-log plot (constant pressure dimensionless cumulative production solution) for the power law flow model combined with the exponential time-dependent skin effects for select values of  $s_\infty$ -parameter.

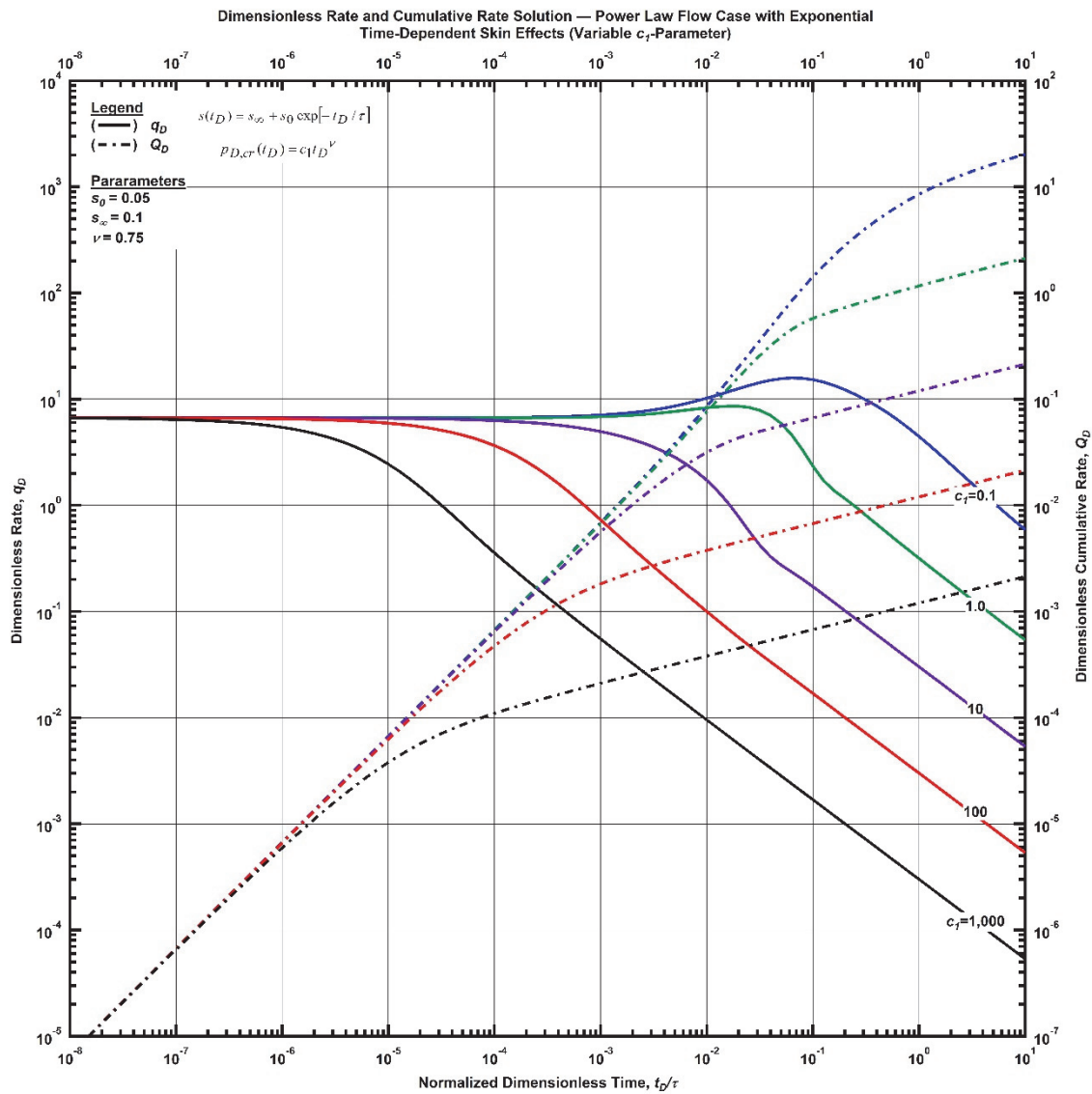


Figure F. 31—Log-log plot (constant pressure dimensionless cumulative production solution) for the power law flow model combined with the exponential time-dependent skin effects for select values of  $c_1$ -parameter.

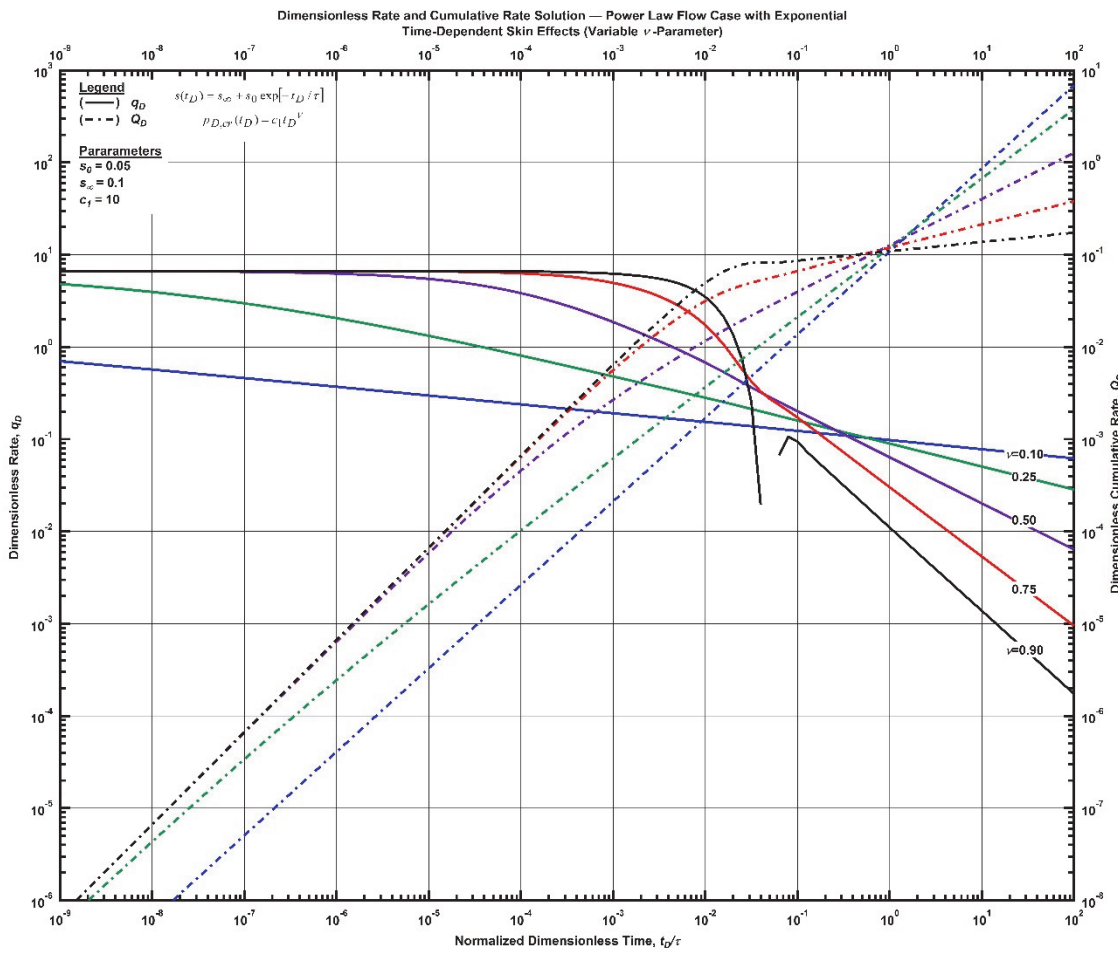


Figure F. 32—Log-log plot (constant pressure dimensionless cumulative production solution) for the power law flow model combined with the exponential time-dependent skin effects for select values of  $\nu$ -parameter.

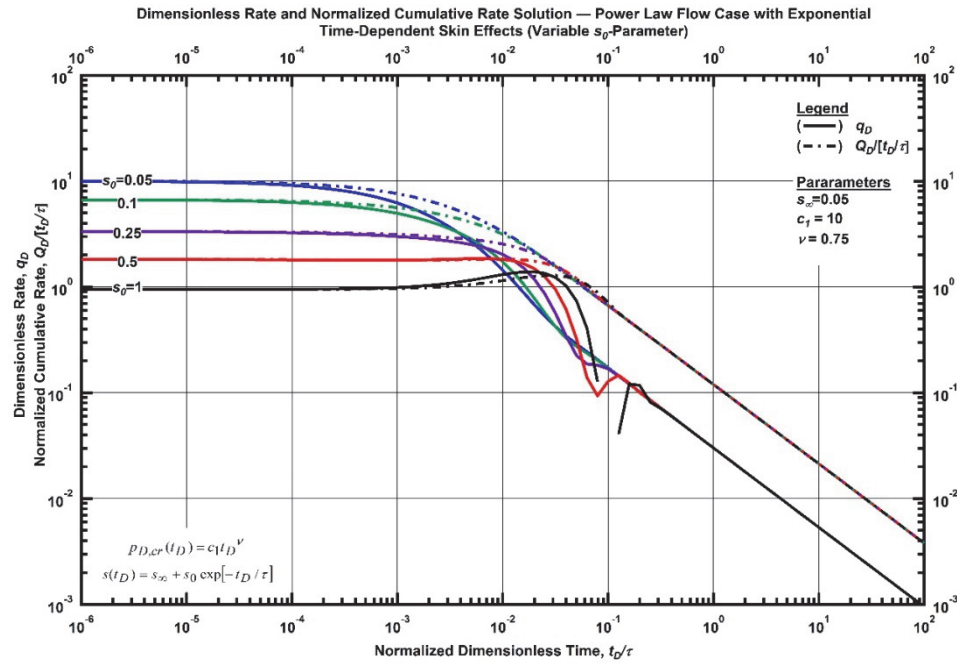


Figure F. 33—Log-log plot (constant pressure time-normalized dimensionless cumulative rate solution) for the power law flow model combined with the exponential time-dependent skin effects for select values of  $s_0$ -parameter.

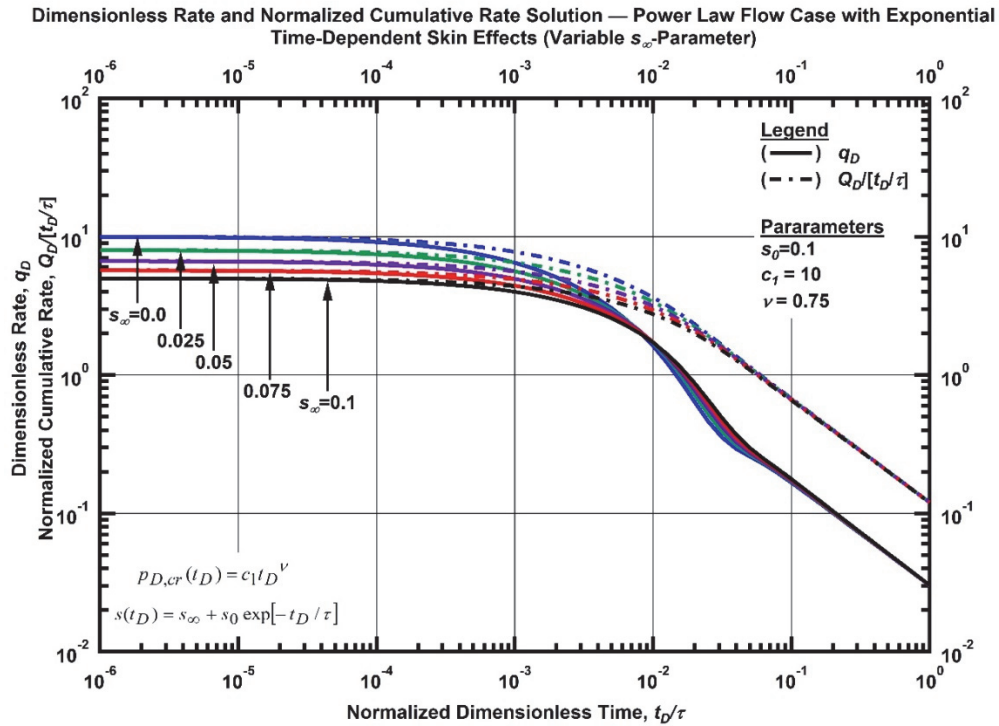


Figure F. 34—Log-log plot (constant pressure time-normalized dimensionless cumulative rate solution) for the power law flow model combined with the exponential time-dependent skin effects for select values of  $s_\infty$ -parameter.

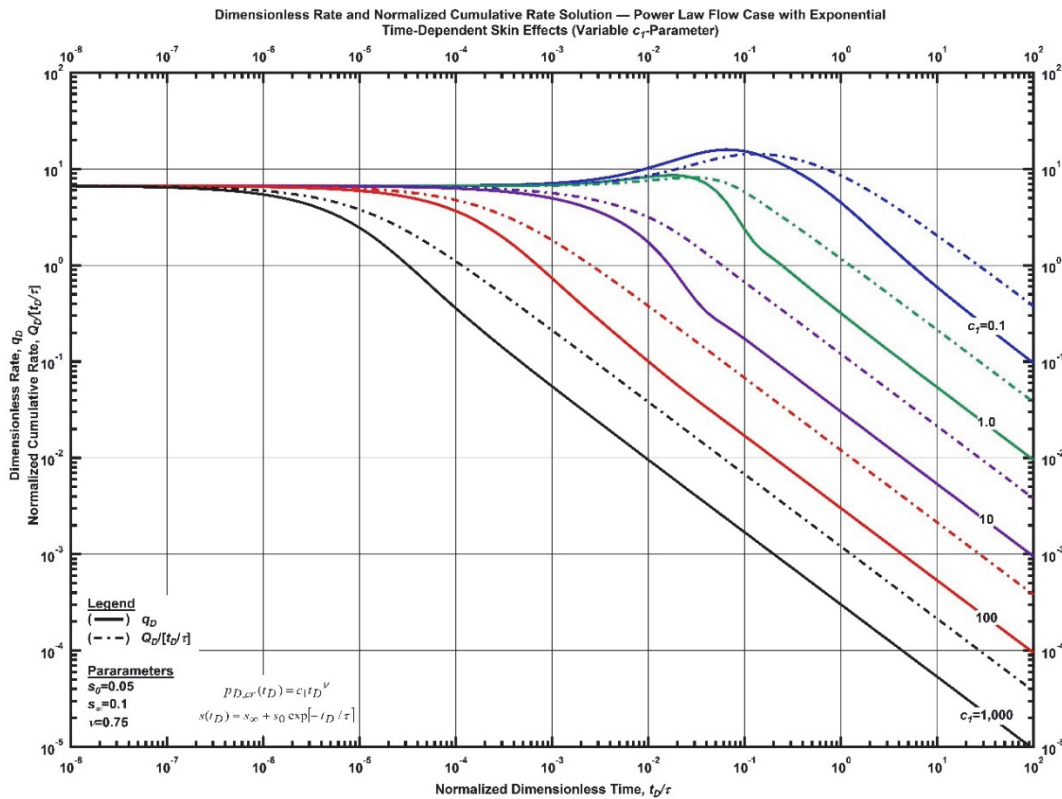


Figure F. 35—Log-log plot (constant pressure time-normalized dimensionless cumulative rate solution) for the power law flow model combined with the exponential time-dependent skin effects for select values of  $c_1$ -parameter.

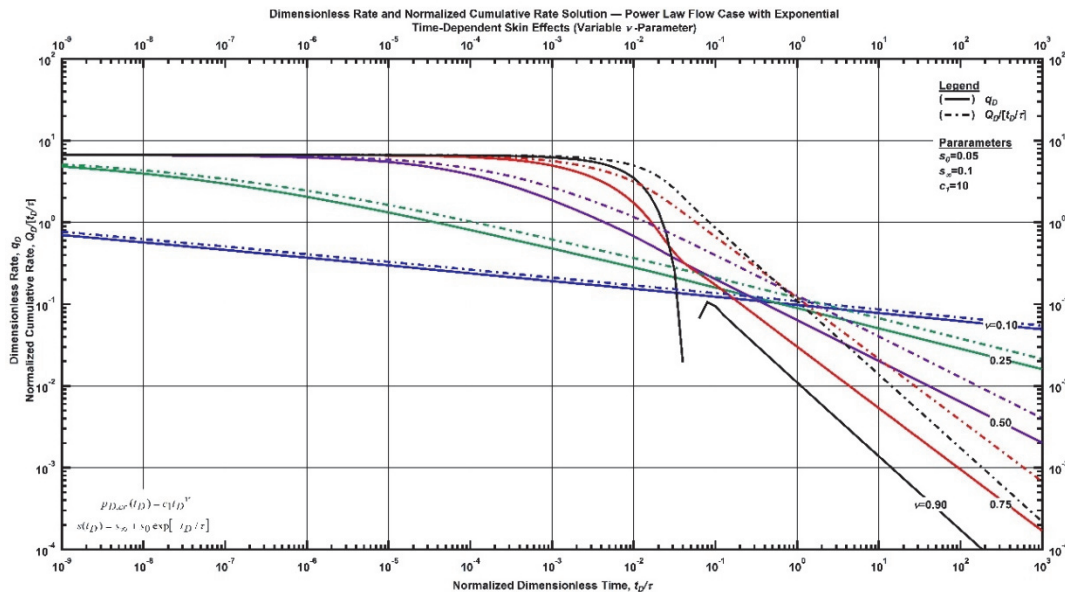


Figure F. 36—Log-log plot (constant pressure time-normalized dimensionless cumulative rate solution) for the power law flow model combined with the exponential time-dependent skin effects for select values of  $v$ -parameter.

### Power-Law Flow Relation with Hyperbolic Time-Dependent Skin

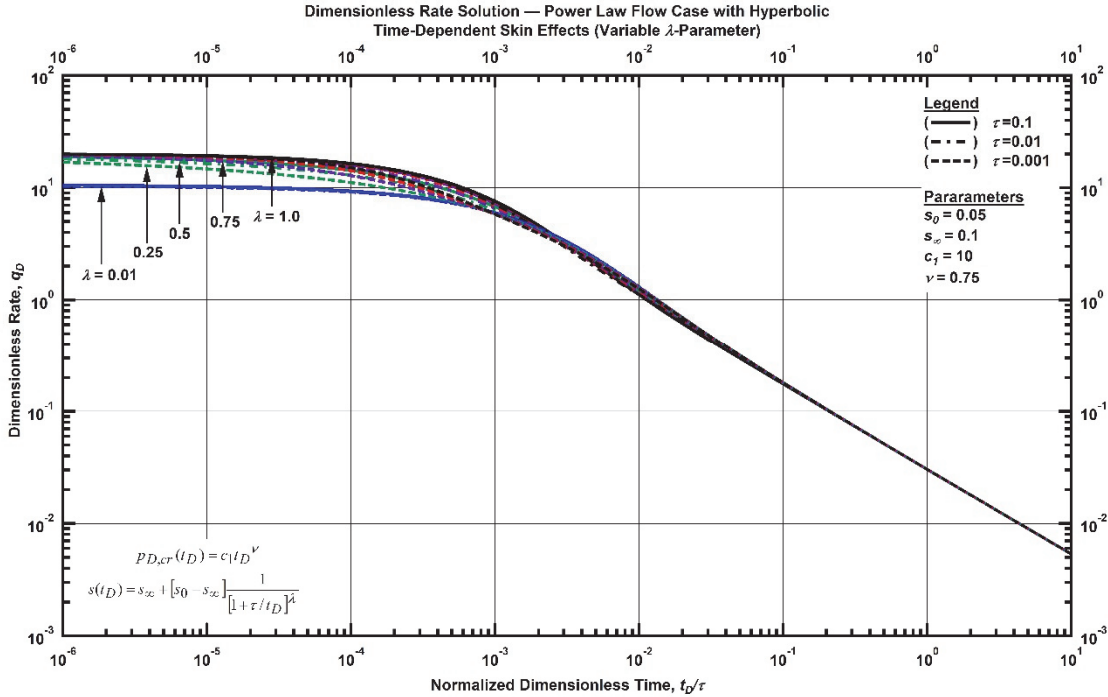


Figure F. 37—Log-log plot (constant pressure dimensionless rate solution) for the power law flow model combined with the hyperbolic time-dependent skin effects for select values of  $\lambda$ -parameter.

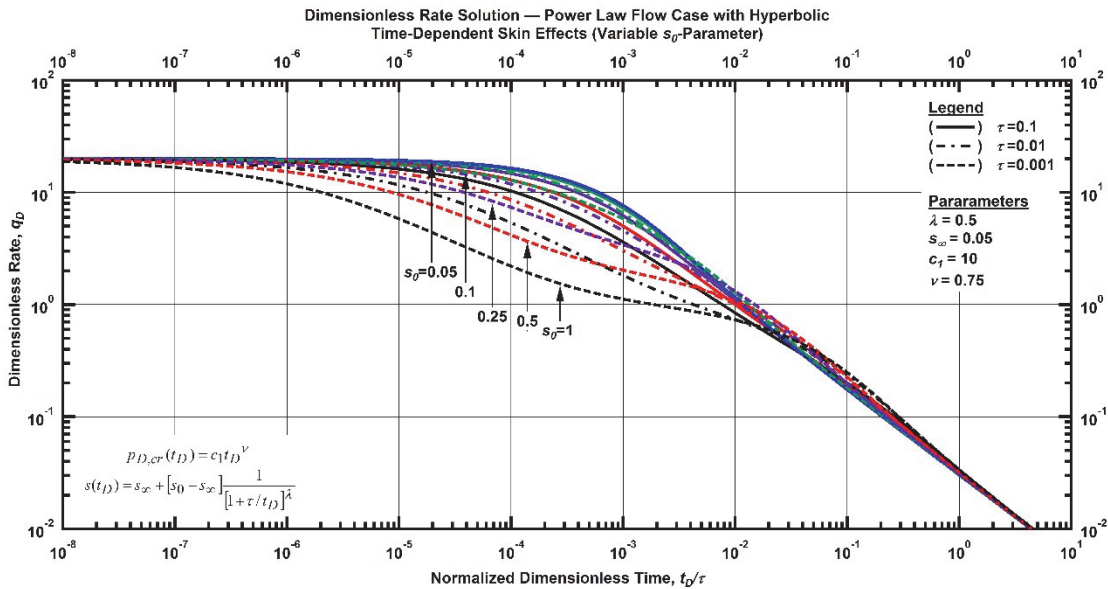


Figure F. 38—Log-log plot (constant pressure dimensionless rate solution) for the power law flow model combined with the hyperbolic time-dependent skin effects for select values of  $s_0$ -parameter.

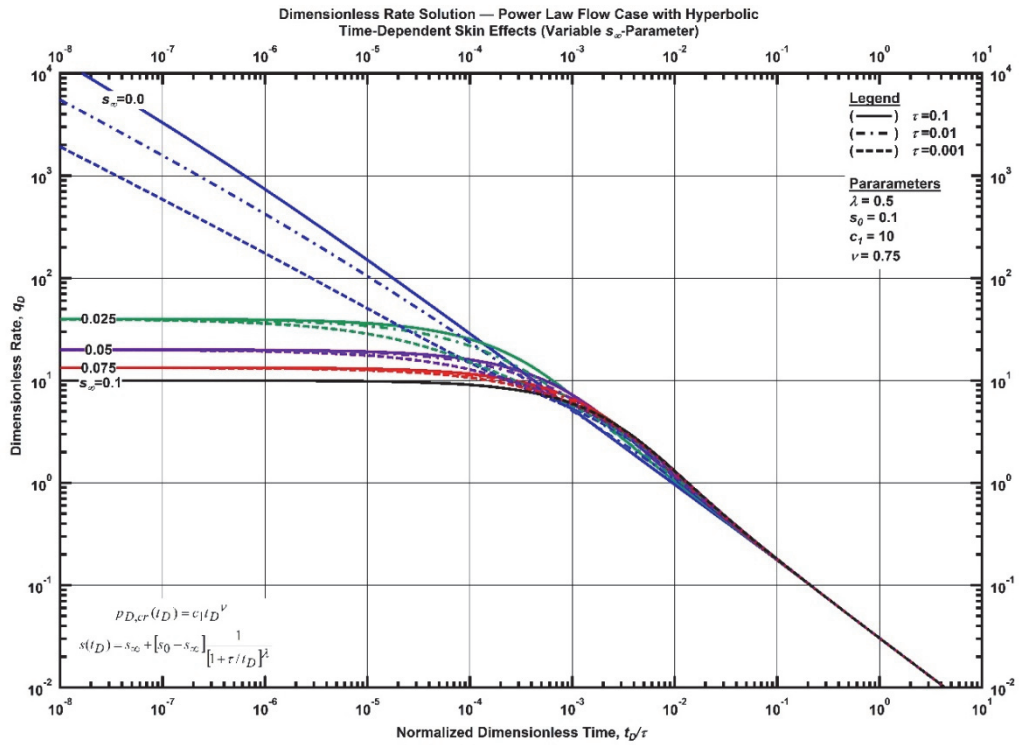


Figure F. 39—Log-log plot (constant pressure dimensionless rate solution) for the power law flow model combined with the hyperbolic time-dependent skin effects for select values of  $s_\infty$ -parameter.

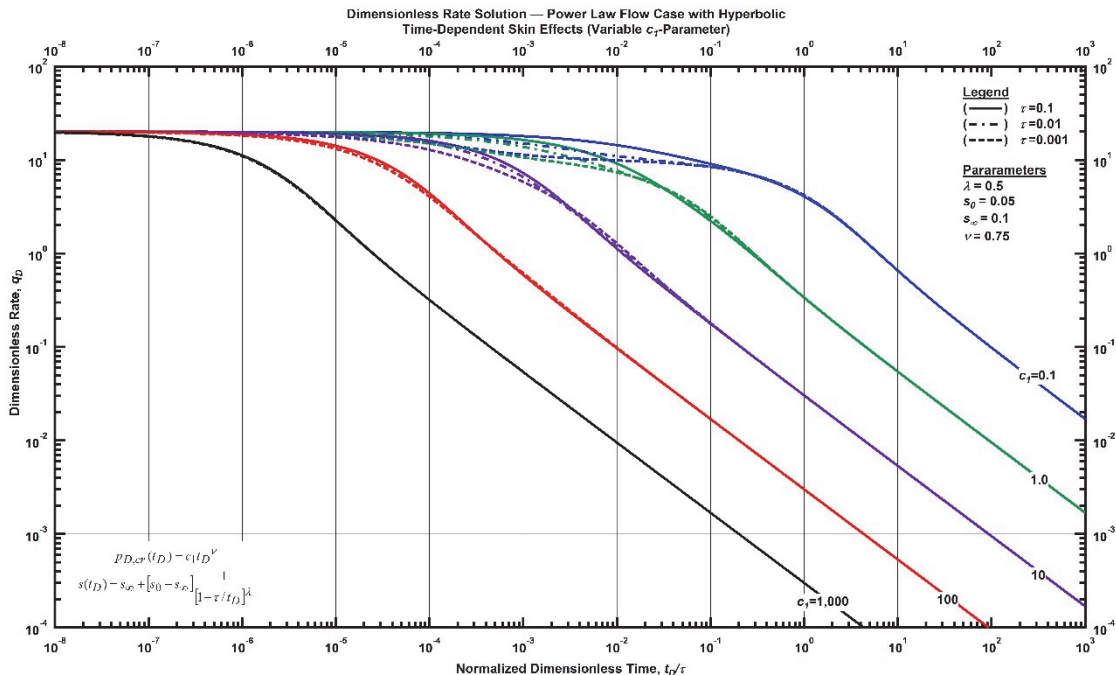


Figure F. 40—Log-log plot (constant pressure dimensionless rate solution) for the power law flow model combined with the hyperbolic time-dependent skin effects for select values of  $c_1$ -parameter.

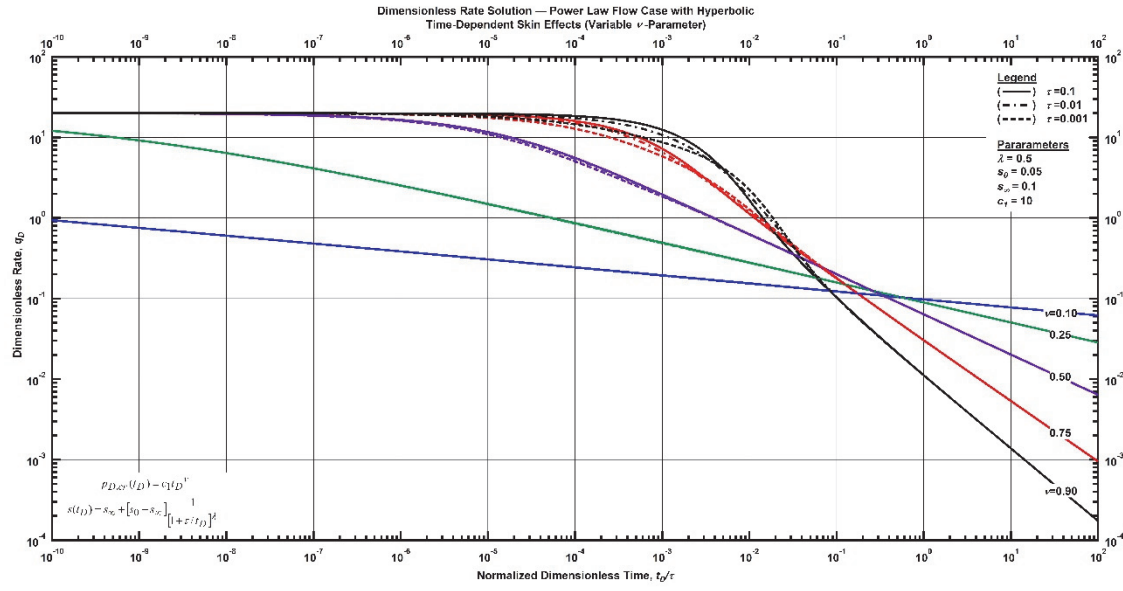


Figure F. 41—Log-log plot (constant pressure dimensionless rate solution) for the power law flow model combined with the hyperbolic time-dependent skin effects for select values of  $\nu$ -parameter.

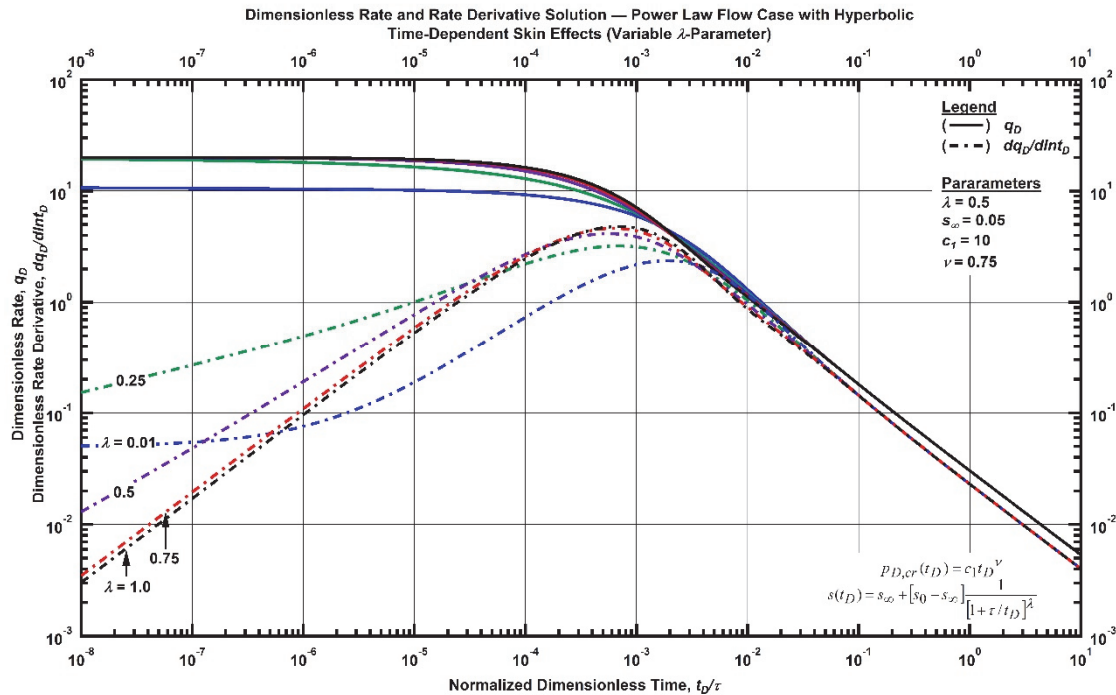


Figure F. 42—Log-log plot (constant pressure dimensionless derivative rate solution) for the power law flow model combined with the hyperbolic time-dependent skin effects for select values of  $\lambda$ -parameter.

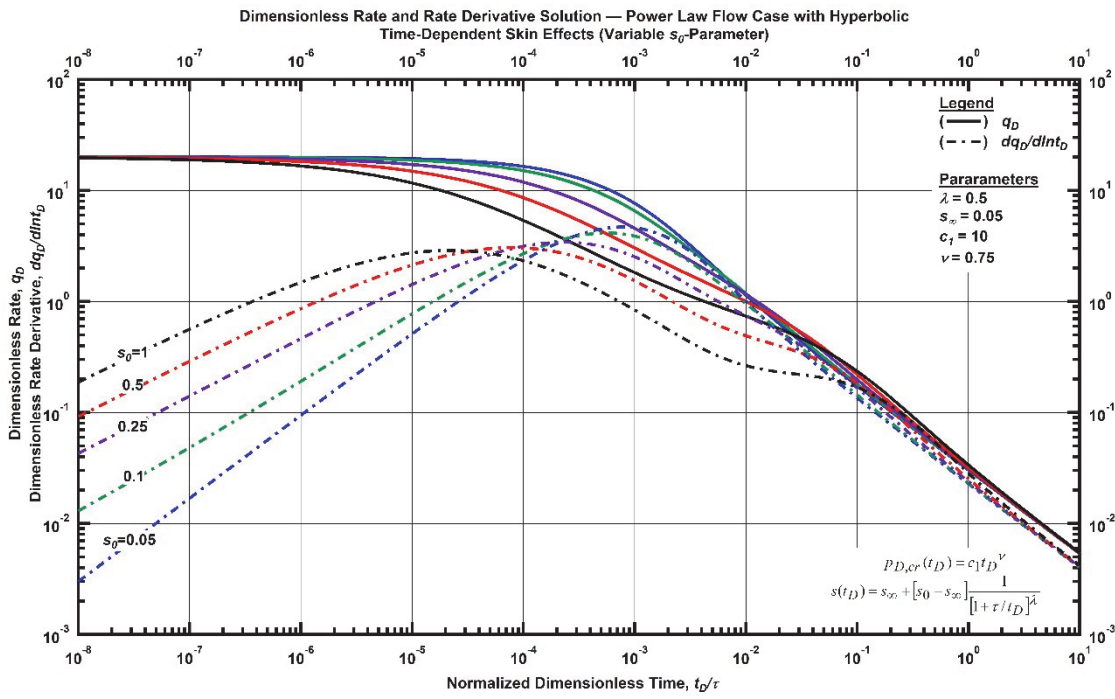


Figure F. 43—Log-log plot (constant pressure dimensionless derivative rate solution) for the power law flow model combined with the hyperbolic time-dependent skin effects for select values of  $s_0$ -parameter.

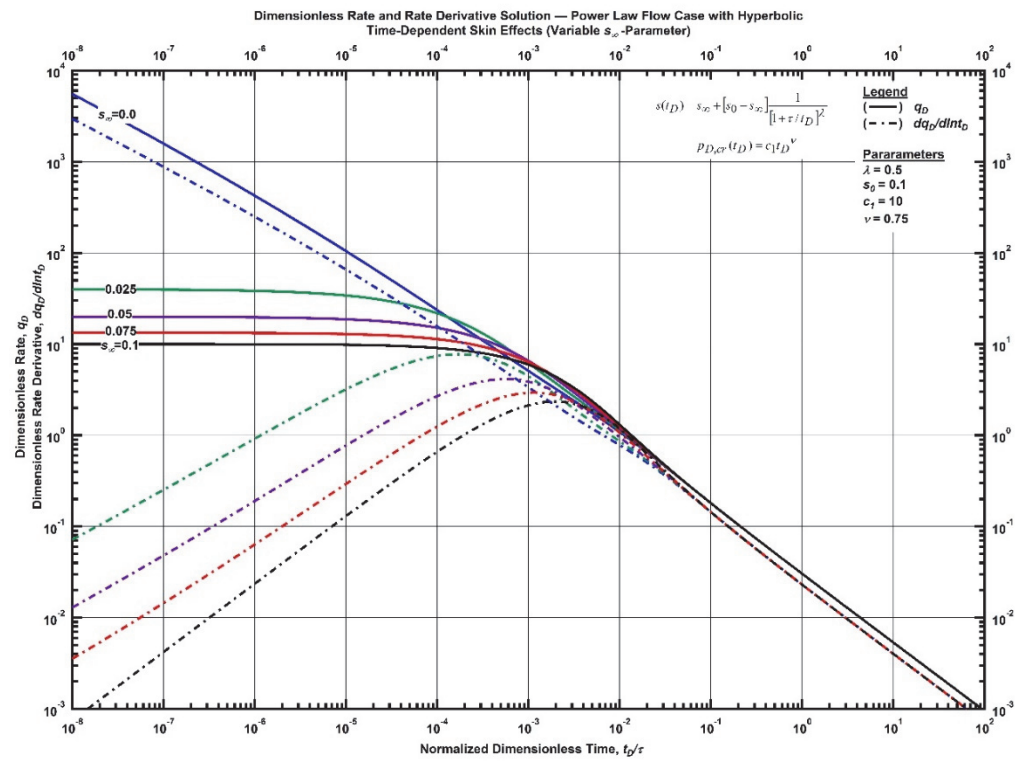


Figure F. 44—Log-log plot (constant pressure dimensionless derivative rate solution) for the power law flow model combined with the hyperbolic time-dependent skin effects for select values of  $s_\infty$ -parameter.

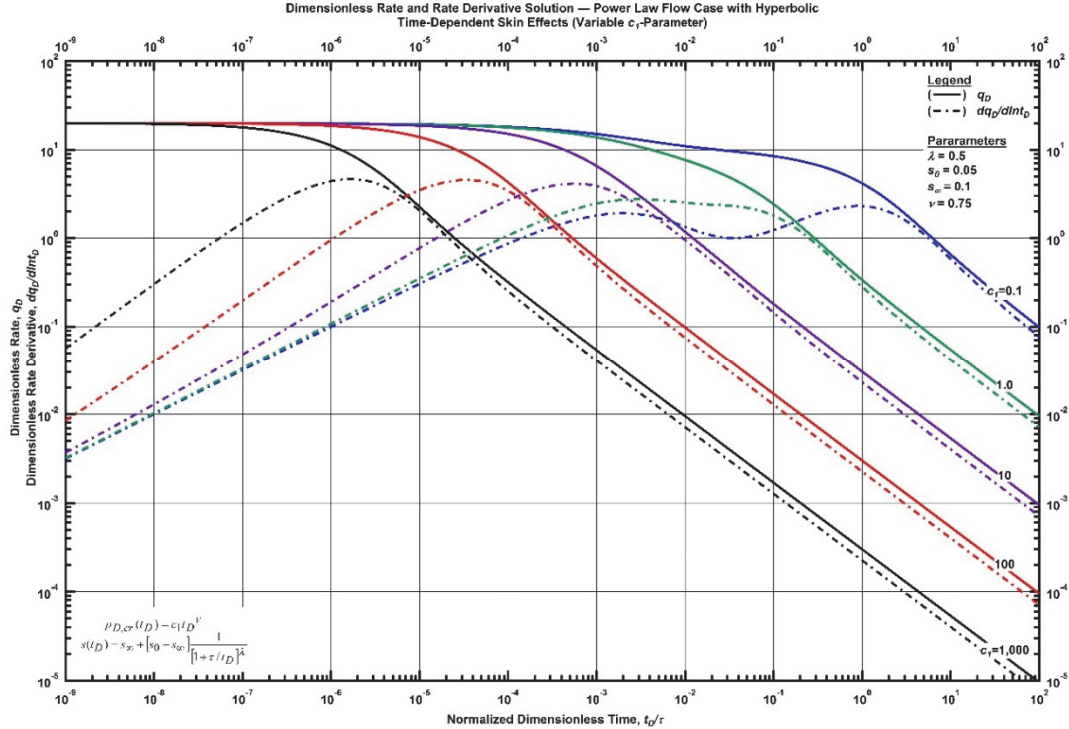


Figure F. 45—Log-log plot (constant pressure dimensionless derivative rate solution) for the power law flow model combined with the hyperbolic time-dependent skin effects for select values of  $c_1$ -parameter.

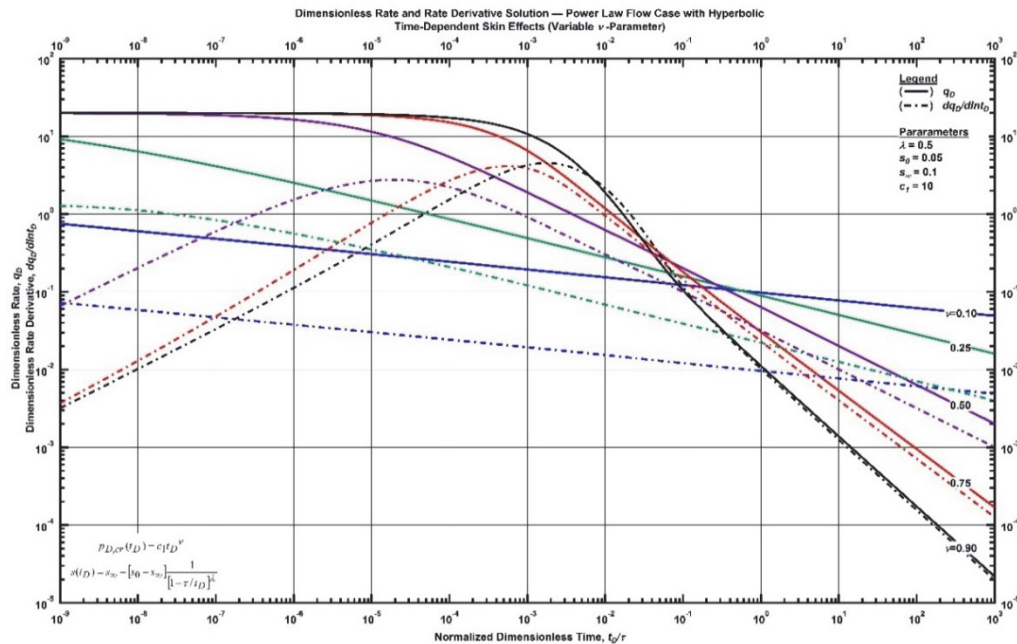


Figure F. 46—Log-log plot (constant pressure dimensionless derivative rate solution) for the power law flow model combined with the hyperbolic time-dependent skin effects for select values of  $\nu$ -parameter.

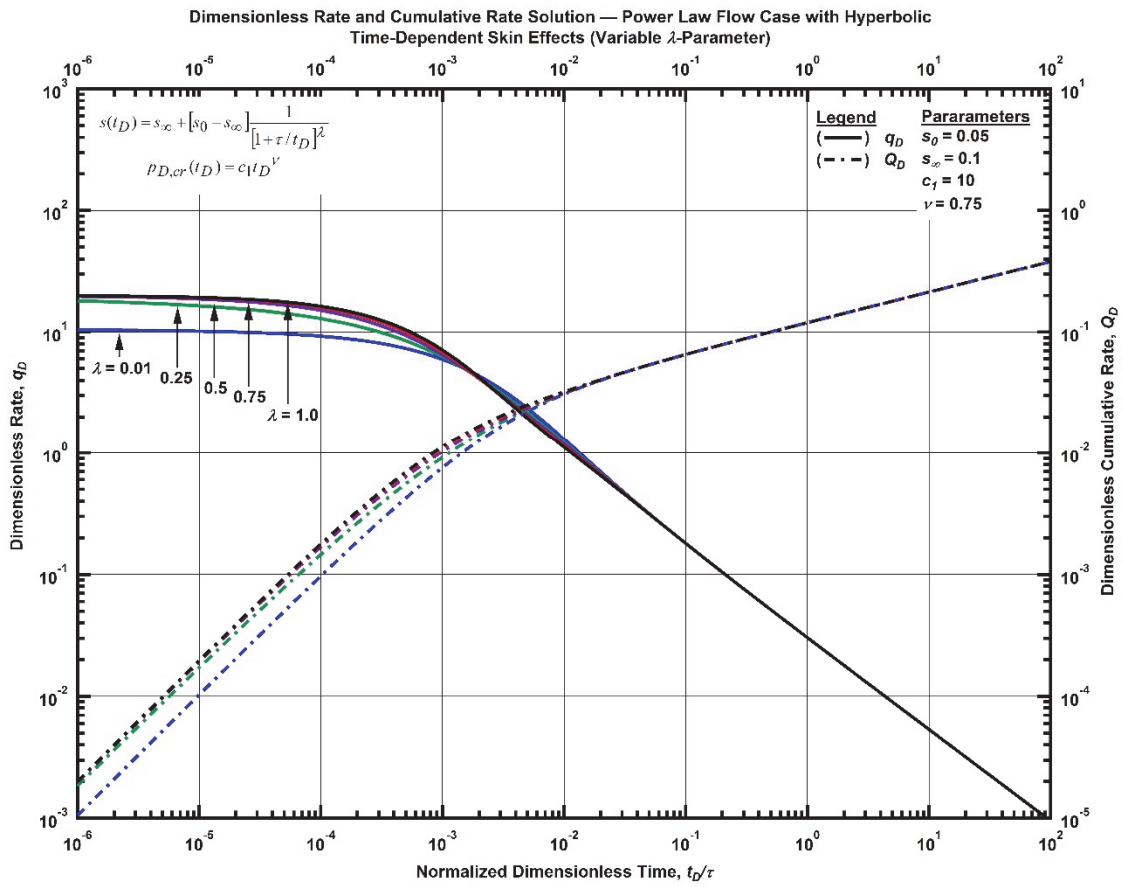


Figure F. 47—Log-log plot (constant pressure dimensionless cumulative production solution) for the power law flow model combined with the hyperbolic time-dependent skin effects for select values of  $\lambda$ -parameter.

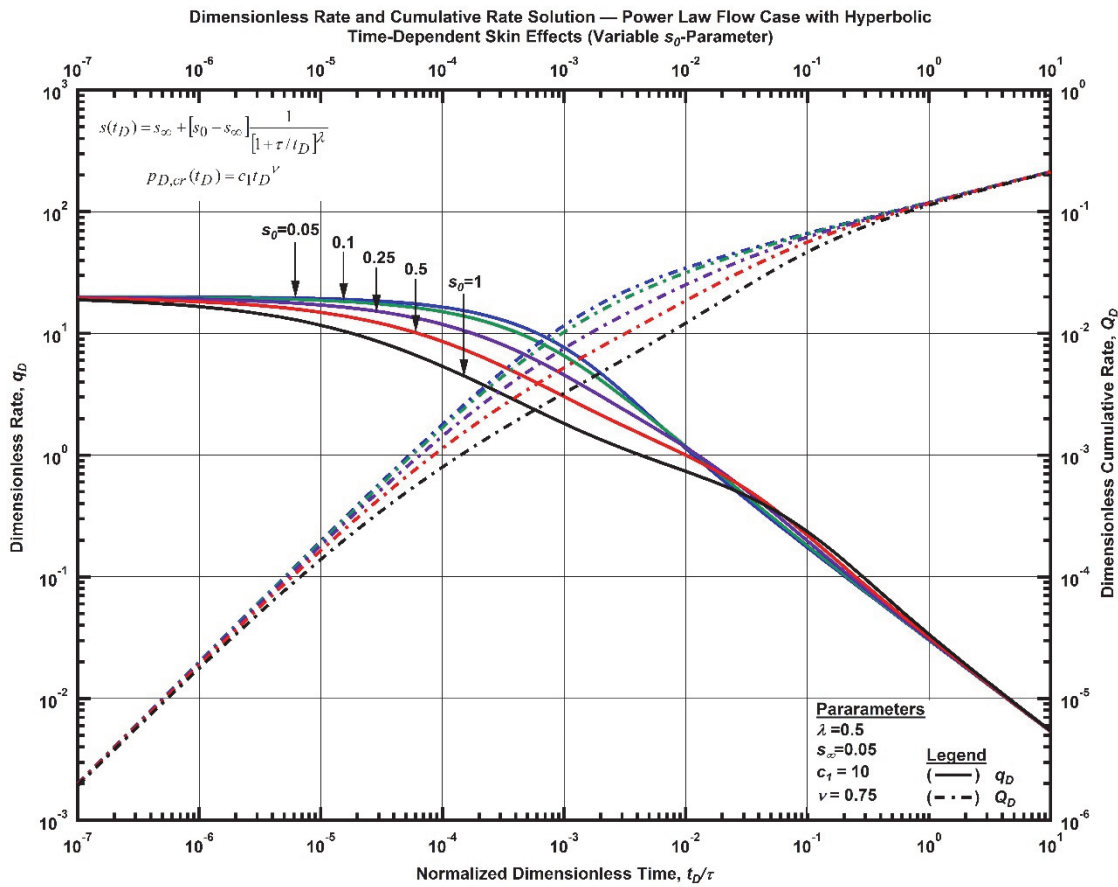


Figure F. 48—Log-log plot (constant pressure dimensionless cumulative production solution) for the power law flow model combined with the hyperbolic time-dependent skin effects for select values of  $s_0$ -parameter.

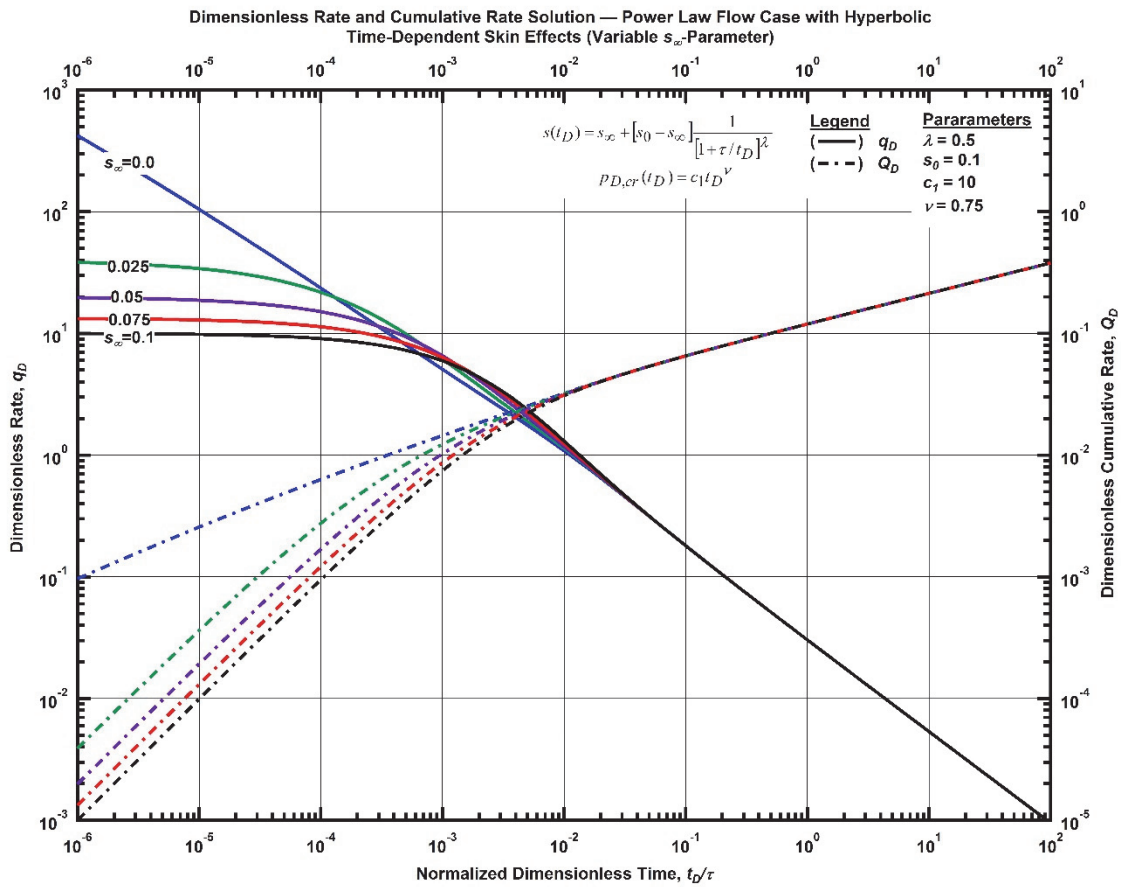


Figure F. 49—Log-log plot (constant pressure dimensionless cumulative production solution) for the power law flow model combined with the hyperbolic time-dependent skin effects for select values of  $s_\infty$ -parameter.

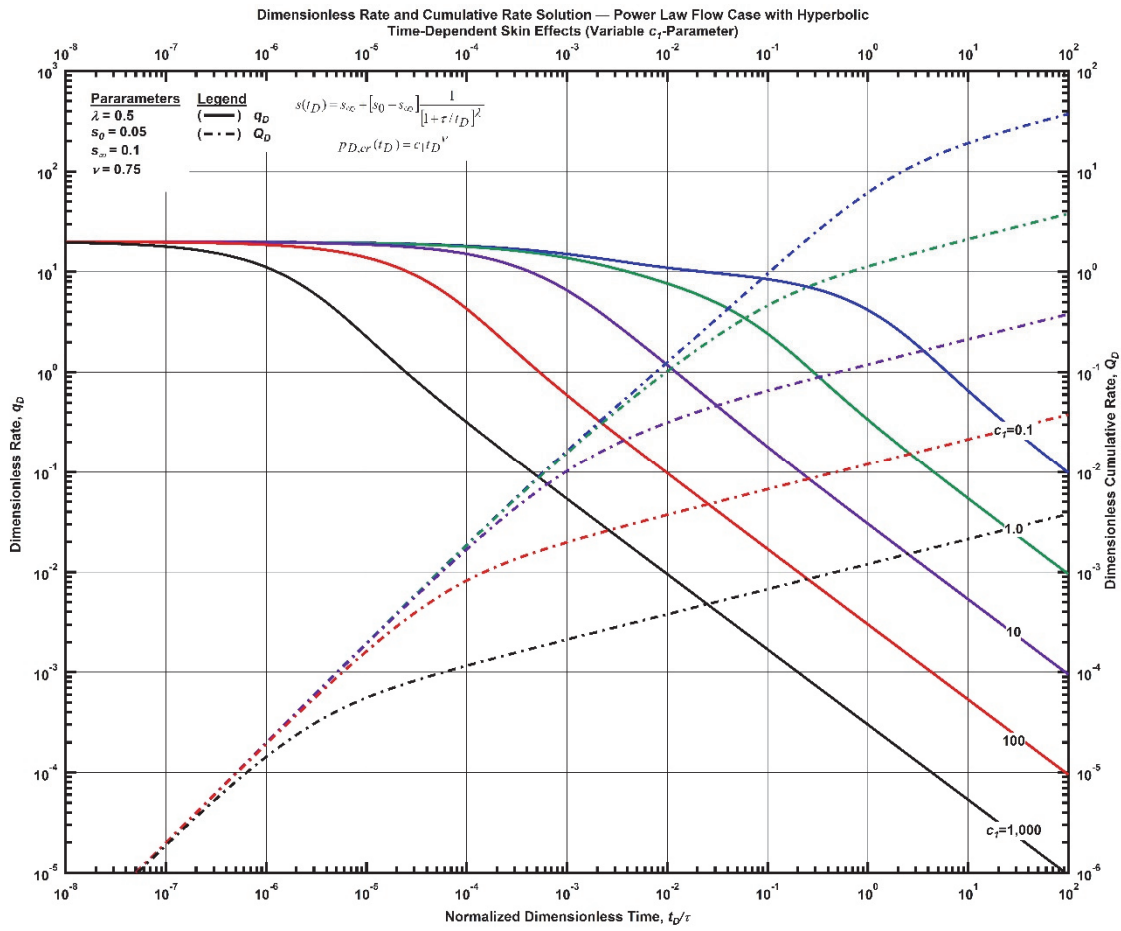


Figure F. 50—Log-log plot (constant pressure dimensionless cumulative production solution) for the power law flow model combined with the hyperbolic time-dependent skin effects for select values of  $c_1$ -parameter.

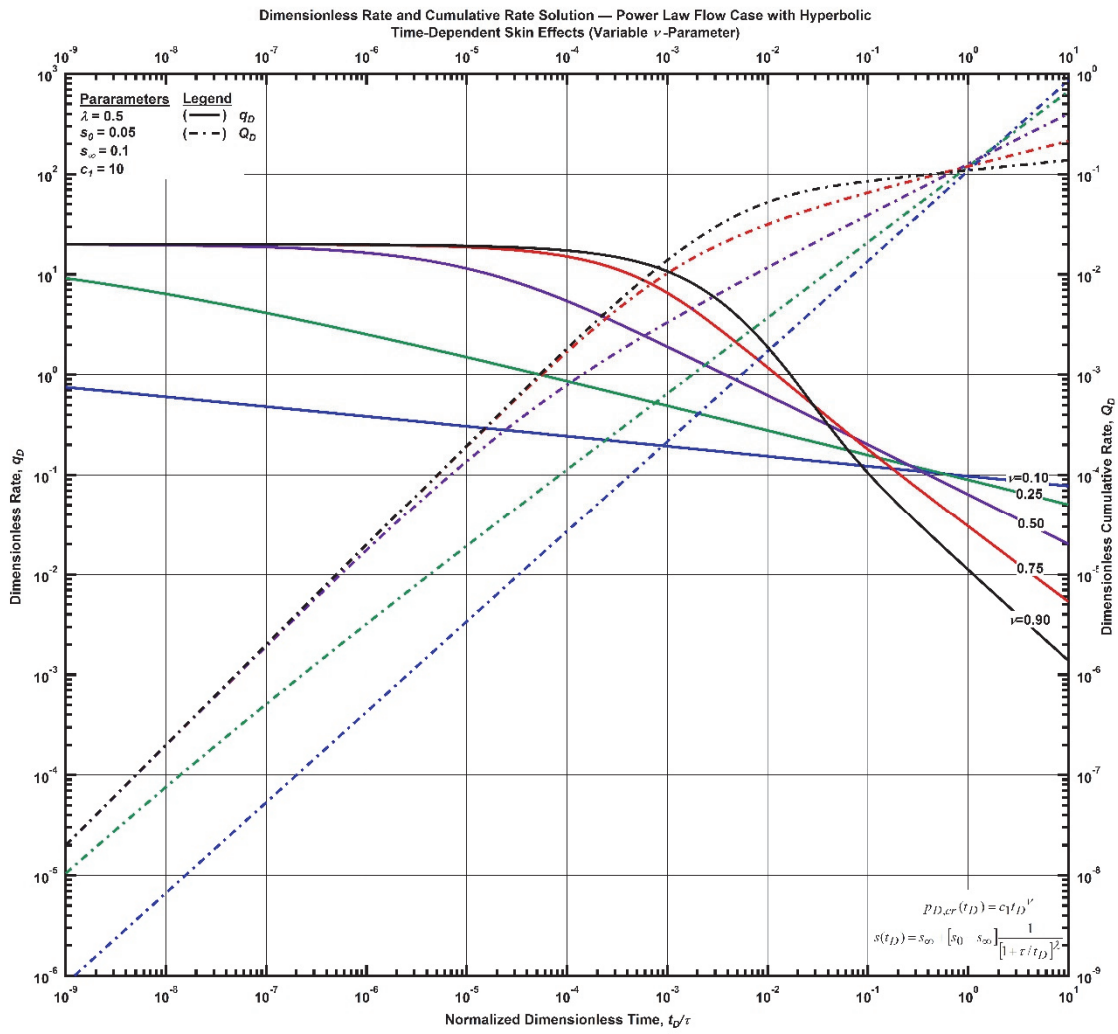


Figure F. 51—Log-log plot (constant pressure dimensionless cumulative production solution) for the power law flow model combined with the hyperbolic time-dependent skin effects for select values of  $\nu$ -parameter.

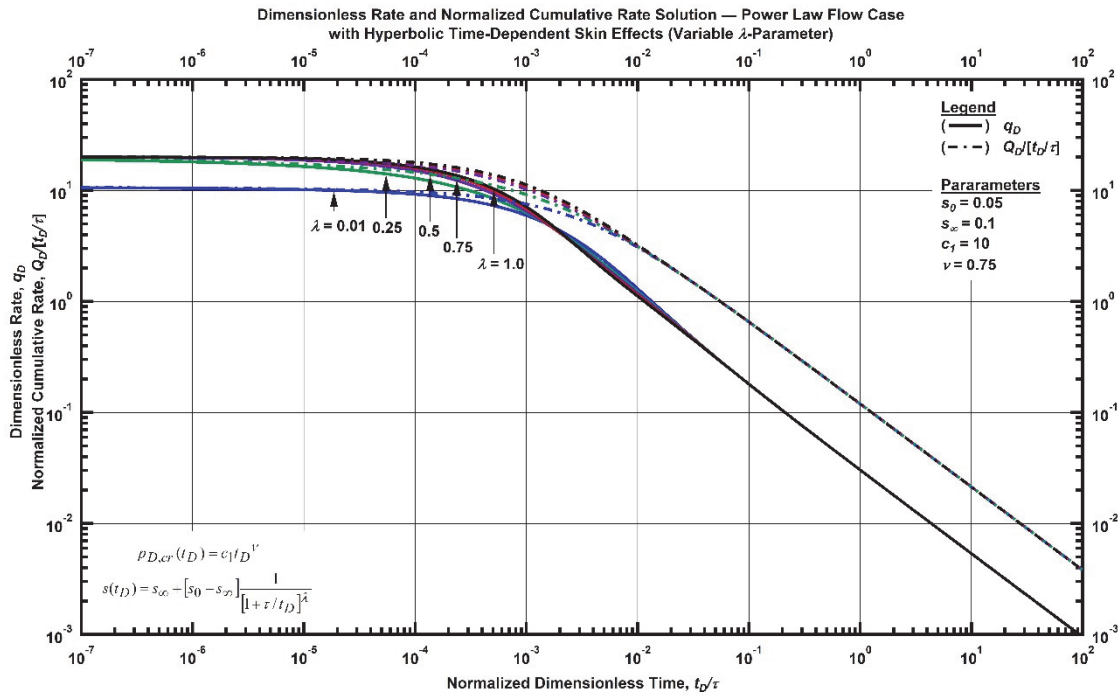


Figure F. 52—Log-log plot (constant pressure time-normalized dimensionless cumulative rate solution) for the power law flow model combined with the hyperbolic time-dependent skin effects for select values of  $\lambda$ -parameter.

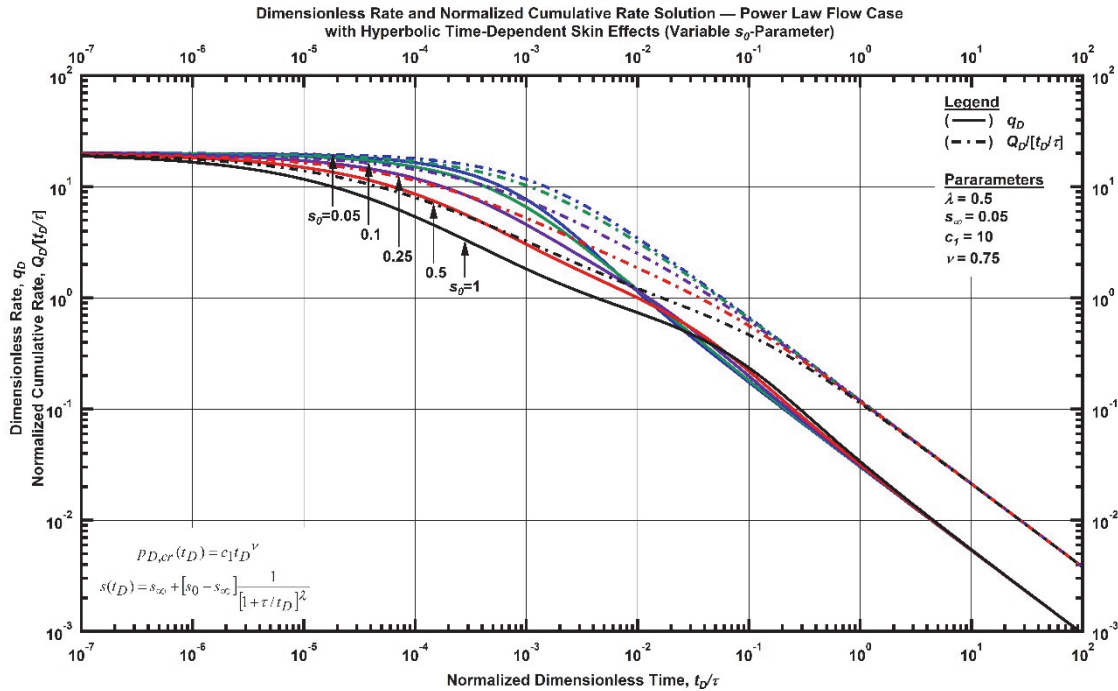


Figure F. 53—Log-log plot (constant pressure time-normalized dimensionless cumulative rate solution) for the power law flow model combined with the hyperbolic time-dependent skin effects for select values of  $s_0$ -parameter.

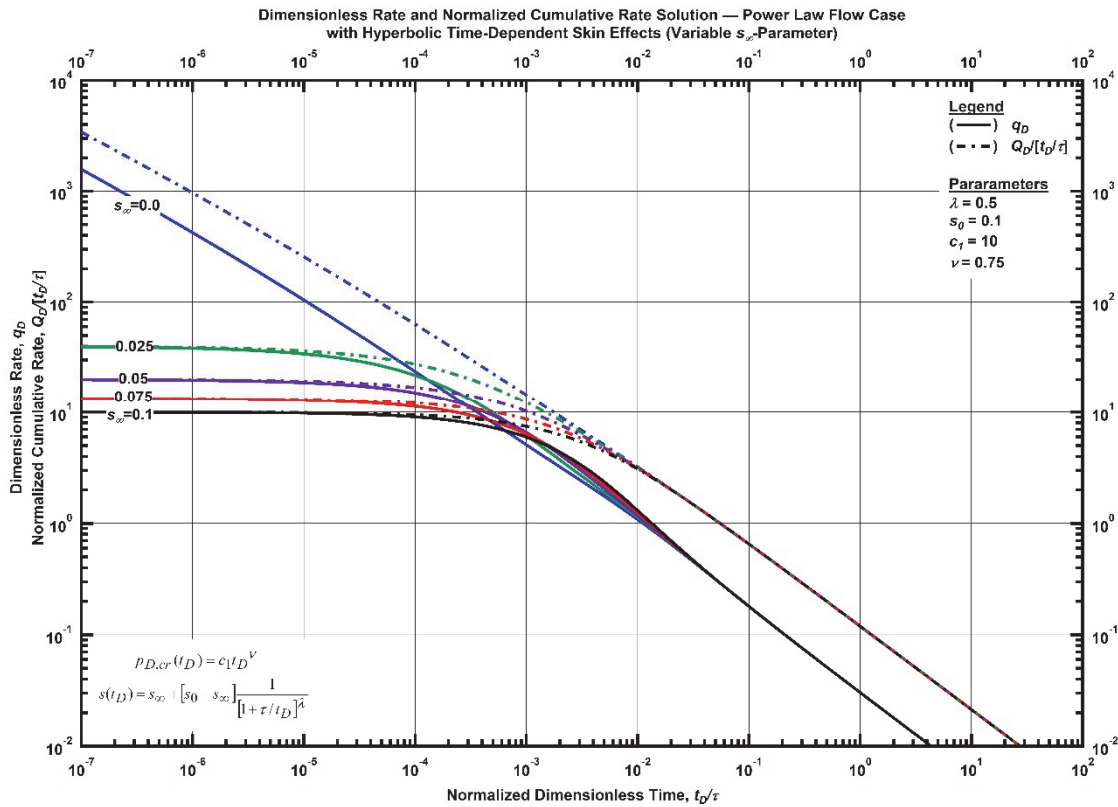


Figure F. 54—Log-log plot (constant pressure time-normalized dimensionless cumulative rate solution) for the power law flow model combined with the hyperbolic time-dependent skin effects for select values of  $s_\infty$ -parameter.

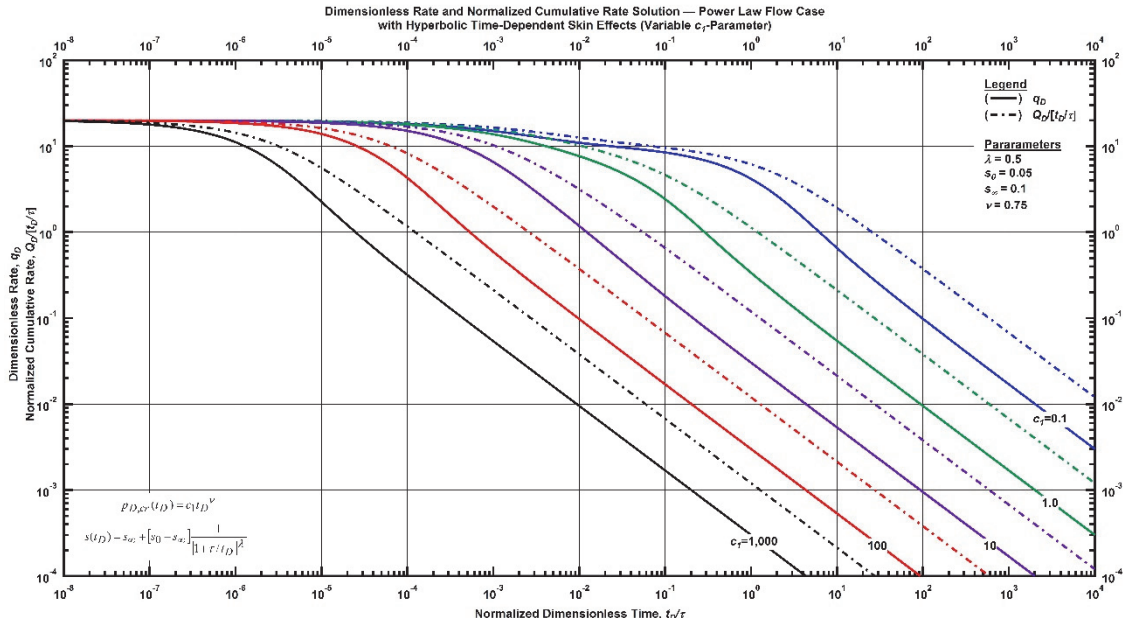


Figure F. 55—Log-log plot (constant pressure time-normalized dimensionless cumulative rate solution) for the power law flow model combined with the hyperbolic time-dependent skin effects for select values of  $c_1$ -parameter.

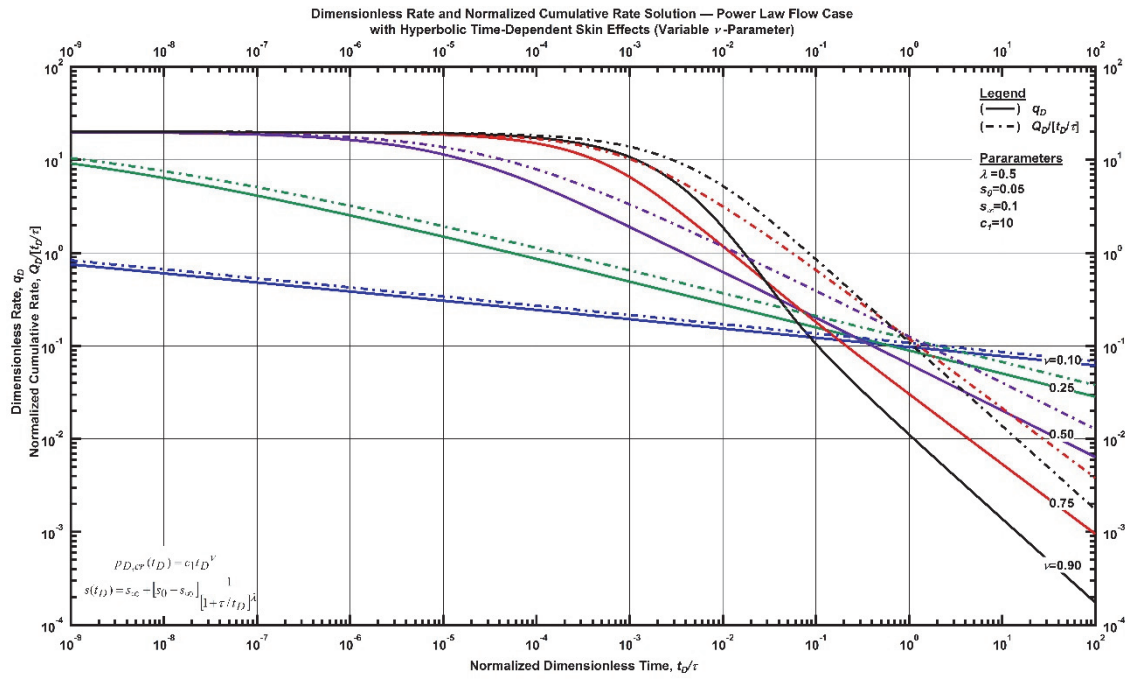


Figure F. 56—Log-log plot (constant pressure time-normalized dimensionless cumulative rate solution) for the power law flow model combined with the hyperbolic time-dependent skin effects for select values of  $\nu$ -parameter.

#### Power-Law Flow Relation with Time-Dependent Wellbore Storage

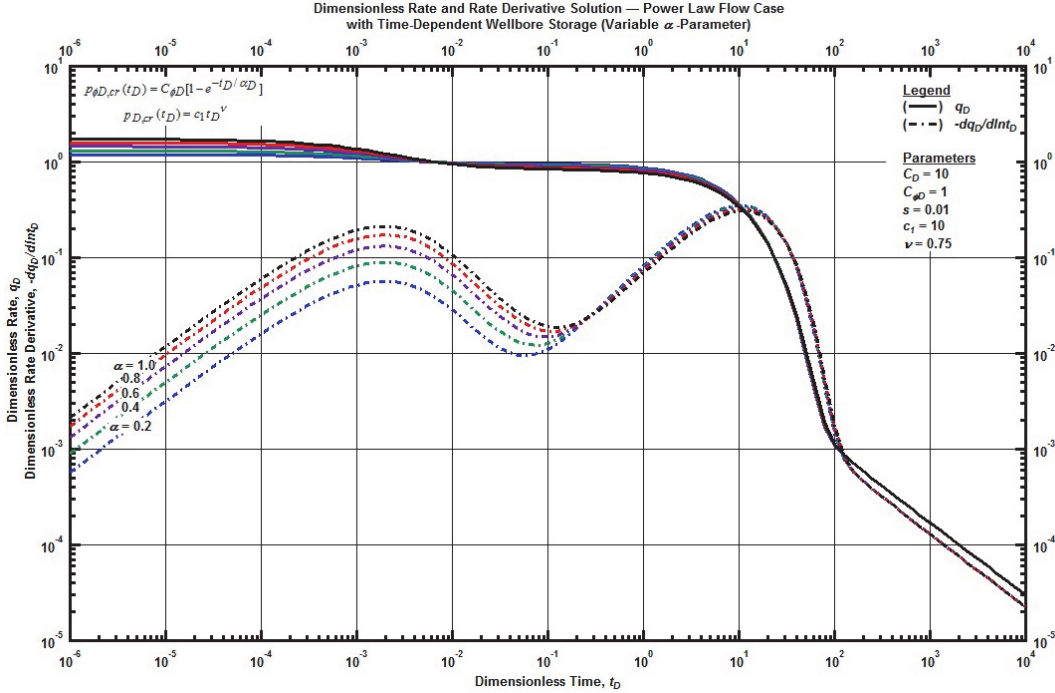


Figure F. 57—Log-log plot (constant pressure dimensionless rate solution) for the power law flow model combined with the time-dependent wellbore storage for select values of  $\alpha$ -parameter.

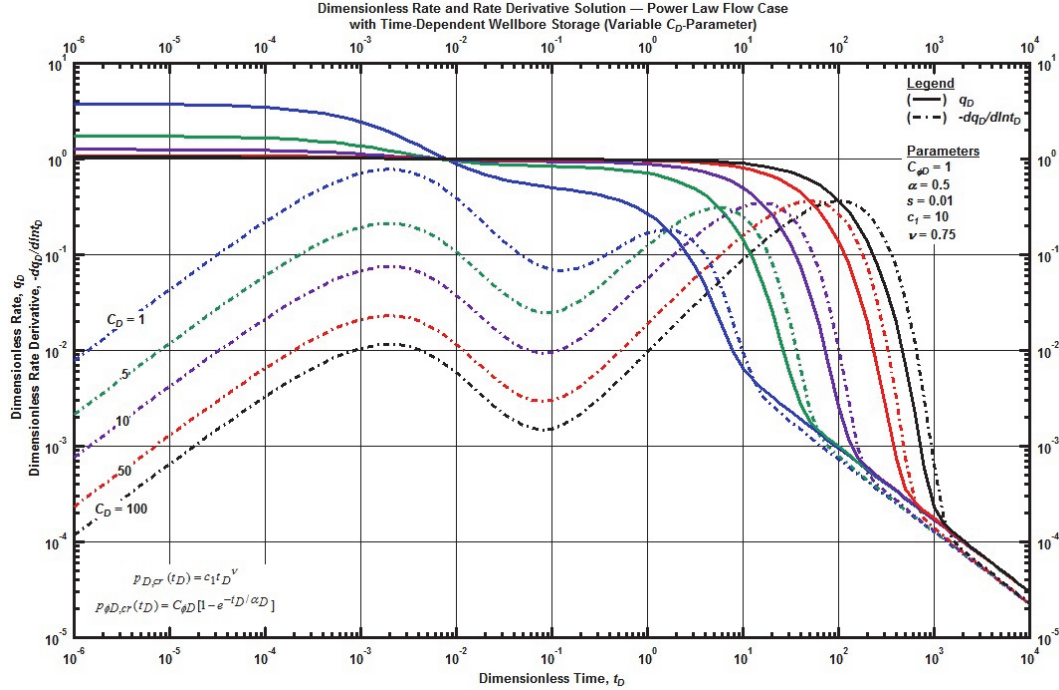


Figure F. 58—Log-log plot (constant pressure dimensionless rate solution) for the power law flow model combined with the time-dependent wellbore storage for select values of the dimensionless wellbore storage constant.

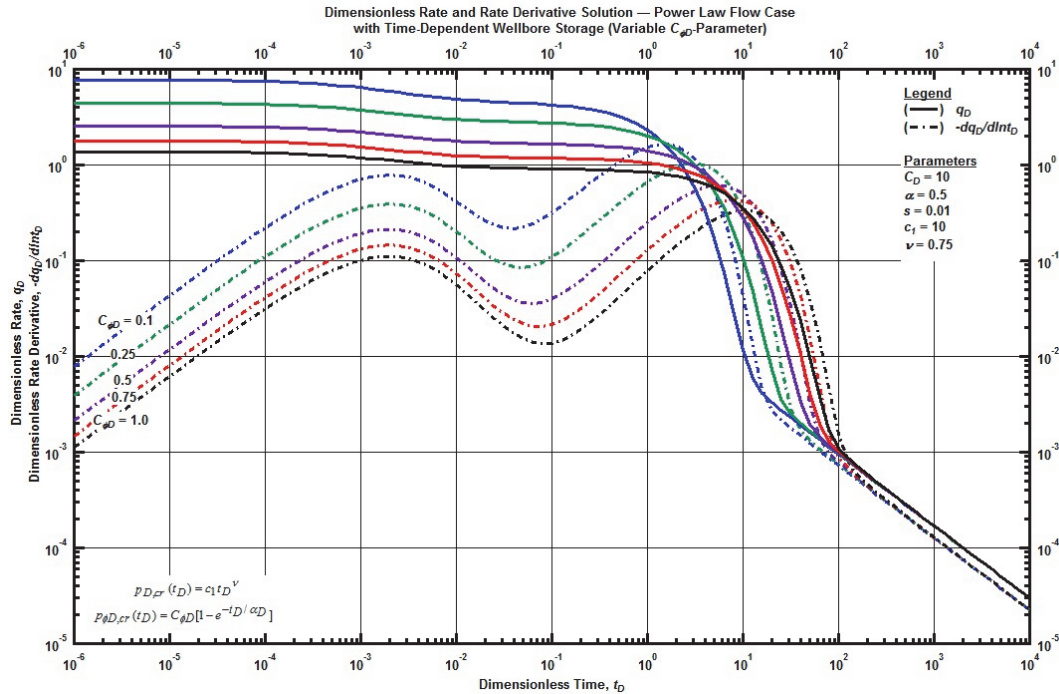


Figure F. 59—Log-log plot (constant pressure dimensionless rate solution) for the power law flow model combined with the time-dependent wellbore storage for select values phase redistribution constant.

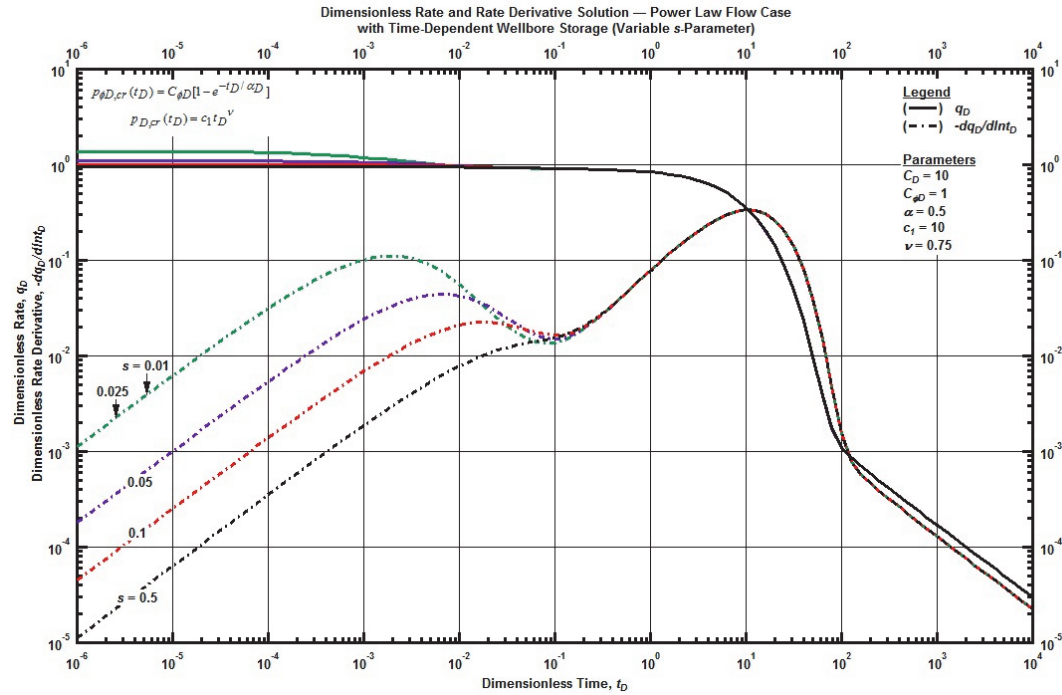


Figure F. 60—Log-log plot (constant pressure dimensionless rate solution) for the power law flow model combined with the time-dependent wellbore storage for select dimensionless constant skin factor.

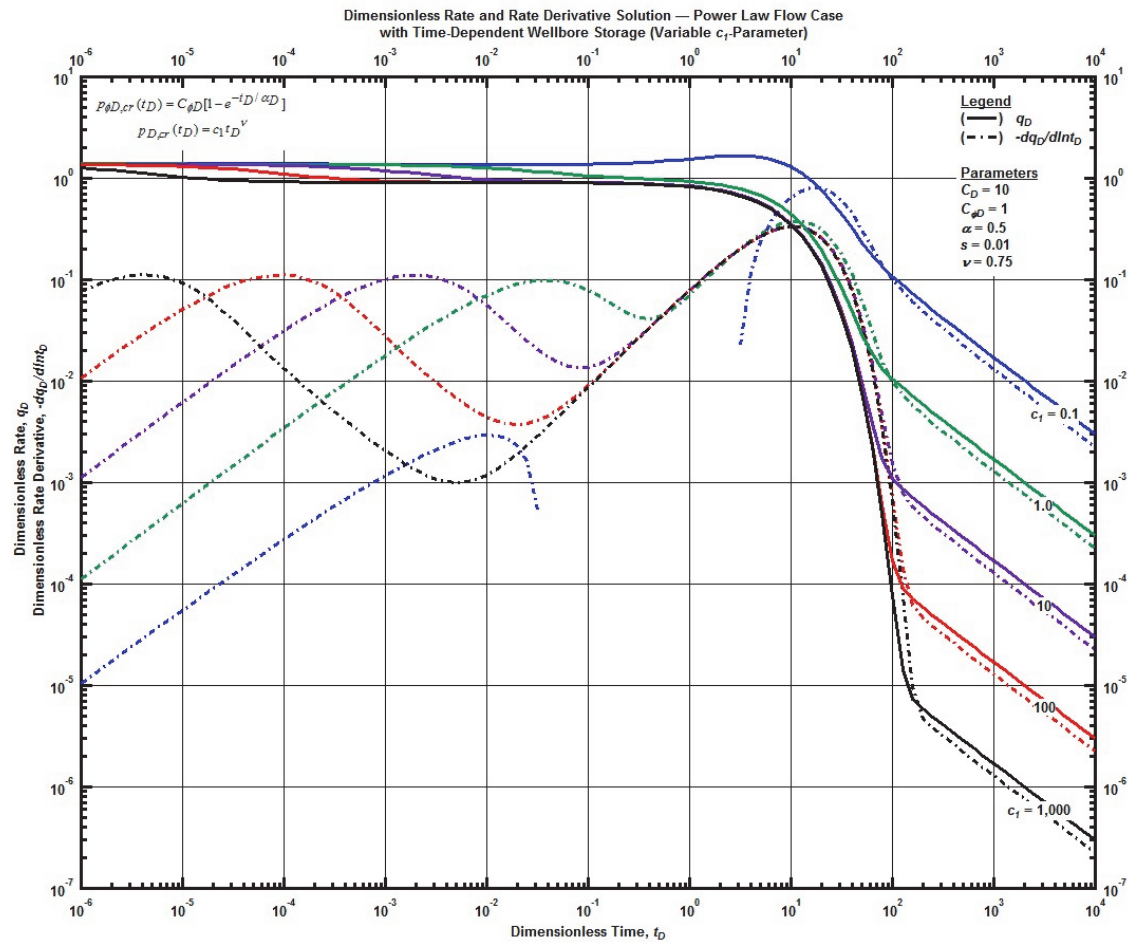


Figure F. 61—Log-log plot (constant pressure dimensionless rate solution) for the power law flow model combined with the time-dependent wellbore storage for select values of  $c_1$ -parameter.

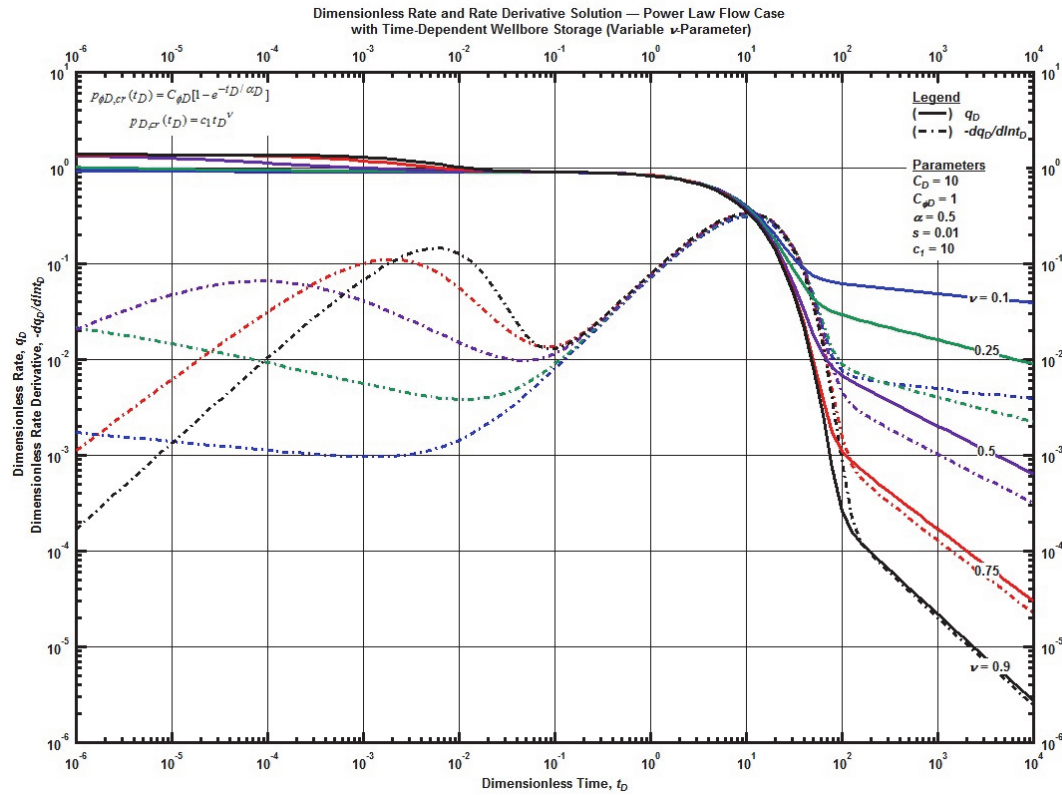


Figure F. 62—Log-log plot (constant pressure dimensionless rate solution) for the power law flow model combined with the time-dependent wellbore storage for select values of  $\nu$ -parameter.

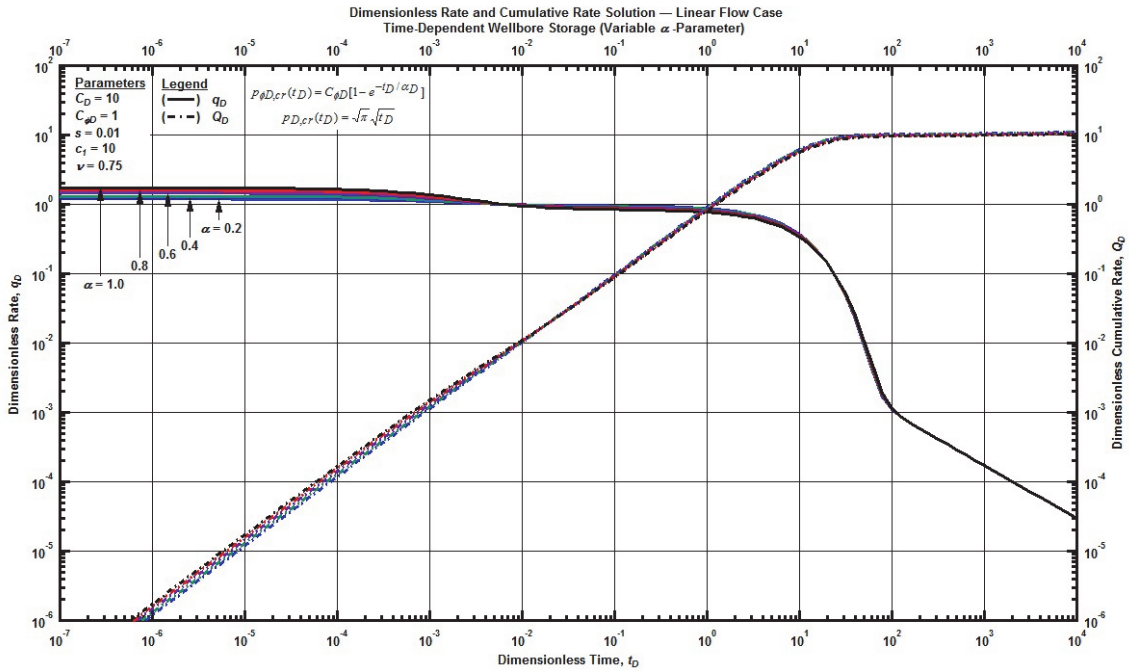


Figure F. 63—Log-log plot (constant pressure dimensionless cumulative production solution) for the power law flow model combined with the time-dependent wellbore storage for select values of  $\alpha$ -parameter.

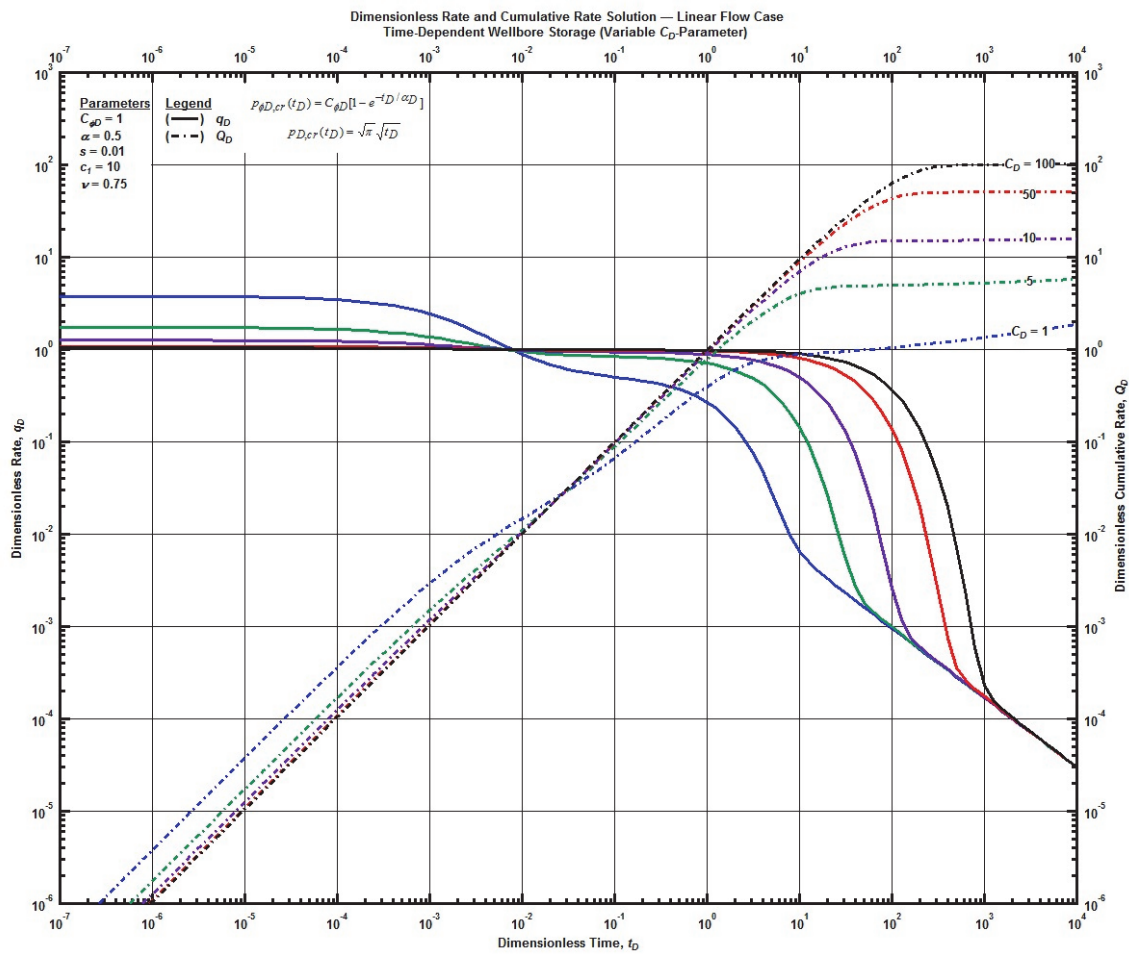


Figure F. 64—Log-log plot (constant pressure dimensionless cumulative production solution) for the power law flow model combined with the time-dependent wellbore storage for select values of the dimensionless wellbore storage constant.

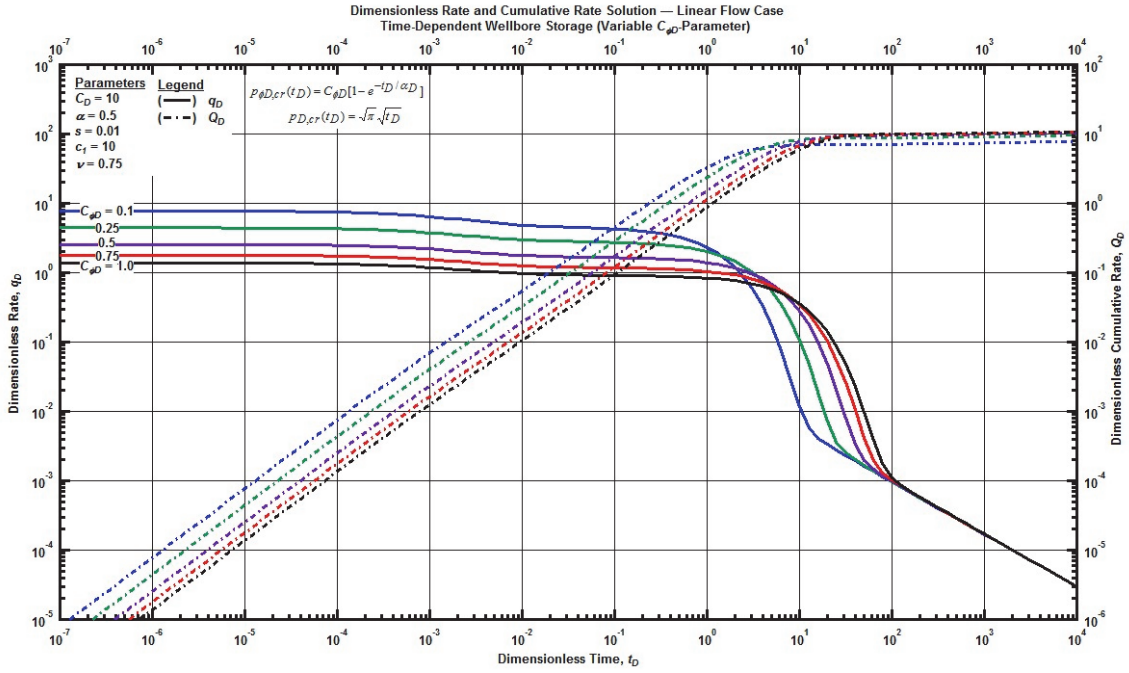


Figure F. 65—Log-log plot (constant pressure dimensionless cumulative production solution) for the power law flow model combined with the time-dependent wellbore storage for select values phase redistribution constant.

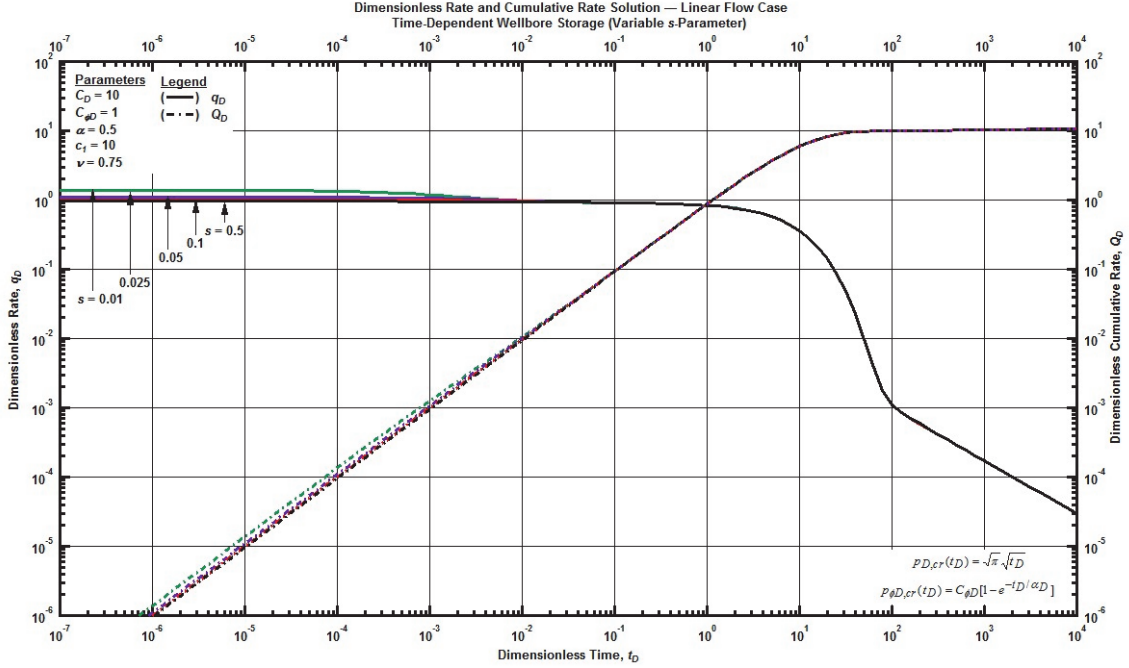


Figure F. 66—Log-log plot (constant pressure dimensionless cumulative production solution) for the power law flow model combined with the time-dependent wellbore storage for select dimensionless constant skin factor.

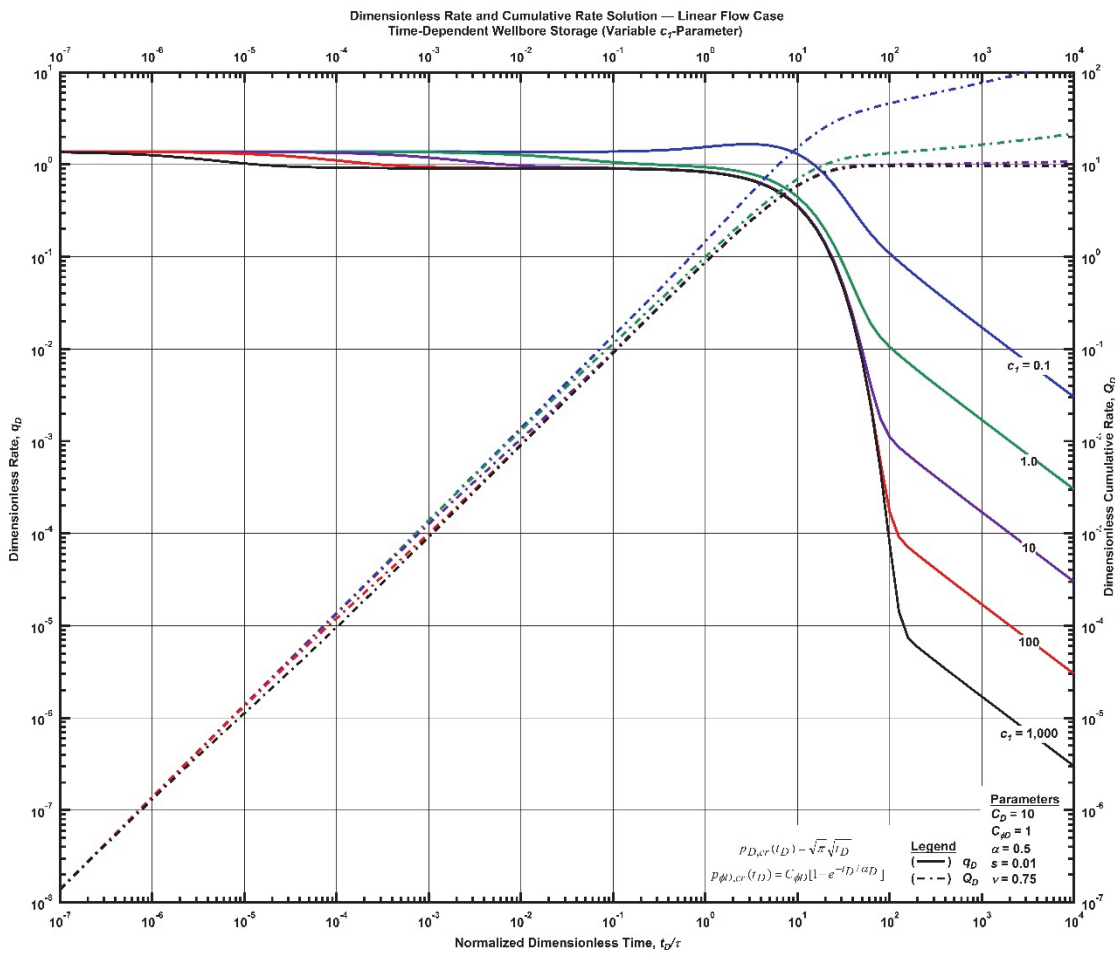


Figure F. 67—Log-log plot (constant pressure dimensionless cumulative production solution) for the power law flow model combined with the time-dependent wellbore storage for select values of  $c_1$ -parameter.

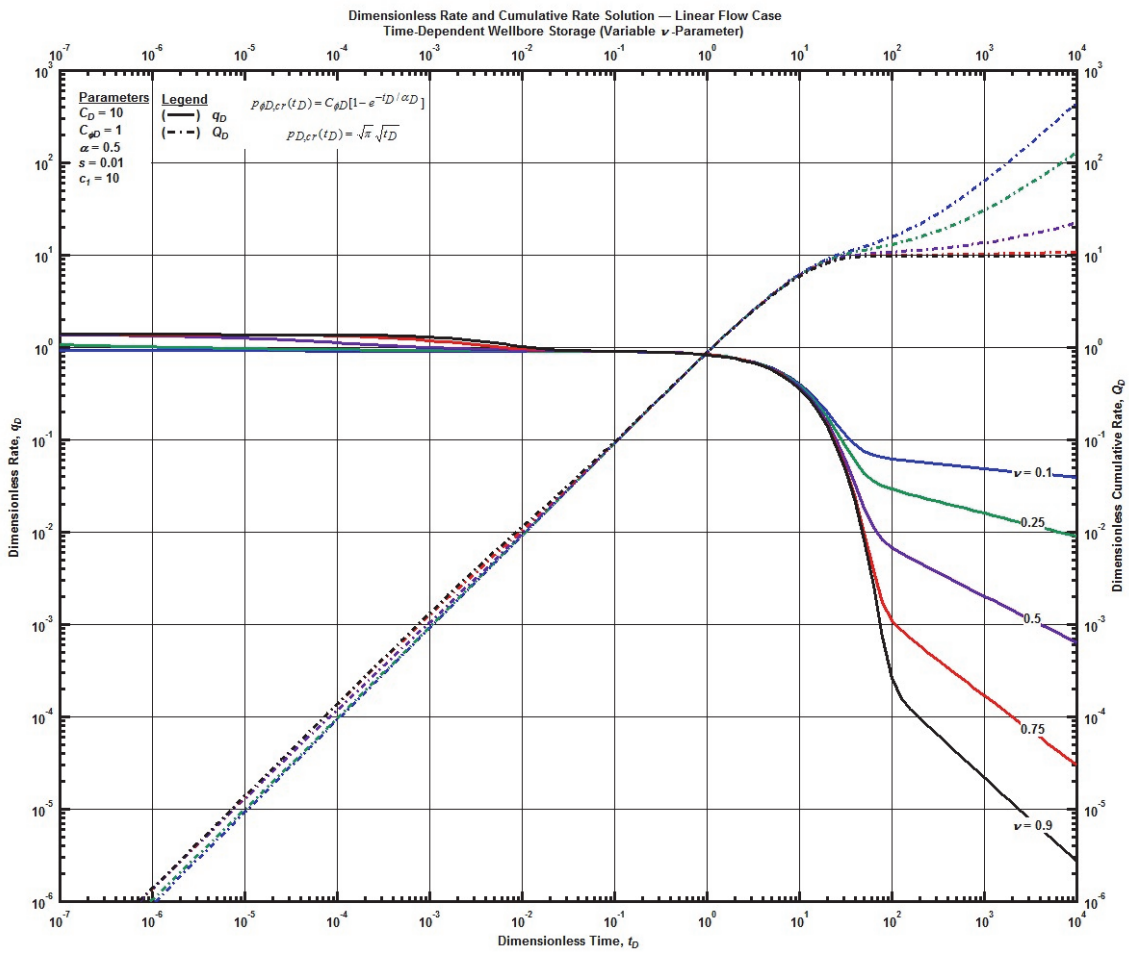


Figure F. 68 — Log-log plot (constant pressure dimensionless cumulative production solution) for the power law flow model combined with the time-dependent wellbore storage for select values of  $\nu$ -parameter.

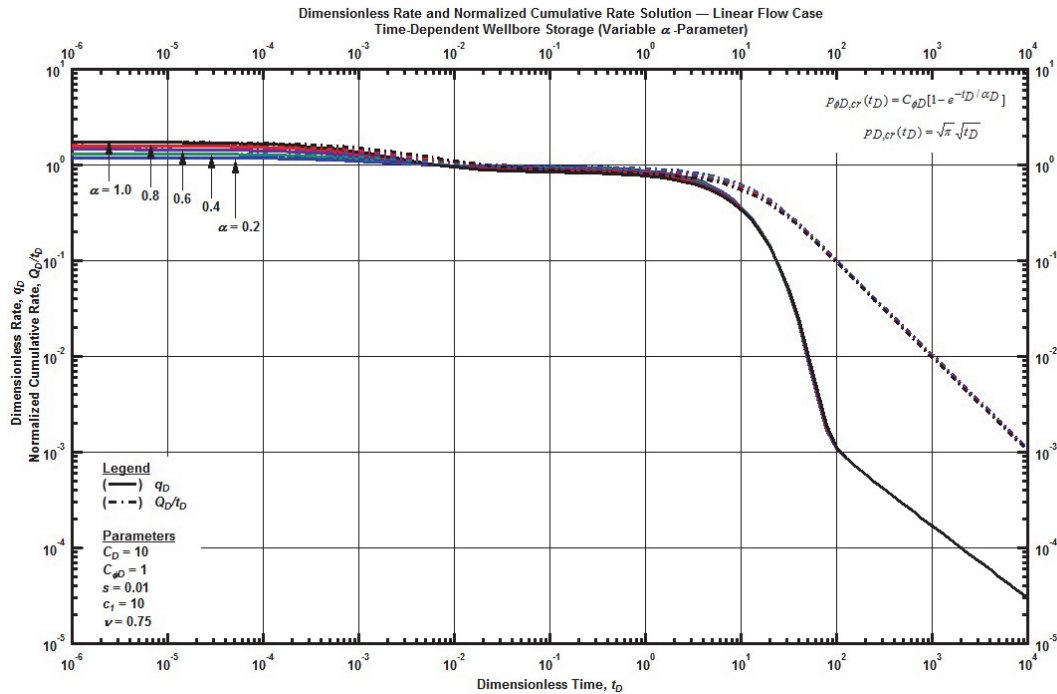


Figure F. 69—Log-log plot (constant pressure time-normalized dimensionless cumulative rate solution) for the power law flow model combined with the time-dependent wellbore storage for select values of  $\alpha$ -parameter.

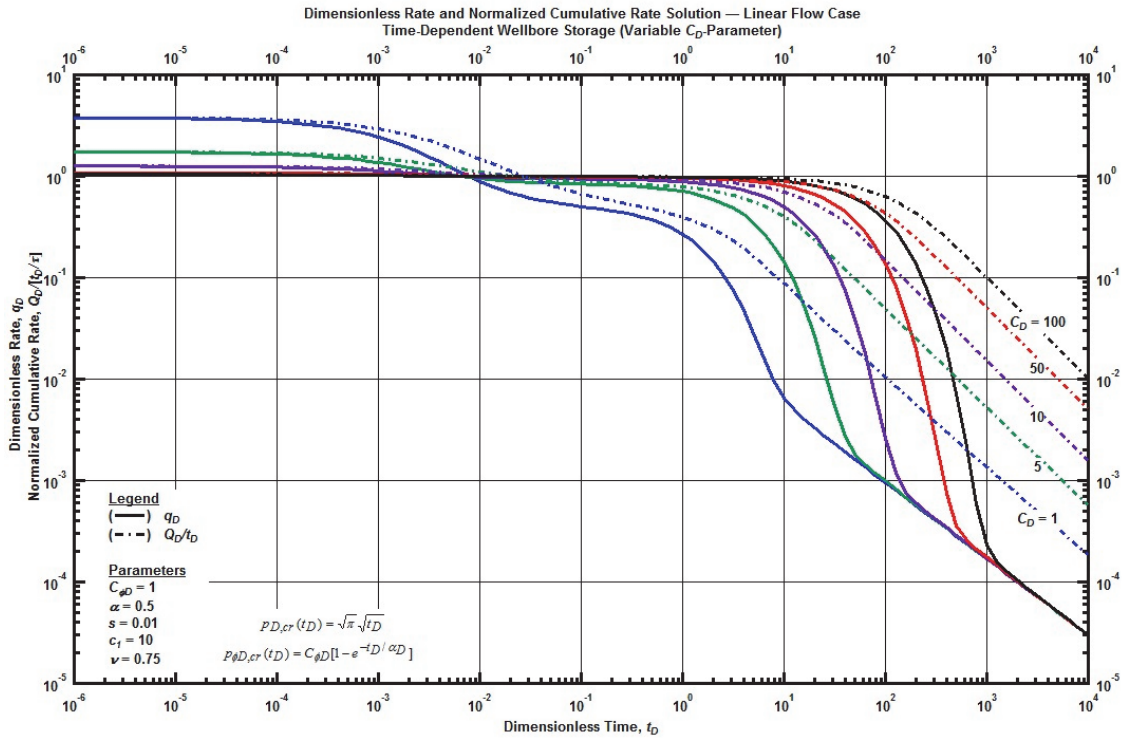


Figure F. 70—Log-log plot (constant pressure time-normalized dimensionless cumulative rate solution) for the power law flow model combined with the time-dependent wellbore storage for select values of the dimensionless wellbore storage constant.

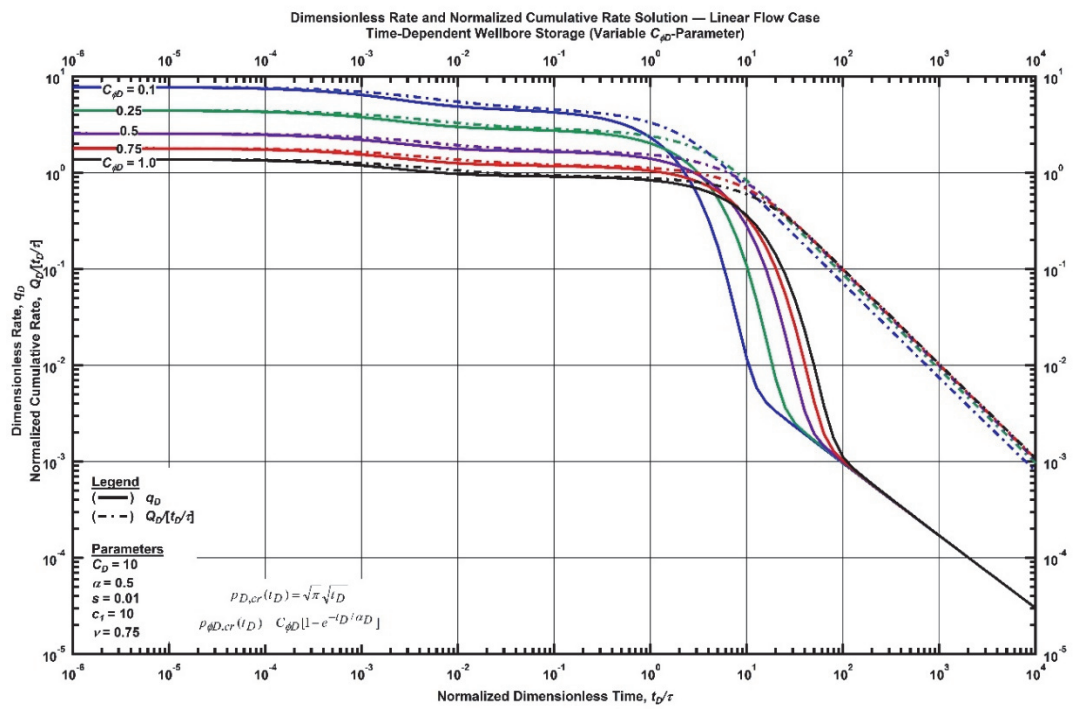


Figure F. 71 — Log-log plot (constant pressure time-normalized dimensionless cumulative rate solution) for the power law flow model combined with the time-dependent wellbore storage for select values phase redistribution constant.

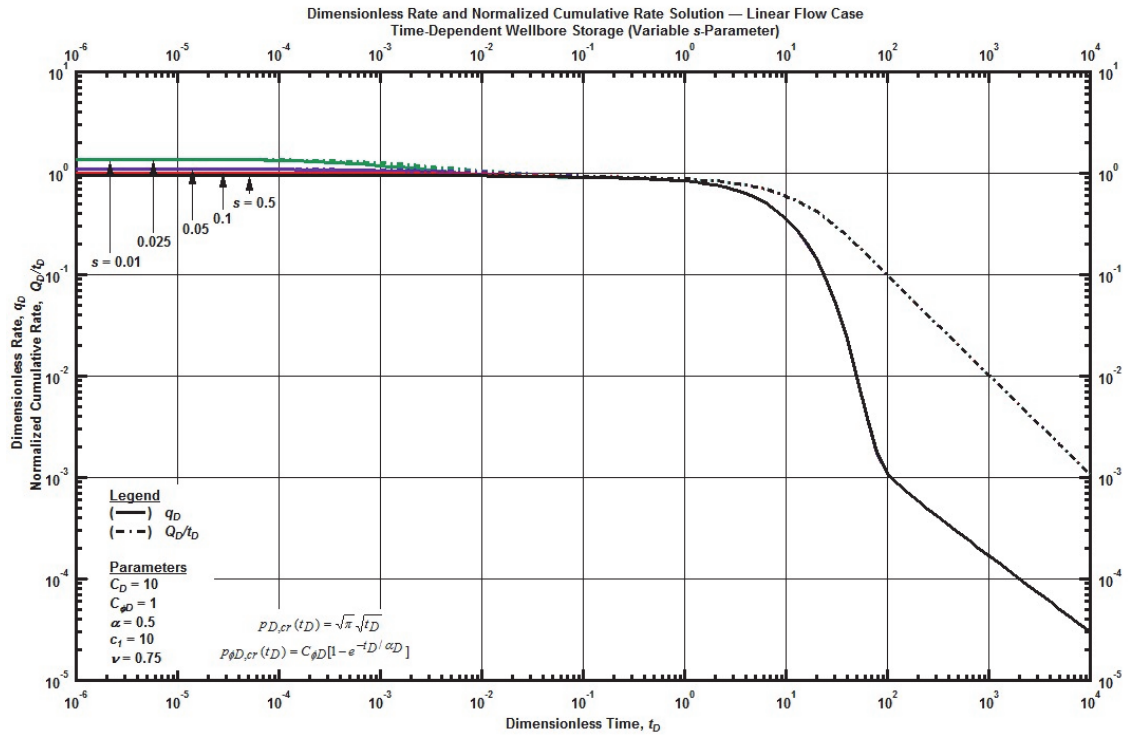


Figure F. 72—Log-log plot (constant pressure time-normalized dimensionless cumulative rate solution) for the power law flow model combined with the time-dependent wellbore storage for select dimensionless constant skin factor.

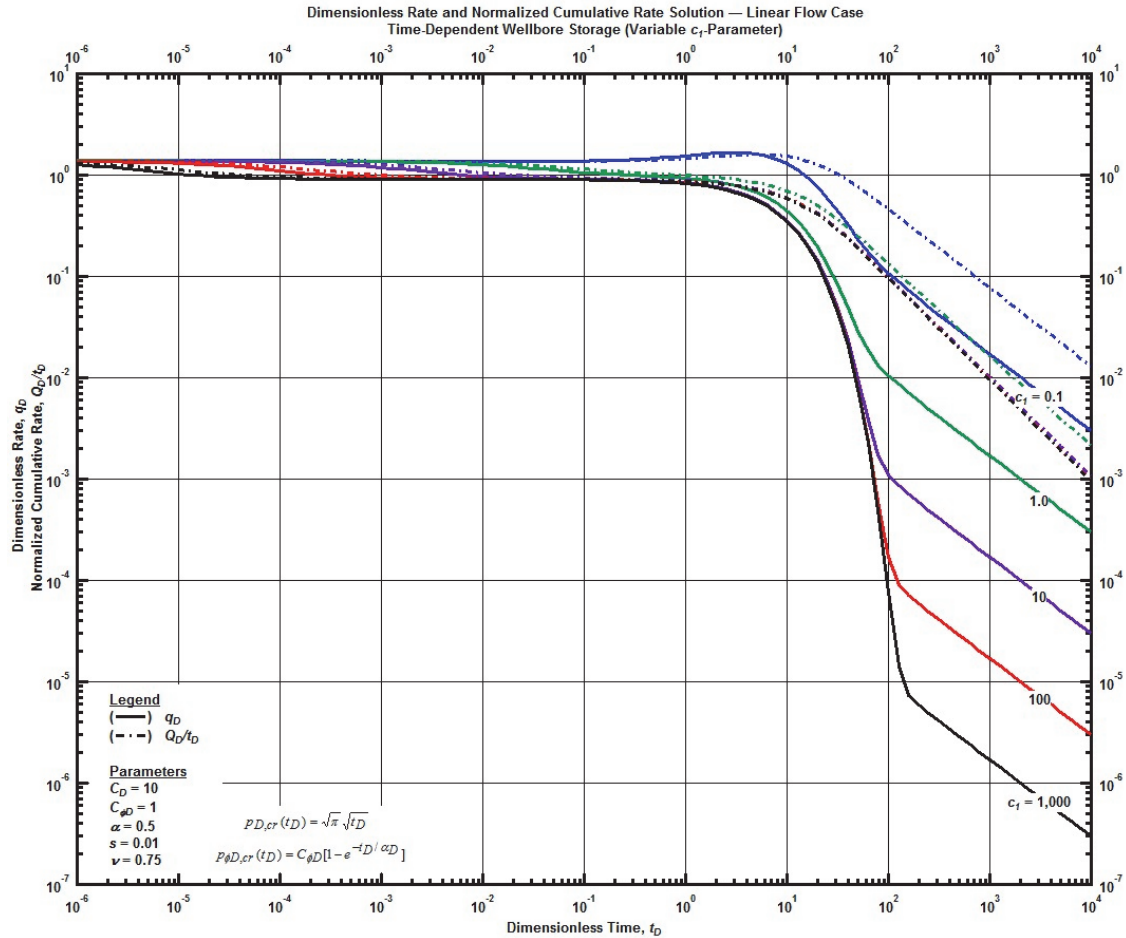


Figure F. 73—Log-log plot (constant pressure time-normalized dimensionless cumulative rate solution) for the power law flow model combined with the time-dependent wellbore storage for select values of  $c_1$ -parameter.

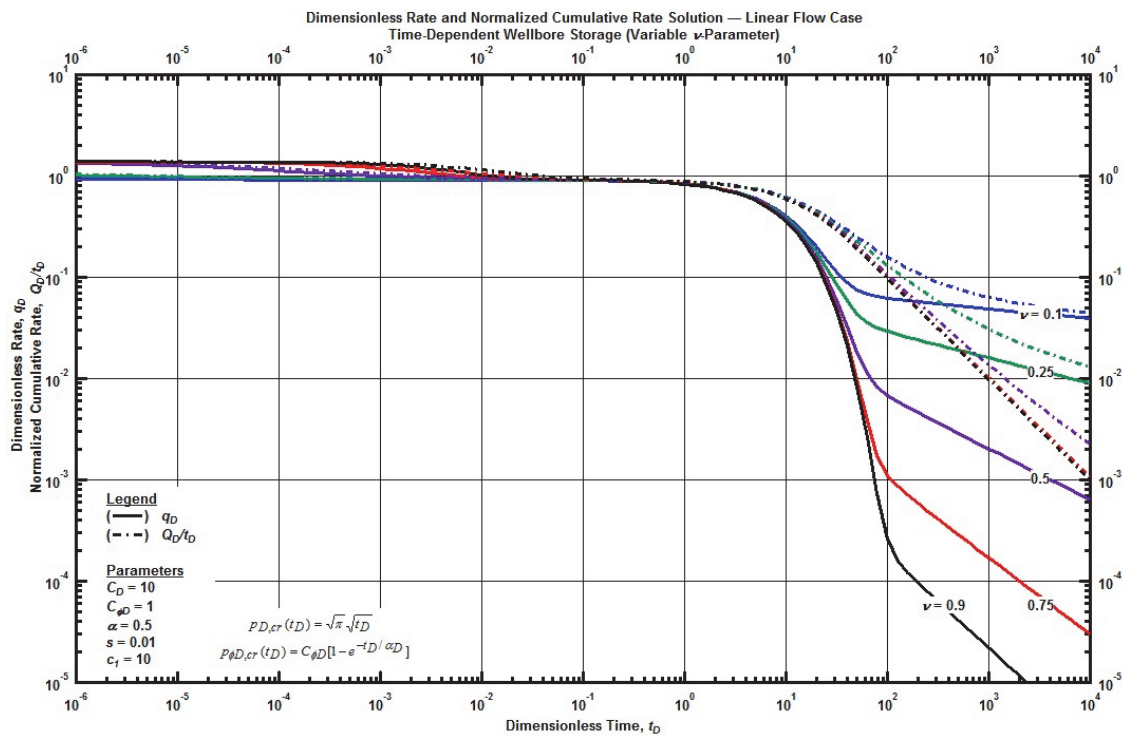


Figure F. 74—Log-log plot (constant pressure time-normalized dimensionless cumulative rate solution) for the power law flow model combined with the time-dependent wellbore storage for select values of  $\nu$ -parameter.

## F.2 Linear Flow Relation

*Linear Flow Relation with Cumulative-Exponential Time-Dependent Skin*

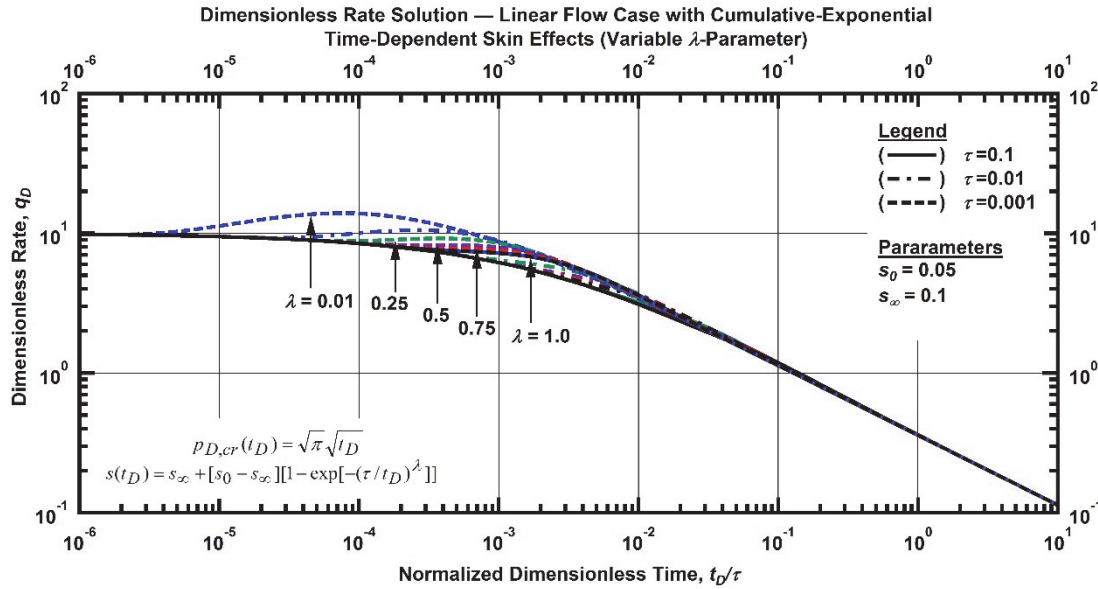


Figure F. 75—Log-log plot (constant pressure dimensionless rate solution) for the linear flow model combined with the cumulative-exponential time-dependent for select values of  $\lambda$ -parameter.

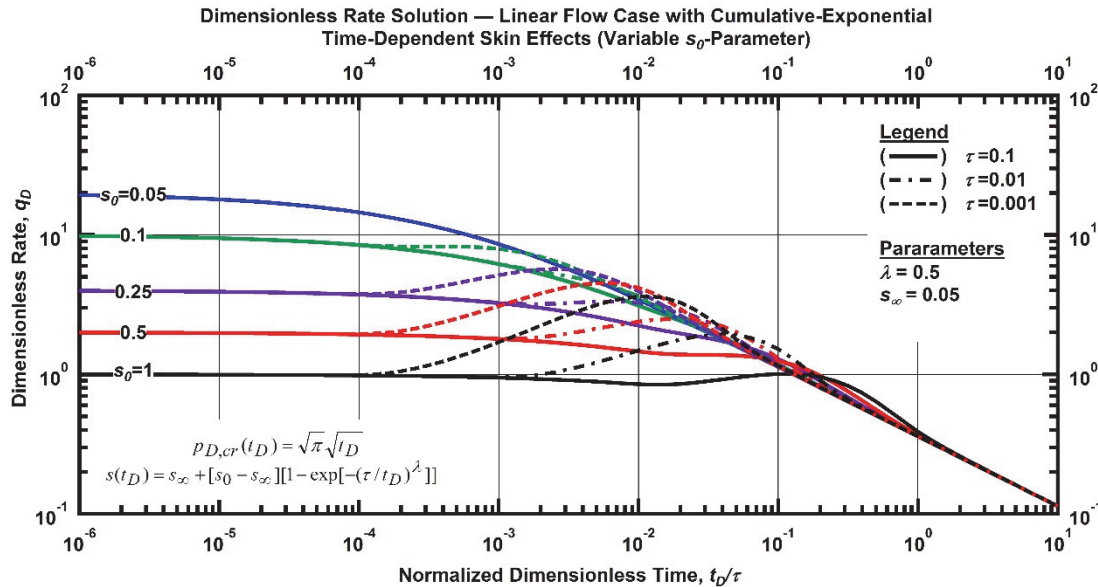


Figure F. 76—Log-log plot (constant pressure dimensionless rate solution) for the linear flow model combined with the cumulative-exponential time-dependent for select values of  $s_0$ -parameter.

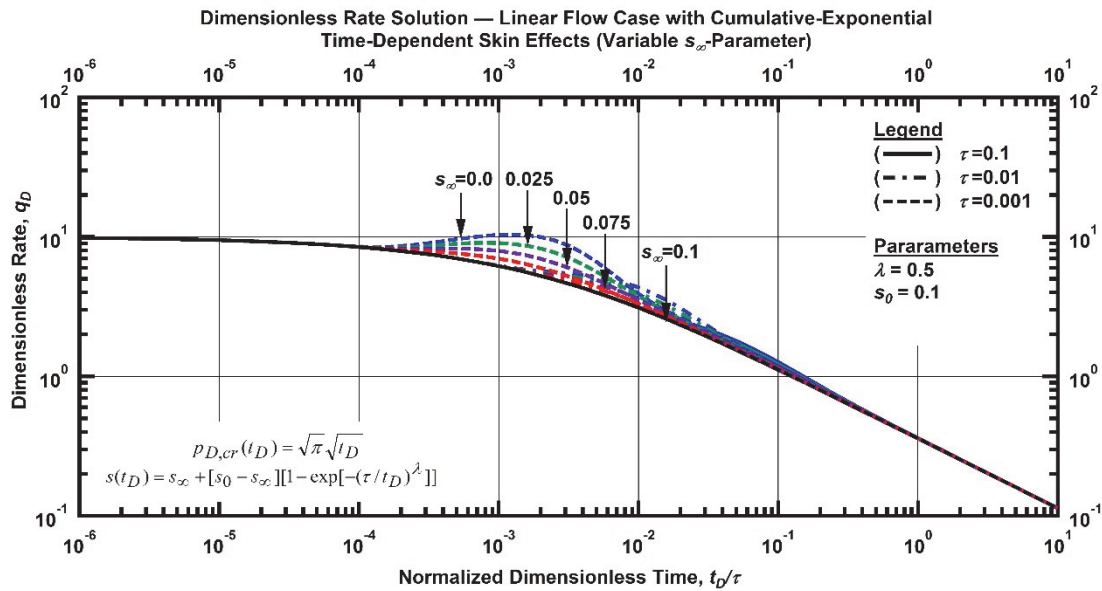


Figure F. 77—Log-log plot (constant pressure dimensionless rate solution) for the linear flow model combined with the cumulative-exponential time-dependent for select values of  $s_\infty$ -parameter.

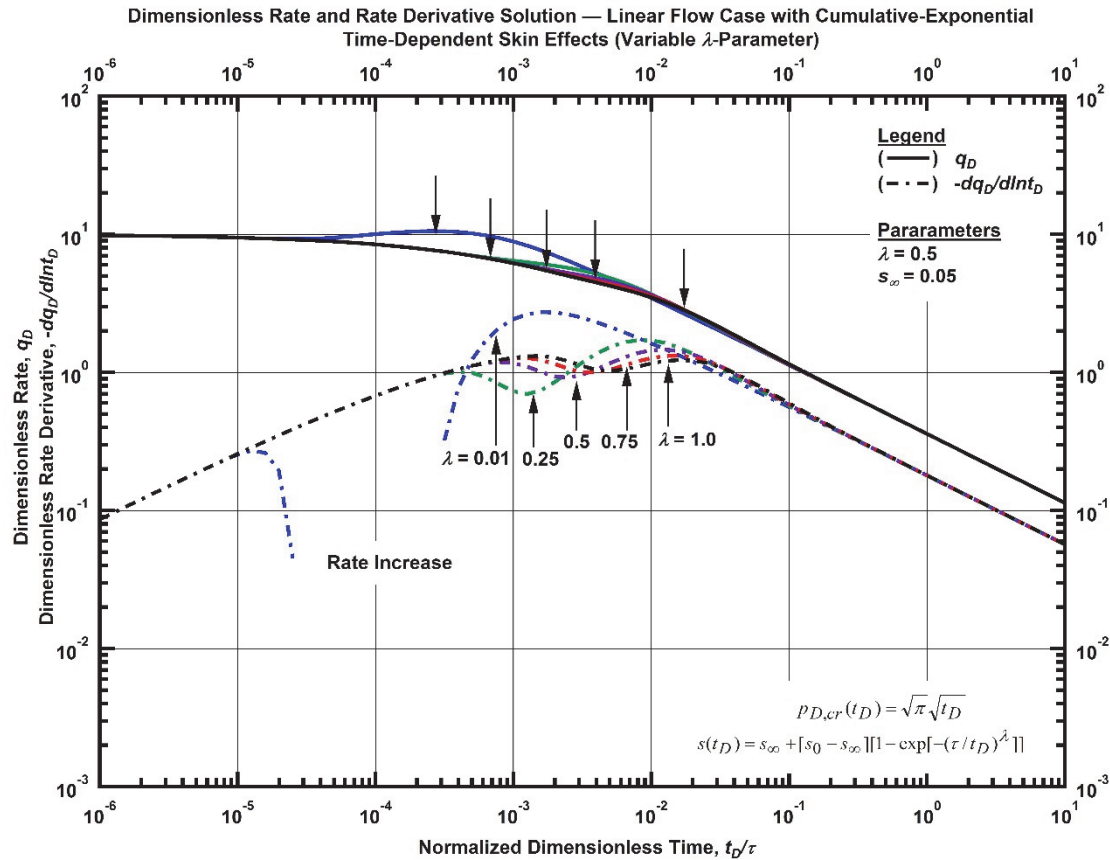


Figure F. 78—Log-log plot (constant pressure dimensionless rate derivative solution) for the linear flow model combined with the cumulative-exponential time-dependent for select values of  $\lambda$ -parameter.

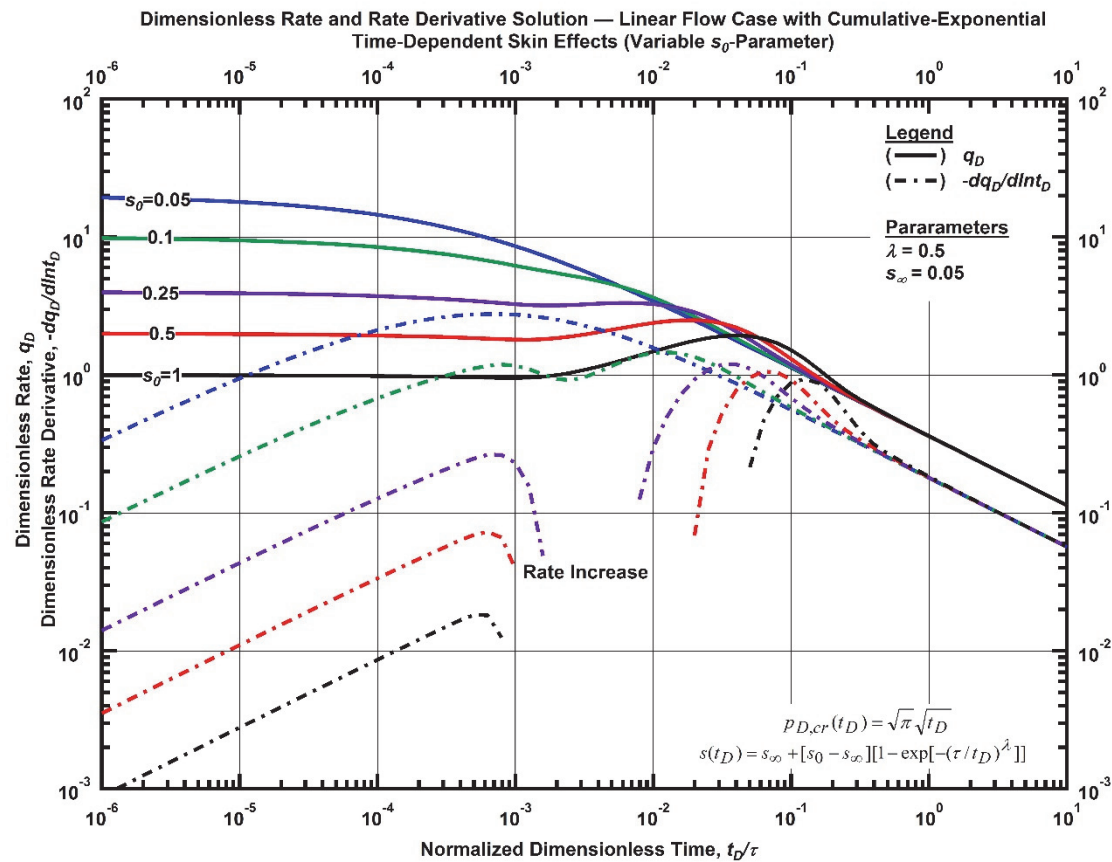


Figure F. 79—Log-log plot (constant pressure dimensionless derivative rate solution) for the linear flow model combined with the cumulative-exponential time-dependent for select values of  $s_0$ -parameter.

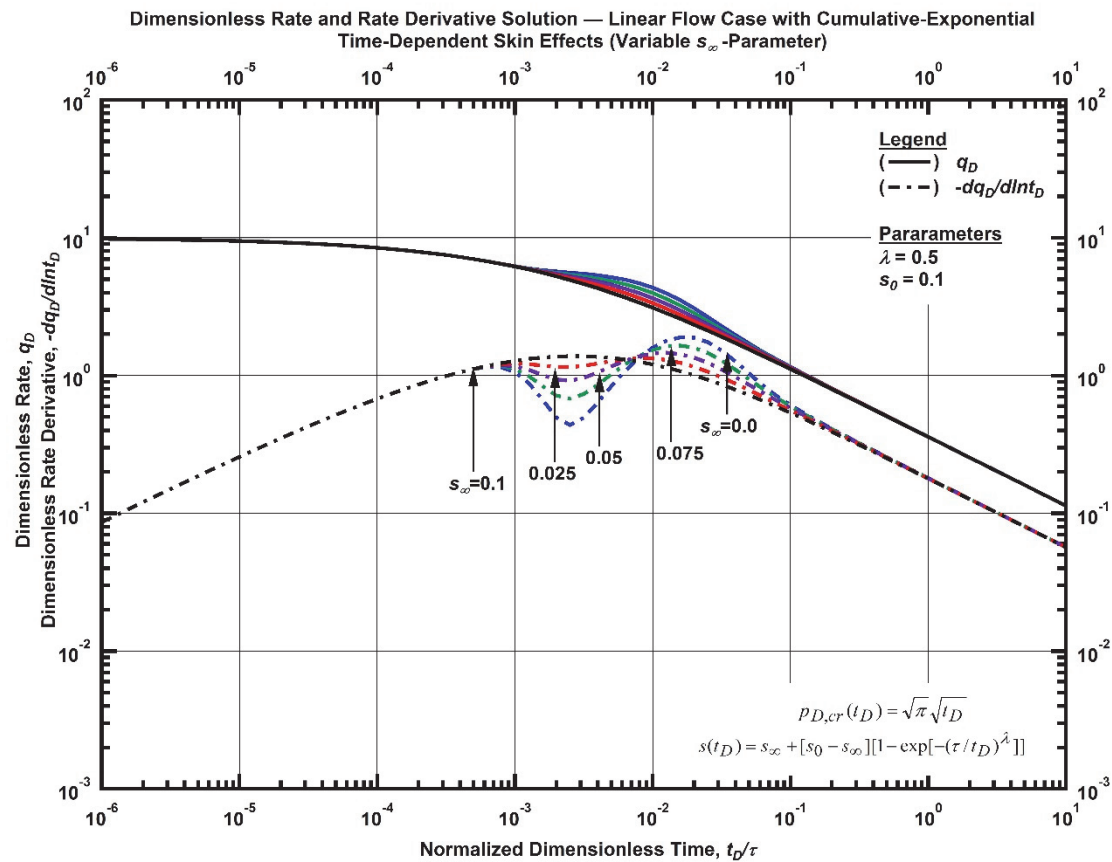


Figure F. 80—Log-log plot (constant pressure dimensionless derivative rate solution) for the linear flow model combined with the cumulative-exponential time-dependent for select values of  $s_\infty$ -parameter.

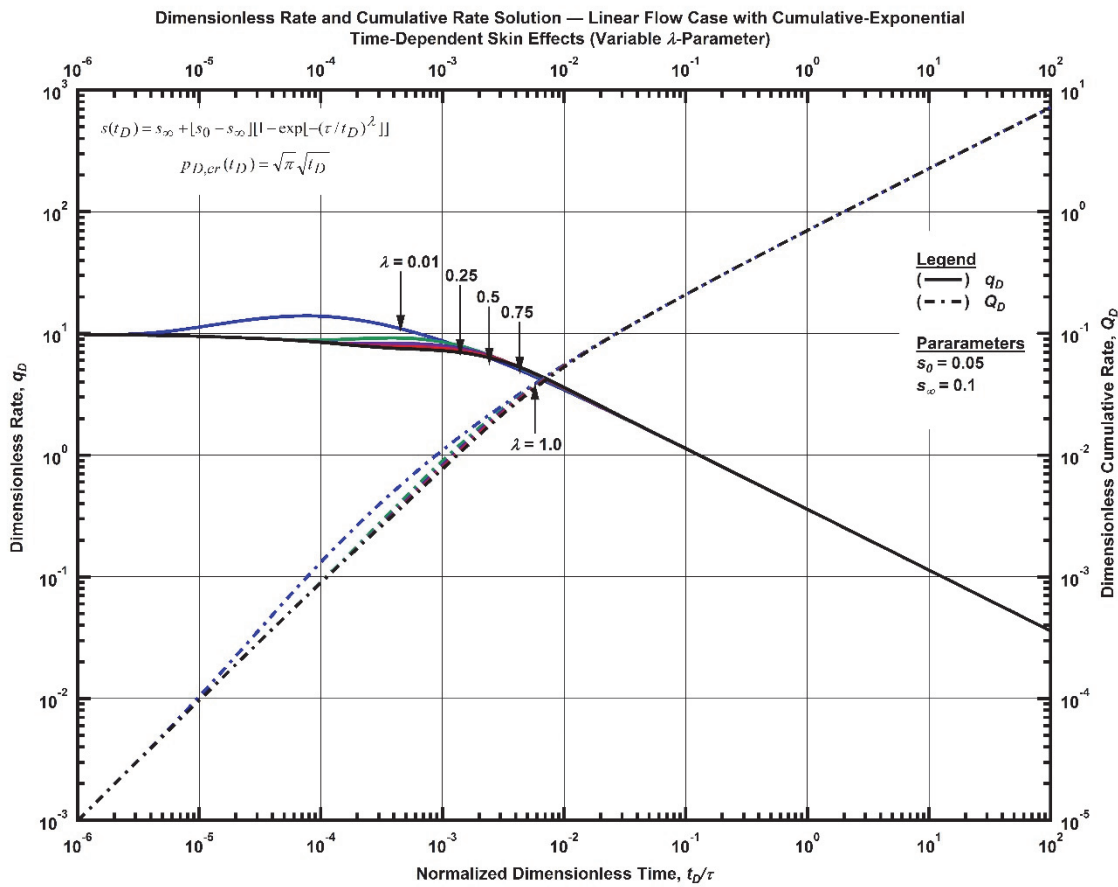


Figure F. 81—Log-log plot (constant pressure dimensionless cumulative production solution) for the linear flow model combined with the cumulative-exponential time-dependent for select values of  $\lambda$ -parameter.

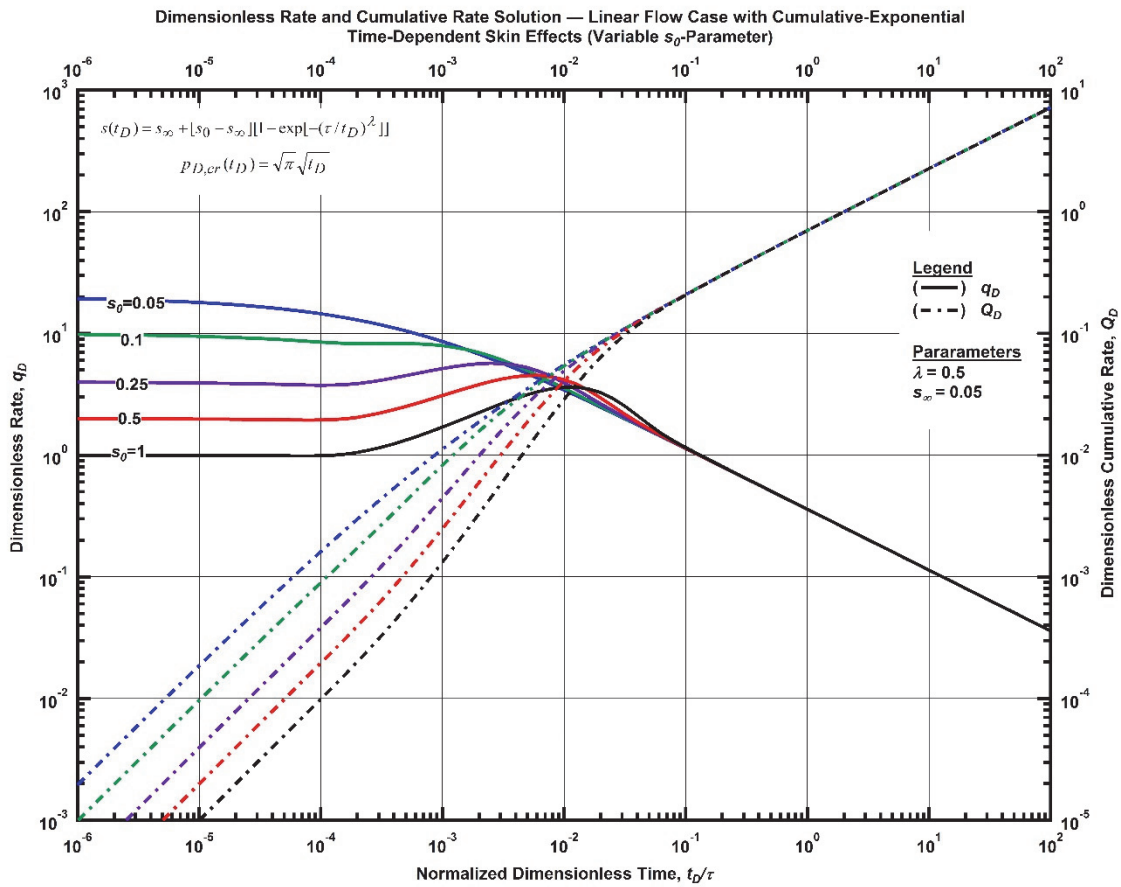


Figure F. 82—Log-log plot (constant pressure dimensionless cumulative production solution) for the linear flow model combined with the cumulative-exponential time-dependent for select values of  $s_0$ -parameter.

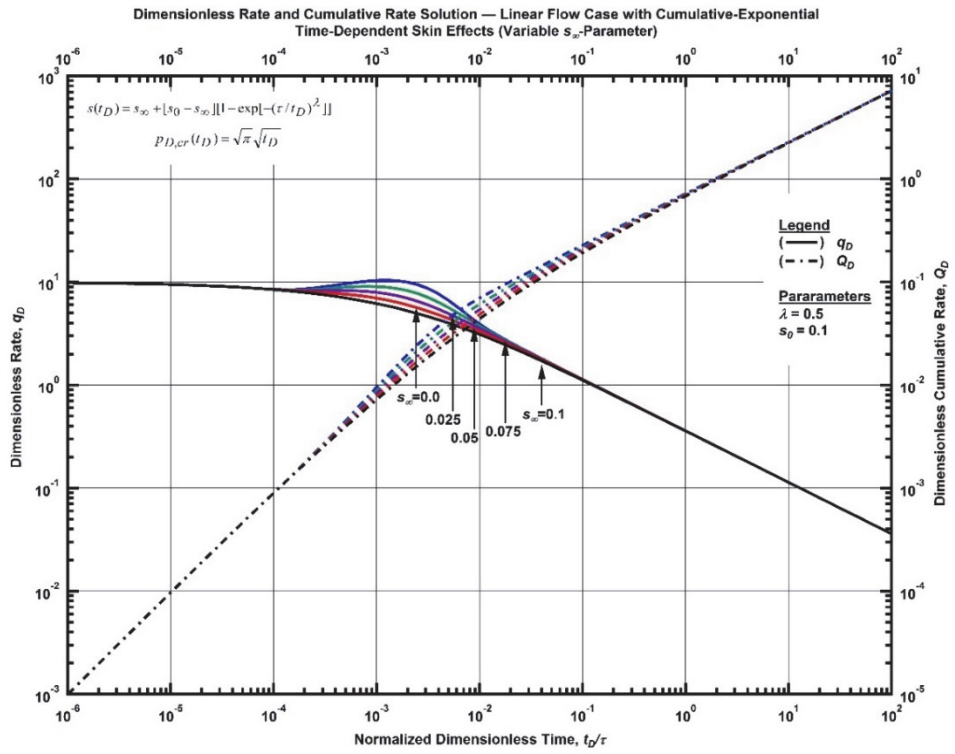


Figure F. 83—Log-log plot (constant pressure dimensionless cumulative production solution) for the linear flow model combined with the cumulative-exponential time-dependent for select values of  $s_\infty$ -parameter.

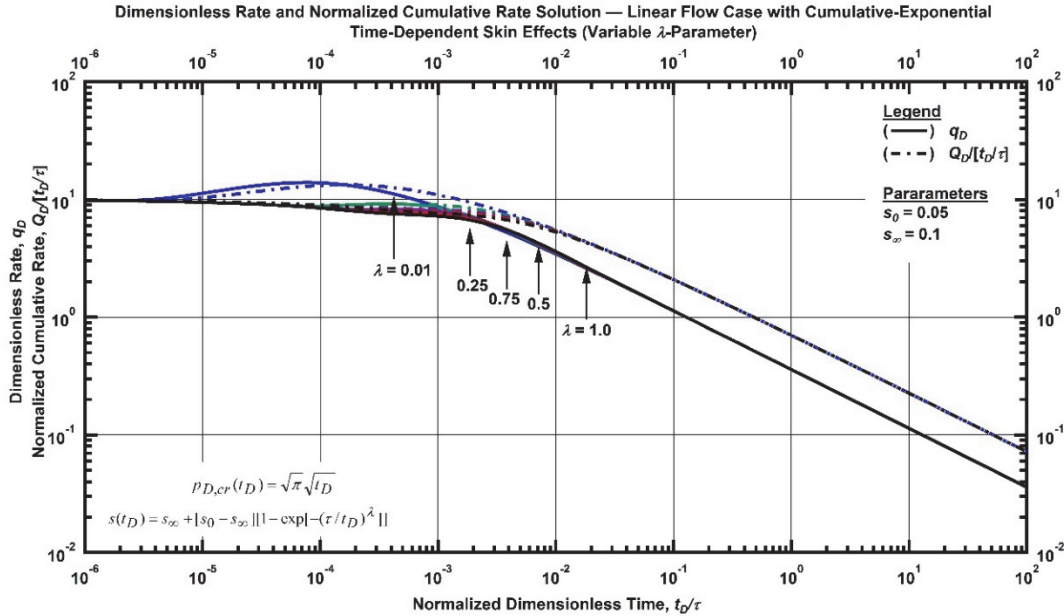


Figure F. 84—Log-log plot (constant pressure time-normalized dimensionless cumulative rate solution) for the linear flow model combined with the cumulative-exponential time-dependent for select values of  $\lambda$ -parameter.

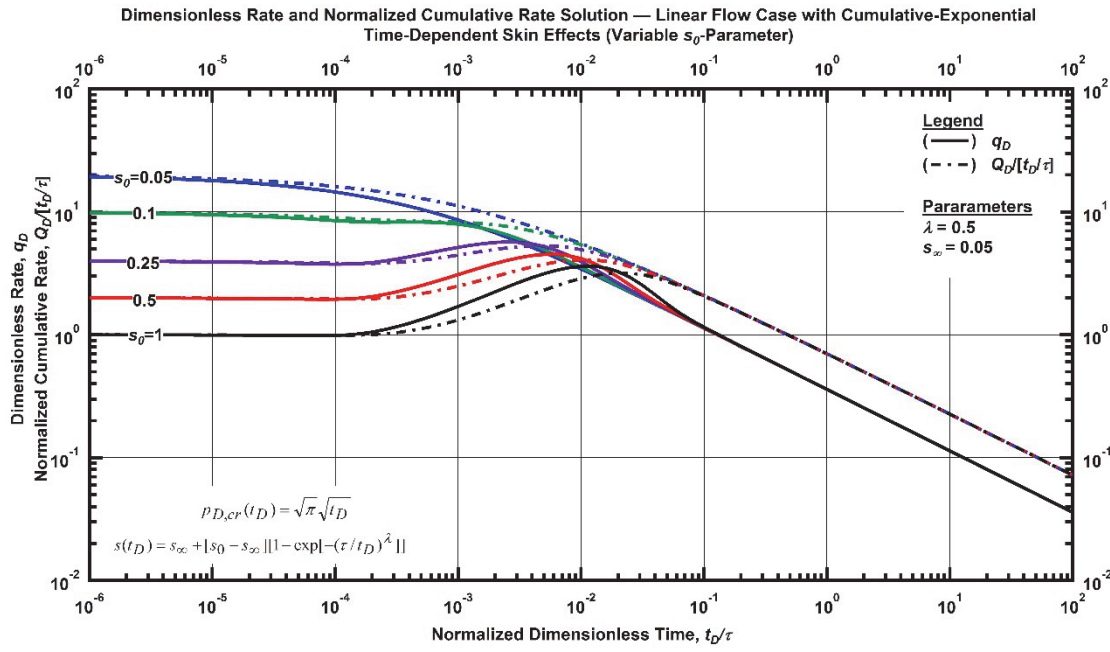


Figure F. 85—Log-log plot (constant pressure time-normalized dimensionless cumulative rate solution) for the linear flow model combined with the cumulative-exponential time-dependent for select values of  $s_0$ -parameter.

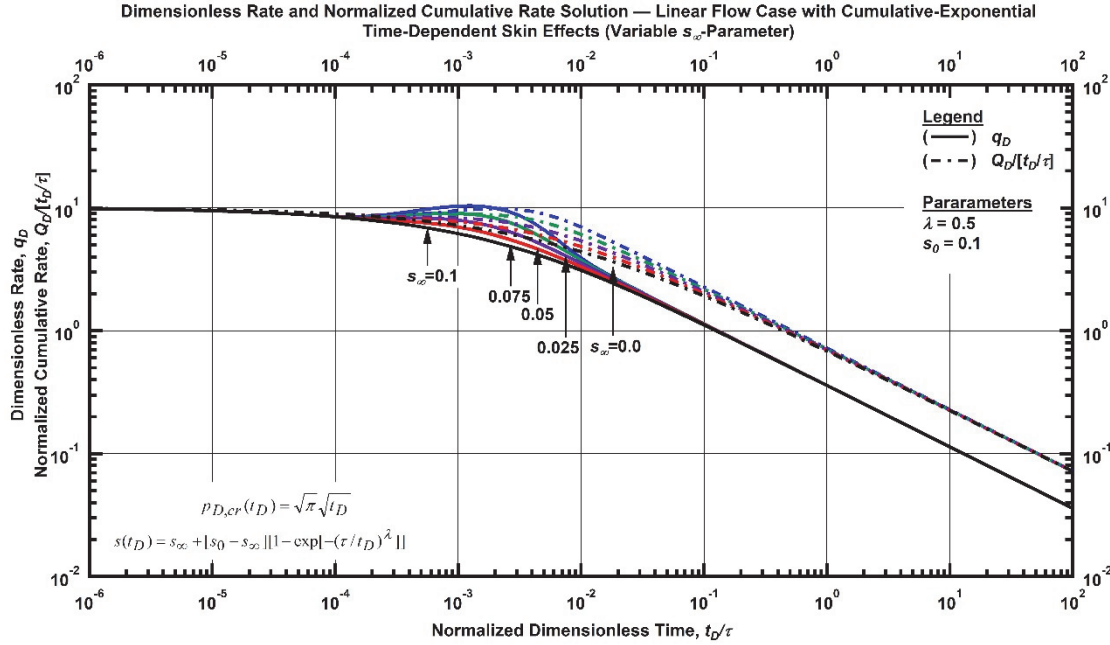


Figure F. 86—Log-log plot (constant pressure time-normalized dimensionless cumulative rate solution) for the linear flow model combined with the cumulative-exponential time-dependent for select values of  $s_\infty$ -parameter.

### Linear Flow Relation with Exponential Time-Dependent Skin Effects

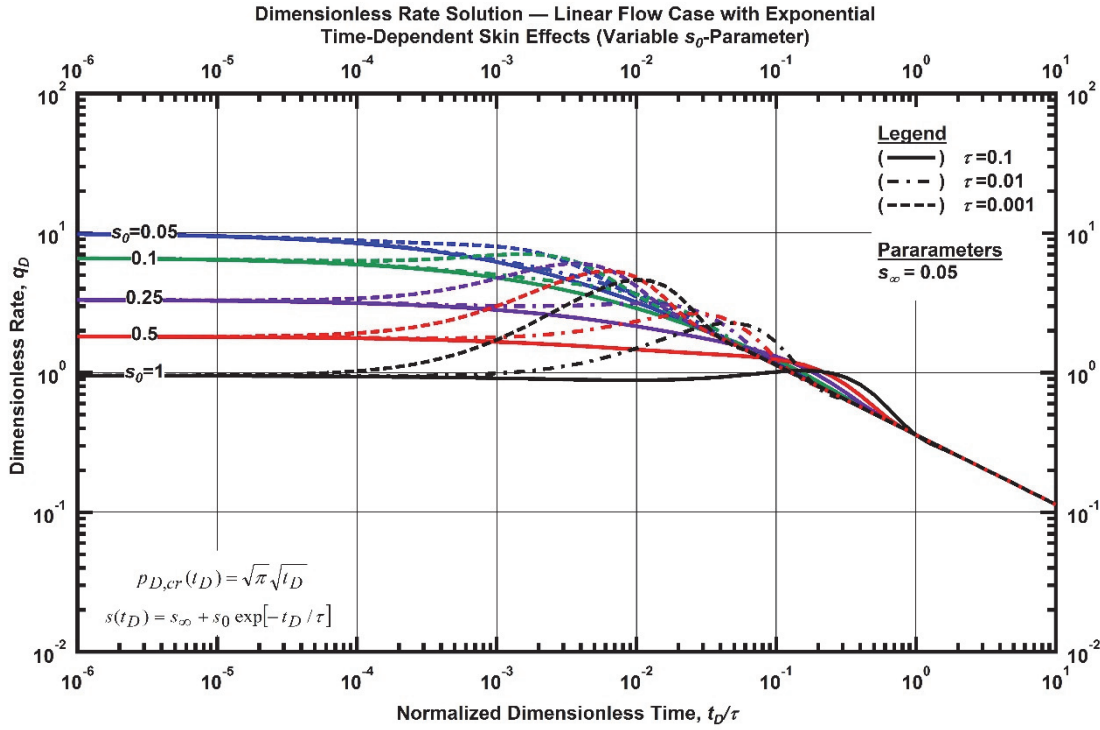


Figure F. 87—Log-log plot (constant pressure dimensionless rate solution) for the linear flow model combined with the exponential time-dependent for select values of  $s_0$ -parameter.

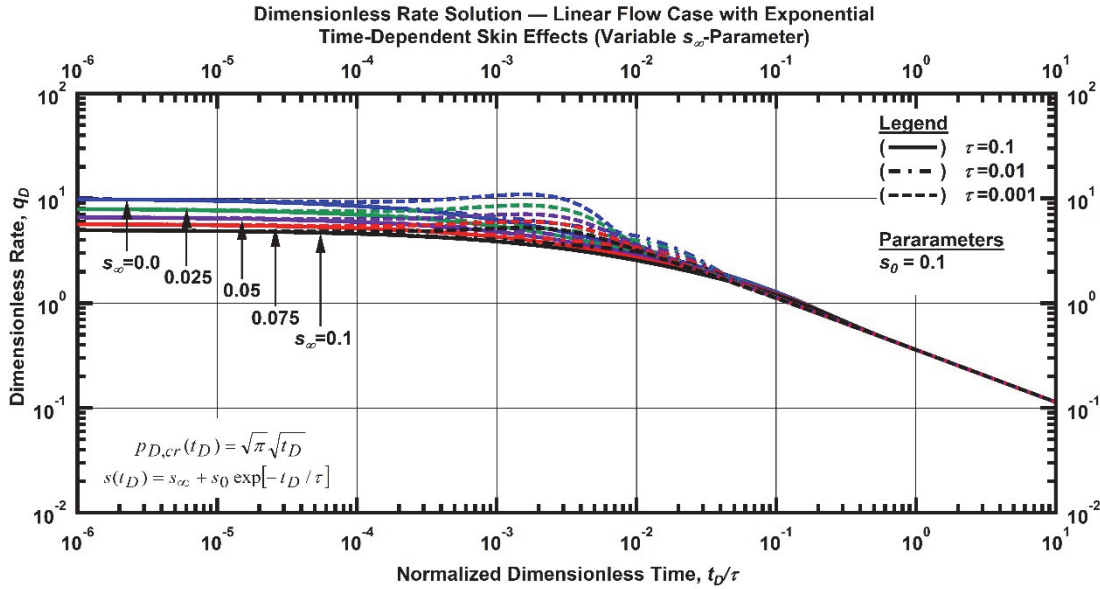


Figure F. 88—Log-log plot (constant pressure dimensionless rate solution) for the linear flow model combined with the exponential time-dependent for select values of  $s_\infty$ -parameter.

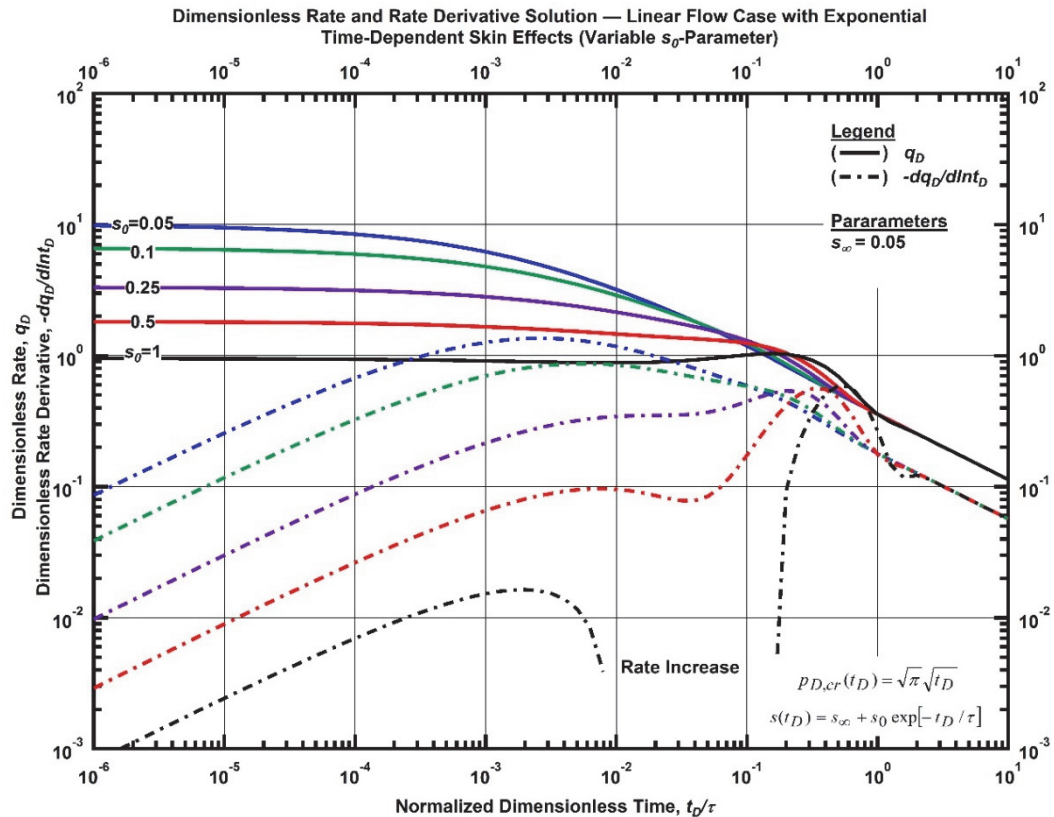


Figure F. 89—Log-log plot (constant pressure dimensionless rate derivative solution) for the linear flow model combined with the exponential time-dependent for select values of  $s_0$ -parameter.

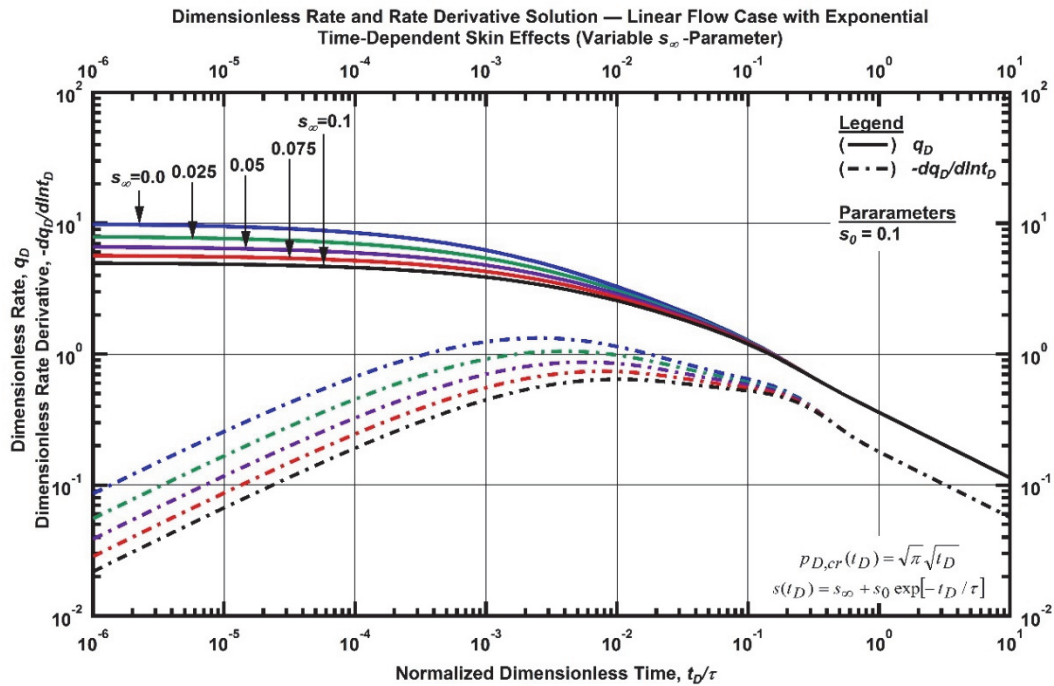


Figure F. 90—Log-log plot (constant pressure dimensionless rate derivative solution) for the linear flow model combined with the exponential time-dependent for select values of  $s_\infty$ -parameter.

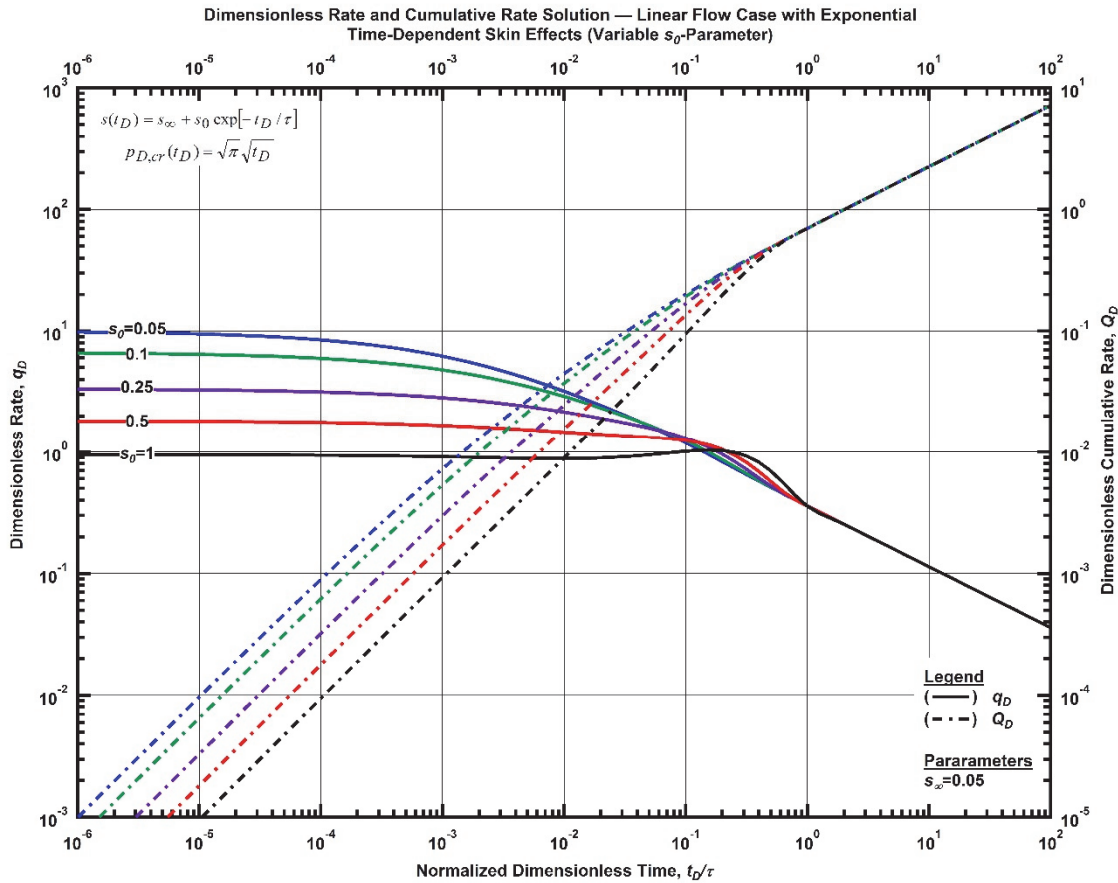


Figure F. 91—Log-log plot (constant pressure dimensionless cumulative production solution) for the linear flow model combined with the exponential time-dependent for select values of  $s_0$ -parameter.

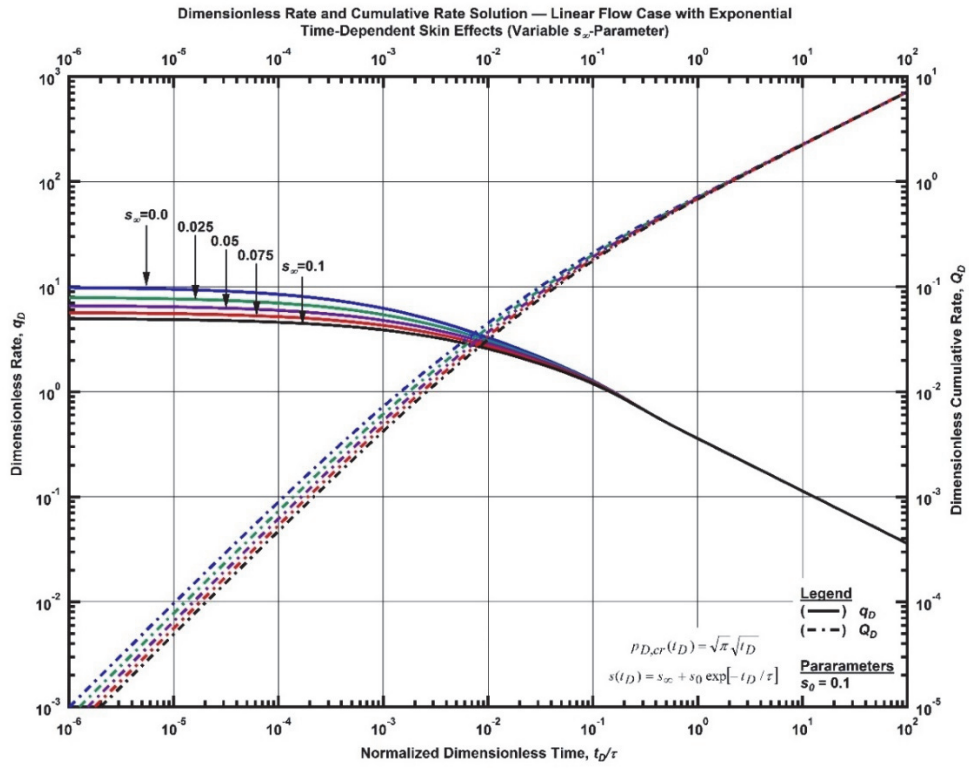


Figure F. 92—Log-log plot (constant pressure dimensionless cumulative production solution) for the linear flow model combined with the exponential time-dependent for select values of  $s_\infty$ -parameter.

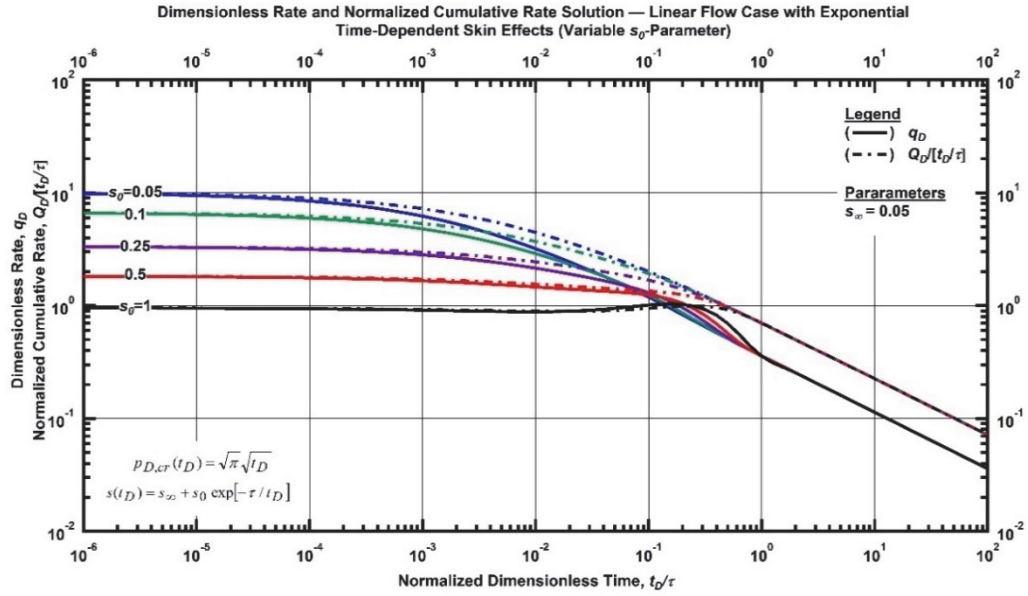


Figure F. 93—Log-log plot (constant pressure time-normalized dimensionless cumulative rate solution) for the linear flow model combined with the exponential time-dependent for select values of  $s_0$ -parameter.

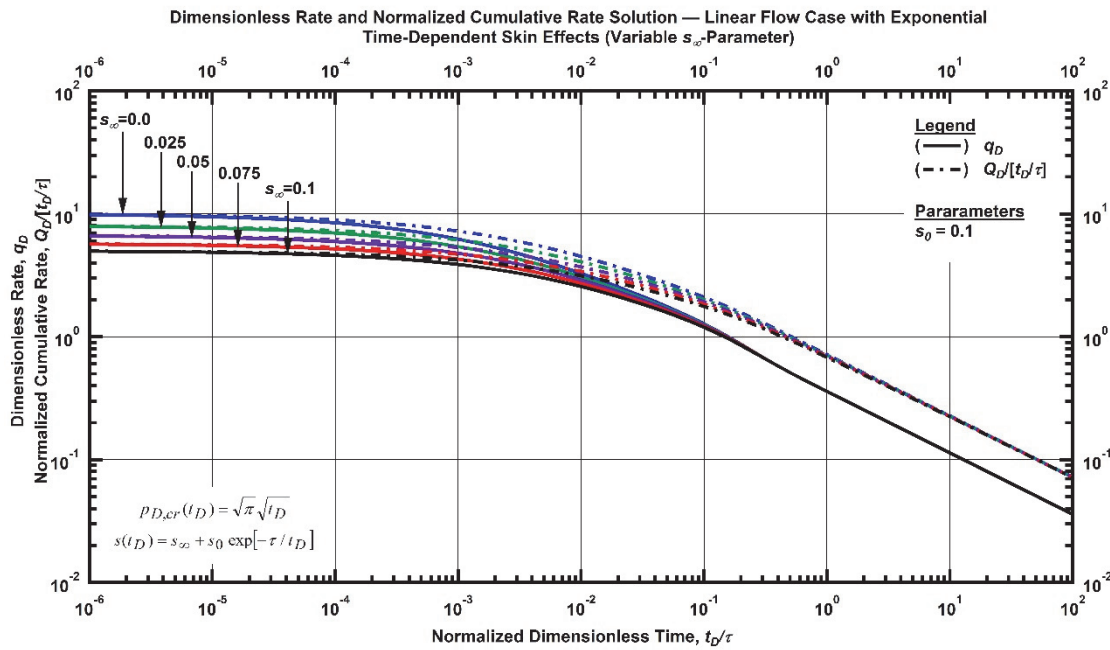


Figure F. 94—Log-log plot (constant pressure time-normalized dimensionless cumulative rate solution) for the linear flow model combined with the exponential time-dependent for select values of  $s_\infty$ -parameter.

#### *Linear Flow Relation with Hyperbolic Time-Dependent Skin Effects*

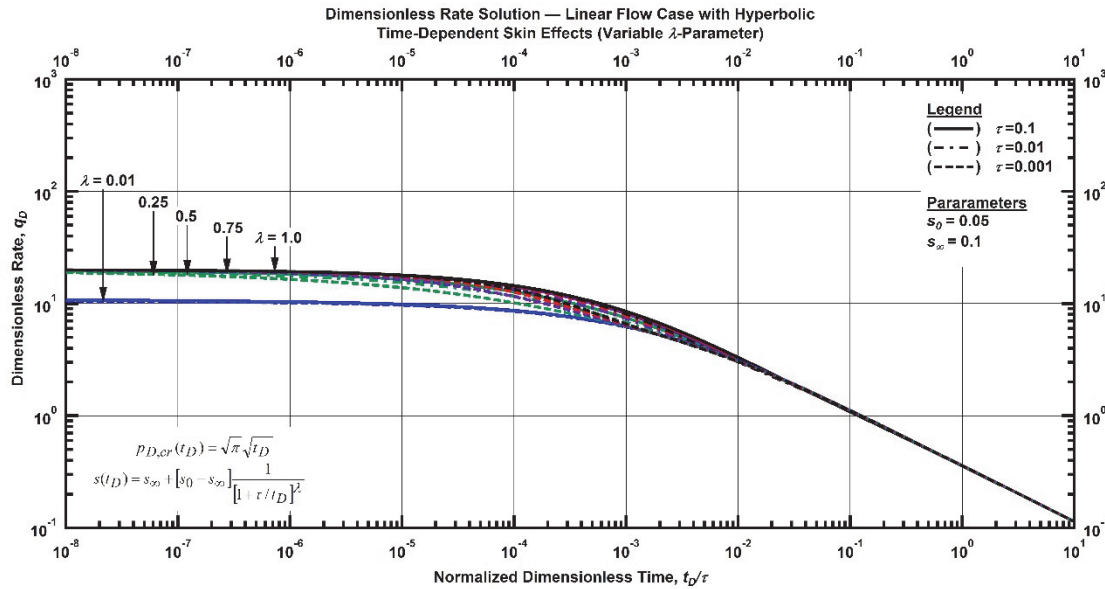


Figure F. 95—Log-log plot (constant pressure dimensionless rate solution) for the linear flow model combined with the hyperbolic time-dependent for select values of  $\lambda$ -parameter.

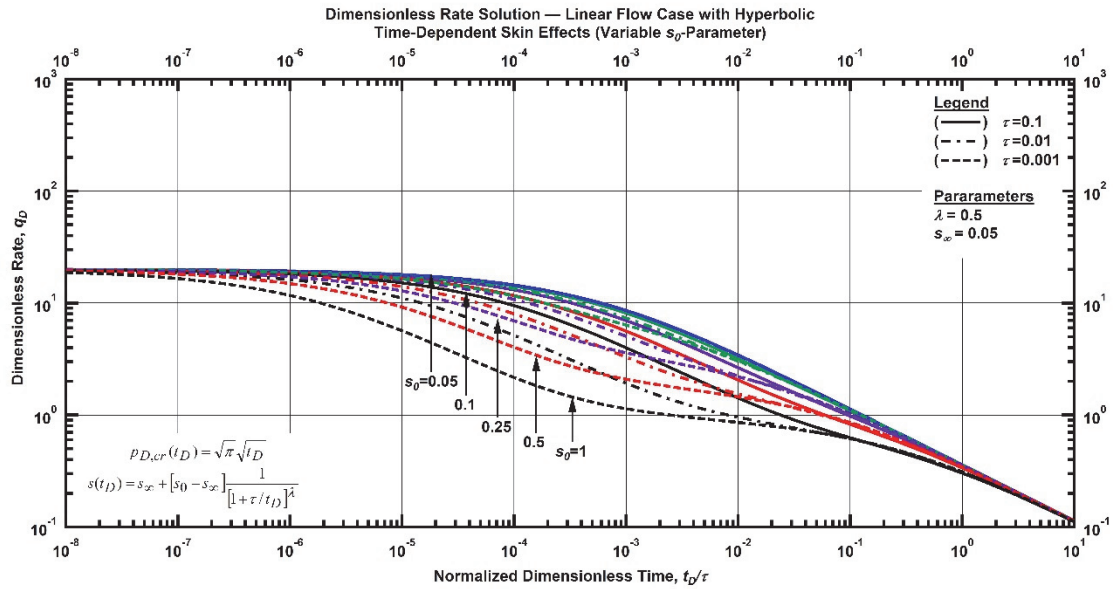


Figure F. 96—Log-log plot (constant pressure dimensionless rate solution) for the linear flow model combined with the hyperbolic time-dependent for select values of  $s_0$ -parameter.

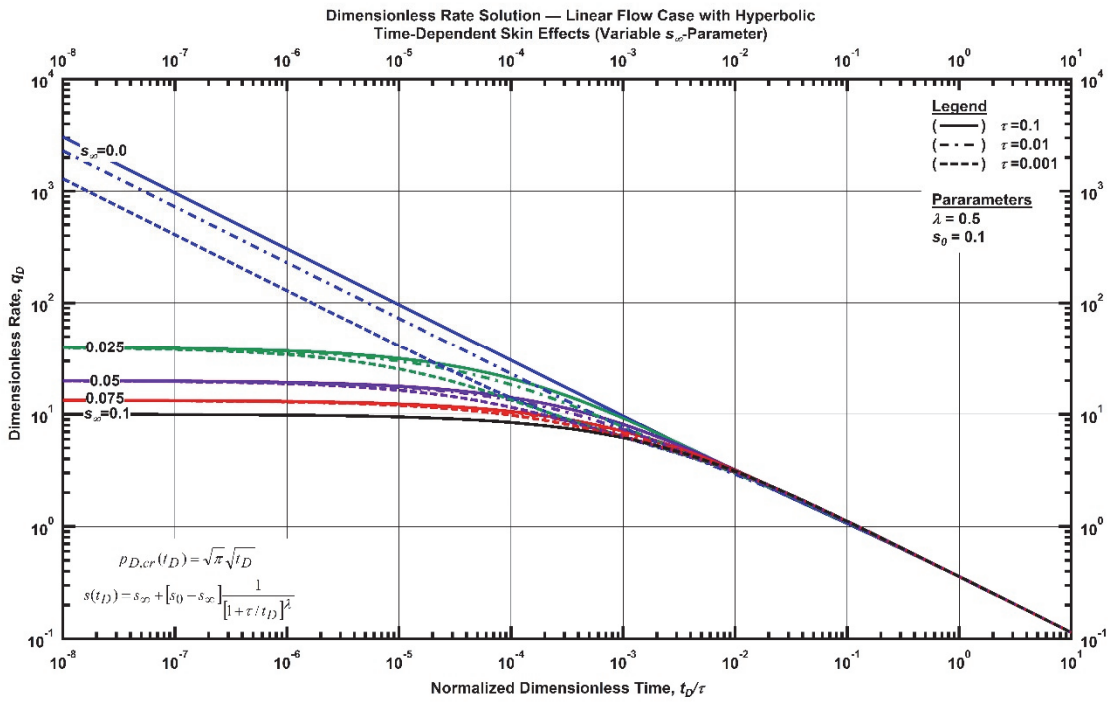


Figure F. 97—Log-log plot (constant pressure dimensionless rate solution) for the linear flow model combined with the hyperbolic time-dependent for select values of  $s_\infty$ -parameter.

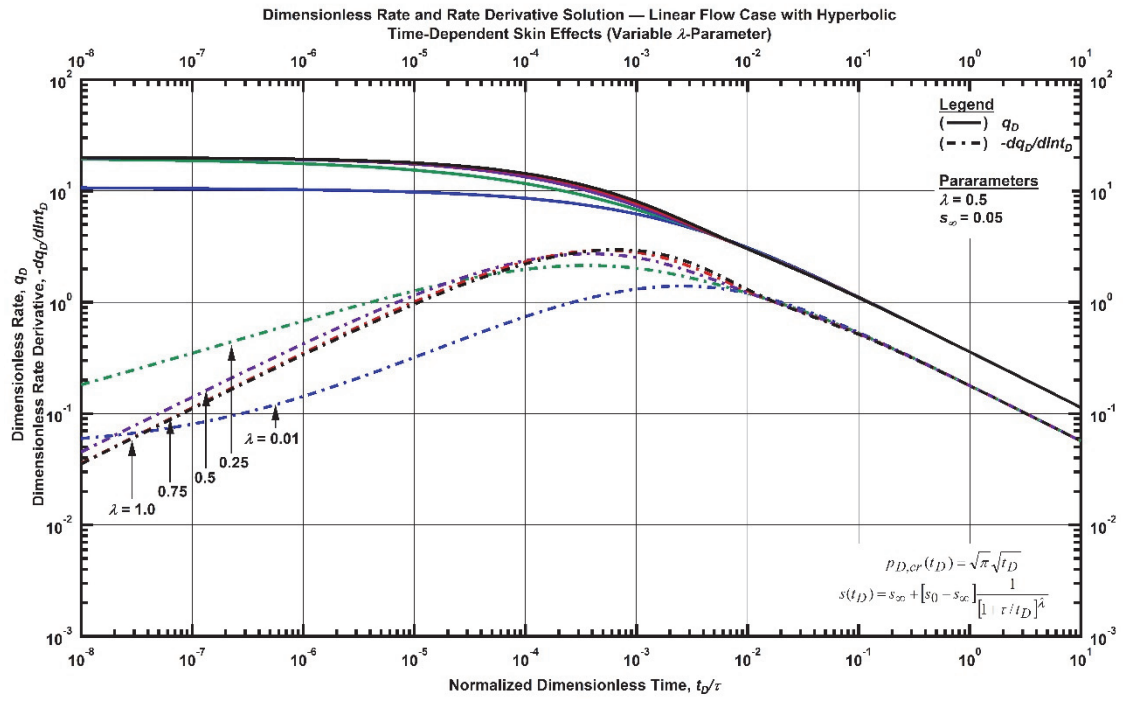


Figure F. 98—Log-log plot (constant pressure dimensionless rate derivative solution) for the linear flow model combined with the hyperbolic time-dependent for select values of  $\lambda$ -parameter.

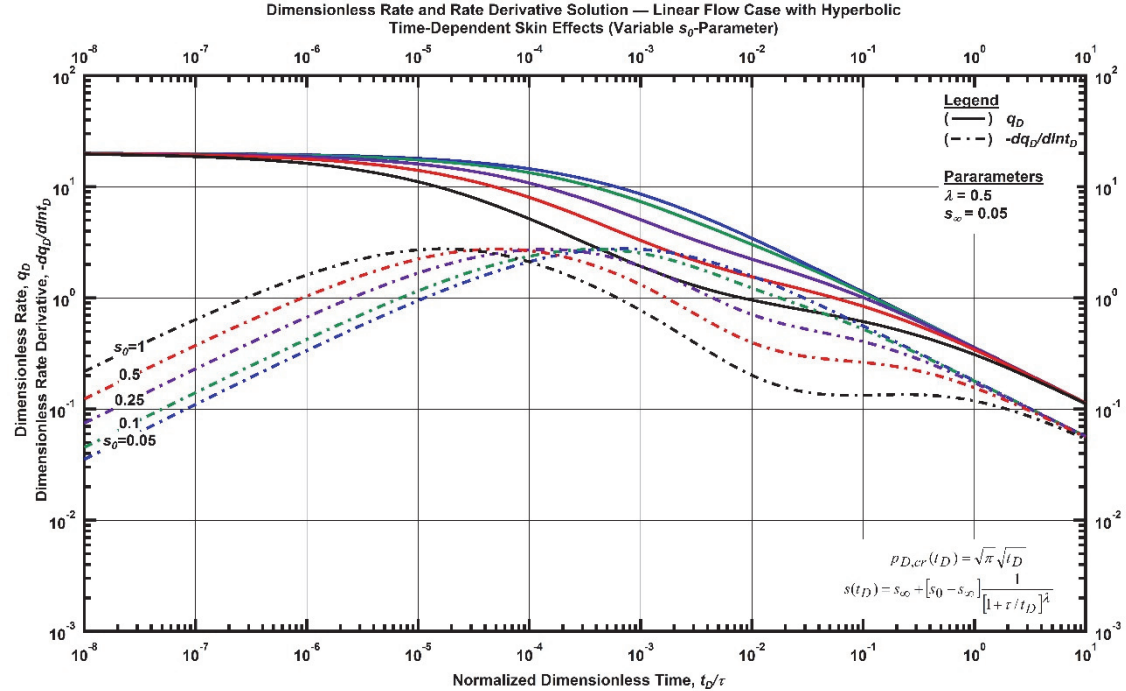


Figure F. 99—Log-log plot (constant pressure dimensionless rate derivative solution) for the linear flow model combined with the hyperbolic time-dependent for select values of  $s_0$ -parameter.

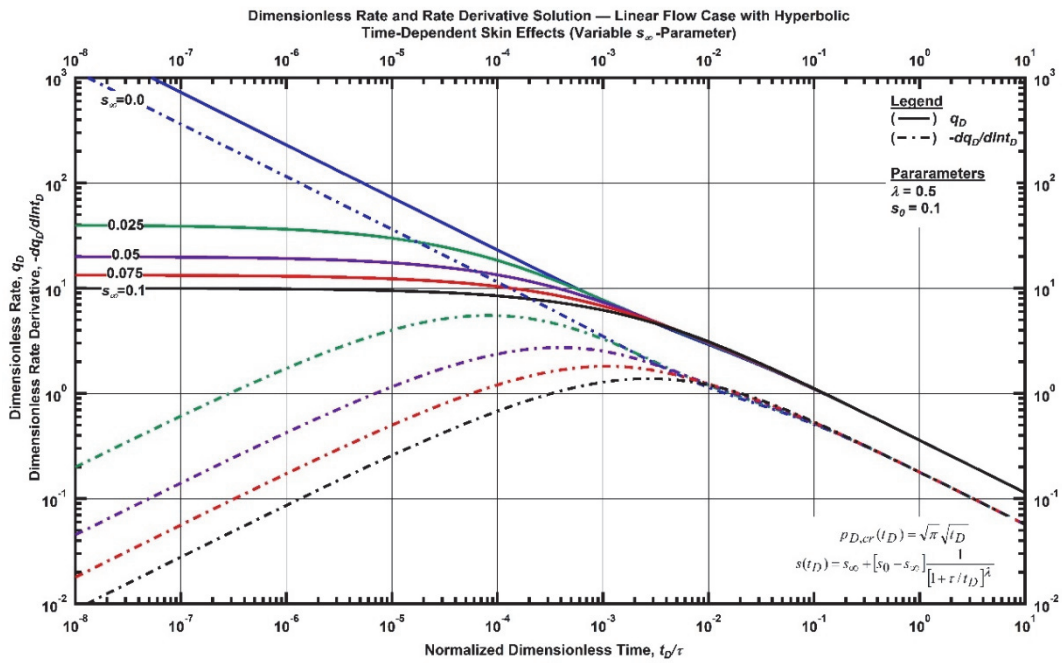


Figure F. 100 — Log-log plot (constant pressure dimensionless rate derivative solution) for the linear flow model combined with the hyperbolic time-dependent for select values of  $s_\infty$ -parameter.

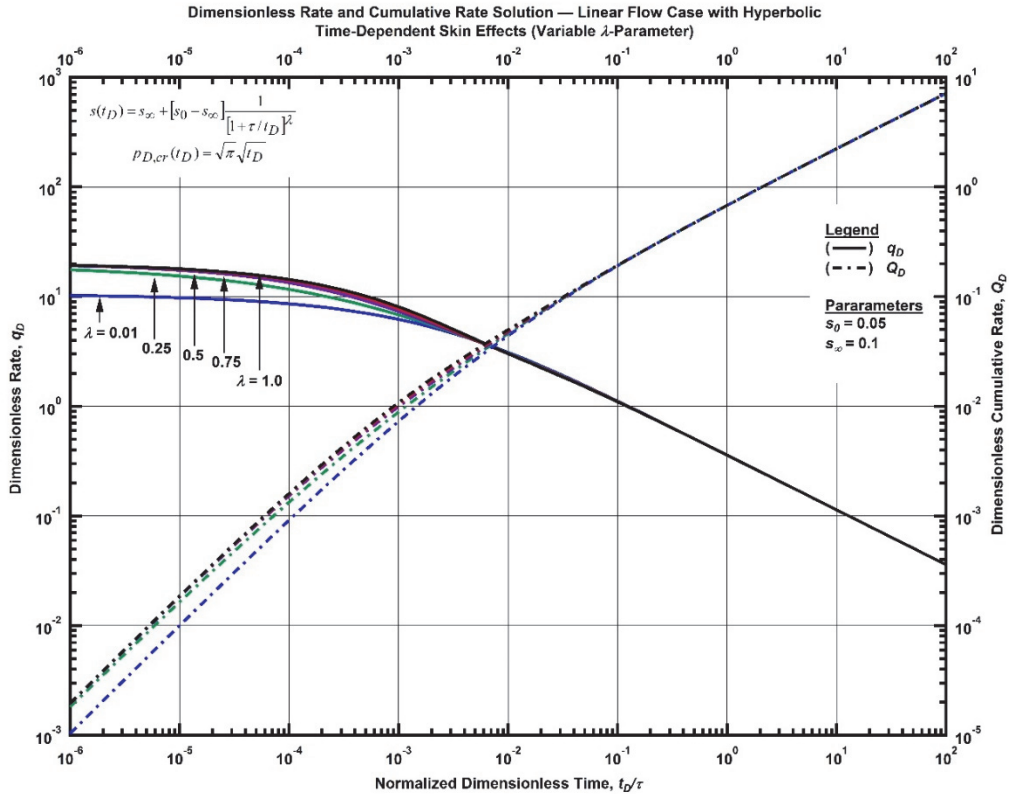


Figure F. 101 — Log-log plot (constant pressure dimensionless cumulative production solution) for the linear flow model combined with the hyperbolic time-dependent for select values of  $\lambda$ -parameter.

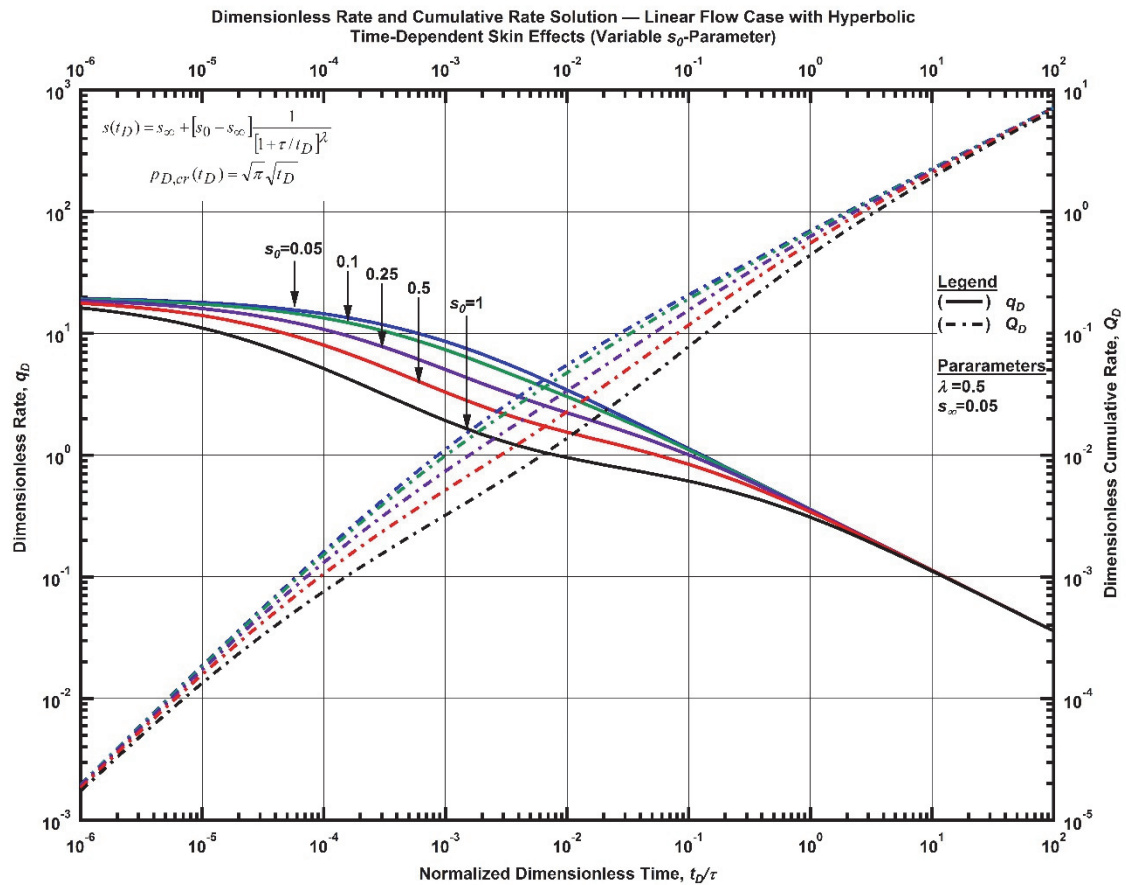


Figure F. 102 — Log-log plot (constant pressure dimensionless cumulative production solution) for the linear flow model combined with the hyperbolic time-dependent for select values of  $s_0$ -parameter.

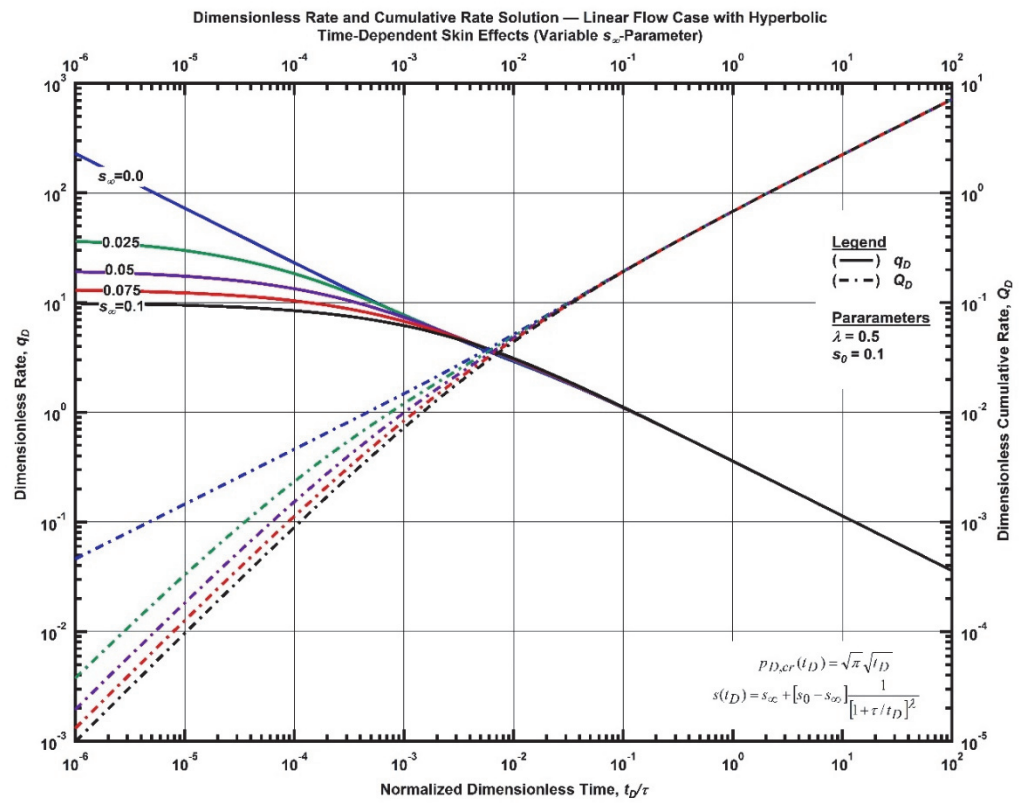


Figure F. 103 — Log-log plot (constant pressure dimensionless cumulative production solution) for the linear flow model combined with the hyperbolic time-dependent for select values of  $s_\infty$ -parameter.

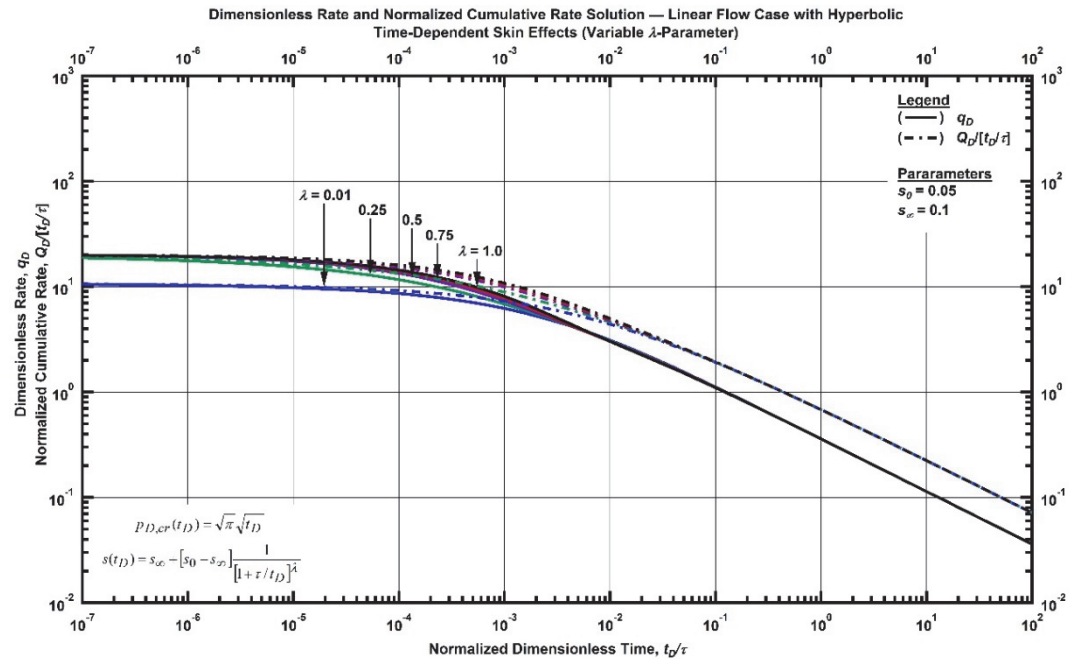


Figure F. 104 — Log-log plot (constant pressure time-normalized dimensionless cumulative rate solution) for the linear flow model combined with the hyperbolic time-dependent for select values of  $\lambda$ -parameter.

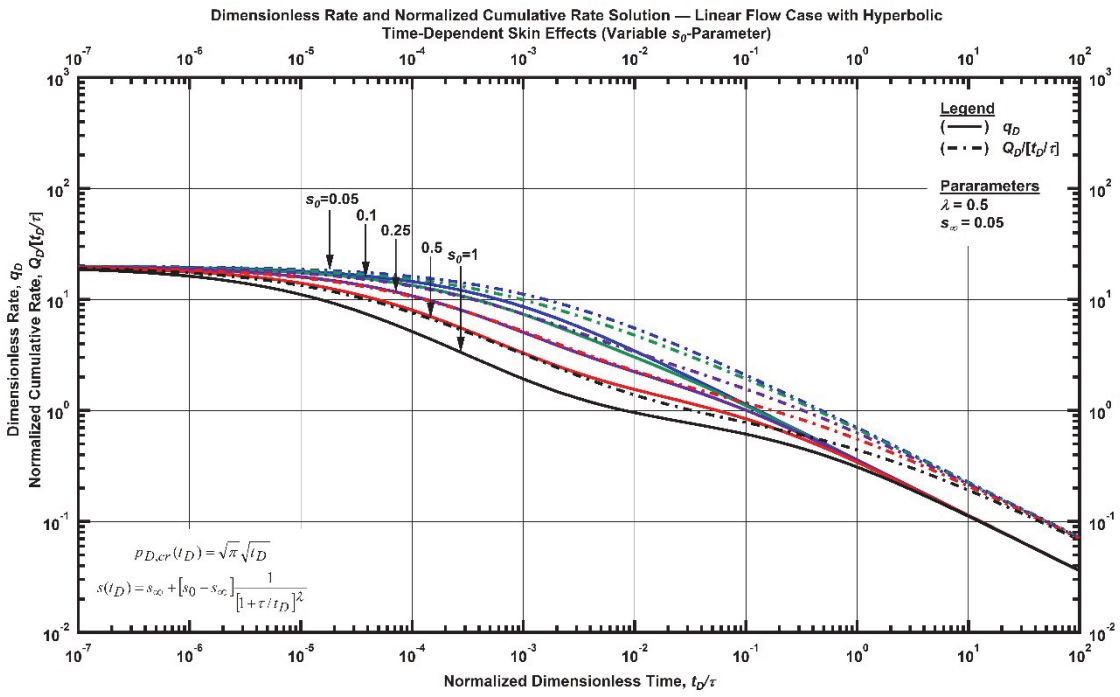


Figure F. 105 — Log-log plot (constant pressure time-normalized dimensionless cumulative rate solution) for the linear flow model combined with the hyperbolic time-dependent for select values of  $s_0$ -parameter.

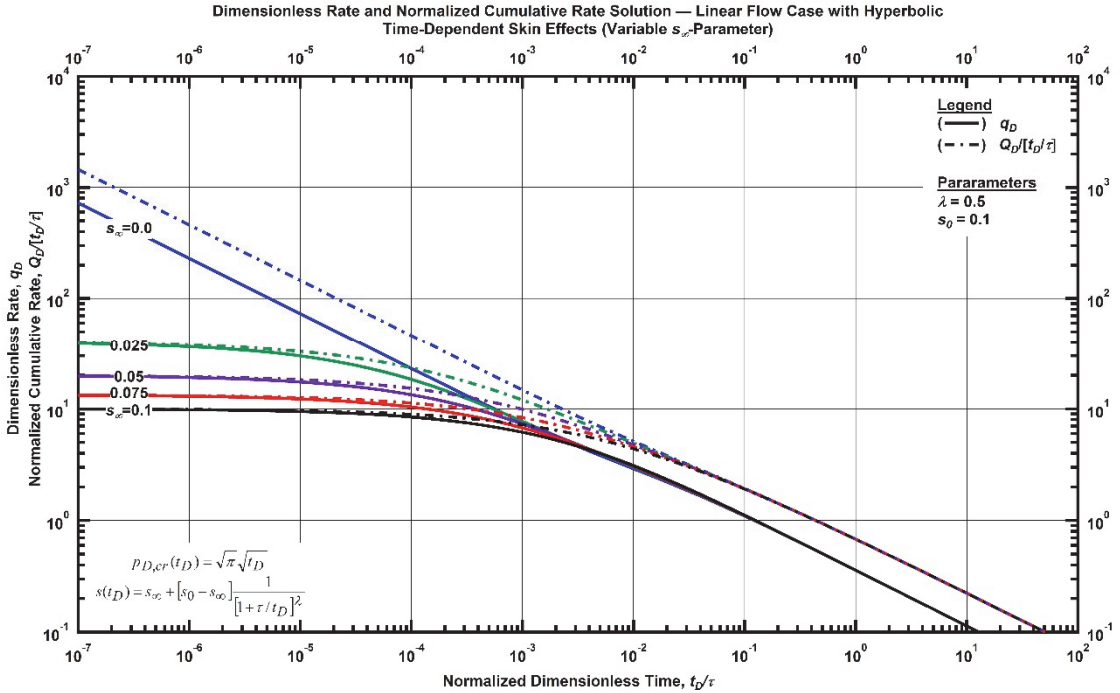


Figure F. 106 — Log-log plot (constant pressure time-normalized dimensionless cumulative rate solution) for the linear flow model combined with the hyperbolic time-dependent for select values of  $s_\infty$ -parameter.

### Linear Flow Relation with Time-Dependent Wellbore Storage

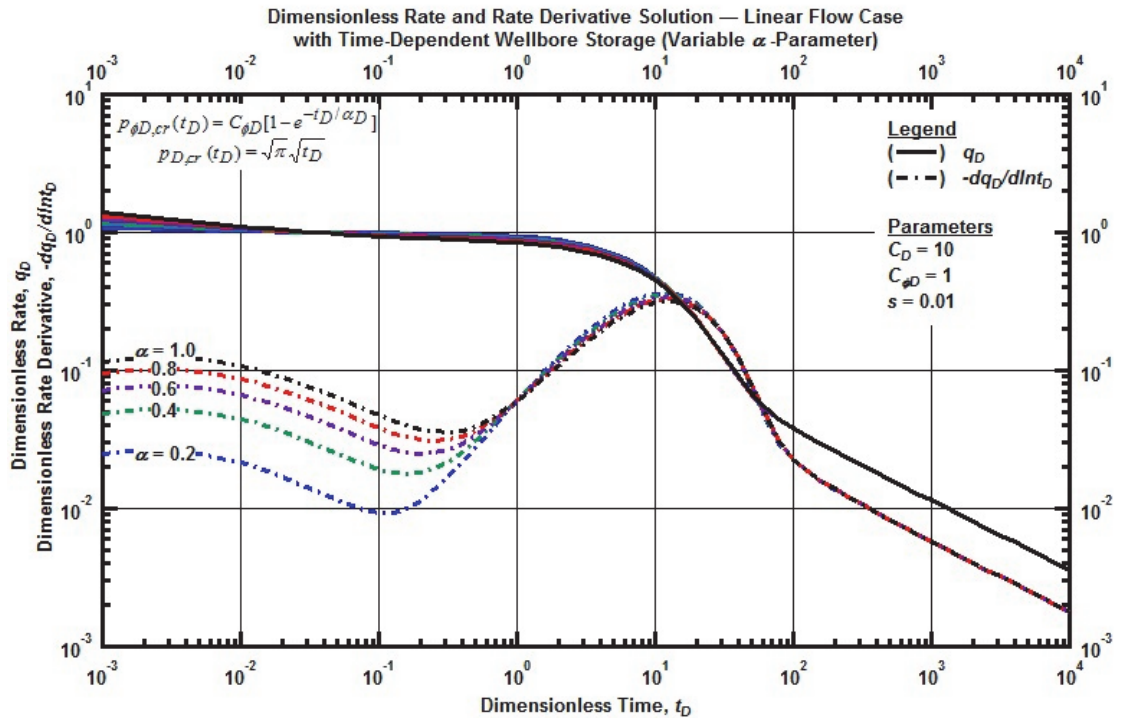


Figure F. 107 — Log-log plot (constant pressure dimensionless rate solution) for the linear flow model combined with the time-dependent wellbore storage for select values of  $\alpha$ -parameter.

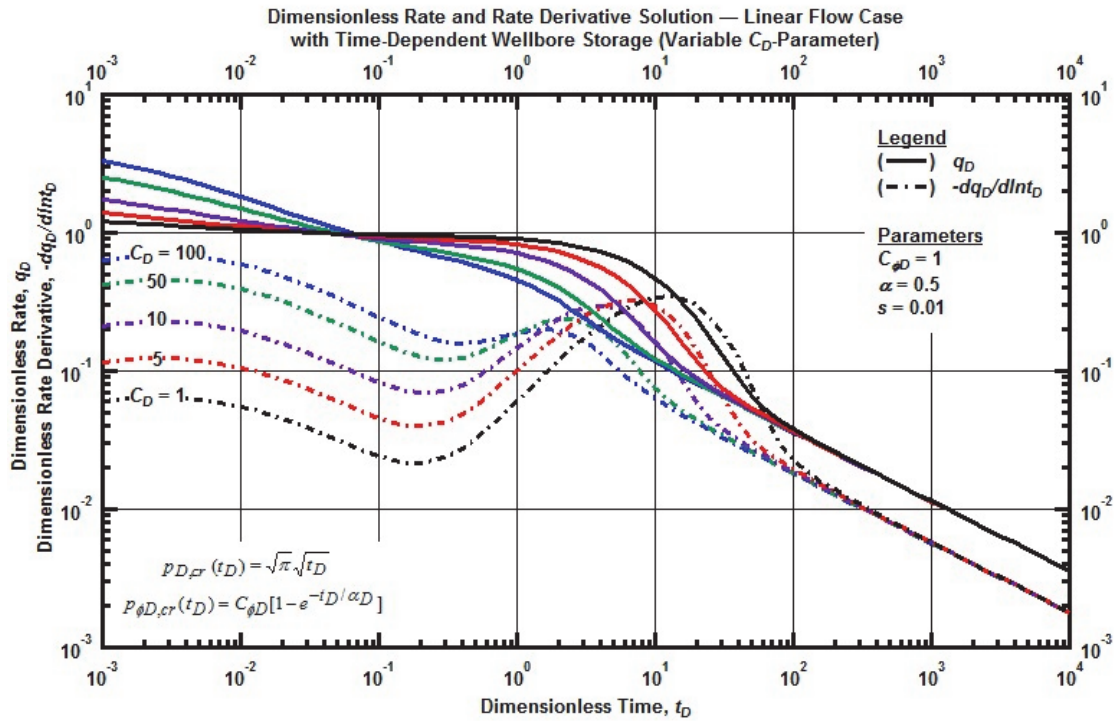


Figure F. 108 — Log-log plot (constant pressure dimensionless rate solution) for the linear flow model combined with the time-dependent wellbore storage for select values of the dimensionless wellbore storage constant.

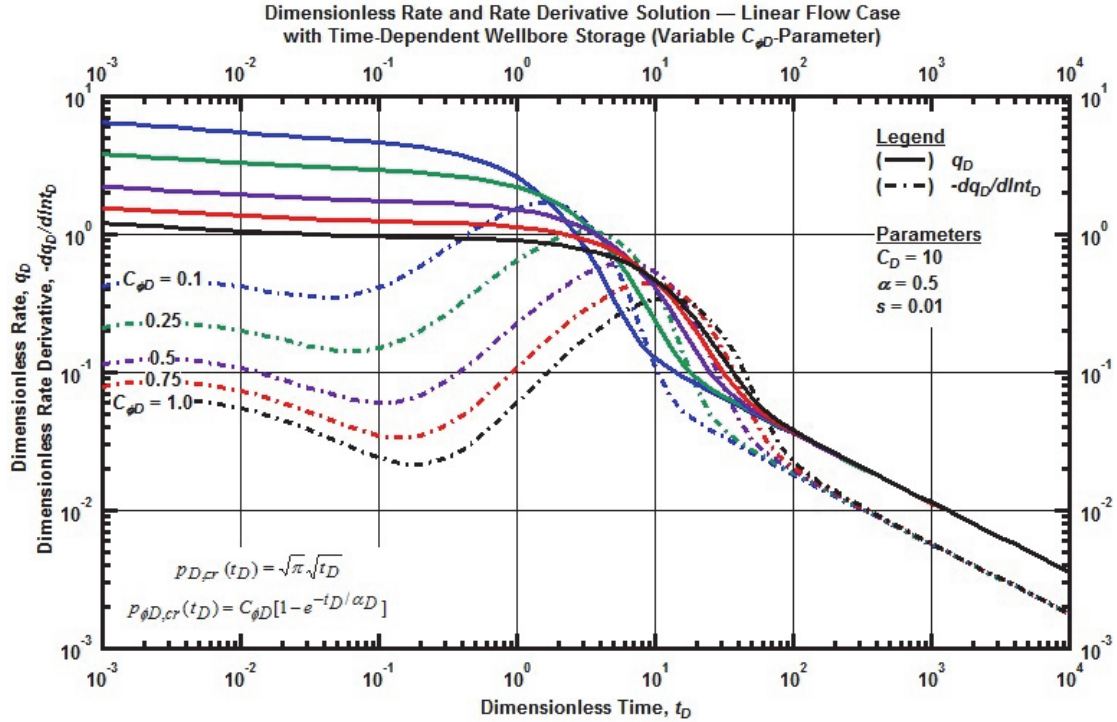


Figure F. 109 — Log-log plot (constant pressure dimensionless rate solution) for the linear flow model combined with the time-dependent wellbore storage for select phase redistribution constant.

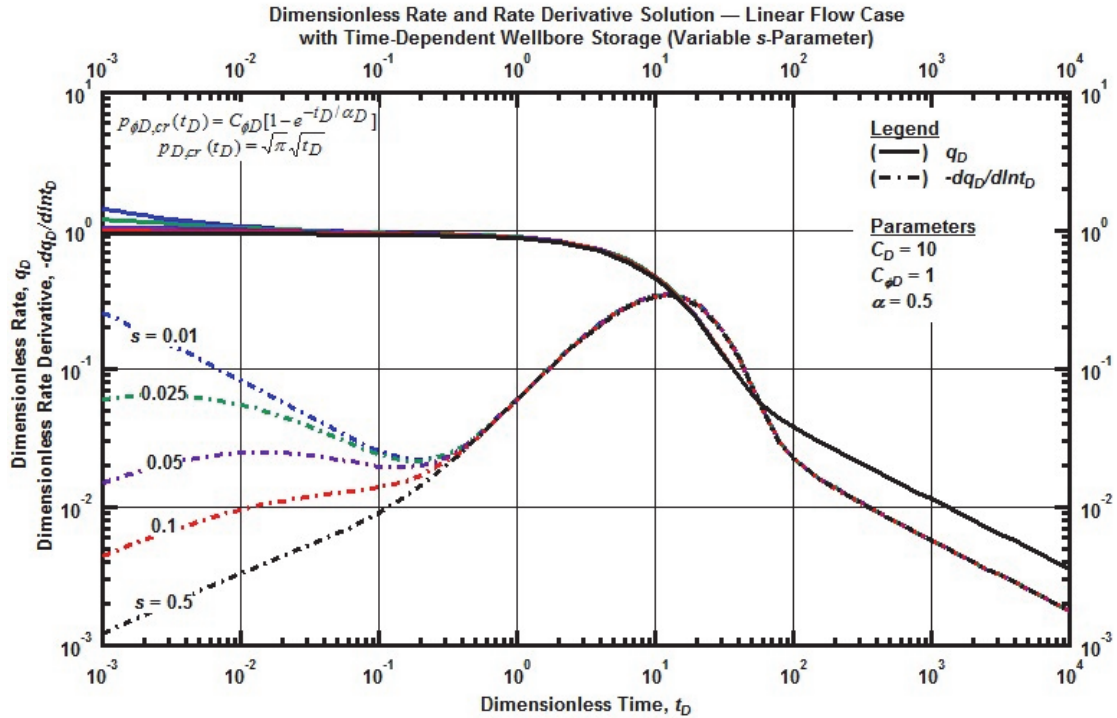


Figure F. 110 — Log-log plot (constant pressure dimensionless rate solution) for the linear flow model combined with the time-dependent wellbore storage for select dimensionless constant skin factor.

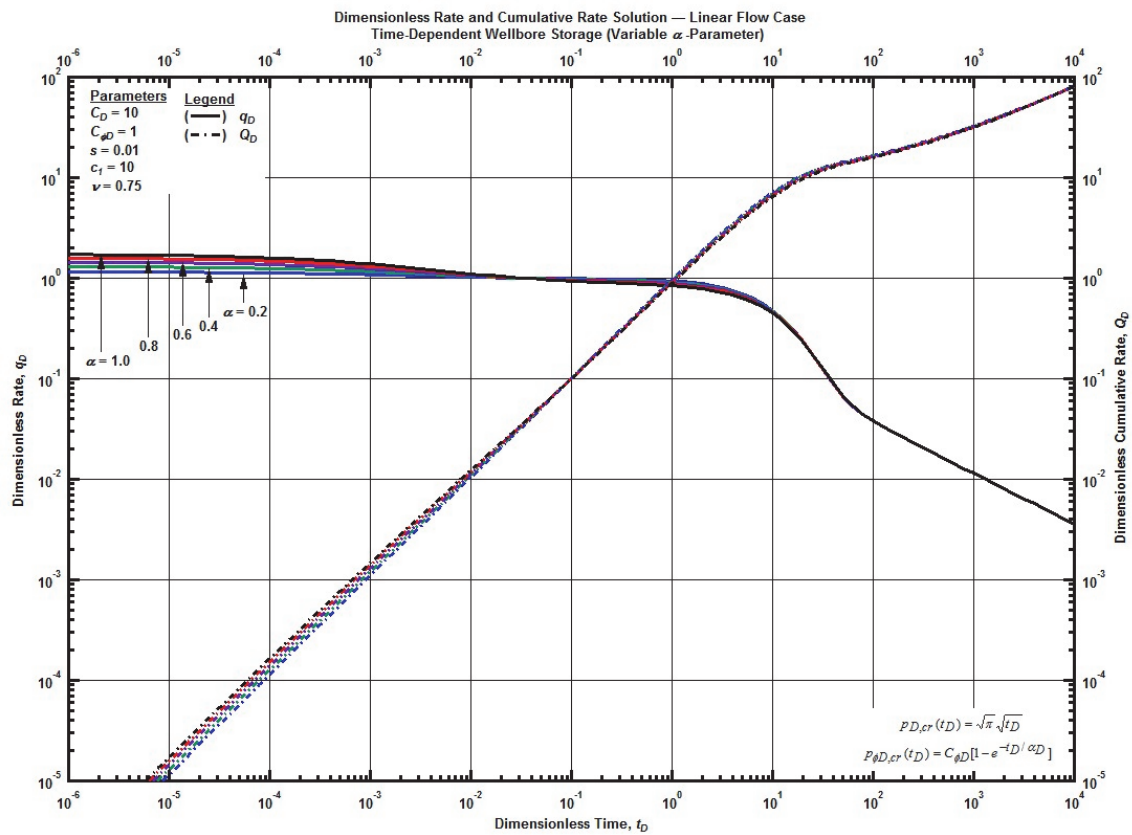


Figure F. 111 — Log-log plot (constant pressure dimensionless cumulative production solution) for the linear flow model combined with the time-dependent wellbore storage for select values of  $\alpha$ -parameter.

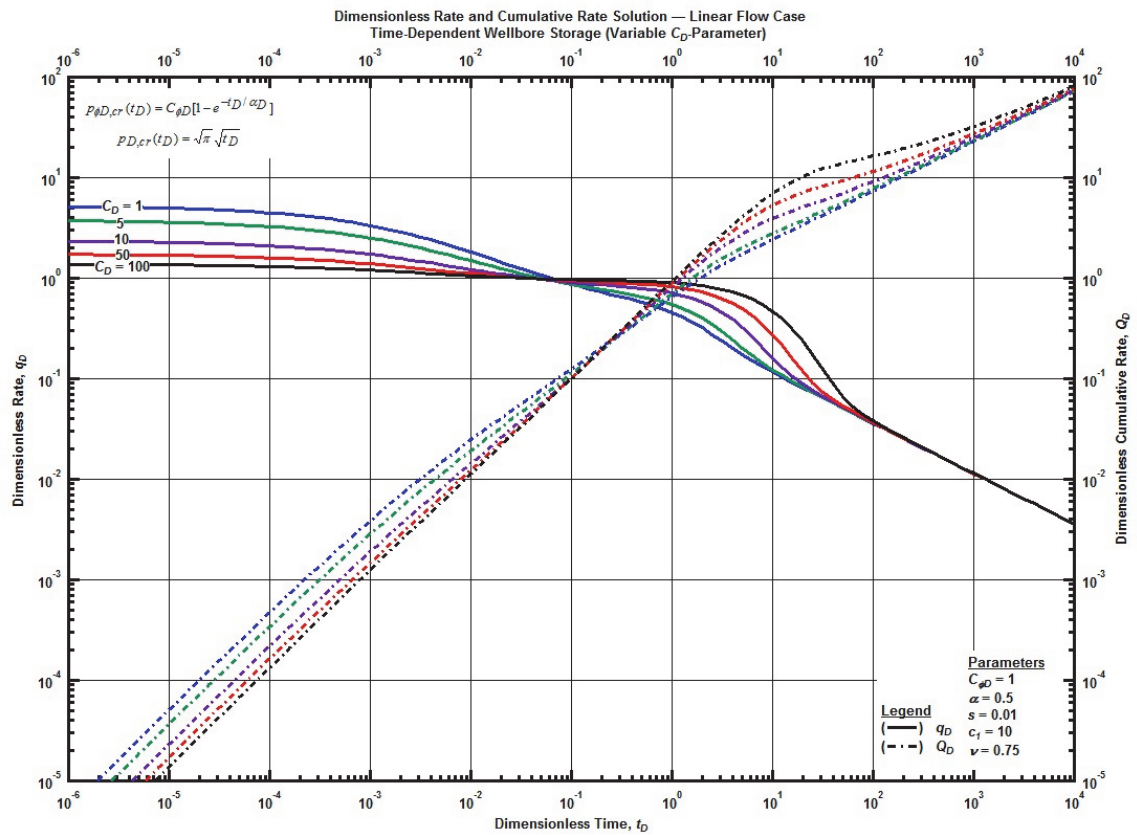


Figure F. 112 — Log-log plot (constant pressure dimensionless cumulative production solution) for the linear flow model combined with the time-dependent wellbore storage for select values of the dimensionless wellbore storage constant.

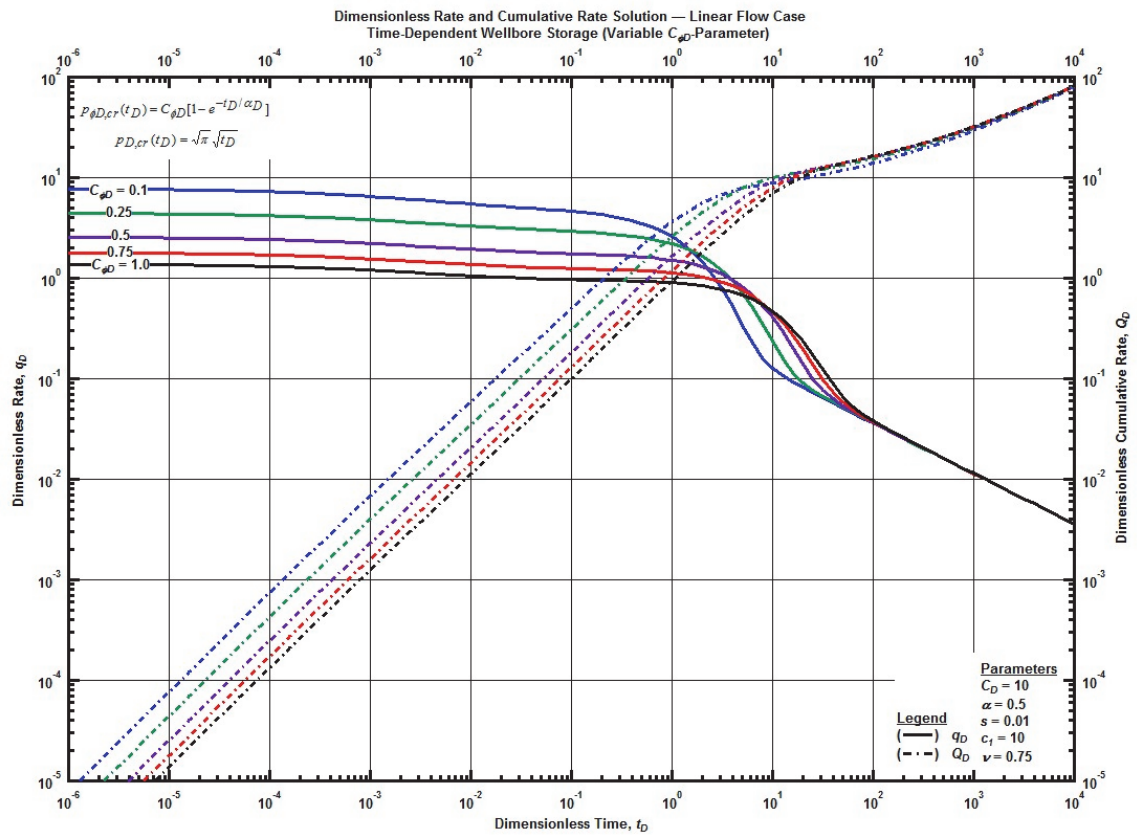


Figure F. 113 — Log-log plot (constant pressure dimensionless cumulative production solution) for the linear flow model combined with the time-dependent wellbore storage for select values phase redistribution constant.

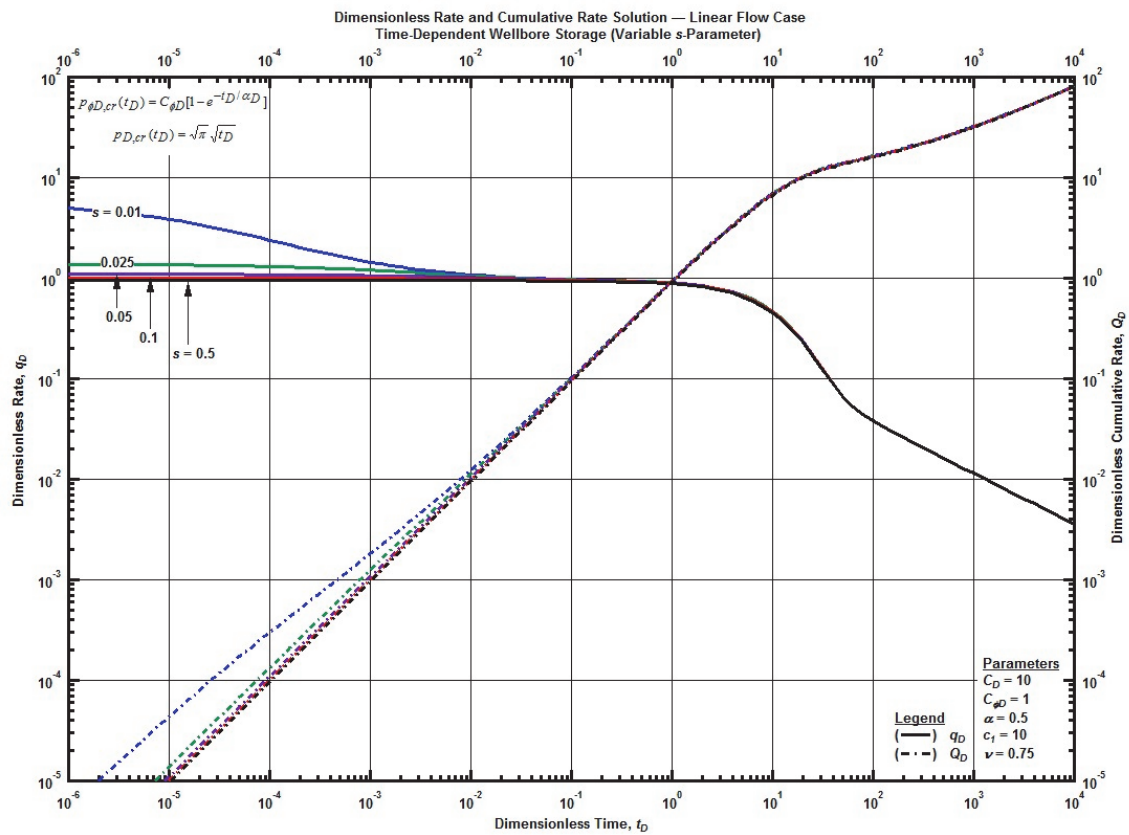


Figure F. 114 — Log-log plot (constant pressure dimensionless cumulative production solution) for the linear flow model combined with the time-dependent wellbore storage for select dimensionless constant skin factor.

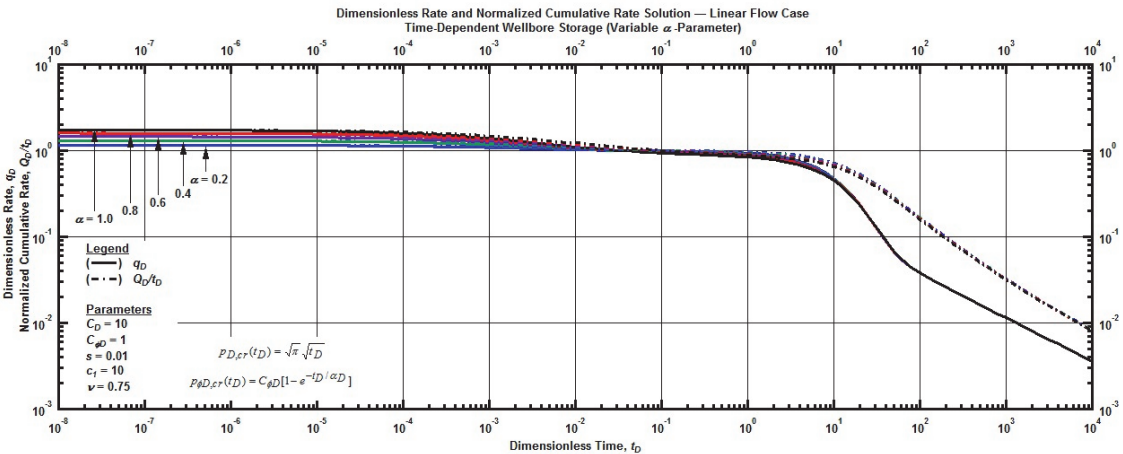


Figure F. 115 — Log-log plot (constant pressure time-normalized dimensionless cumulative rate solution) for the linear flow model combined with the time-dependent wellbore storage for select values of  $\alpha$ -parameter.

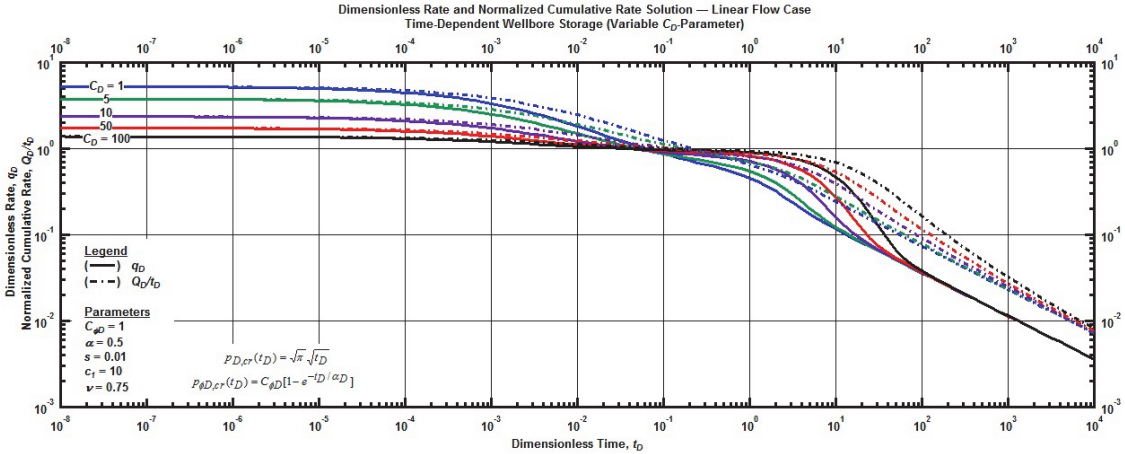


Figure F. 116 — Log-log plot (constant pressure time-normalized dimensionless cumulative rate solution) for the linear flow model combined with the time-dependent wellbore storage for select values of the dimensionless wellbore storage constant.

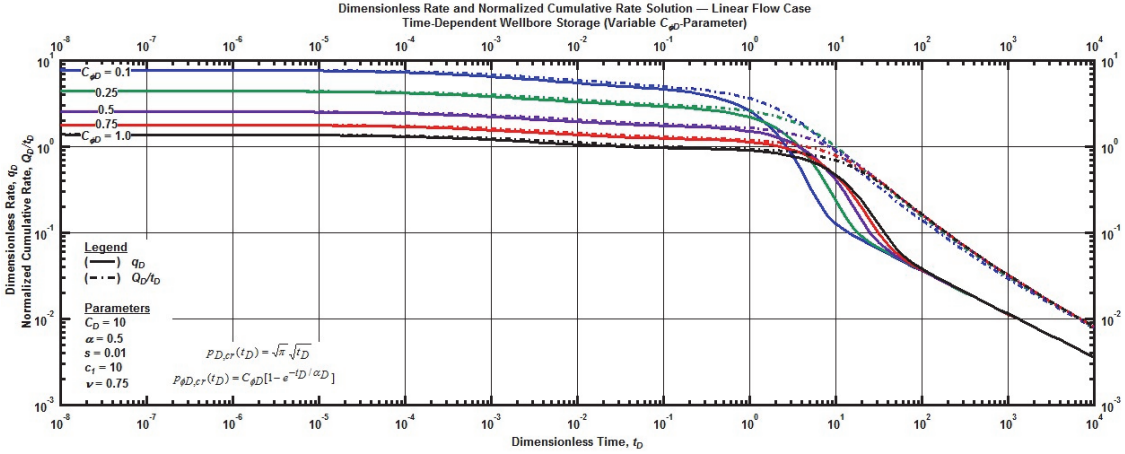


Figure F. 117 — Log-log plot (constant pressure time-normalized dimensionless cumulative rate solution) for the linear flow model combined with the time-dependent wellbore storage for select values phase redistribution constant.

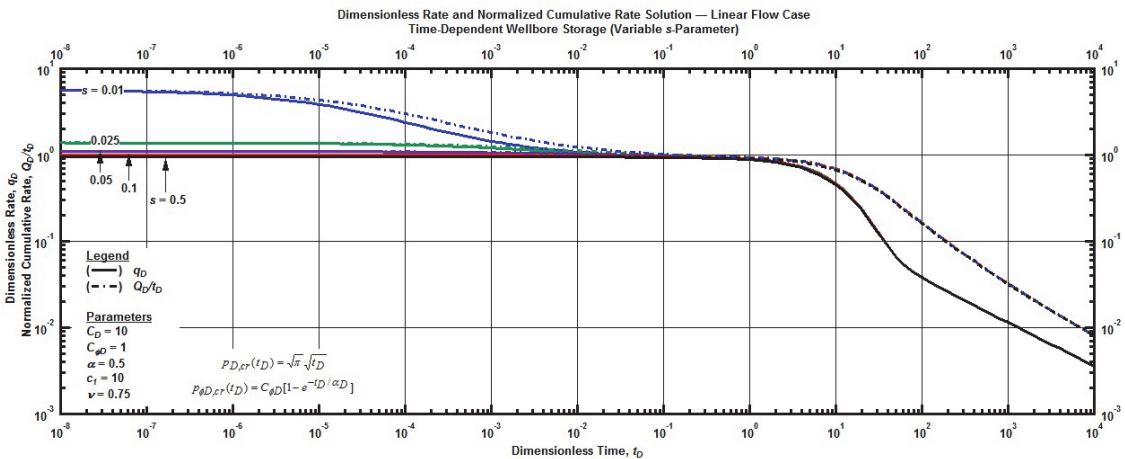


Figure F. 118 — Log-log plot (constant pressure time-normalized dimensionless cumulative rate solution) for the linear flow model combined with the time-dependent wellbore storage for select dimensionless constant skin factor.

### Linear Flow Regime with Time-Dependent Wellbore Storage and Cumulative-Exponential Skin Effects

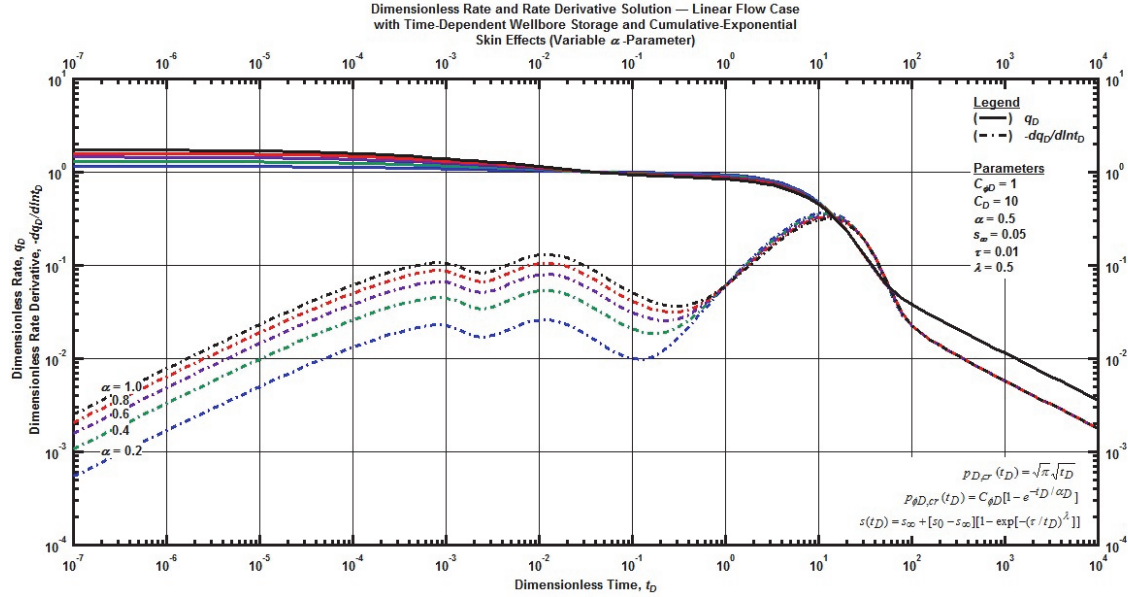


Figure F. 119 — Log-log plot (constant pressure dimensionless rate solution) for the bilinear flow model combined with the time-dependent wellbore storage and cumulative-exponential skin effects for select values of  $\alpha$ -parameter.

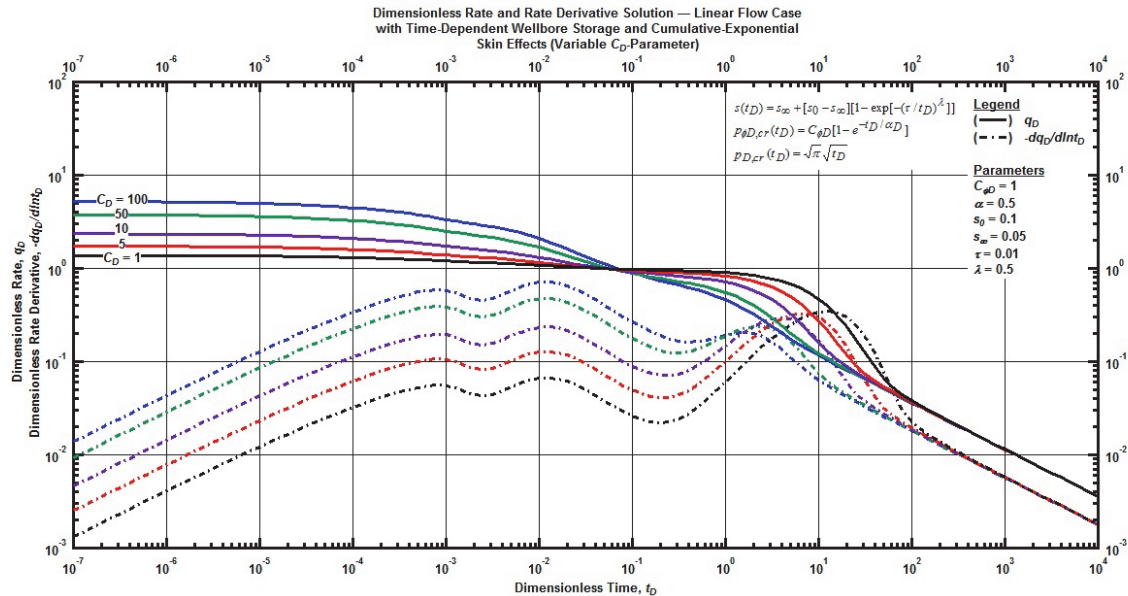


Figure F. 120 — Log-log plot (constant pressure dimensionless rate solution) for the bilinear flow model combined with the time-dependent wellbore storage and cumulative-exponential skin effects for select values of the dimensionless wellbore storage constant.

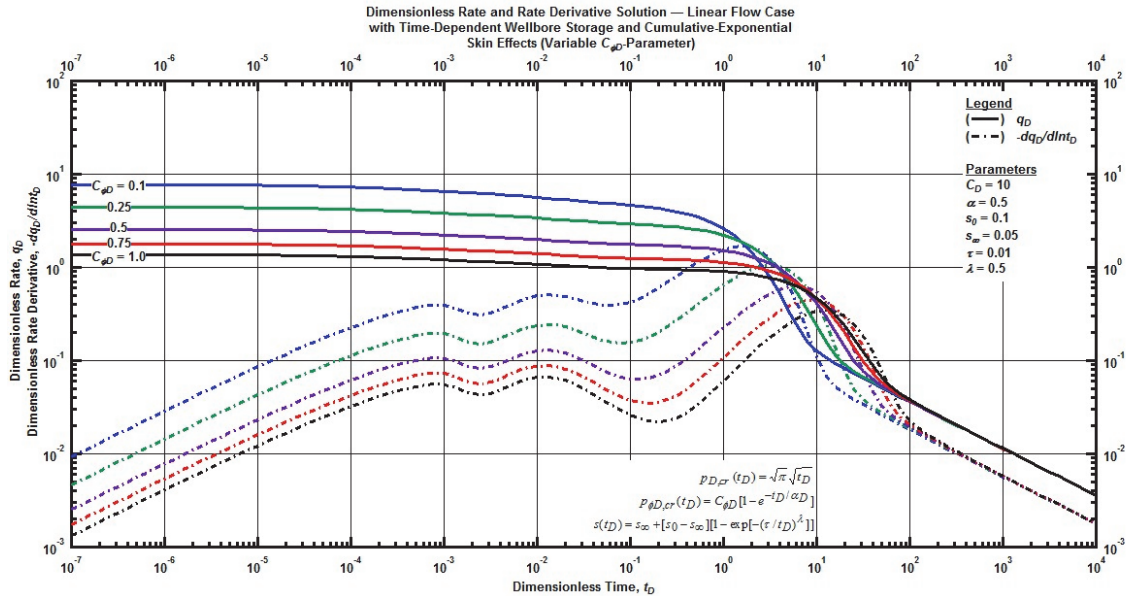


Figure F. 121 — Log-log plot (constant pressure dimensionless rate solution) for the bilinear flow model combined with the time-dependent wellbore storage and cumulative-exponential skin effects for select values phase redistribution constant.

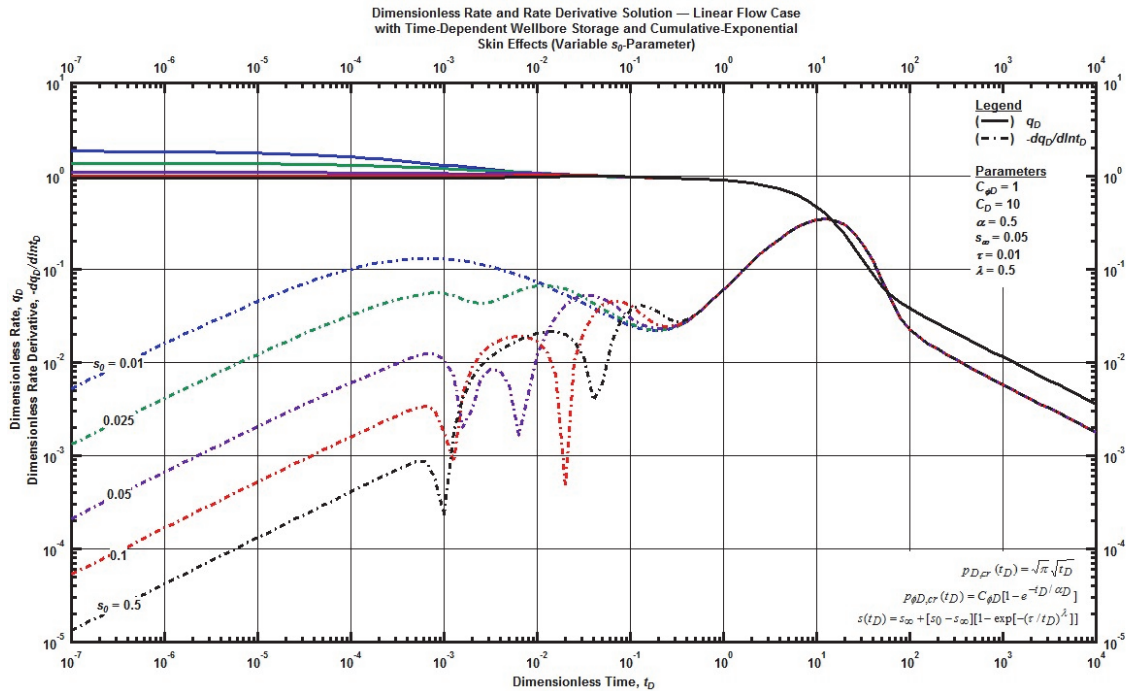


Figure F. 122 — Log-log plot (constant pressure dimensionless rate solution) for the bilinear flow model combined with the time-dependent wellbore storage and cumulative-exponential skin effects for select values of  $s_0$ -parameter.

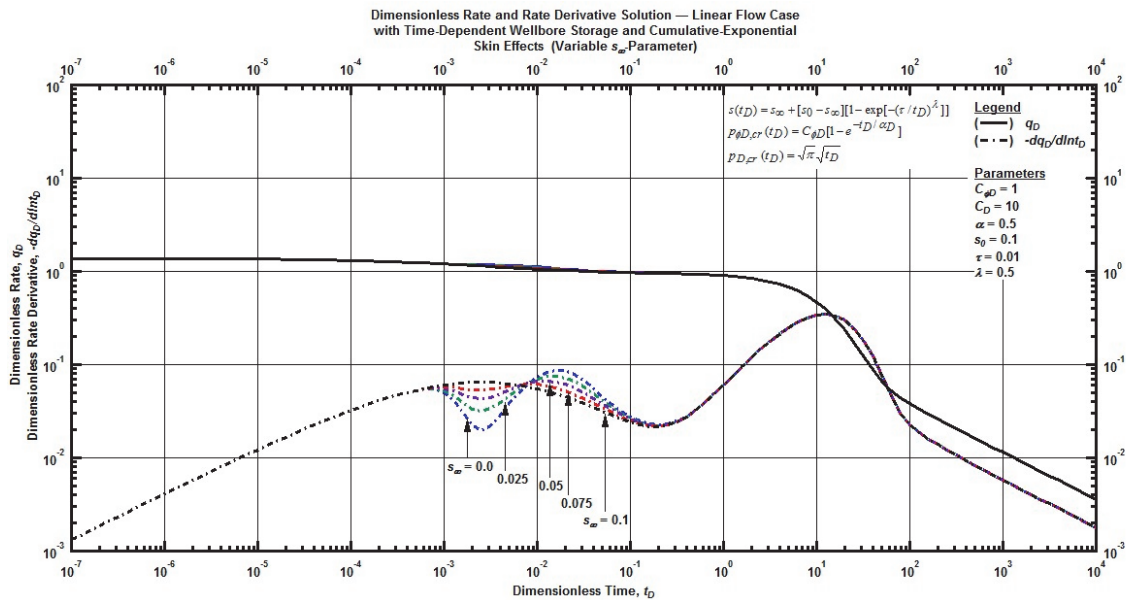


Figure F. 123 — Log-log plot (constant pressure dimensionless rate solution) for the bilinear flow model combined with the time-dependent wellbore storage and cumulative-exponential skin effects for select values of  $s_\infty$ -parameter.

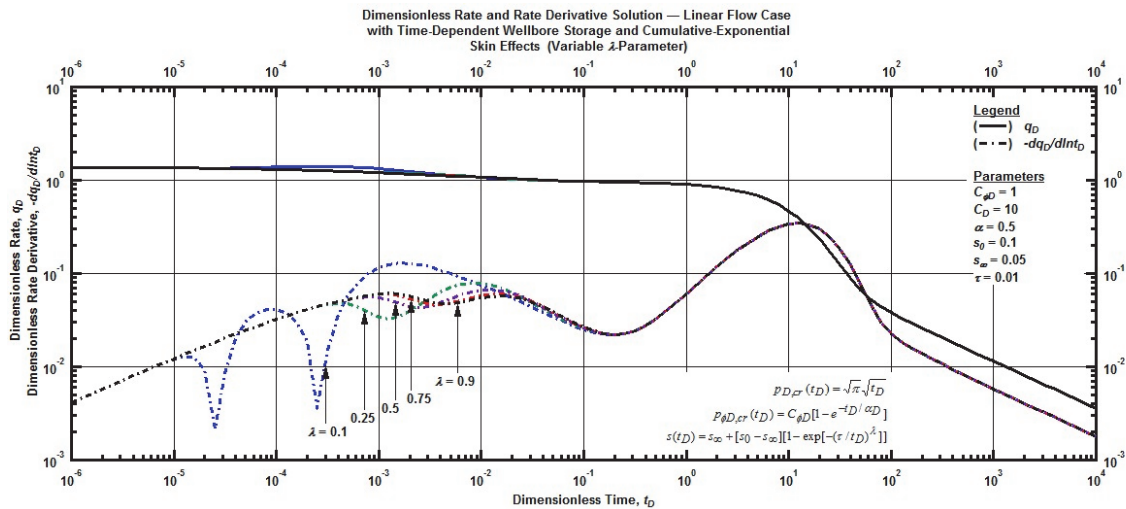


Figure F. 124 — Log-log plot (constant pressure dimensionless rate solution) for the bilinear flow model combined with the time-dependent wellbore storage and cumulative-exponential skin effects for select values of  $\lambda$ -parameter.

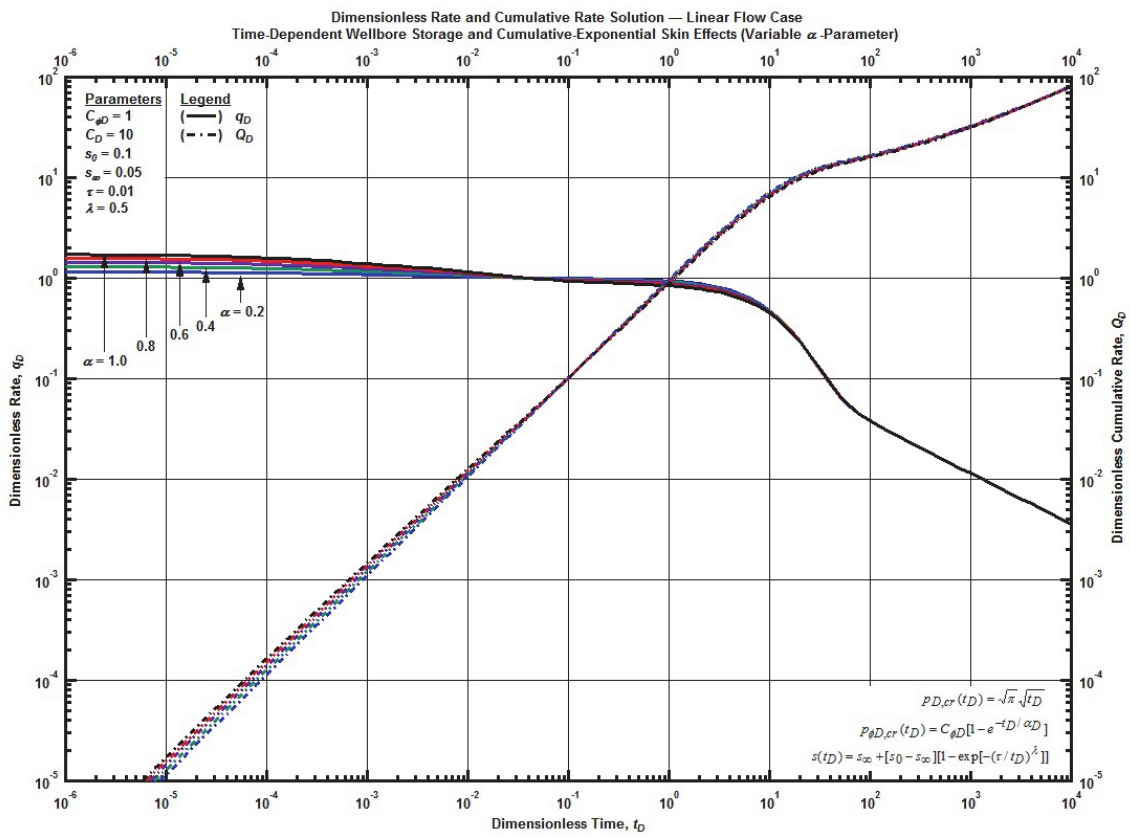


Figure F. 125 — Log-log plot (constant pressure dimensionless cumulative production solution) for the bilinear flow model combined with the time-dependent wellbore storage and cumulative-exponential skin effects for select values of  $\alpha$ -parameter.

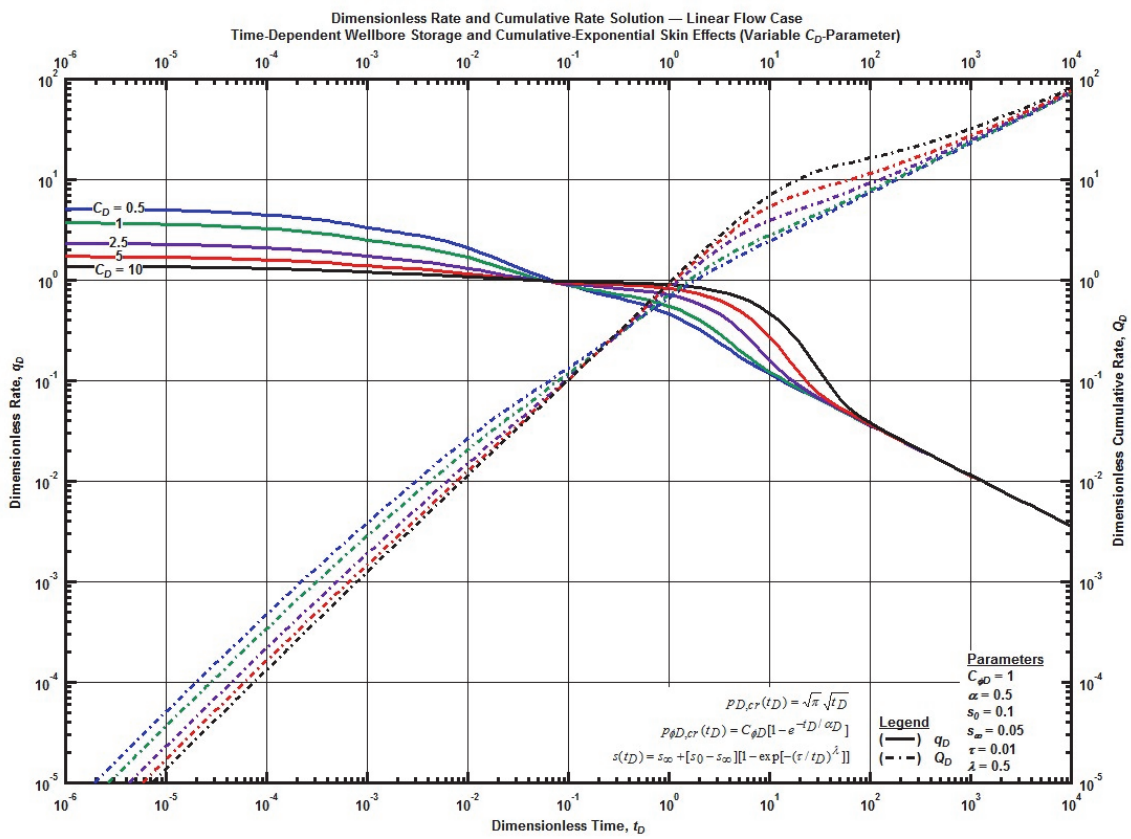


Figure F. 126 — Log-log plot (constant pressure dimensionless cumulative production solution) for the bilinear flow model combined with the time-dependent wellbore storage and cumulative-exponential skin effects for select values of the dimensionless wellbore storage constant.

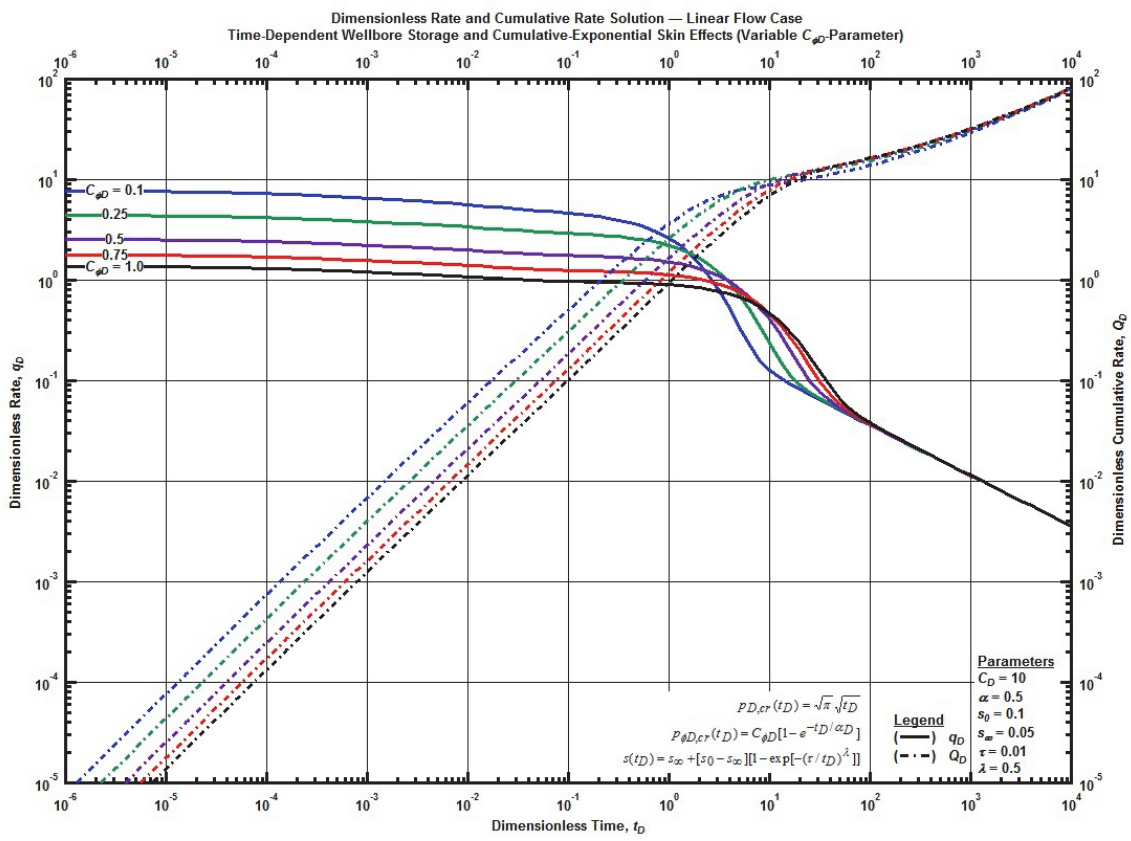


Figure F. 127 — Log-log plot (constant pressure dimensionless cumulative production solution) for the bilinear flow model combined with the time-dependent wellbore storage and cumulative-exponential skin effects for select values phase redistribution constant.

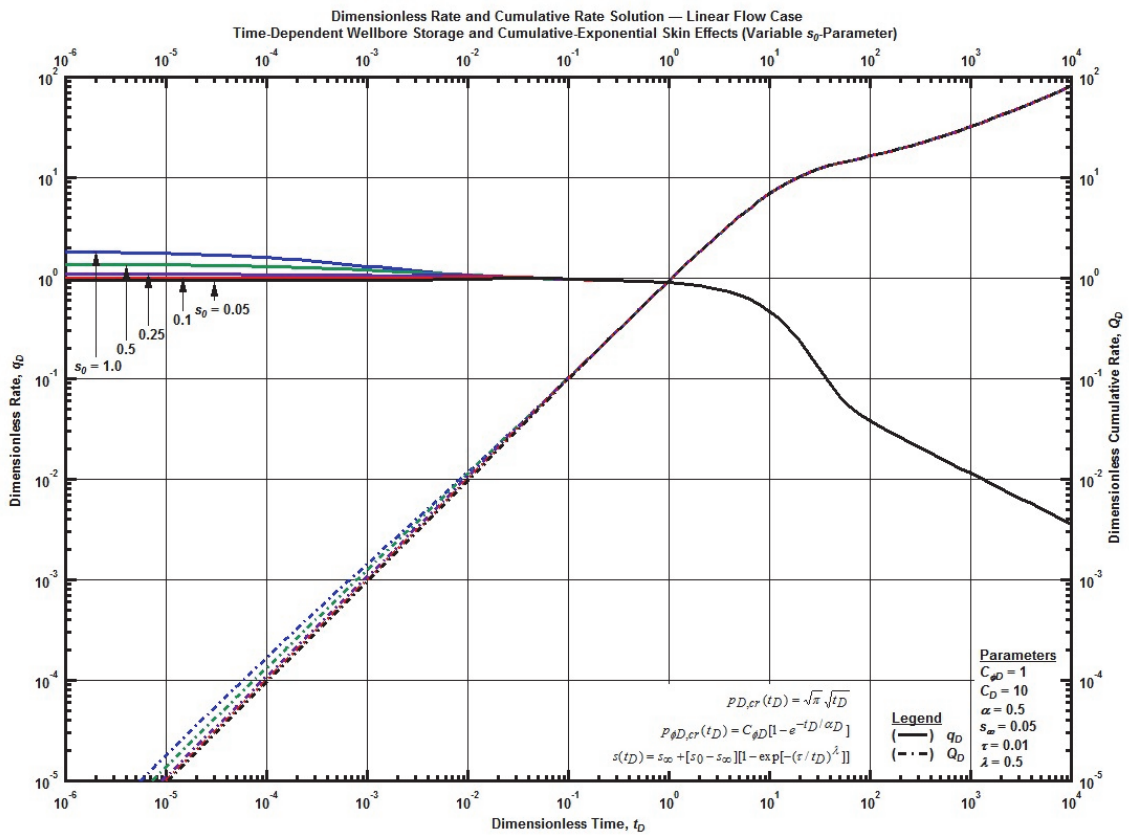


Figure F. 128 — Log-log plot (constant pressure dimensionless cumulative production solution) for the bilinear flow model combined with the time-dependent wellbore storage and cumulative-exponential skin effects for select values of  $s_0$ -parameter.

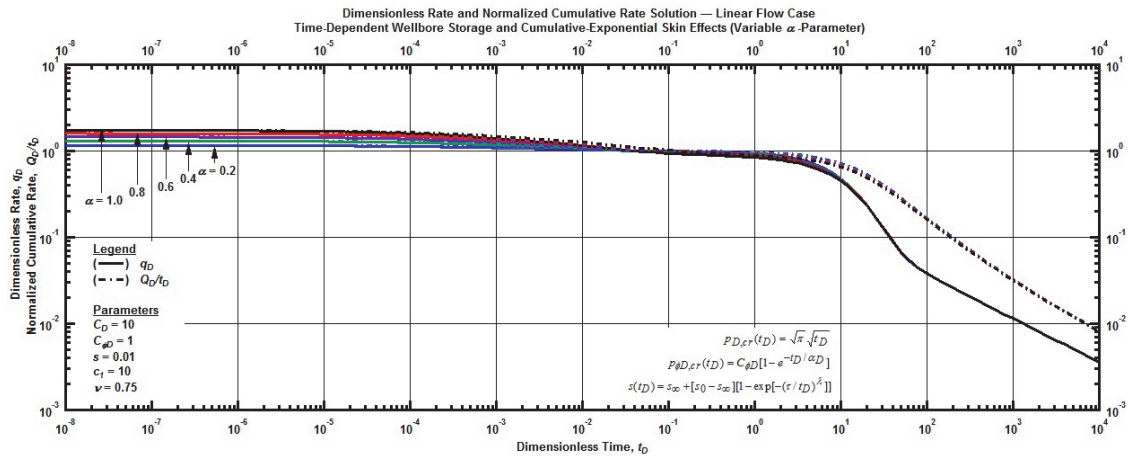


Figure F. 129 — Log-log plot (constant pressure dimensionless cumulative production solution) for the bilinear flow model combined with the time-dependent wellbore storage and cumulative-exponential skin effects for select values of  $\alpha$ -parameter.

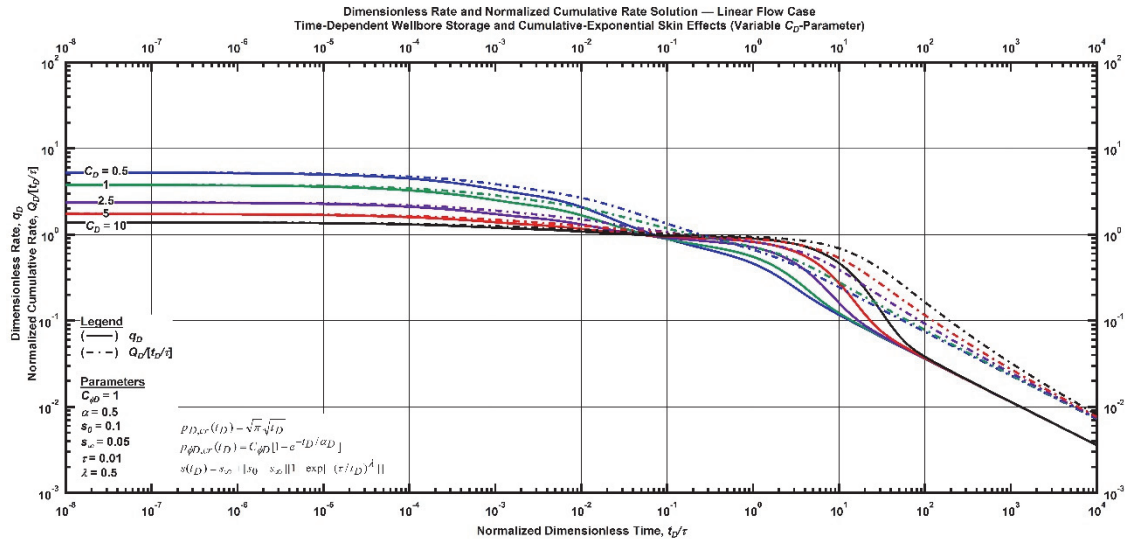


Figure F. 130 — Log-log plot (constant pressure time-normalized dimensionless cumulative rate solution) for the bilinear flow model combined with the time-dependent wellbore storage and cumulative-exponential skin effects for select values of the dimensionless wellbore storage constant.

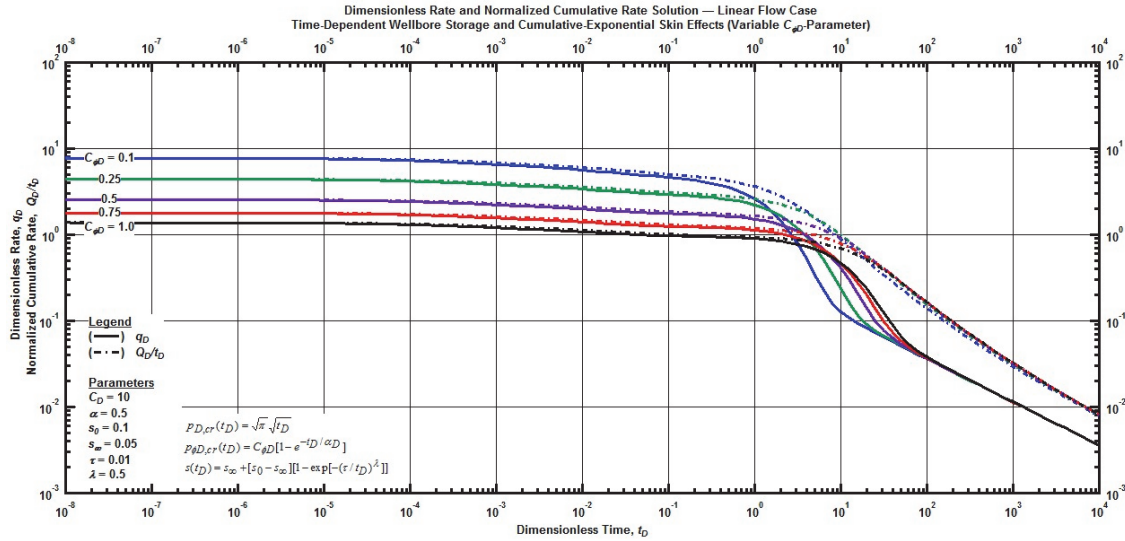


Figure F. 131 — Log-log plot (constant pressure time-normalized dimensionless cumulative rate solution) for the bilinear flow model combined with the time-dependent wellbore storage and cumulative-exponential skin effects for select values phase redistribution constant.

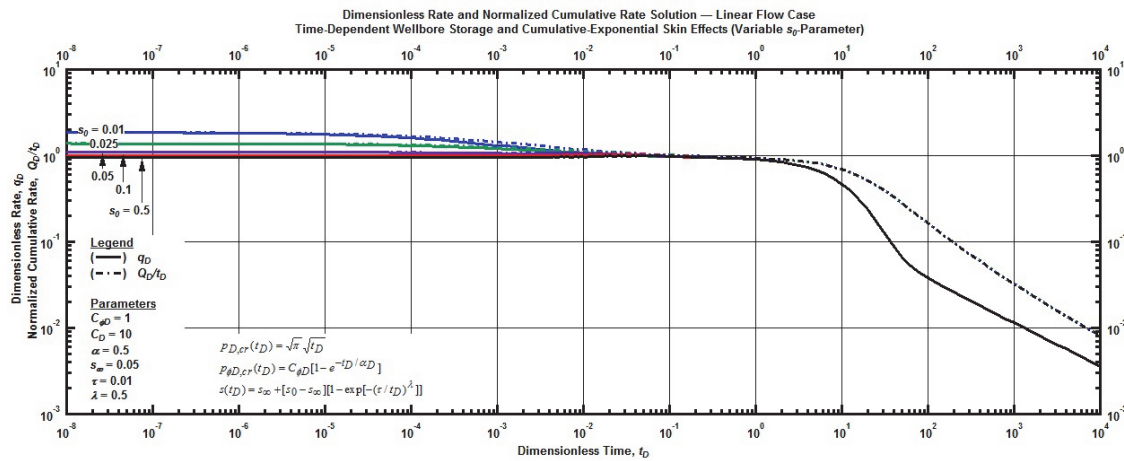


Figure F. 132 — Log-log plot (constant pressure time-normalized dimensionless cumulative rate solution) for the bilinear flow model combined with the time-dependent wellbore storage and cumulative-exponential skin effects for select values of  $s_0$ -parameter.

### F.3 Bilinear Flow Relation

*Bilinear Flow Relation with Cumulative-Exponential Time-Dependent Skin*

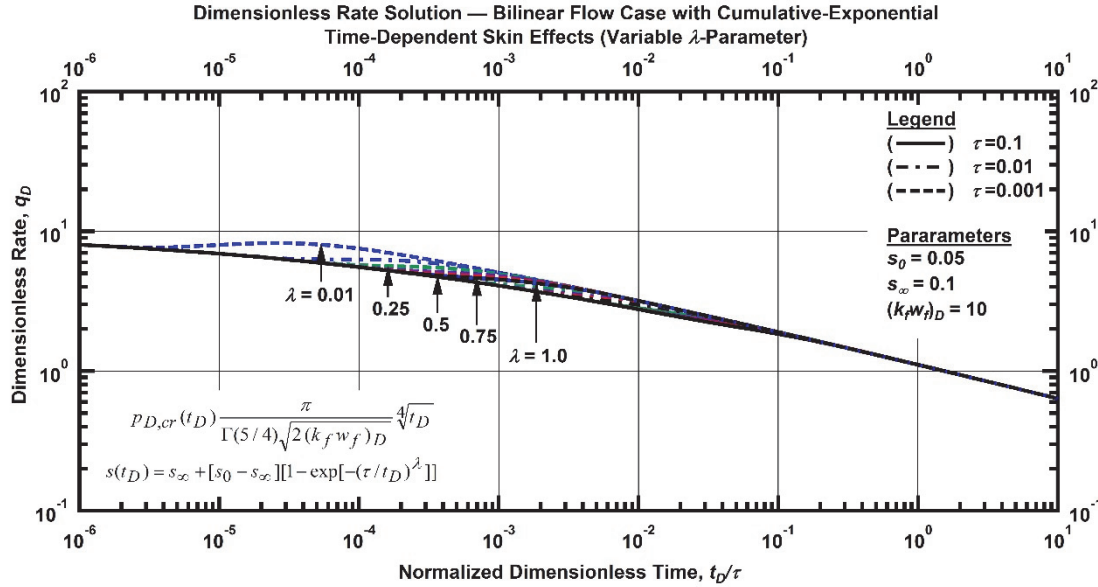


Figure F. 133 — Log-log plot (constant pressure dimensionless rate solution) for the bilinear flow model combined with the cumulative-exponential time-dependent for select values of  $\lambda$ -parameter.

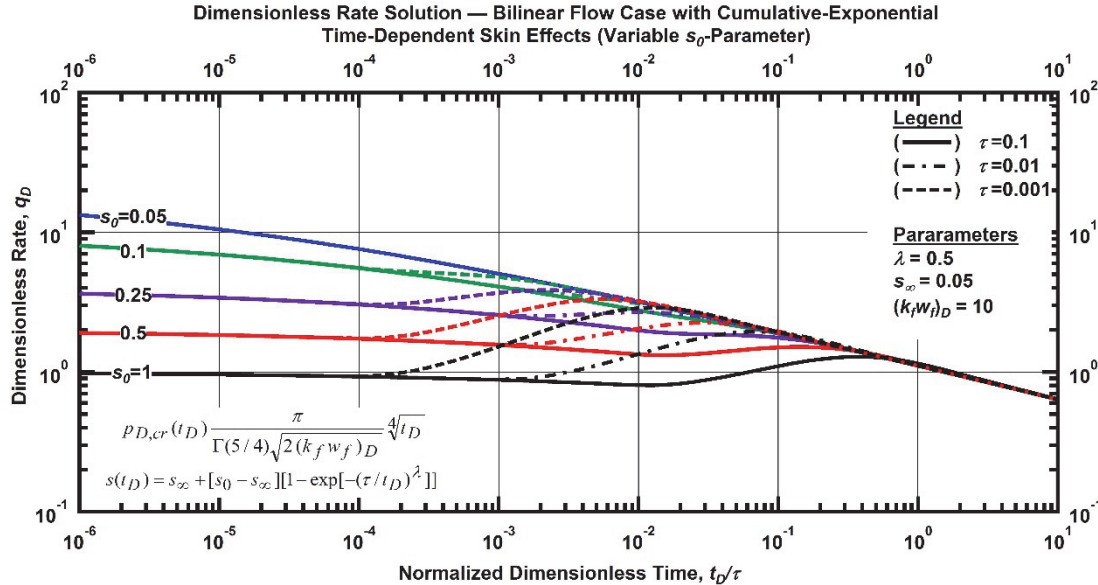


Figure F. 134 — Log-log plot (constant pressure dimensionless rate solution) for the bilinear flow model combined with the cumulative-exponential time-dependent for select values of  $s_0$ -parameter.

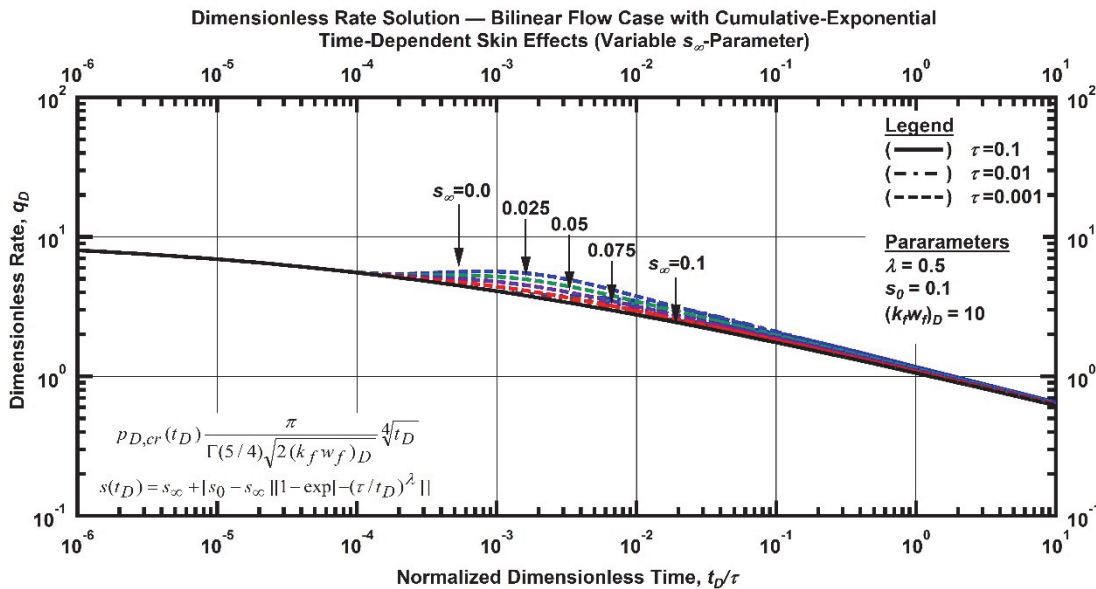


Figure F. 135 — Log-log plot (constant pressure dimensionless rate solution) for the bilinear flow model combined with the cumulative-exponential time-dependent for select values of  $s_\infty$ -parameter.

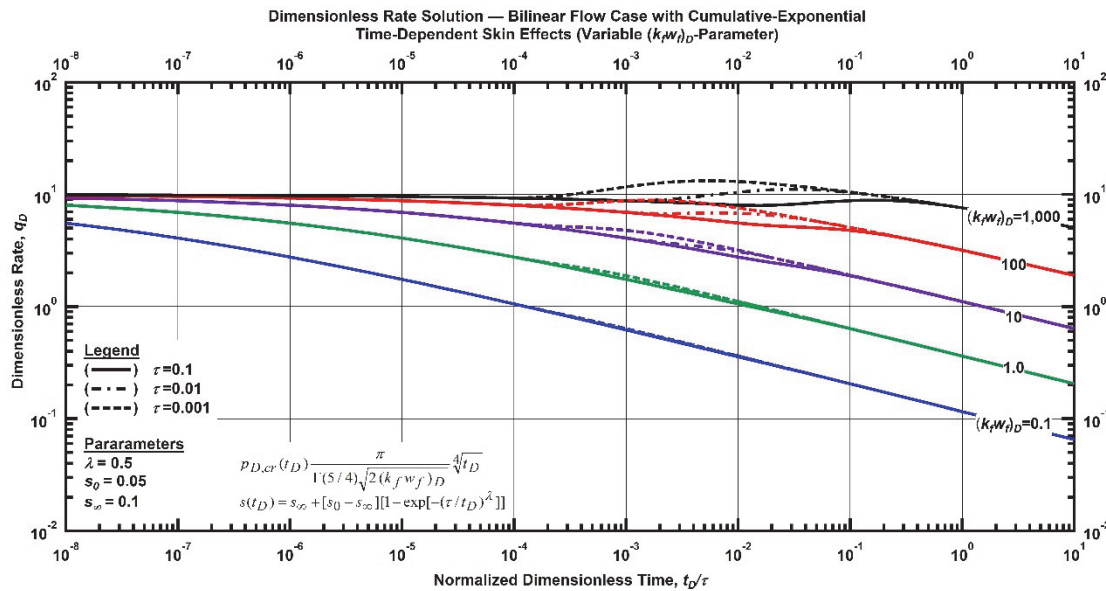


Figure F. 136 — Log-log plot (constant pressure dimensionless rate solution) for the bilinear flow model combined with the cumulative-exponential time-dependent for select values of dimensionless fracture conductivity.

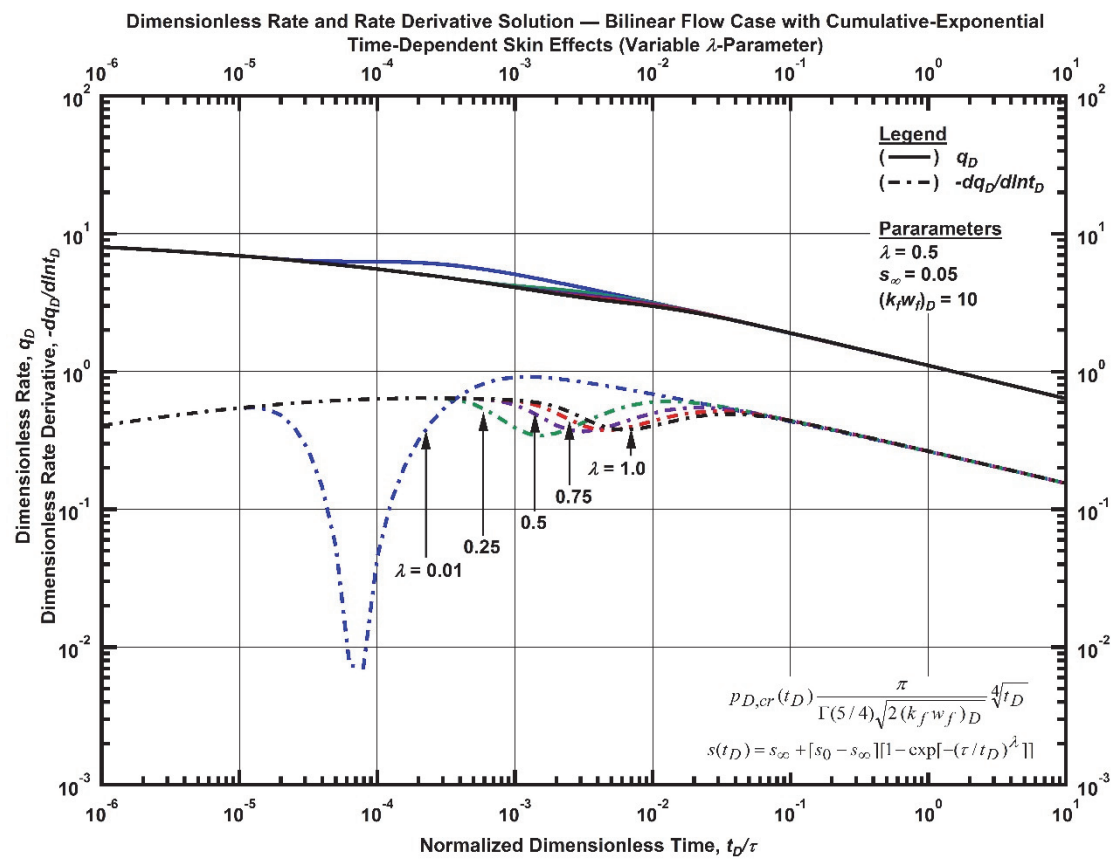


Figure F. 137 — Log-log plot (constant pressure dimensionless rate derivative solution) for the bilinear flow model combined with the cumulative-exponential time-dependent for select values of  $\lambda$ -parameter.

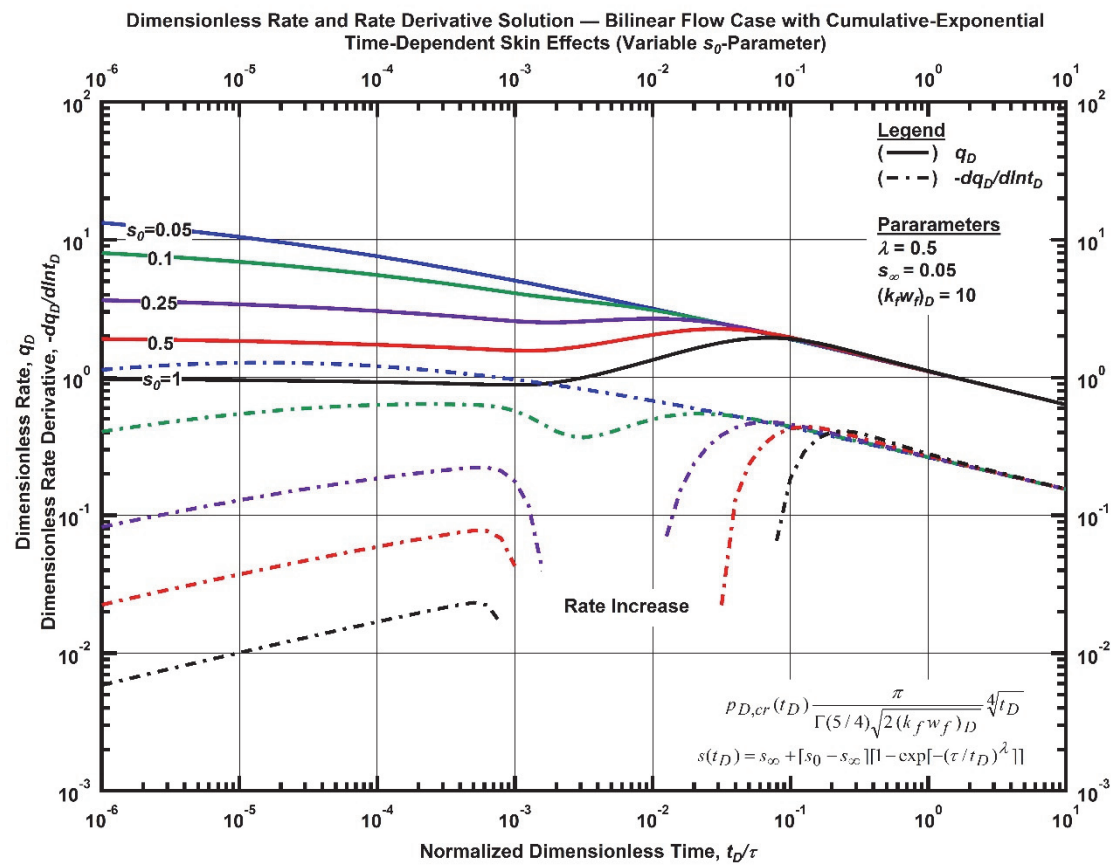


Figure F. 138 — Log-log plot (constant pressure dimensionless rate derivative solution) for the bilinear flow model combined with the cumulative-exponential time-dependent for select values of  $s_0$ -parameter.

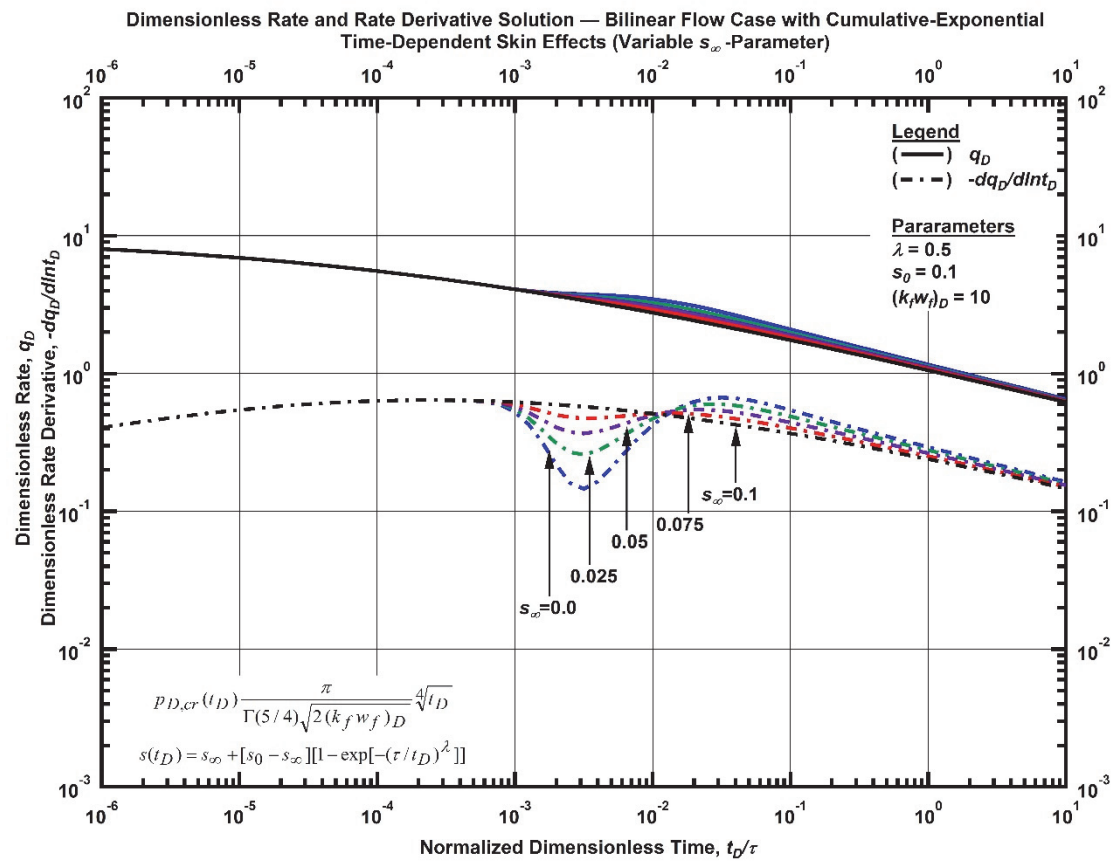


Figure F. 139 — Log-log plot (constant pressure dimensionless rate derivative solution) for the bilinear flow model combined with the cumulative-exponential time-dependent for select values of  $s_\infty$ -parameter.

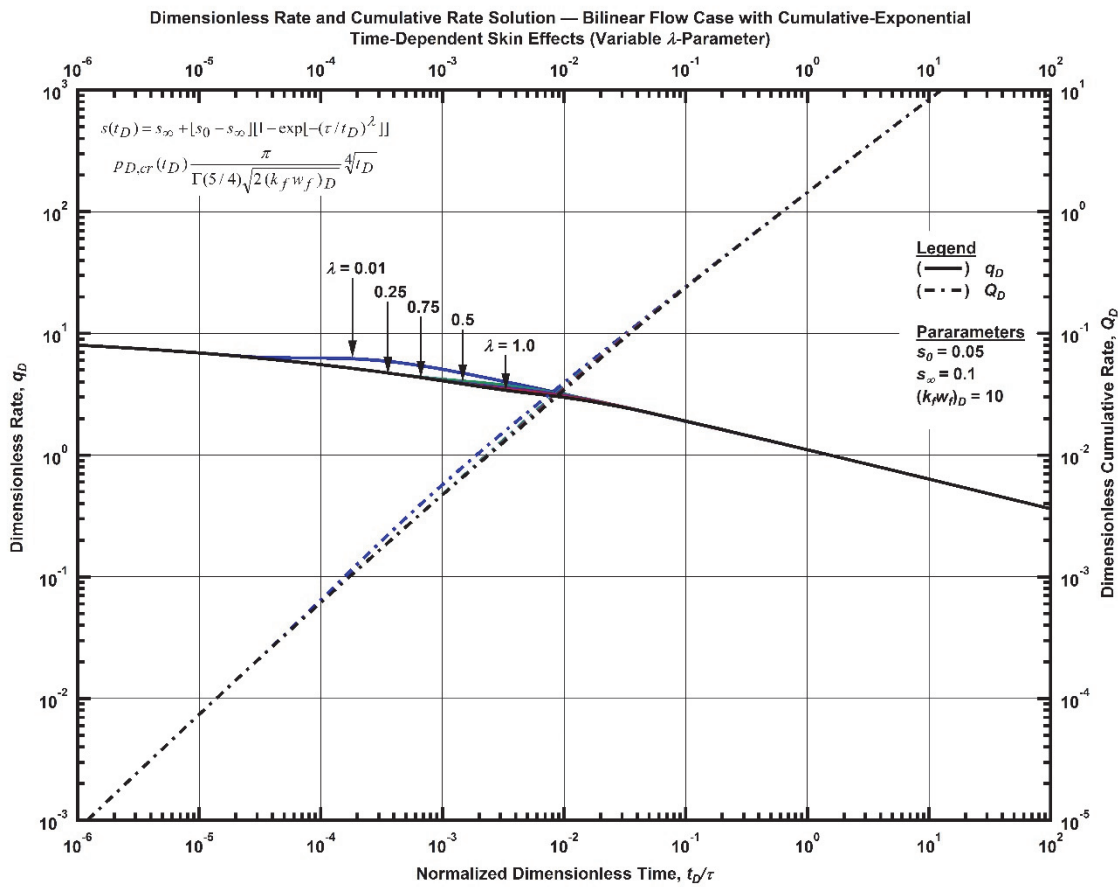


Figure F. 140 — Log-log plot (constant pressure dimensionless cumulative production solution) for the bilinear flow model combined with the cumulative-exponential time-dependent for select values of  $\lambda$ -parameter.

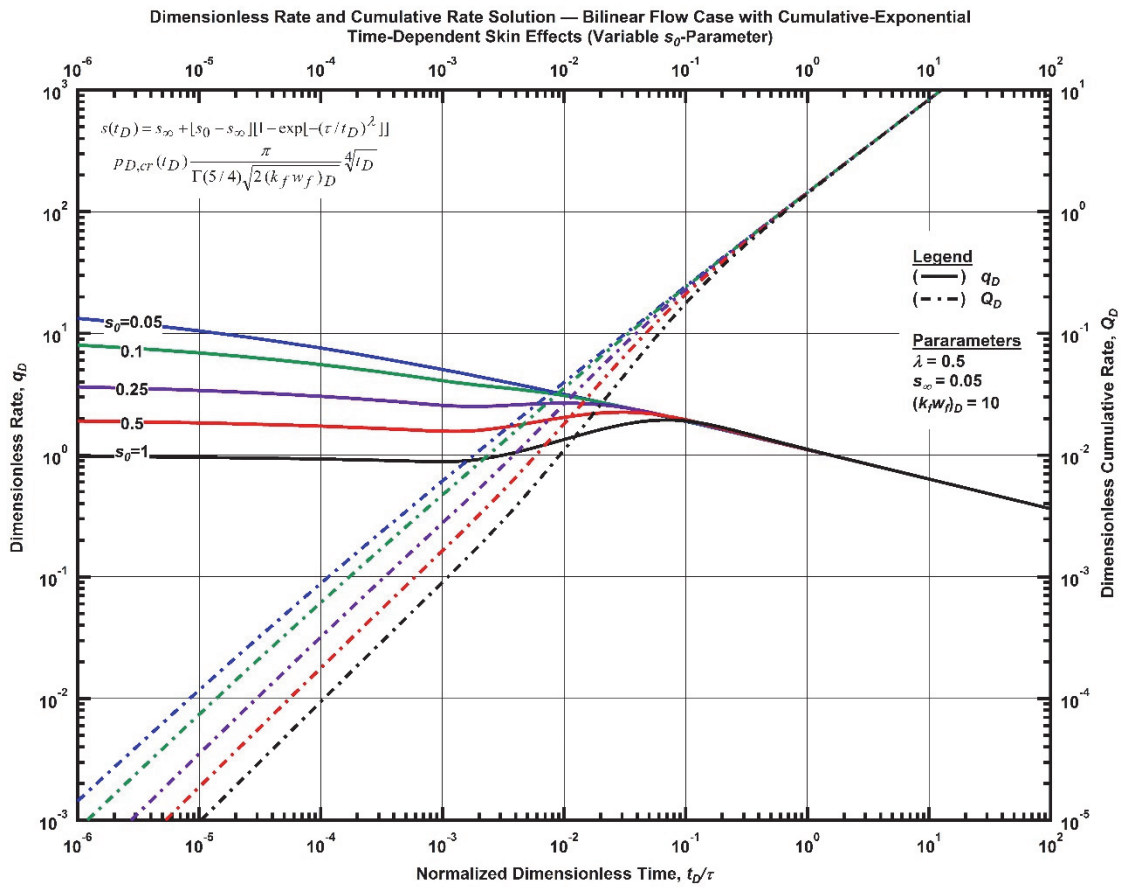


Figure F. 141 — Log-log plot (constant pressure dimensionless cumulative production solution) for the bilinear flow model combined with the cumulative-exponential time-dependent for select values of  $s_0$ -parameter.

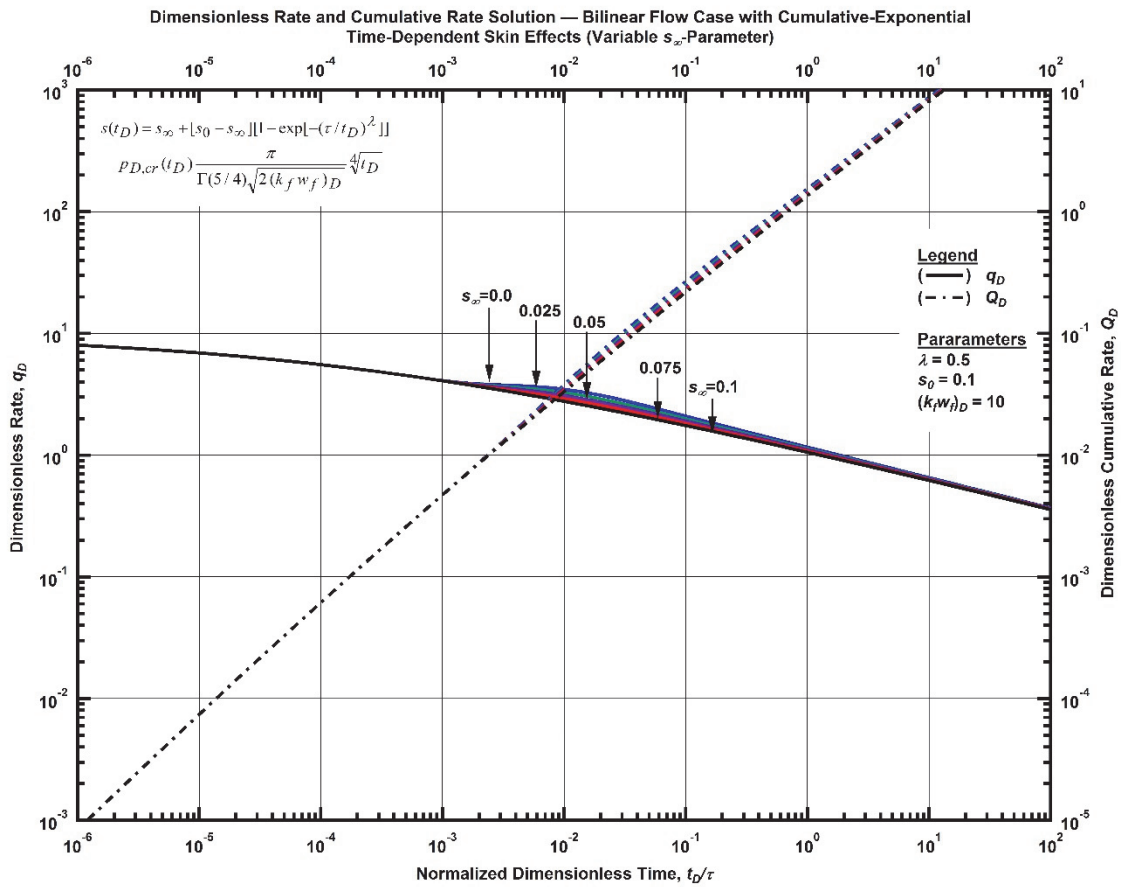


Figure F. 142 — Log-log plot (constant pressure dimensionless cumulative production solution) for the bilinear flow model combined with the cumulative-exponential time-dependent for select values of  $s_\infty$ -parameter.

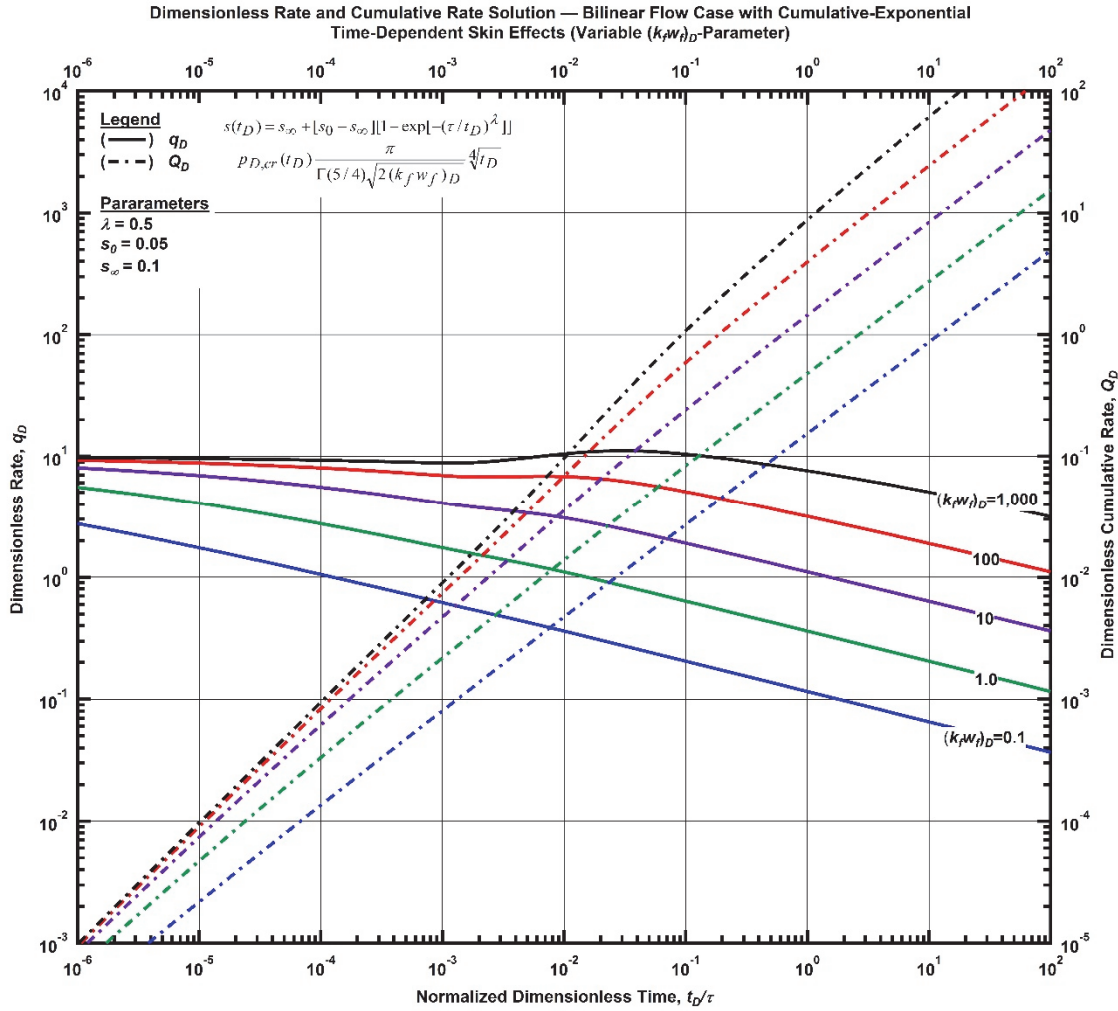


Figure F. 143 — Log-log plot (constant pressure dimensionless cumulative production solution) for the bilinear flow model combined with the cumulative-exponential time-dependent for select values of dimensionless fracture conductivity.

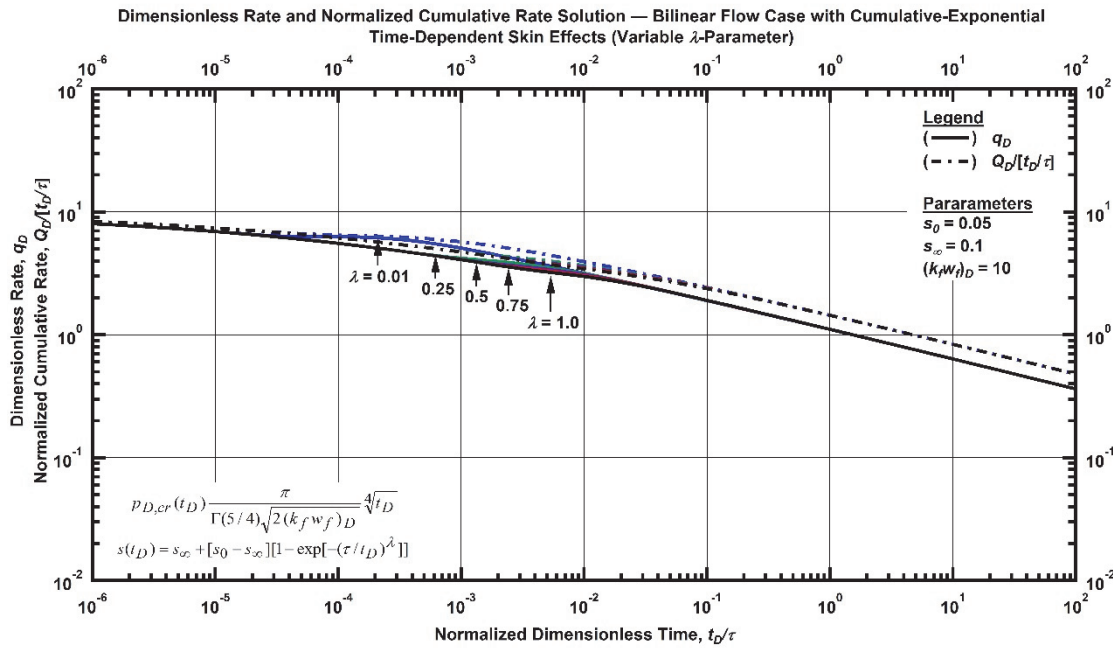


Figure F. 144 — Log-log plot (constant pressure time-normalized dimensionless cumulative rate solution) for the bilinear flow model combined with the cumulative-exponential time-dependent for select values of  $\lambda$ -parameter.

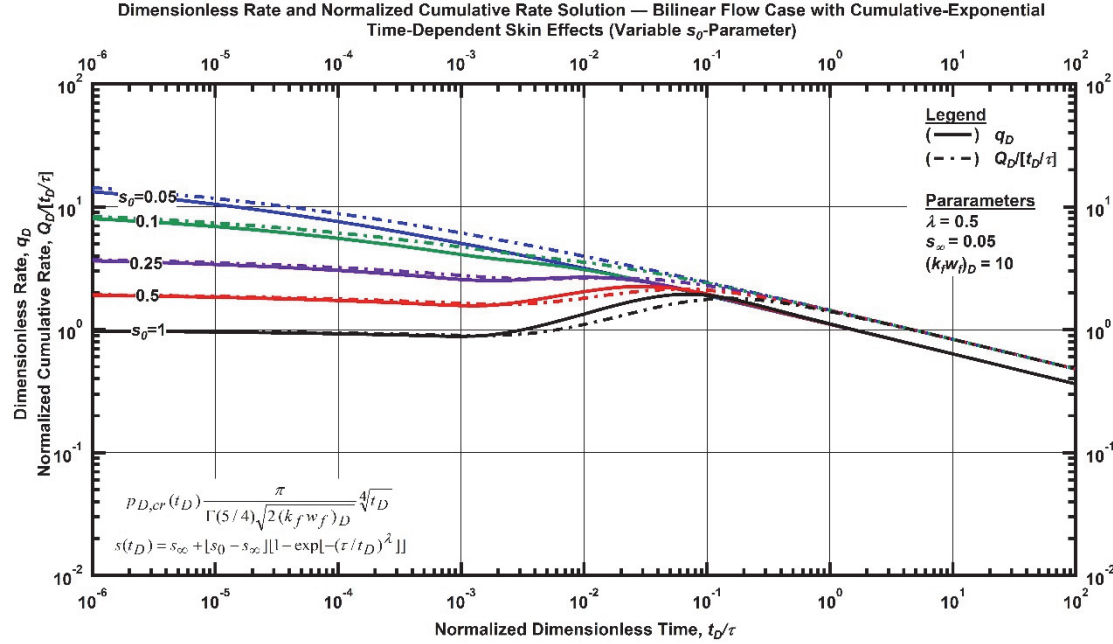


Figure F. 145 — Log-log plot (constant pressure time-normalized dimensionless cumulative rate solution) for the bilinear flow model combined with the cumulative-exponential time-dependent for select values of  $s_0$ -parameter.

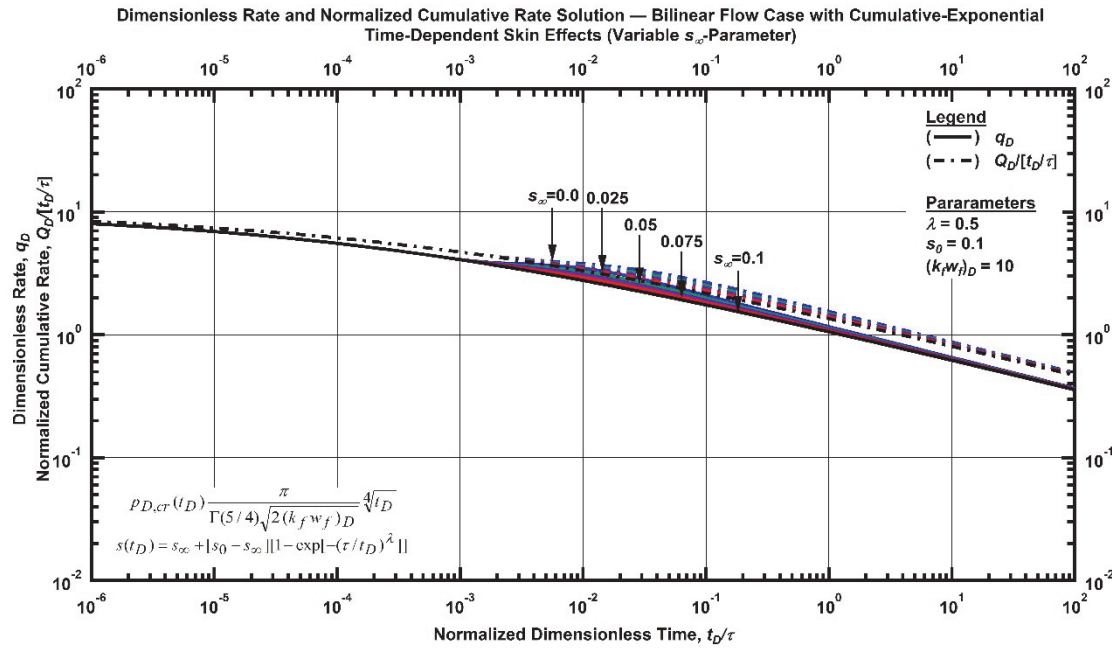


Figure F. 146 — Log-log plot (constant pressure time-normalized dimensionless cumulative rate solution) for the bilinear flow model combined with the cumulative-exponential time-dependent for select values of  $s_\infty$ -parameter.

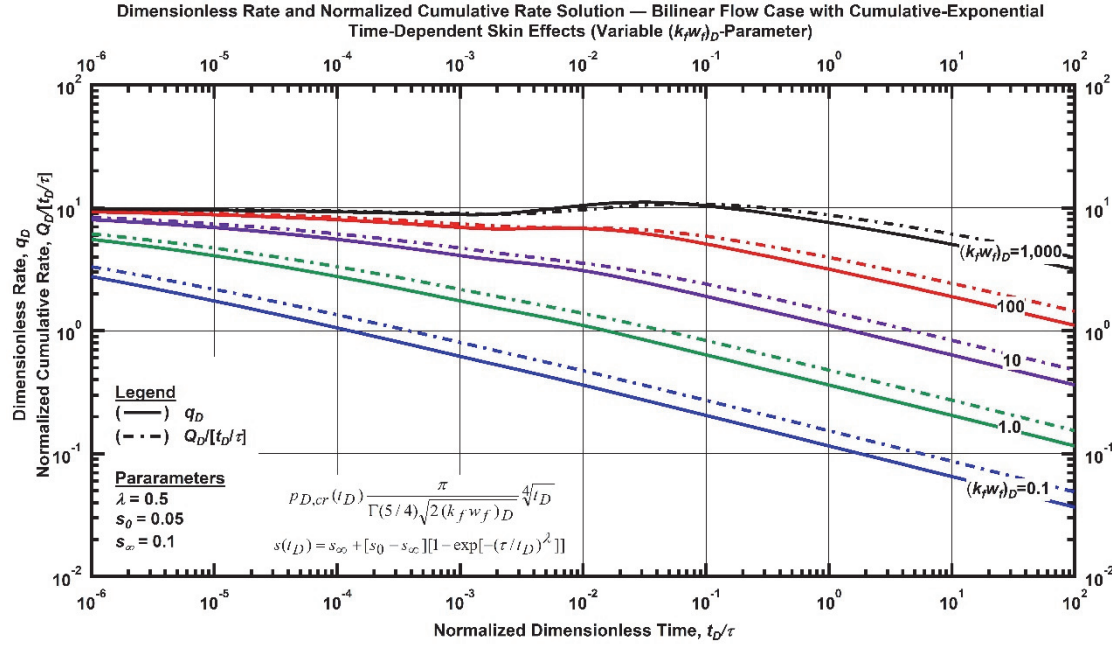


Figure F. 147 — Log-log plot (constant pressure time-normalized dimensionless cumulative rate solution) for the bilinear flow model combined with the cumulative-exponential time-dependent for select values of dimensionless fracture conductivity.

### Bilinear Flow Relation with Exponential Time-Dependent Skin

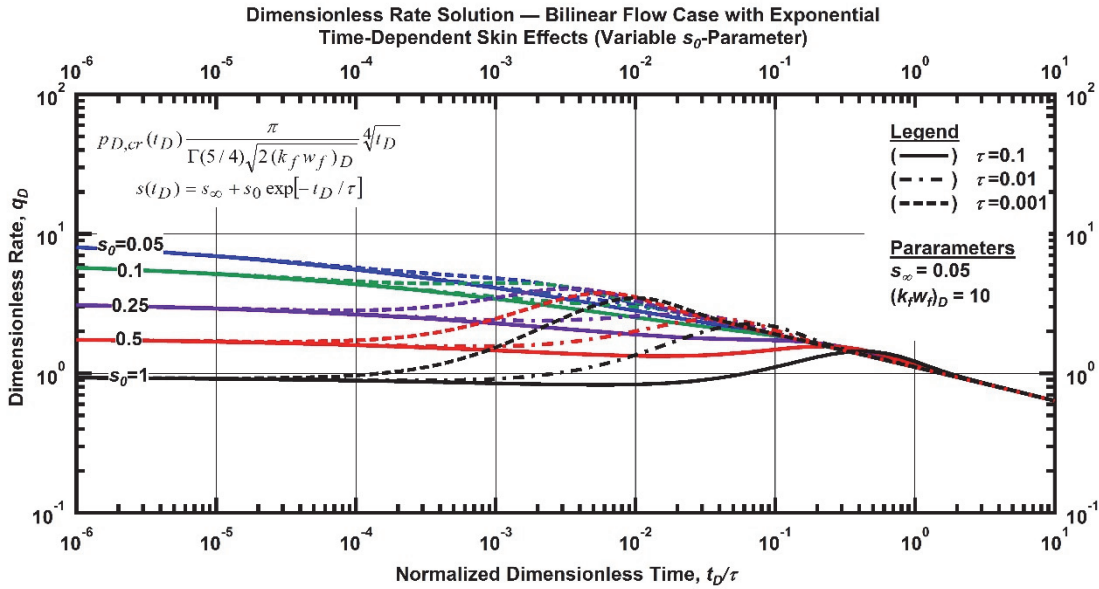


Figure F. 148 — Log-log plot (constant pressure dimensionless rate solution) for the bilinear flow model combined with the exponential time-dependent for select values of  $s_0$ -parameter.

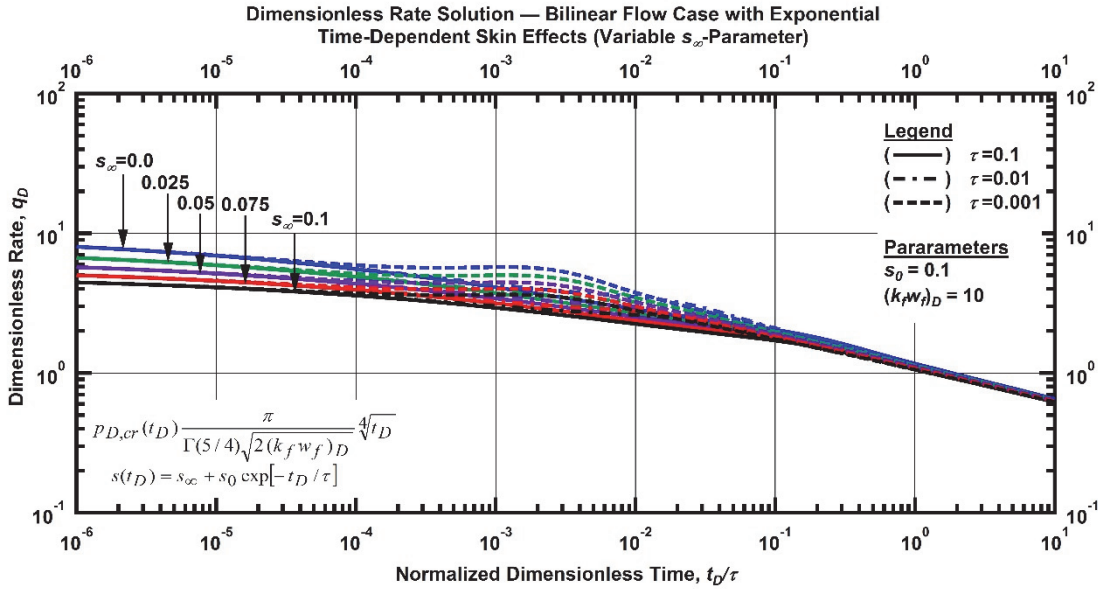


Figure F. 149 — Log-log plot (constant pressure dimensionless rate solution) for the bilinear flow model combined with the exponential time-dependent for select values of  $s_\infty$ -parameter.

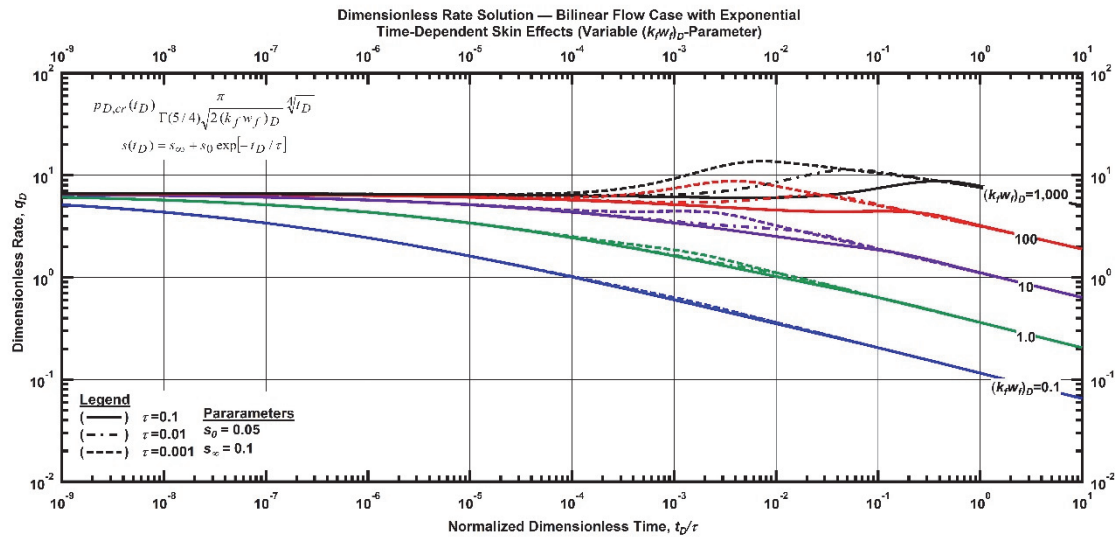


Figure F. 150 — Log-log plot (constant pressure dimensionless rate solution) for the bilinear flow model combined with the exponential time-dependent for select values of dimensionless fracture conductivity.

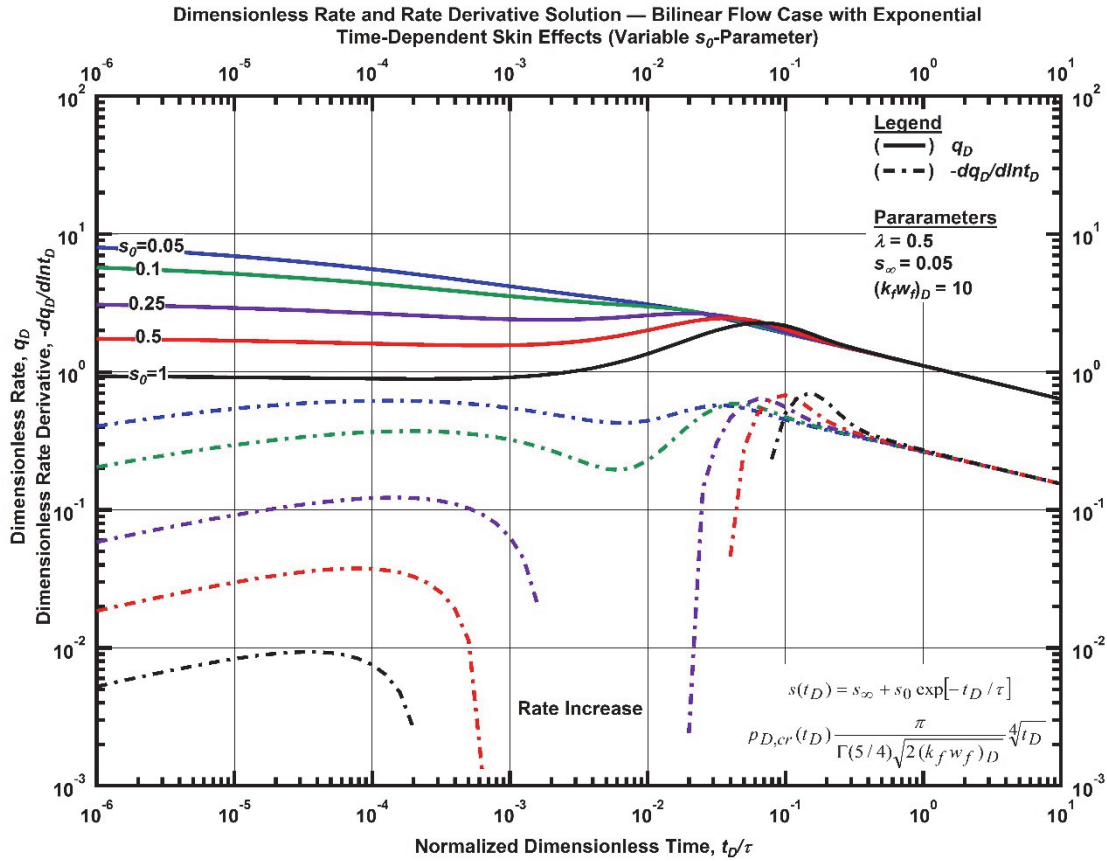


Figure F. 151 — Log-log plot (constant pressure dimensionless rate derivative solution) for the bilinear flow model combined with the exponential time-dependent for select values of  $s_0$ -parameter.

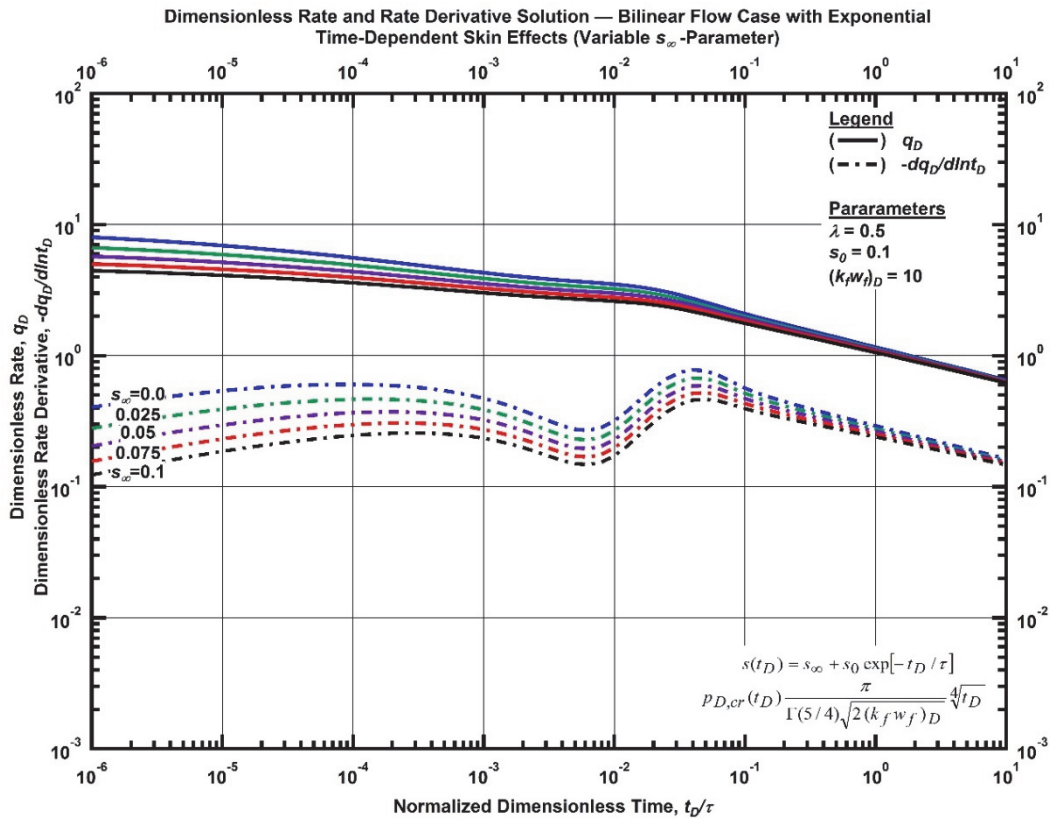


Figure F. 152 — Log-log plot (constant pressure dimensionless rate derivative solution) for the bilinear flow model combined with the exponential time-dependent for select values of  $s_\infty$ -parameter.

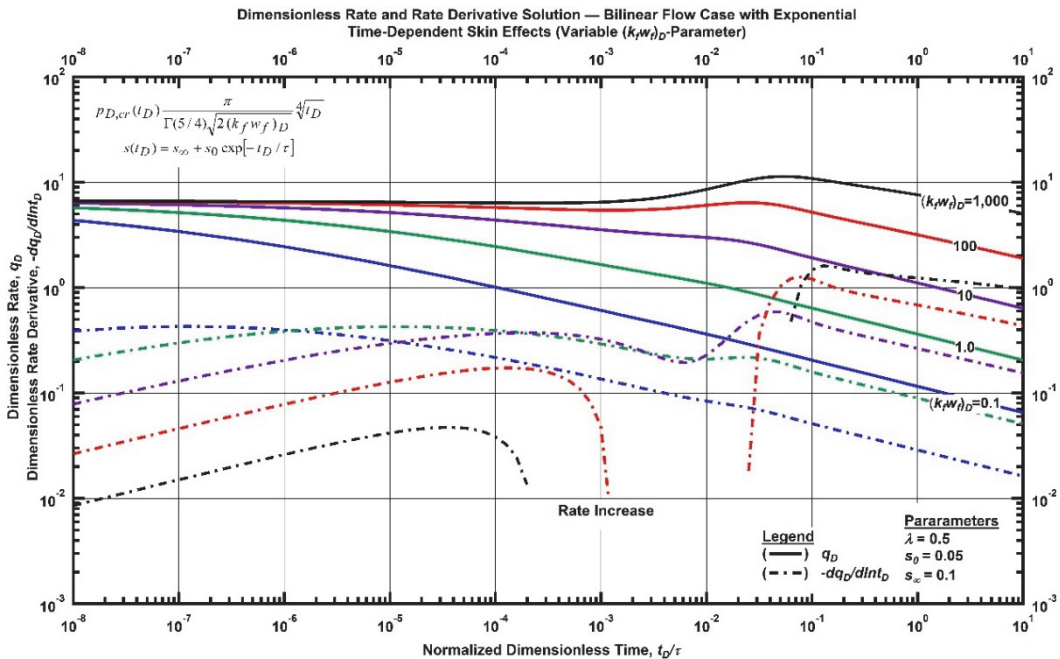


Figure F. 153 — Log-log plot (constant pressure dimensionless rate derivative solution) for the bilinear flow model combined with the exponential time-dependent for select values of dimensionless fracture conductivity.

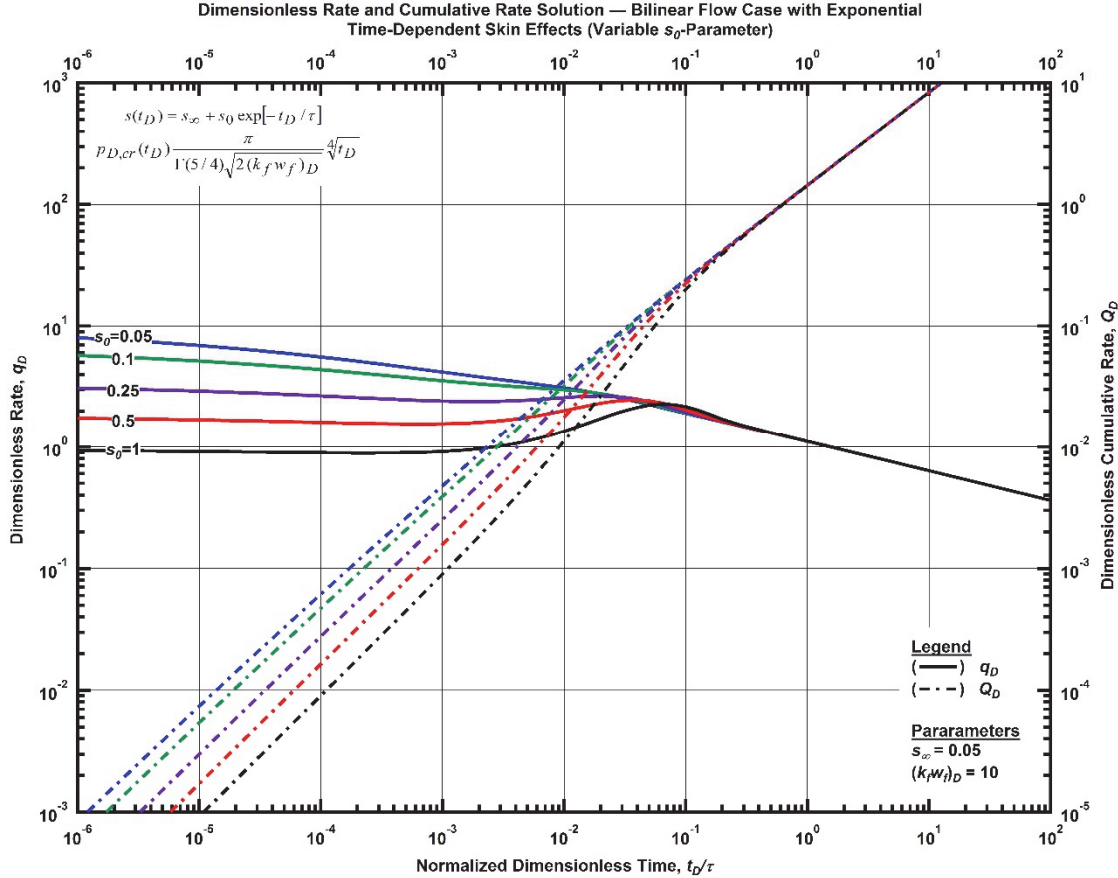


Figure F. 154 — Log-log plot (constant pressure dimensionless cumulative production solution) for the bilinear flow model combined with the exponential time-dependent for select values of  $s_0$ -parameter.

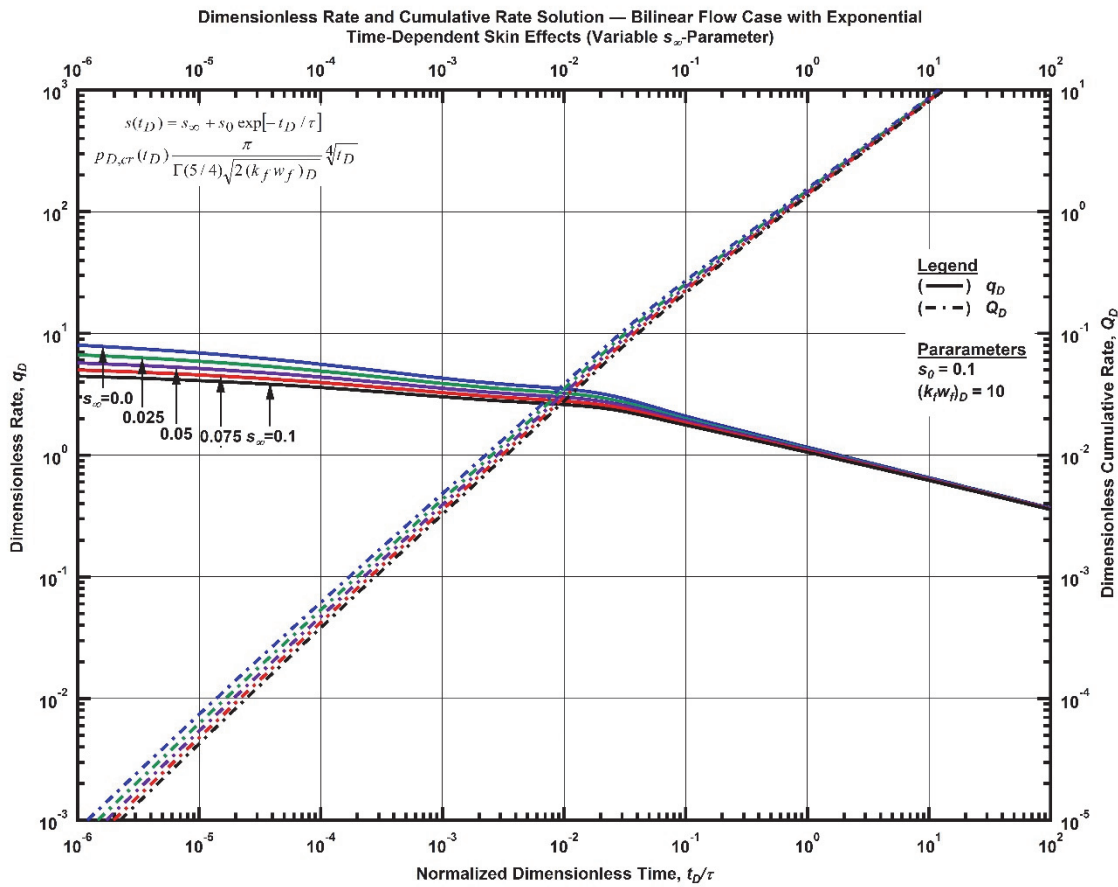


Figure F. 155 — Log-log plot (constant pressure dimensionless cumulative production solution) for the bilinear flow model combined with the exponential time-dependent for select values of  $s_\infty$ -parameter.

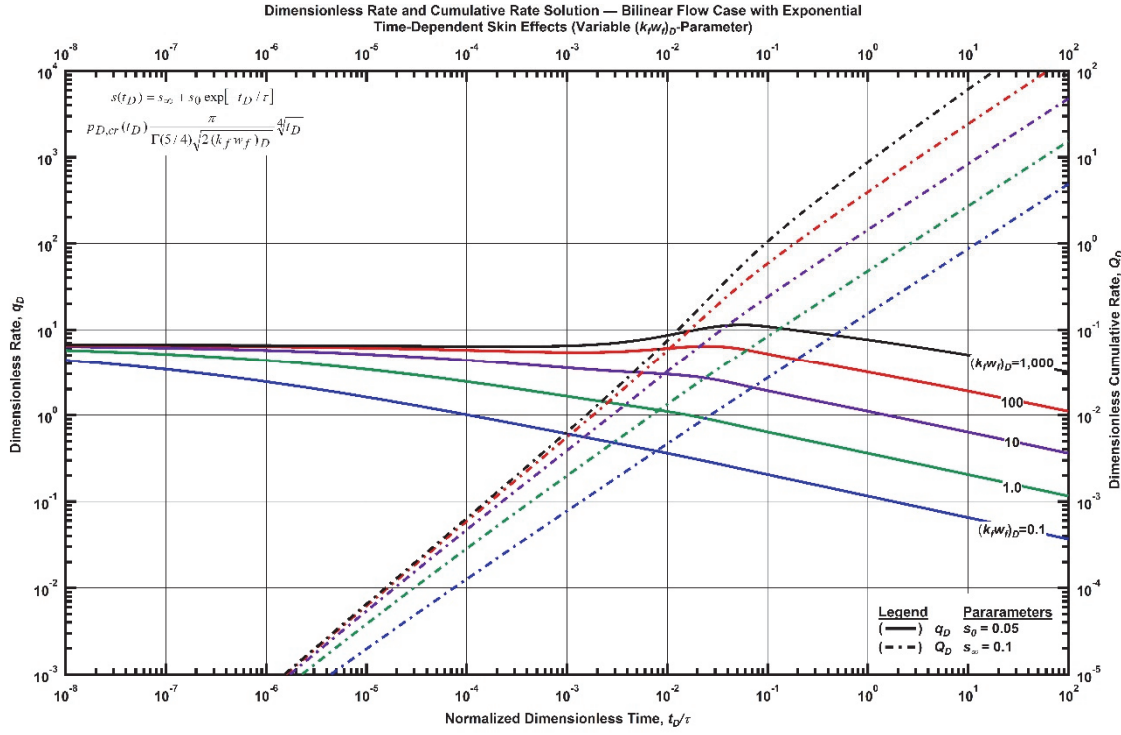


Figure F. 156 — Log-log plot (constant pressure dimensionless cumulative production solution) for the bilinear flow model combined with the exponential time-dependent for select values of dimensionless fracture conductivity.

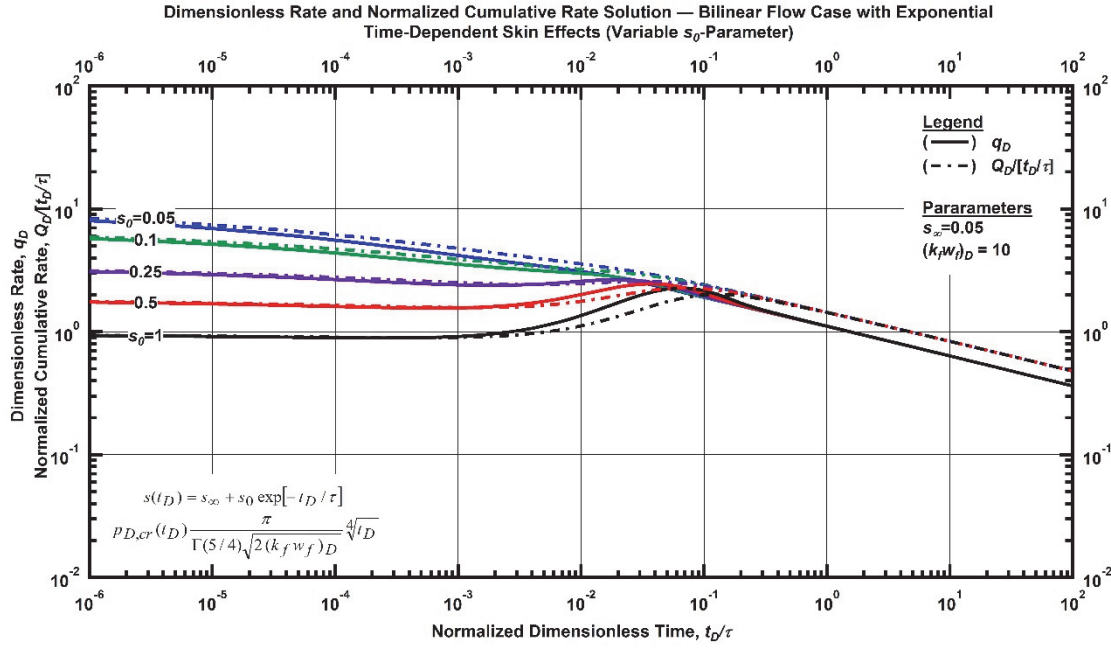


Figure F. 157 — Log-log plot (constant pressure time-normalized dimensionless cumulative rate solution) for the bilinear flow model combined with the exponential time-dependent for select values of  $s_0$ -parameter.

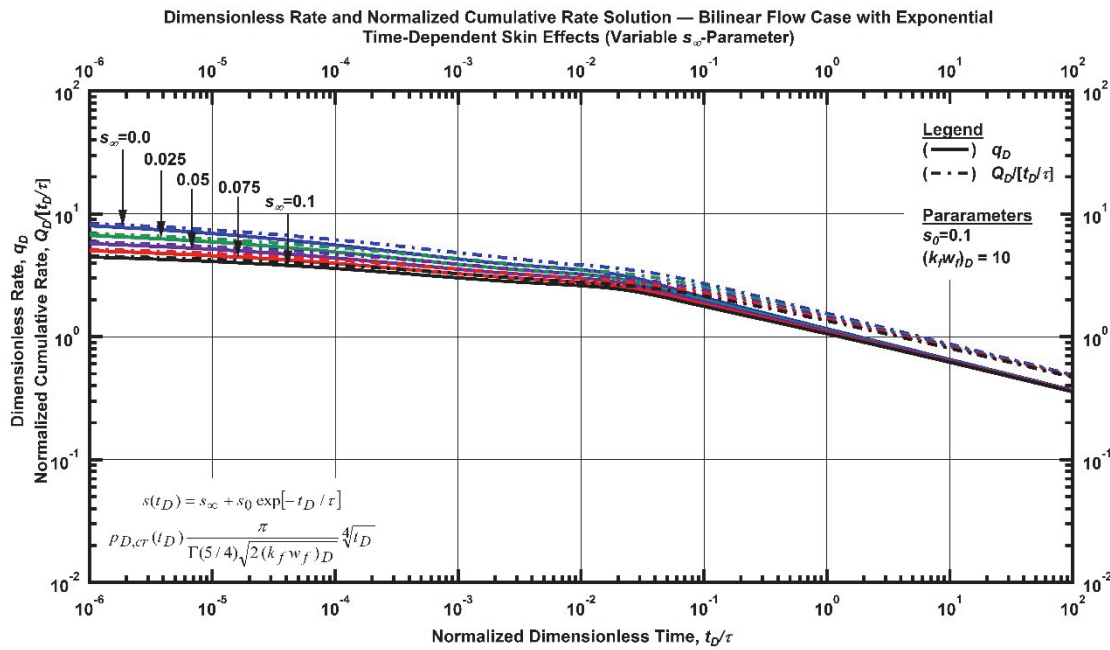


Figure F. 158 — Log-log plot (constant pressure time-normalized dimensionless cumulative rate solution) for the bilinear flow model combined with the exponential time-dependent for select values of  $s_\infty$ -parameter.

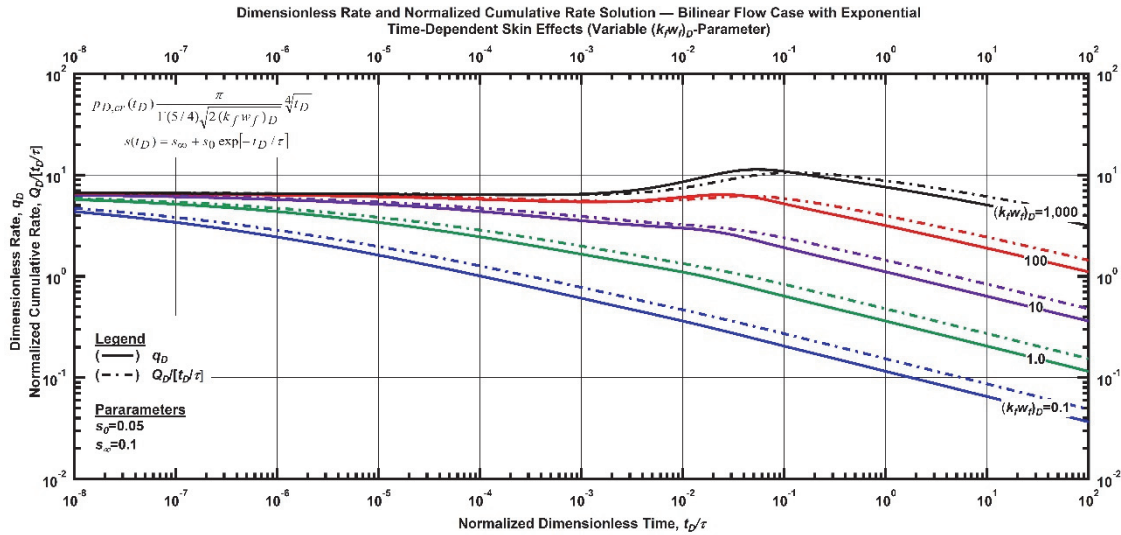


Figure F. 159 — Log-log plot (constant pressure time-normalized dimensionless cumulative rate solution) for the bilinear flow model combined with the exponential time-dependent for select values of dimensionless fracture conductivity.

### Bilinear Flow Relation with Hyperbolic Time-Dependent Skin Effects

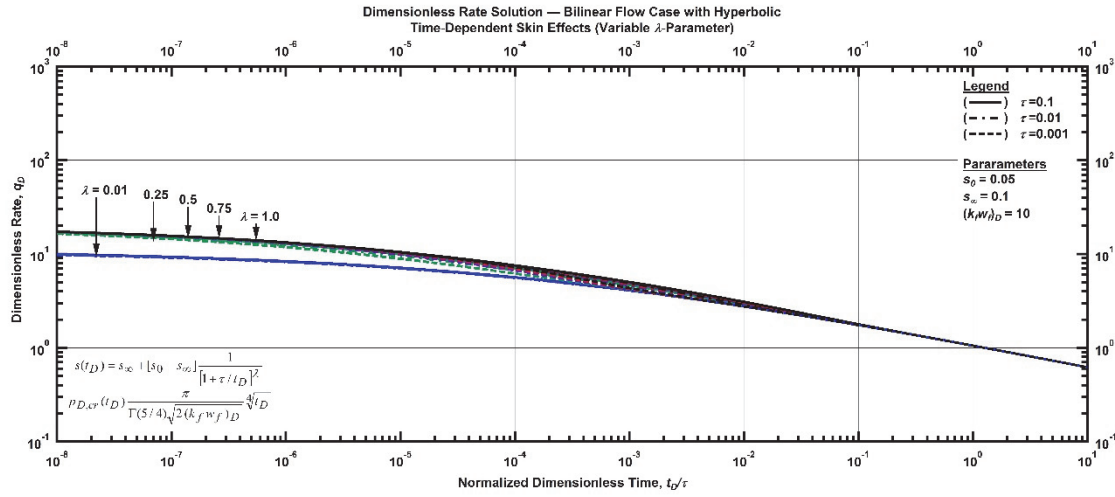


Figure F. 160 — Log-log plot (constant pressure dimensionless rate solution) for the bilinear flow model combined with the hyperbolic time-dependent for select values of  $\lambda$ -parameter.

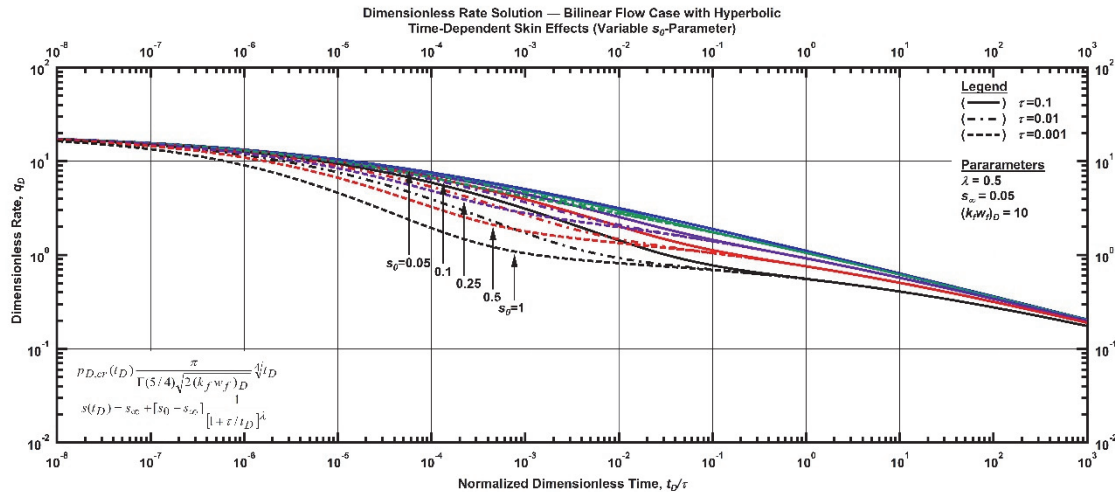


Figure F. 161 — Log-log plot (constant pressure dimensionless rate solution) for the bilinear flow model combined with the hyperbolic time-dependent for select values of  $s_0$ -parameter.

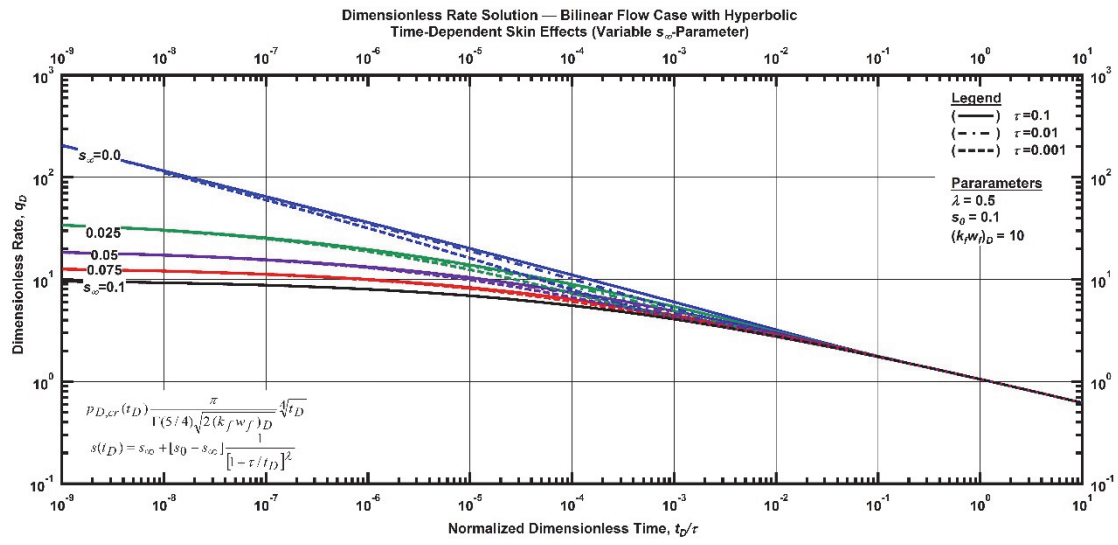


Figure F. 162 — Log-log plot (constant pressure dimensionless rate solution) for the bilinear flow model combined with the hyperbolic time-dependent for select values of  $s_\infty$ -parameter.

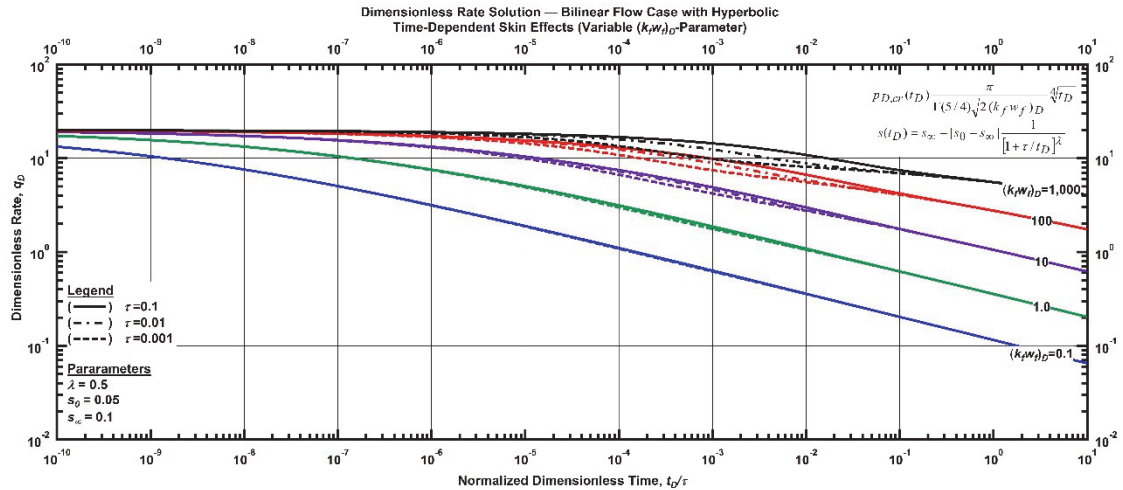


Figure F. 163 — Log-log plot (constant pressure dimensionless rate solution) for the bilinear flow model combined with the hyperbolic time-dependent for select values of dimensionless fracture conductivity.

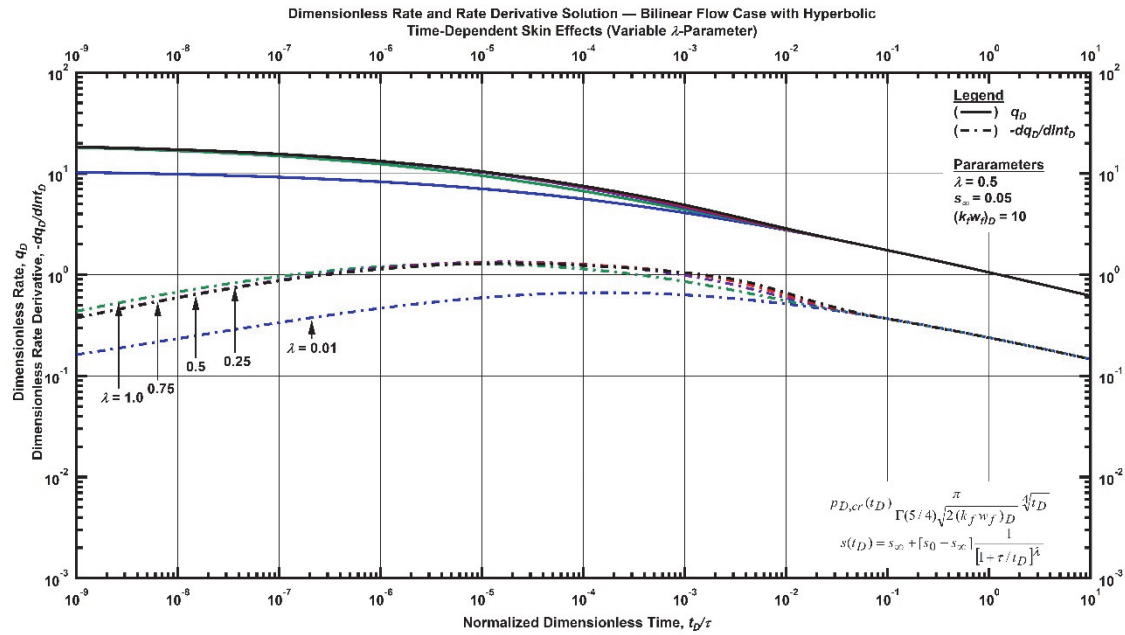


Figure F. 164 — Log-log plot (constant pressure dimensionless rate derivative solution) for the bilinear flow model combined with the hyperbolic time-dependent for select values of  $\lambda$ -parameter.

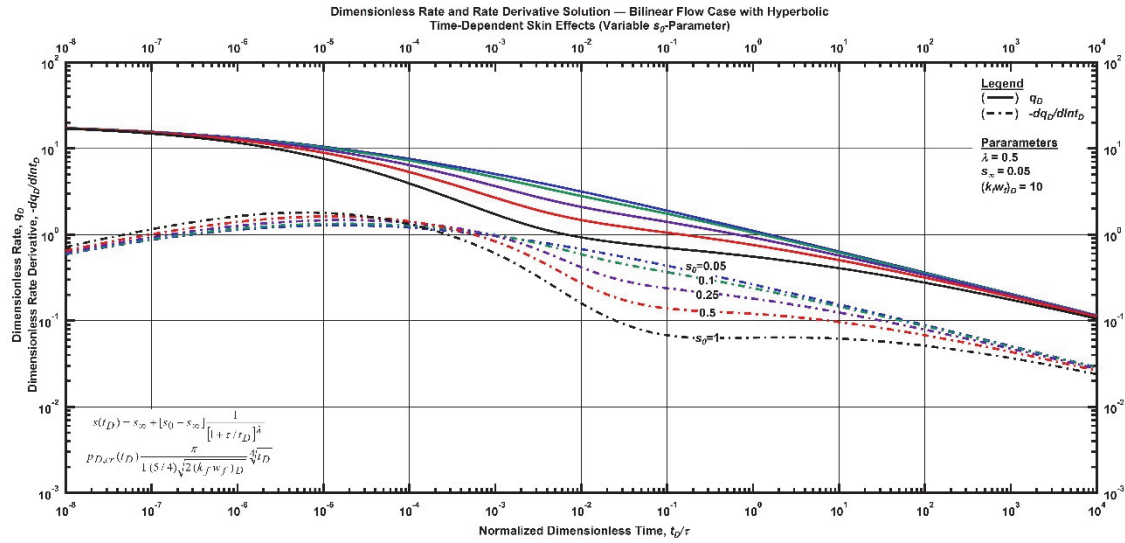


Figure F. 165 — Log-log plot (constant pressure dimensionless rate derivative solution) for the bilinear flow model combined with the hyperbolic time-dependent for select values of  $s_0$ -parameter.

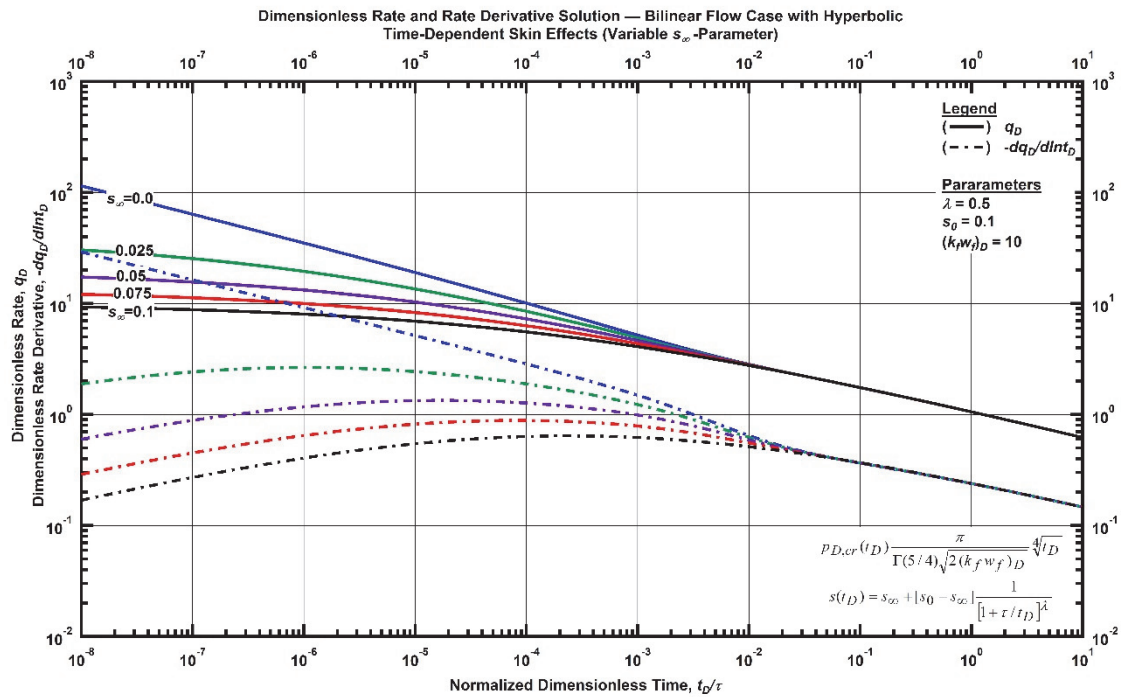


Figure F. 166 — Log-log plot (constant pressure dimensionless rate derivative solution) for the bilinear flow model combined with the hyperbolic time-dependent for select values of  $s_\infty$ -parameter.

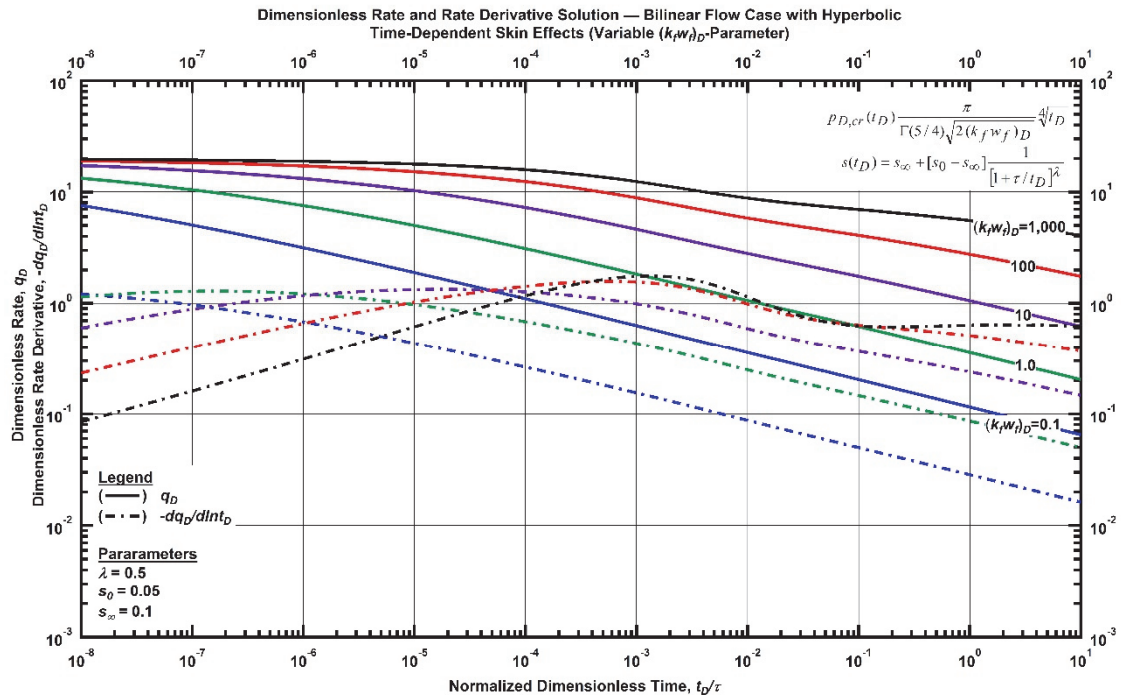


Figure F. 167 — Log-log plot (constant pressure dimensionless rate derivative solution) for the bilinear flow model combined with the hyperbolic time-dependent for select values of dimensionless fracture conductivity.

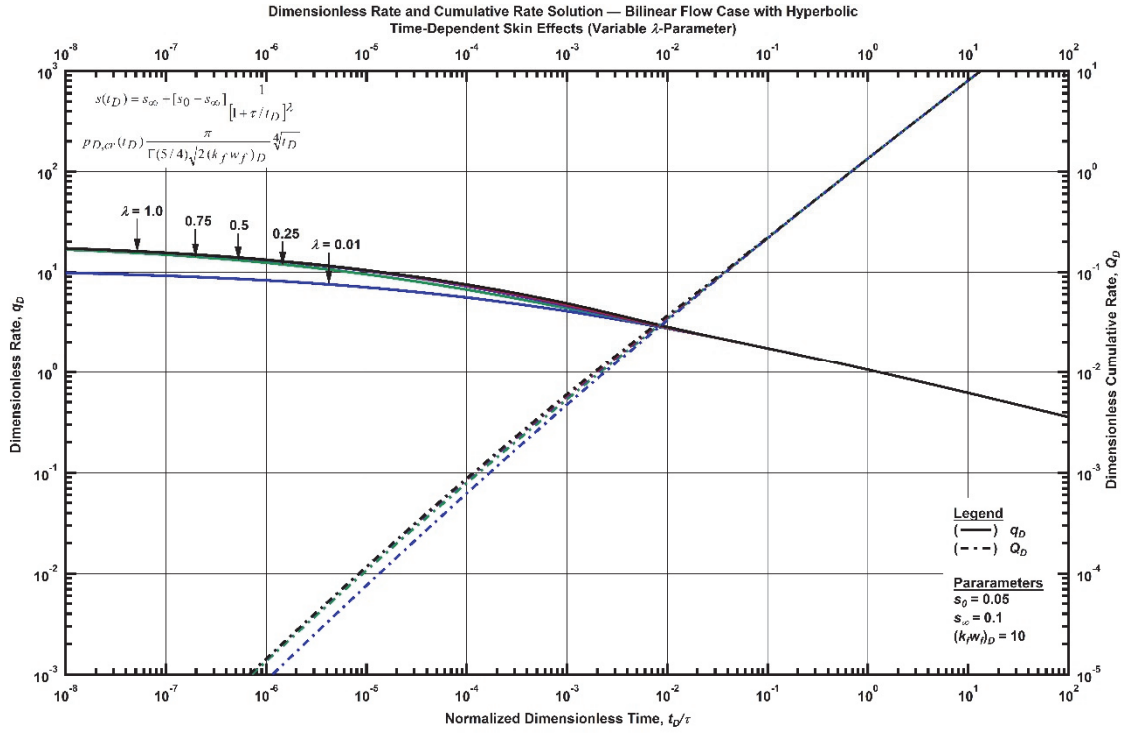


Figure F. 168 — Log-log plot (constant pressure dimensionless cumulative production solution) for the bilinear flow model combined with the hyperbolic time-dependent for select values of  $\lambda$ -parameter.

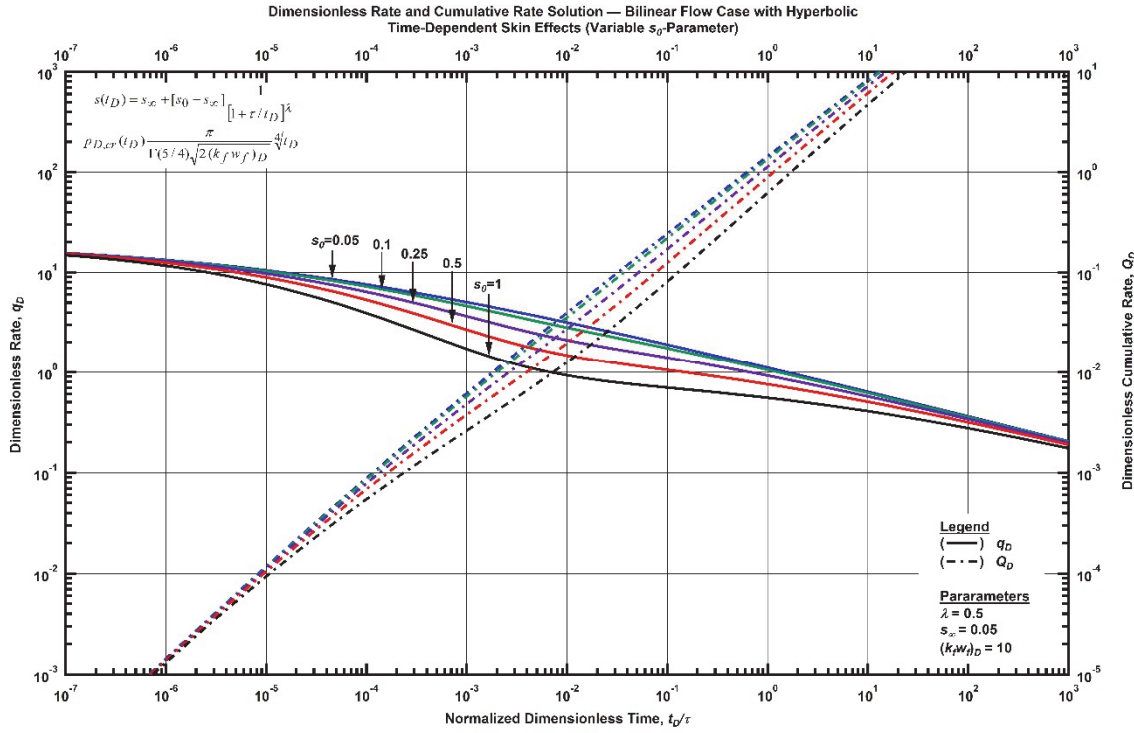


Figure F. 169 — Log-log plot (constant pressure dimensionless cumulative production solution) for the bilinear flow model combined with the hyperbolic time-dependent for select values of  $s_0$ -parameter.

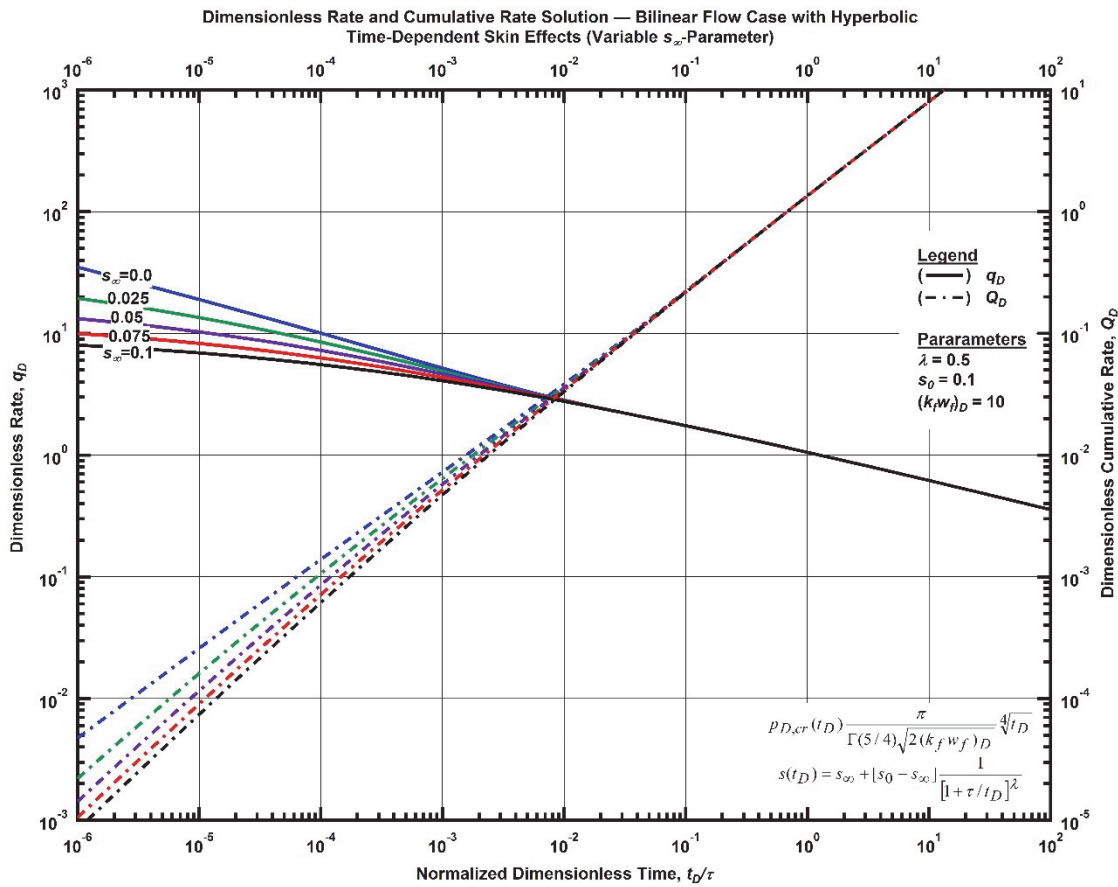


Figure F. 170 — Log-log plot (constant pressure dimensionless cumulative production solution) for the bilinear flow model combined with the hyperbolic time-dependent for select values of  $s_\infty$ -parameter.

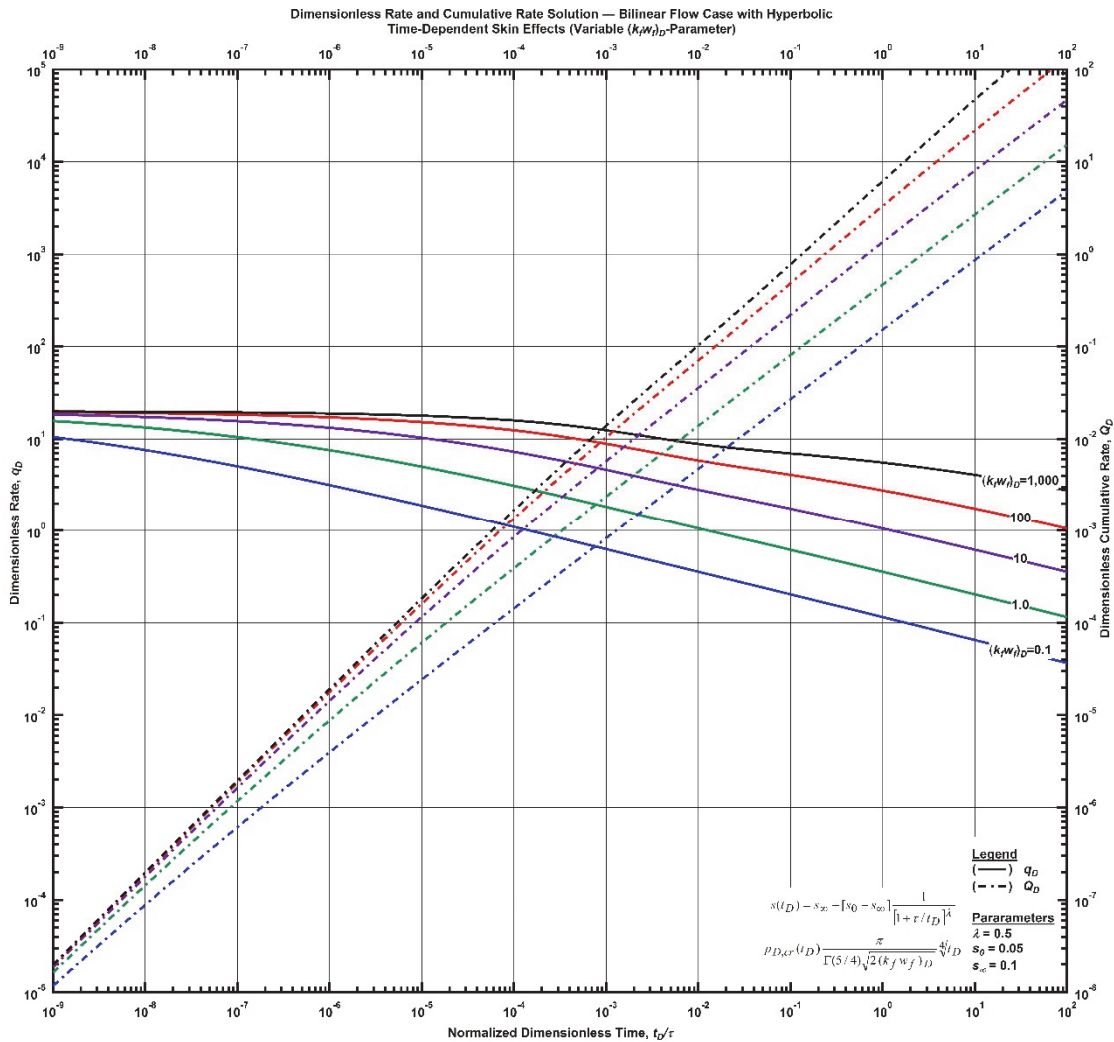


Figure F. 171 — Log-log plot (constant pressure dimensionless cumulative production solution) for the bilinear flow model combined with the hyperbolic time-dependent for select values of dimensionless fracture conductivity.

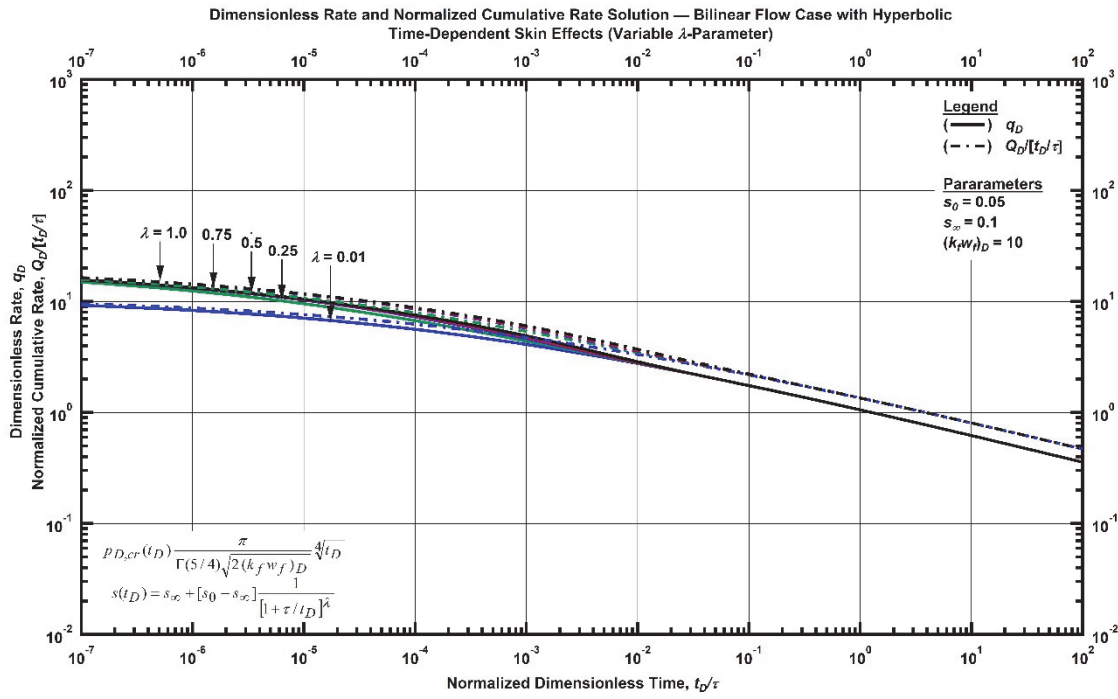


Figure F. 172 — Log-log plot (constant pressure time-normalized dimensionless cumulative rate solution) for the bilinear flow model combined with the hyperbolic time-dependent for select values of  $\lambda$ -parameter.

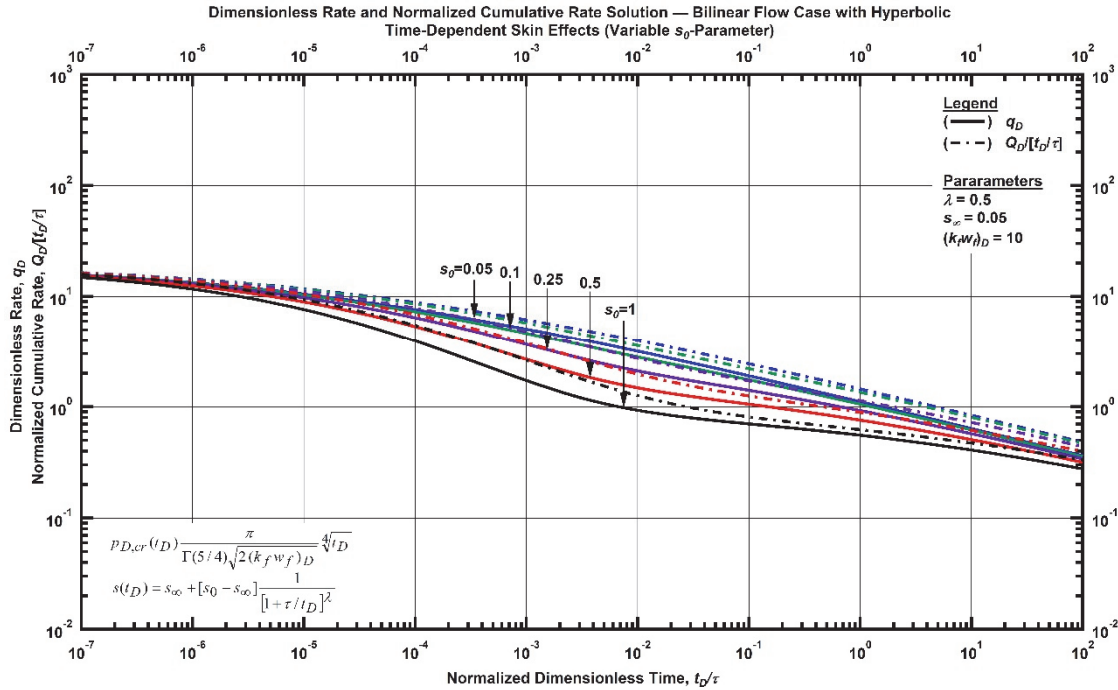


Figure F. 173 — Log-log plot (constant pressure time-normalized dimensionless cumulative rate solution) for the bilinear flow model combined with the hyperbolic time-dependent for select values of  $s_0$ -parameter.

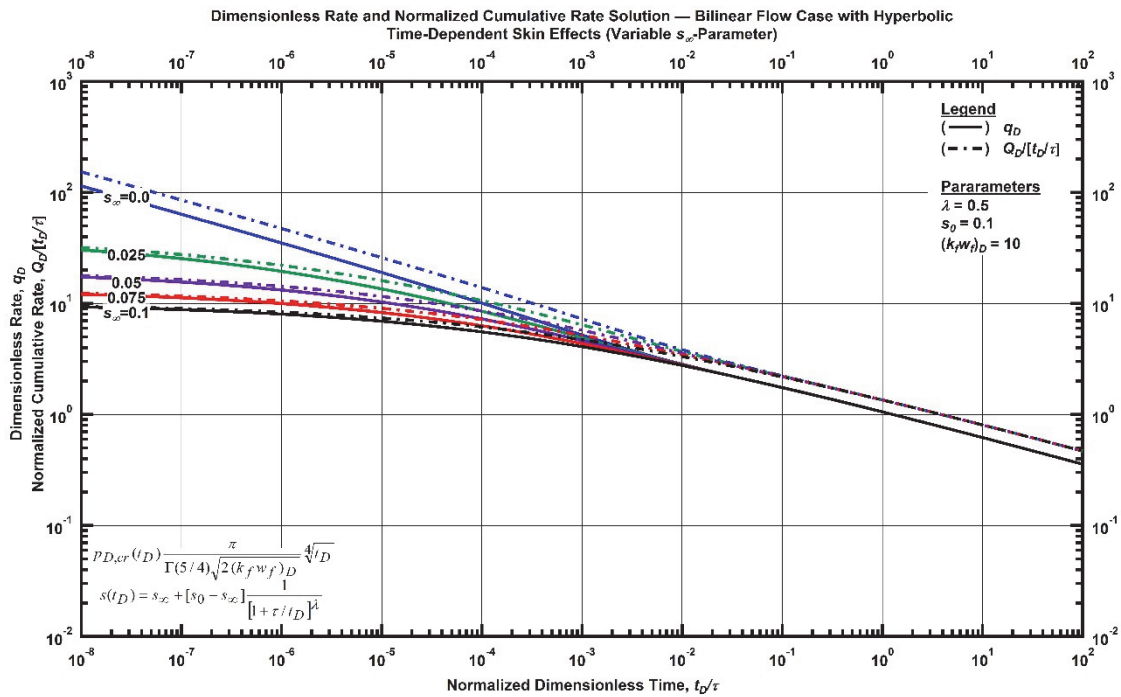


Figure F. 174 — Log-log plot (constant pressure time-normalized dimensionless cumulative rate solution) for the bilinear flow model combined with the hyperbolic time-dependent for select values of  $s_\infty$ -parameter.

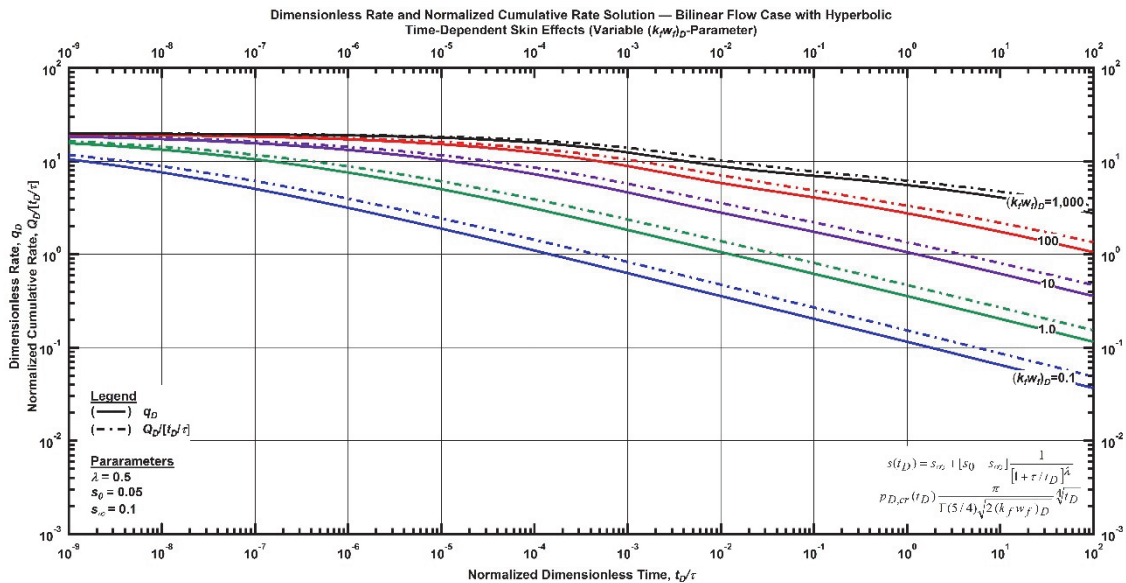


Figure F. 175 — Log-log plot (constant pressure time-normalized dimensionless cumulative rate solution) for the bilinear flow model combined with the hyperbolic time-dependent for select values of dimensionless fracture conductivity.

### Bilinear Flow Relation with Time-Dependent Wellbore Storage

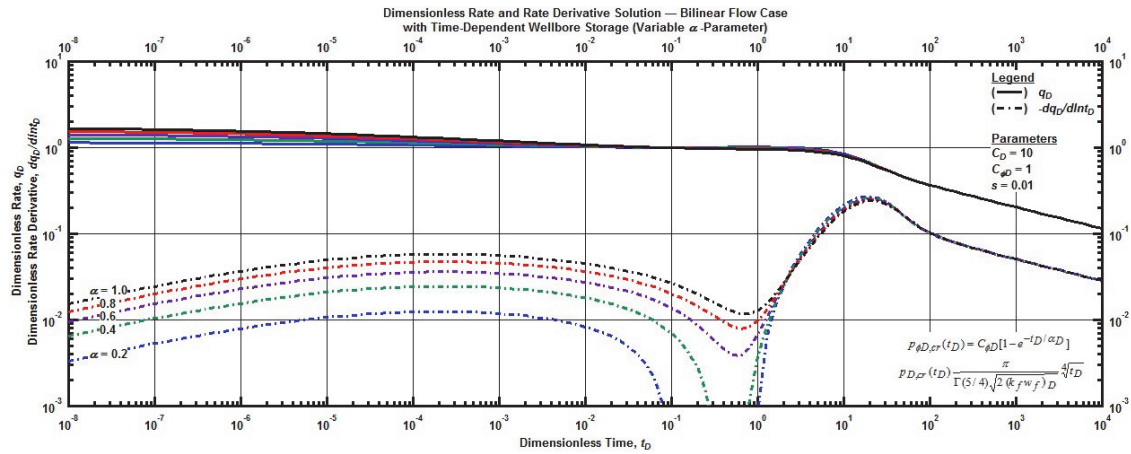


Figure F. 176 — Log-log plot (constant pressure dimensionless rate solution) for the bilinear flow model combined with the time-dependent wellbore storage for select values of  $\alpha$ -parameter.

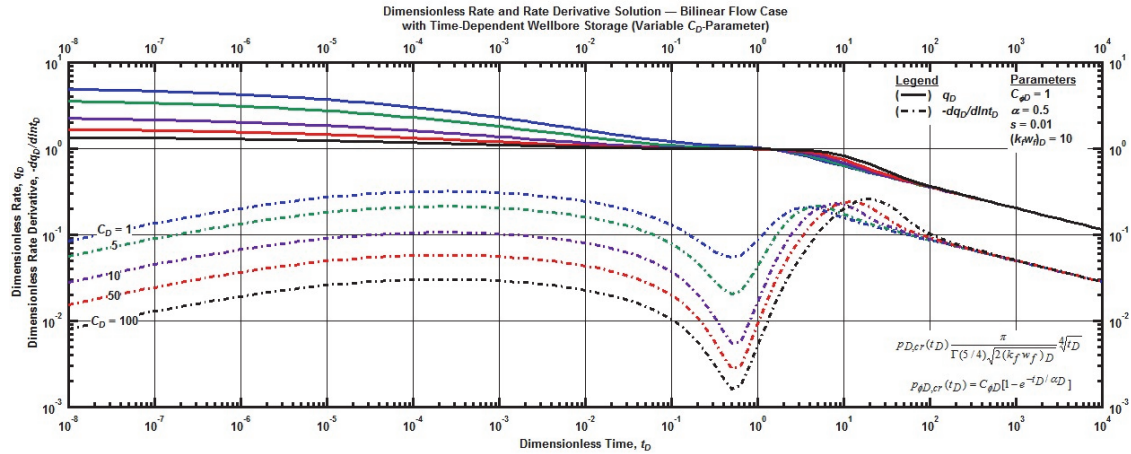


Figure F. 177 — Log-log plot (constant pressure dimensionless rate solution) for the bilinear flow model combined with the time-dependent wellbore storage for select values of the dimensionless wellbore storage constant.

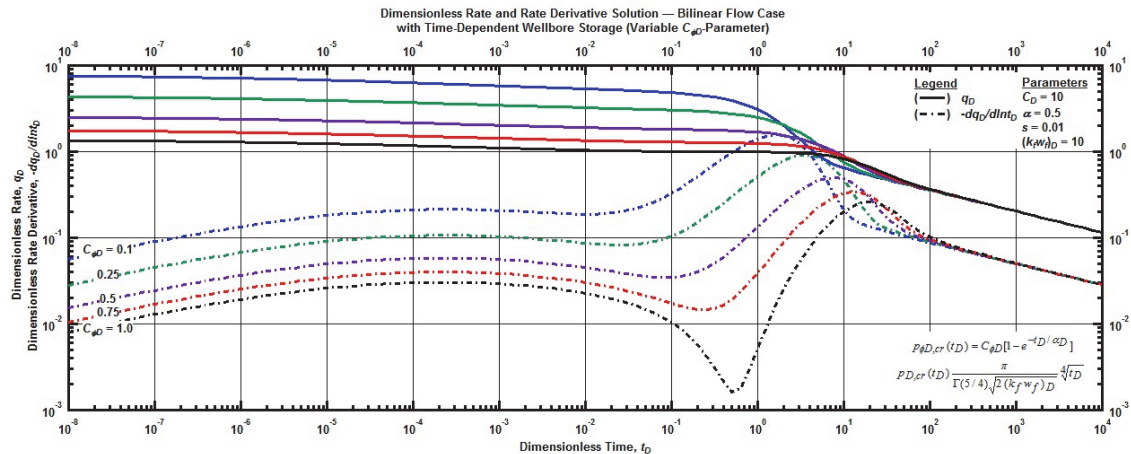


Figure F. 178 — Log-log plot (constant pressure dimensionless rate solution) for the bilinear flow model combined with the time-dependent wellbore storage for select values phase redistribution constant.

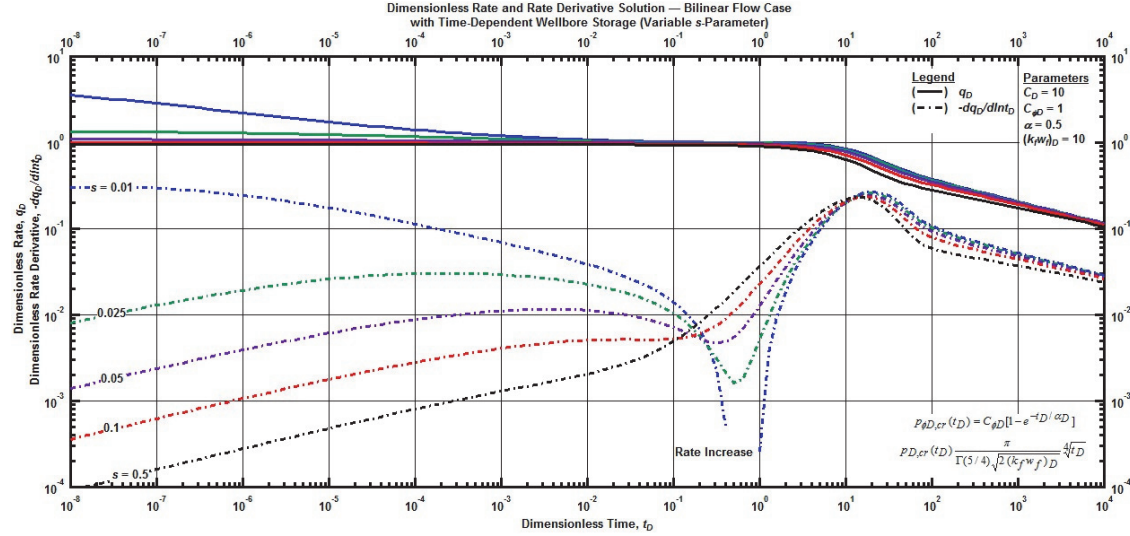


Figure F. 179 — Log-log plot (constant pressure dimensionless rate solution) for the bilinear flow model combined with the time-dependent wellbore storage for select dimensionless constant skin factor.

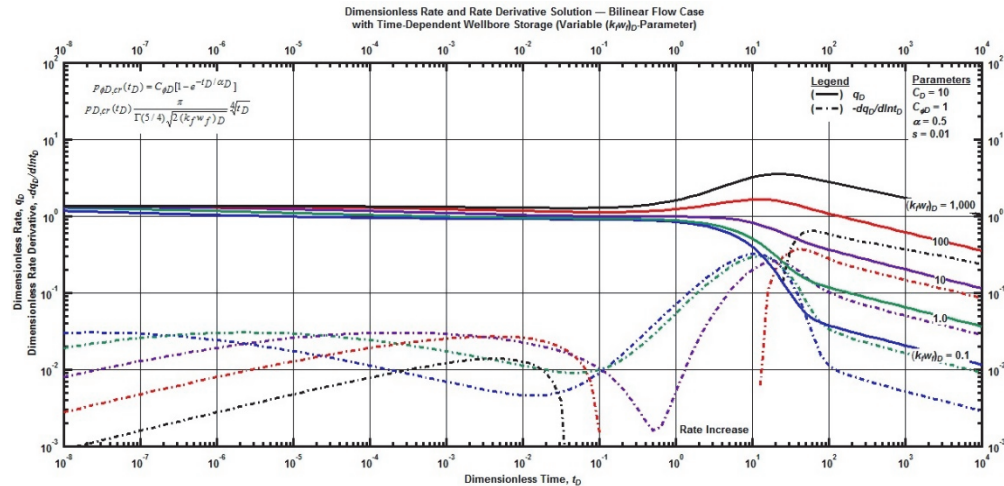


Figure F. 180 — Log-log plot (constant pressure dimensionless rate solution) for the bilinear flow model combined with the time-dependent wellbore storage for select values of  $(k_f w_f)_D$ -parameter.

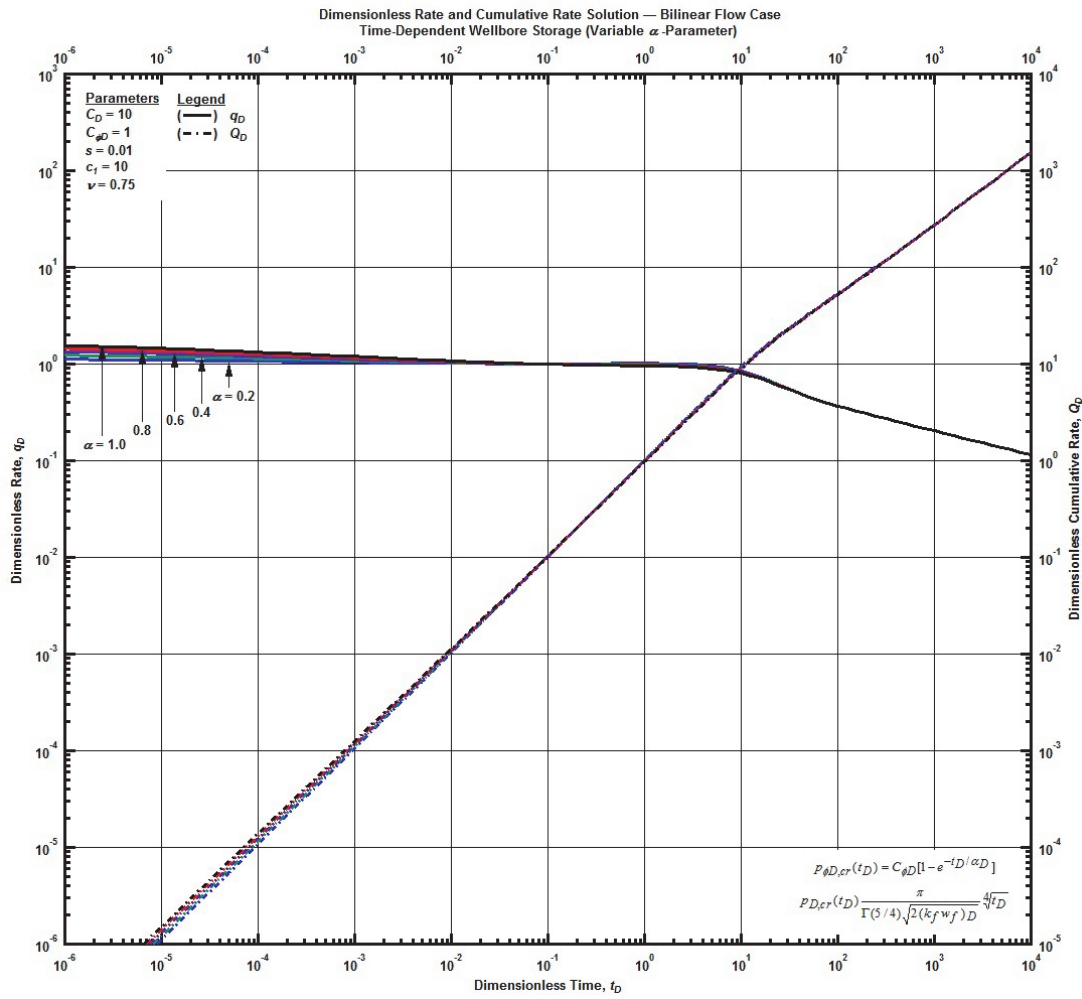


Figure F. 181 — Log-log plot (constant pressure dimensionless cumulative production solution) for the bilinear flow model combined with the time-dependent wellbore storage for select values of  $\alpha$ -parameter.

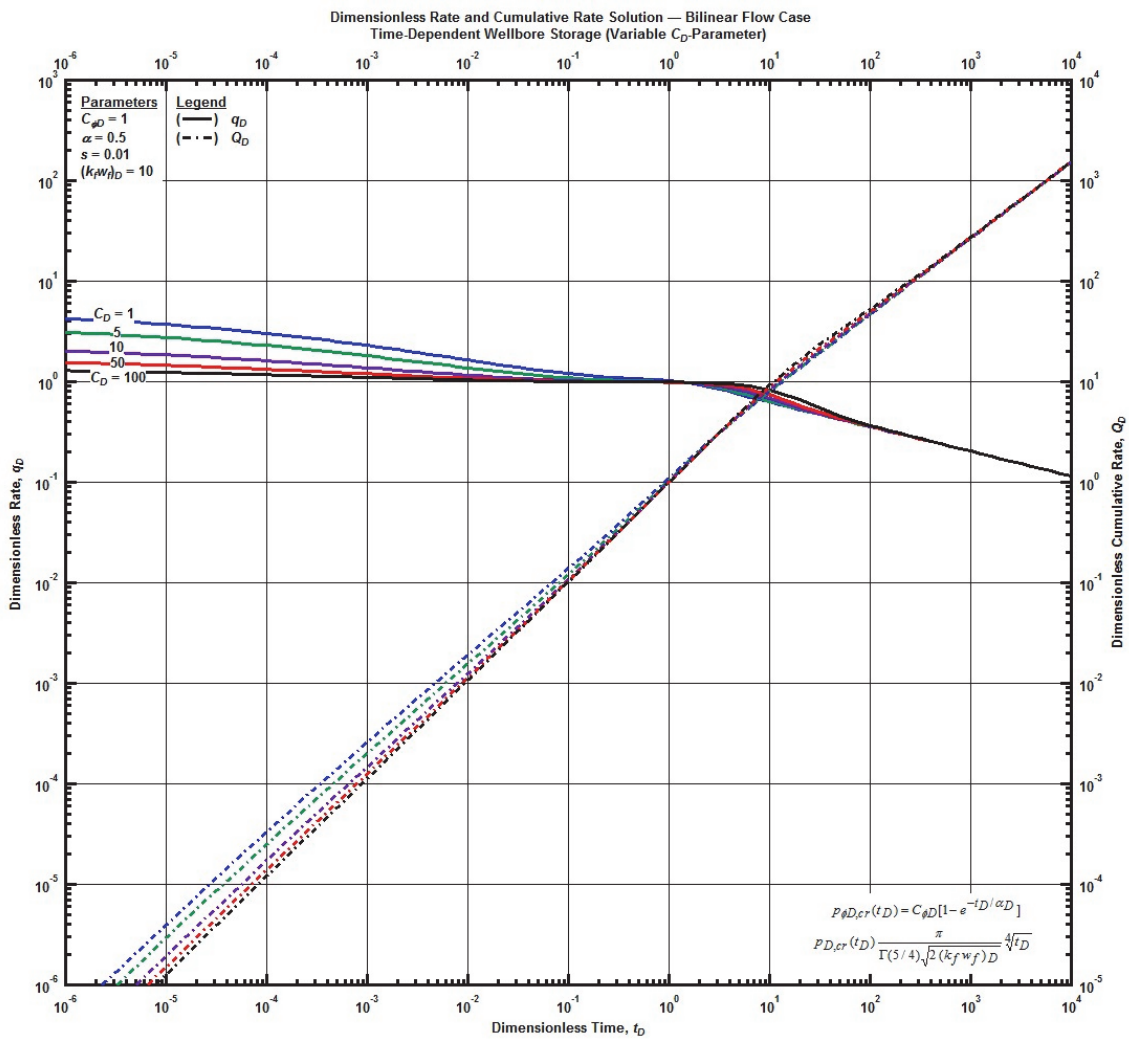


Figure F. 182 — Log-log plot (constant pressure dimensionless cumulative production solution) for the bilinear flow model combined with the time-dependent wellbore storage for select values of the dimensionless wellbore storage constant.

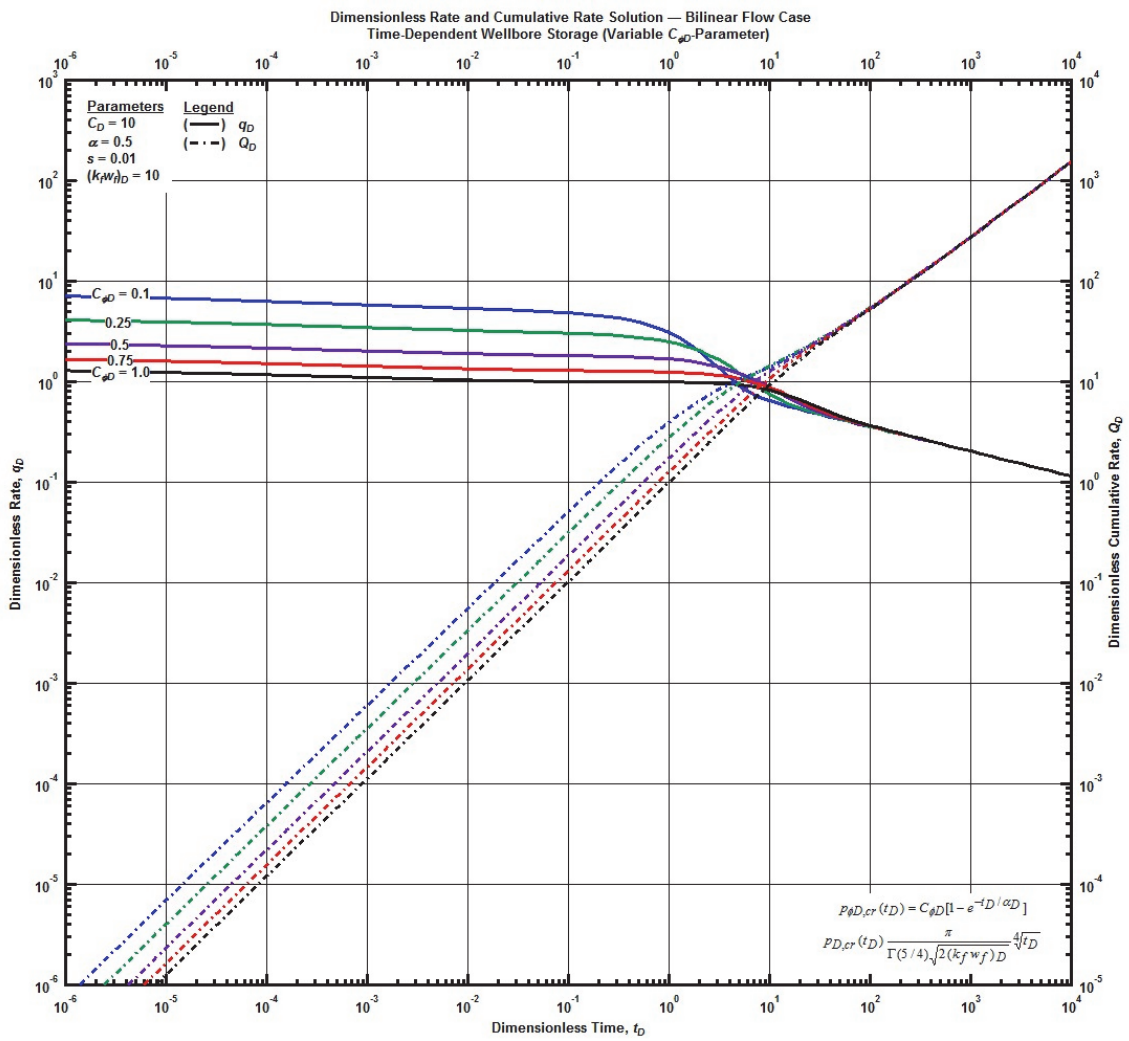


Figure F. 183 — Log-log plot (constant pressure dimensionless cumulative production solution) for the bilinear flow model combined with the time-dependent wellbore storage for select values phase redistribution constant.

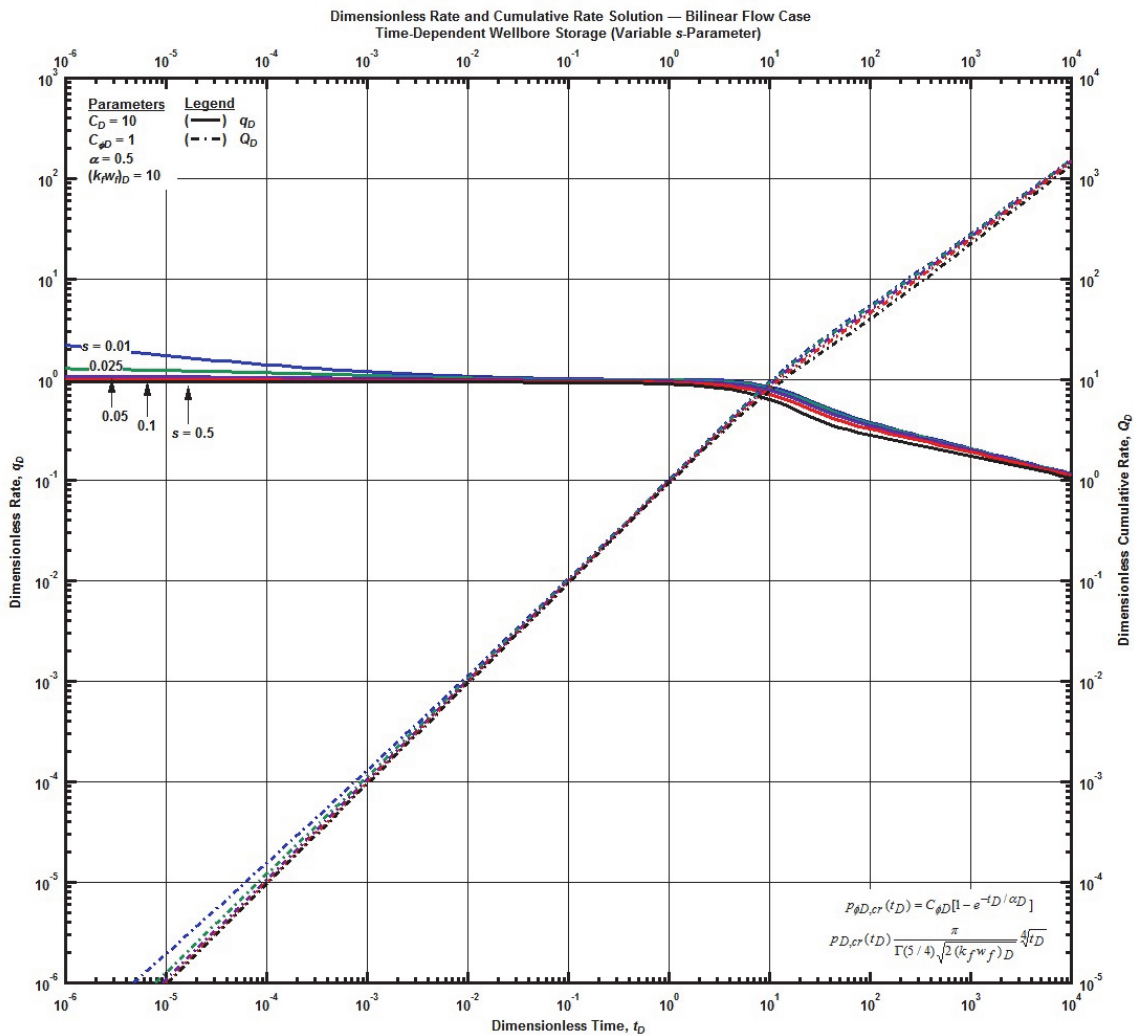


Figure F. 184 — Log-log plot (constant pressure dimensionless cumulative production solution) for the bilinear flow model combined with the time-dependent wellbore storage for select dimensionless constant skin factor.

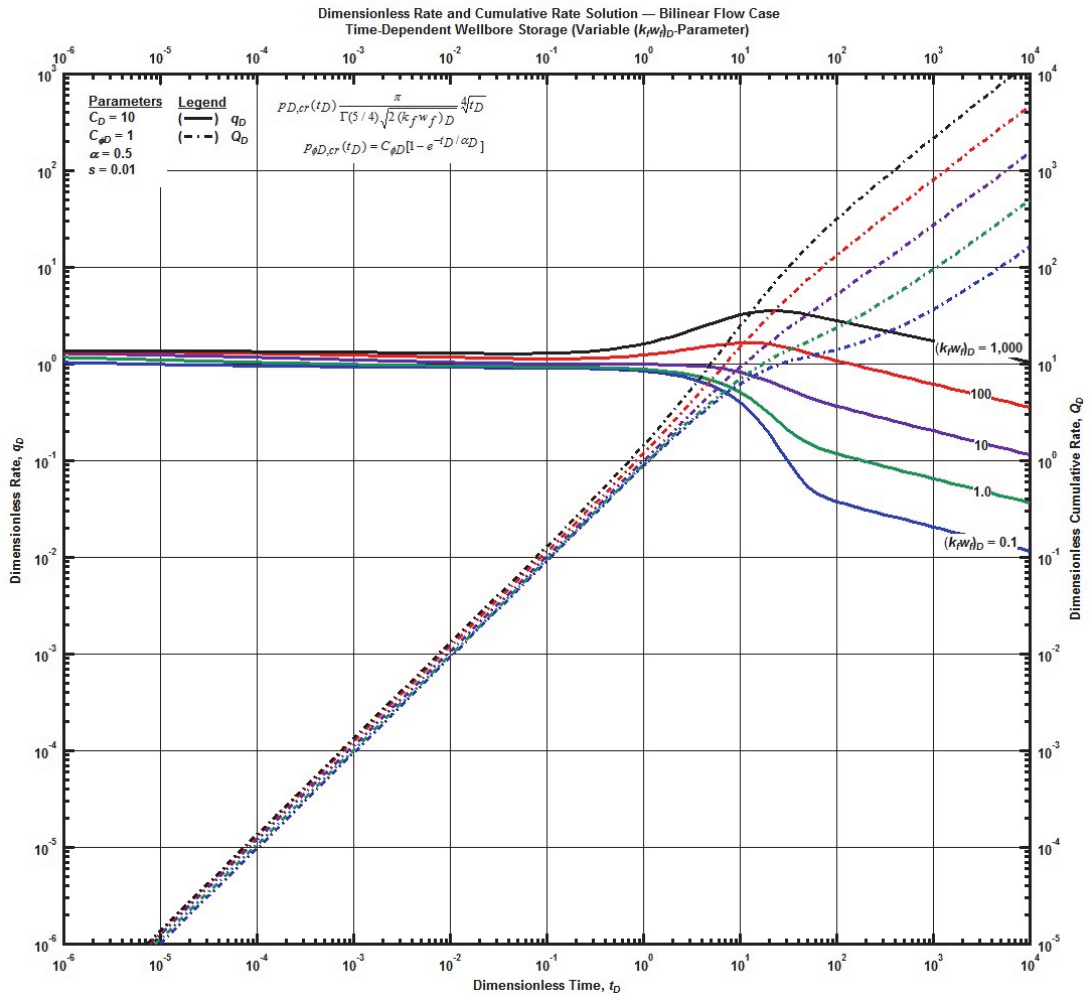


Figure F. 185 — Log-log plot (constant pressure dimensionless cumulative production solution) for the bilinear flow model combined with the time-dependent wellbore storage for select values of  $(k_w)_D$ -parameter.

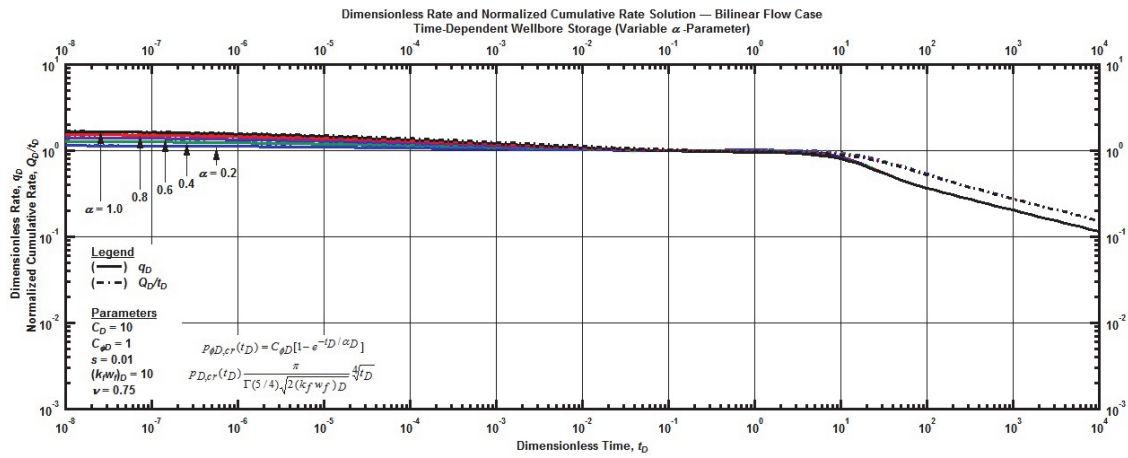


Figure F. 186 — Log-log plot (constant pressure time-normalized dimensionless cumulative rate solution) for the bilinear flow model combined with the time-dependent wellbore storage for select values of  $\alpha$ -parameter.

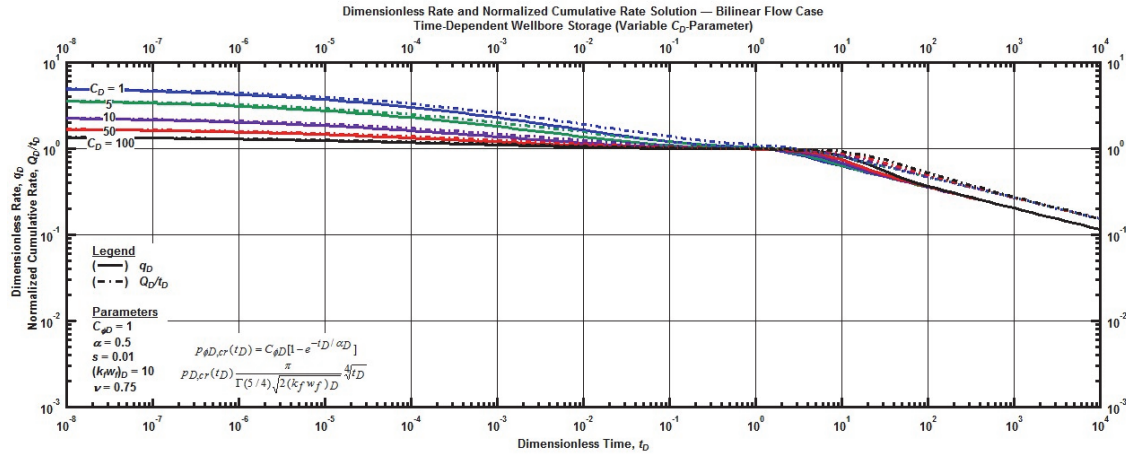


Figure F. 187 — Log-log plot (constant pressure time-normalized dimensionless cumulative rate solution) for the bilinear flow model combined with the time-dependent wellbore storage for select values of the dimensionless wellbore storage constant.

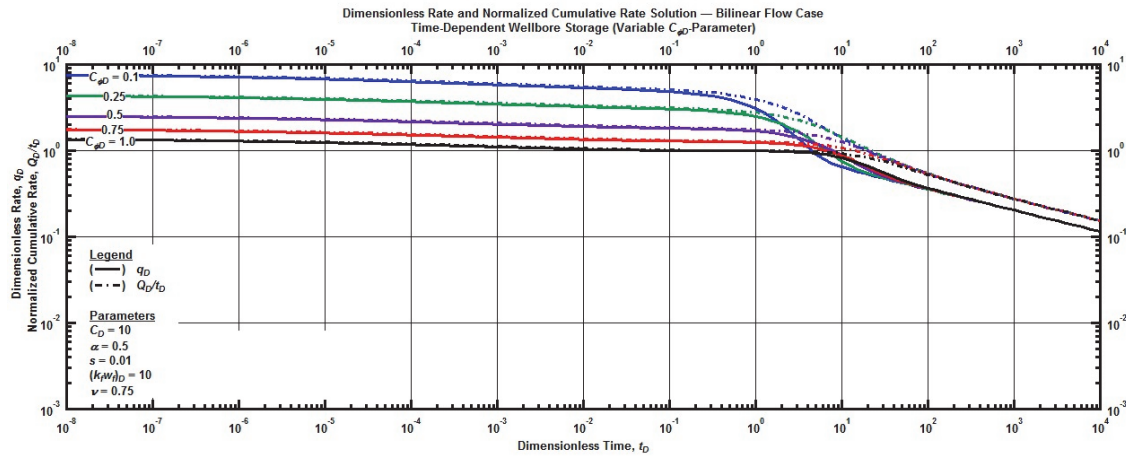


Figure F. 188 — Log-log plot (constant pressure time-normalized dimensionless cumulative rate solution) for the bilinear flow model combined with the time-dependent wellbore storage for select values phase redistribution constant.

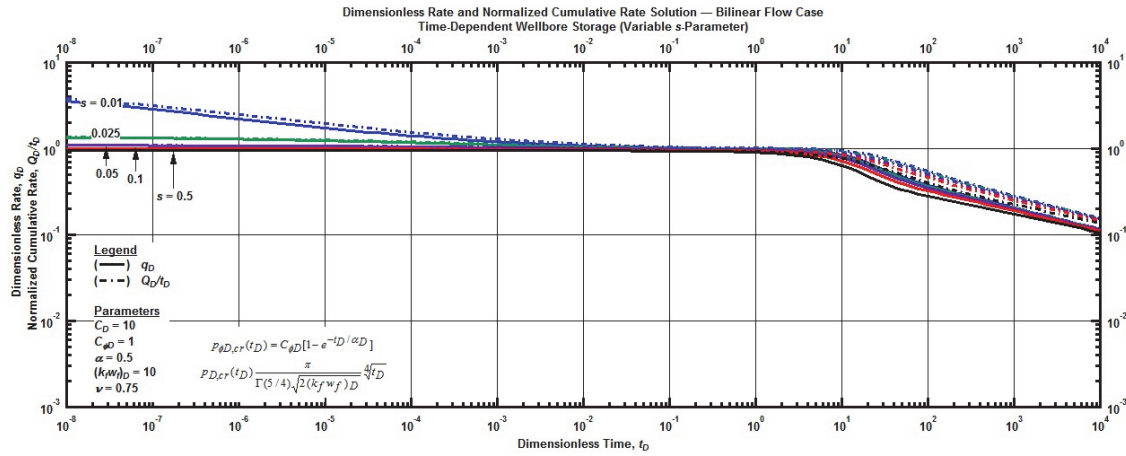


Figure F. 189 — Log-log plot (constant pressure time-normalized dimensionless cumulative rate solution) for the bilinear flow model combined with the time-dependent wellbore storage for select dimensionless constant skin factor.

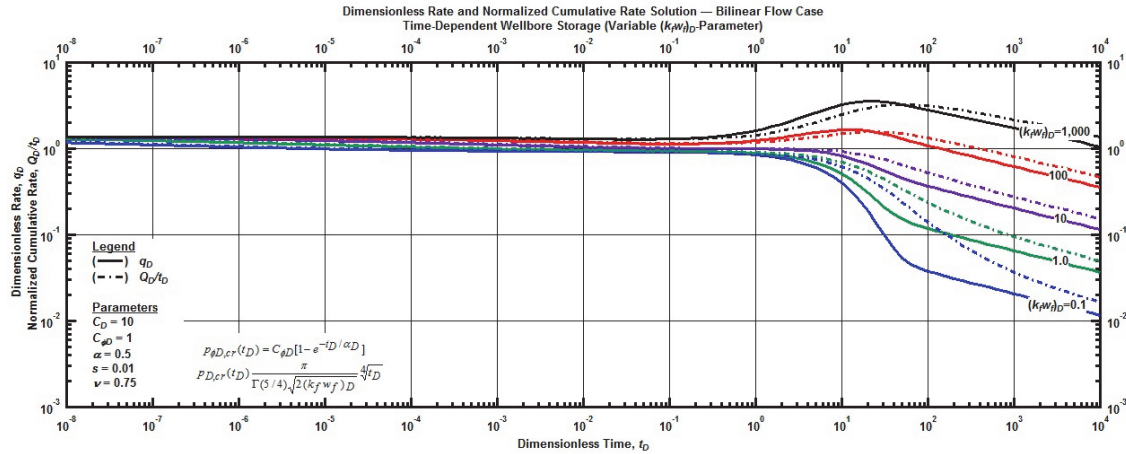


Figure F. 190 — Log-log plot (constant pressure time-normalized dimensionless cumulative rate solution) for the bilinear flow model combined with the time-dependent wellbore storage for select values of  $(k_f w_f)_D$ -parameter.